TECHNICAL REPORT UOME-FM-89-06

TURBULENCE MEASUREMENTS IN THE SWIRLING FLOW AT THE ENTRANCE TO THE CCRL TUNNEL FURNACE FACILITY

FOR THE DEPARTMENT OF ENERGY, MINES AND RESOURCES,
CANMET-ERL DIVISION
(DSS CONTRACT NO. 23440-8-9175/01-SS)

by

A. G. L. Holloway, P. Eng.

S. Tavoularis, Ph.D., P. Eng.
(Principal Investigator)

Department of Mechanical Engineering
University of Ottawa
Ottawa, Ontario, K1N 6N5

MICROMEDIA

May 1989

169 pp

Approved:

89-05406/

Abstract

The mean velocity (axial, radial and circumferential components) and turbulence stresses were measured at the burner exit of the CCRL tunnel furnace for three fixed vane swirl generators and a International Flame Research Foundation (IFRF) variable block type swirl generator for various degrees of swirl and different mass flowrates . Integral length scales were also measured in some cases.

The results suggest that the mean velocity profiles and turbulence stresses may be scaled using the mass flow rate.

Contents

1 Introduction 21

2 Experimental Facility 21

3 Instrumentation and Experimental Procedure 23

4 Measurements 28

4.1 General Description 28

4.2 Sources of Errors 31

4.3 Scaling of the Results 31

4.4 The Fixed Vane Swirl Generators 32

4.4.1 The Primary Flow 33

4.4.2 The Secondary Flow 33

4.5 The IFRF Swirl Generator 34

4.5.1 The Primary Flow 34

4.5.2 The Secondary Flow 34

5 Using the Measurements in Turbulence Models 35

6 Conclusions 37

NOMENCLATURE

b	axial coordinate in the probe oriented system
k	turbulent kinetic energy per unit mass
$\dot{m}$	mass flow rate
n	normal coordinate in the probe oriented system
p	air pressure
q^2	sum of mean squared velocity components
$\Re = \frac{\widehat{U}_x D}{\nu}$	Reynolds number based on the radial weighted axial velocity
r	radial position
S	the swirl setting on the IFRF swirl generator
t	time
u	velocity fluctuation
U	the mean velocity
x	horizontal coordinate
y	vertical coordinate
z	axial coordinate

Greek Symbols

ρ air density

ϕ angle between the z direction and b direction

θ angular position

Suffixes

$(.)_r$ in the radial direction

$(.)_\theta$ in the circumferential direction

$(.)_b$ in the b direction

$(.)_n$ in the n direction

$(.)_p$ in the primary stream

$(.)_s$ in the secondary stream

$\overline{(.)}$ time average

$\widehat{(.)}$ radius weighted average

$\widetilde{(.)}$ instantaneous value

$(.)'$ root mean square value

List of Tables

1 The experimental conditions for the fixed vane swirl generators 39

2 The experimental conditions for the IFRF swirl generator 39

3 Data in the probe oriented system (uncorrected for temperature) for the 30° degree fixed vane swirl generator. When the wires are in the "zx" plane the subscript "+" is to be taken as "n" and when in the "zy" plane as "y"; z=10 mm. 40

4 Data in the probe oriented system (uncorrected for temperature) for the 30° degree fixed vane swirl generator. When the wires are in the "zx" plane the subscript "+" is to be taken as "n" and when in the "zy" plane as "y"; z=5 mm. 41

5 Data in the probe oriented system (uncorrected for temperature) for the 45° degree fixed vane swirl generator. When the wires are in the "zx" plane the subscript "+" is to be taken as "n" and when in the "zy" plane as "y"; z=10 mm. 42

6 Data in the probe oriented system (uncorrected for temperature) for the 45° degree fixed vane swirl generator. When the wires are in the "zx" plane the subscript "+" is to be taken as "n" and when in the "zy" plane as "y"; z=9 mm. 43

7 Data in the probe oriented system (uncorrected for temperature) for the 60° degree fixed vane swirl generator. When the wires are in the "zx" plane the subscript "+" is to be taken as "n" and when in the "zy" plane as "y"; z=6 mm. 44

8 Data in the probe oriented system (uncorrected for temperature) for the primary flow of the IFRF variable swirl generator. When the wires are in the "zx" plane the subscript "+" is to be taken as "n" and when in the "zy" plane as "y"; z=2.5 mm. 45

9 Data in the probe oriented system (uncorrected for temperature) for the primary flow of the IFRF variable swirl generator. When the wires are in the "zx" plane the subscript "+" is to be taken as "n" and when in the "zy" plane as "y"; z=2.5 mm. 46

10 Data in the probe oriented system (uncorrected for temperature) for the secondary flow of the IFRF variable swirl generator. When the wires are in the "zx" plane the subscript "+" is to be taken as "n" and when in the "zy" plane as "y"; S=0.0, z=2.5 mm. 47

11 Data in the probe oriented system (uncorrected for temperature) for the secondary flow of the IFRF variable swirl generator. When the wires are in the "zx" plane the subscript "+" is to be taken as "n" and when in the "zy" plane as "y"; S=1.0, z=4.0 mm. 48

12 Data in the probe oriented system (uncorrected for temperature) for the secondary flow of the IFRF variable swirl generator. When the wires are in the "zx" plane the subscript "+" is to be taken as "n" and when in the "zy" plane as "y"; S=1.0, z=4.0 mm. 49

13 Data in the probe oriented system (uncorrected for temperature) for the secondary flow of the IFRF variable swirl generator. When the wires are in the "zx" plane the subscript "+" is to be taken as "n" and when in the "zy" plane as "y"; S=2.0, z=2.0 mm. 50

14 Data in the probe oriented system (uncorrected for temperature) for the secondary flow of the IFRF variable swirl generator. When the wires are in the "zx" plane the subscript "+" is to be taken as "n" and when in the "zy" plane as "y"; S=2.0, z=2.0 mm. 51

15 Data in the probe oriented system (uncorrected for temperature) for the secondary flow of the IFRF variable swirl generator. When the wires are in the "zx" plane the subscript "+" is to be taken as "n" and when in the "zy" plane as "y"; S=3.0, z=2.0 mm. 52

16 Data in the probe oriented system (uncorrected for temperature) for the secondary flow of the IFRF variable swirl generator. When the wires are in the "zx" plane the subscript "+" is to be taken as "n" and when in the "zy" plane as "y"; S=3.0, z=2.0 mm. 53

17 Data in the probe oriented system (uncorrected for temperature) for the secondary flow of the IFRF variable swirl generator. When the wires are in the "zx" plane the subscript "+" is to be taken as "n" and when in the "zy" plane as "y"; S=4., z=2.0 mm. 54

18 Data in the probe oriented system (uncorrected for temperature) for the secondary flow of the IFRF variable swirl generator. When the wires are in the "zx" plane the subscript "+" is to be taken as "n" and when in the "zy" plane as "y"; S=4.0, z=2.0 mm. 55

19 Data in the probe oriented system (uncorrected for temperature) for the secondary flow of the IFRF variable swirl generator. When the wires are in the "zx" plane the subscript "+" is to be taken as "n" and when in the "zy" plane as "y"; S=4.5, z=2.0 mm. 56

20 Data in the probe oriented system (uncorrected for temperature) for the secondary flow of the IFRF variable swirl generator. When the wires are in the "zx" plane the subscript "+" is to be taken as "n" and when in the "zy" plane as "y"; S=4.5, z=4.5 mm. 57

21 Data for the 30° fixed vane swirl generator presented in cylindrical coordinates; z=10 mm. 58

22 Normalized data for the 30° fixed vane swirl generator; $\hat{U}_z$ = 31.4 m/s for the primary flow and $\hat{U}_z$ = 22.7 m/s for the secondary flow; z=10 mm. 59

23 Data for the 30° fixed vane swirl generator presented in cylindrical coordinates; z=5 mm. 60

24 Normalized data for the 30° fixed vane swirl generator; $\hat{U}_z$ = 15.2 m/s for the primary flow and $\hat{U}_z$ = 12.1 m/s for the secondary flow; z=5 mm. 61

25 Data for the 45° fixed vane swirl generator presented in cylindrical coordinates; z=10 mm. 62

26 Normalized data for the 45° fixed vane swirl generator; $\hat{U}_z$ = 30.3 m/s for the primary flow and $\hat{U}_z$ = 22.4 m/s for the secondary flow; z=10 mm. 63

27 Data for the 45° fixed vane swirl generator presented in cylindrical coordinates; z=9 mm. 64

28 Normalized data for the 45° fixed vane swirl generator; $\hat{U}_z$ = 19.3 m/s for the primary flow and $\hat{U}_z$ = 13.2 m/s for the secondary flow; z=9 mm. 65

29 Data for the 60° fixed vane swirl generator presented in cylindrical coordinates; z=6 mm. 66

30 Normalized data for the 60° fixed vane swirl generator; $\hat{U}_z$ = 15.4 m/s for the primary flow and $\hat{U}_z$ = 10.6 m/s for the secondary flow; z=6 mm. 67

31 Data for the primary flow of the IFRF variable swirl generator presented in cylindrical coordinates; z=2.5 mm. 68

32 Normalized data for the primary flow of the IFRF variable swirl generator; $\hat{U}_z$ = 15.4 m/s, z=2.5 mm. 69

33 Data for the primary flow of the IFRF variable swirl generator presented in cylindrical coordinates; z=2.5 mm. 70

34 Normalized data for the primary flow of the IFRF variable swirl generator; $\hat{U}_z$ = 6.6 m/s, z=10 mm. 71

35 Data for the secondary flow of the IFRF variable swirl generator presented in cylindrical coordinates; S=0.0, z=2.5 mm. 72

36 Normalized data for the secondary flow of the IFRF variable swirl generator; S=0.0, $\hat{U}_z$ = 14.4 m/s, z=2.5 mm. 73

37 Data for the secondary flow of the IFRF variable swirl generator presented in cylindrical coordinates; S=1.0, z=4.0 mm. 74

38 Normalized data for the secondary flow of the IFRF variable swirl generator; S=1.0, $\hat{U}_z$ = 11.9 m/s, z=4.0 mm. 75

39 Data for the secondary flow of the IFRF variable swirl generator presented in cylindrical coordinates; S=1.0, z=4.0 mm. 76

40 Normalized data for the secondary flow of the IFRF variable swirl generator; S=1.0, $\hat{U}_z$ = 7.2 m/s, z=4.0 mm. 77

41 Data for the secondary flow of the IFRF variable swirl generator presented in cylindrical coordinates; S=2.0, z=2.0 mm. 78

42 Normalized data for the secondary flow of the IFRF variable swirl generator; S=2.0, $\hat{U}_z$ = 16.5 m/s, z=2.0 mm. 79

43 Data for the secondary flow of the IFRF variable swirl generator presented in cylindrical coordinates; S=2.0, z=2.0 mm. 80

44 Normalized data for the secondary flow of the IFRF variable swirl generator; S=2.0, $\hat{U}_z$ = 8.2 m/s, z=2.0 mm. 81

45 Data for the secondary flow of the IFRF variable swirl generator presented in cylindrical coordinates; S=3.0, z=2.0 mm. 82

46 Normalized data for the secondary flow of the IFRF variable swirl generator; S=3.0, $\hat{U}_z$ = 15.9 m/s, z=2.0 mm. 83

47 Data for the secondary flow of the IFRF variable swirl generator, presented in cylindrical coordinates; S=3.0, z=2.0 mm. 84

48 Normalized data for the secondary flow of the IFRF variable swirl generator; S=3.0, $\hat{U}_z$ = 7.9 m/s, z=2.0 mm. 85

49 Data for the secondary flow of the IFRF variable swirl generator presented in cylindrical coordinates; S=4.0, z=10 mm. 86

50 Normalized data for the secondary flow of the IFRF variable swirl generator; S=4.0, $\hat{U}_z$ = 19.6 m/s, z=2 mm. 87

51 Data for the secondary flow of the IFRF variable swirl generator presented in cylindrical coordinates; S=4.0, z=2.0 mm. 88

52 Normalized data for the secondary flow of the IFRF variable swirl generator; S=4.0, $\hat{U}_z$ = 7.5 m/s, z=2.0 mm. 89

53 Data for the secondary flow of the IFRF variable swirl generator presented in cylindrical coordinates; S=4.5, z=2.0 mm. 90

54 Normalized data for the secondary flow of the IFRF variable swirl generator; S=4.5, $\hat{U}_z = 17.4$ m/s, z=2.0 mm. 91

55 Data for the secondary flow of the IFRF variable swirl generator presented in cylindrical coordinates; S=4.5, z=4.0 mm. 92

56 Normalized data for the secondary flow of the IFRF variable swirl generator; S=4.5, $\hat{U}_z = 8.3$ m/s, z=4.0 mm. 93

57 The measured integral length scales and estimated quantities useful for turbulence models. 94

List of Figures

1 The fixed vane swirl generators; the primary flow area is 506.5 mm^2; the secondary flow area is 2887 mm^2. 95

2 The IFRF variable swirl generator; the primary flow area is 6 204 mm^2; the secondary flow area is 18 156 mm^2. 96

3 The traversing mechanism. 97

4 The coordinate systems and velocity components. 98

5 Typical hot wire calibration results. 99

6 30° fixed vane swirl generator; $\theta = -90°$, z=10 mm; $\square \frac{\overline{U_\theta}}{\widehat{U}_z}$, $\circ \frac{\overline{U_r}}{\widehat{U}_z}$, $\Delta \frac{\overline{U_z}}{\widehat{U}_z}$; $\widehat{U}_z$ = 23.1 m/s. 100

7 30° fixed vane swirl generator; $\theta = -90°$, z=10 mm; $\square \frac{u'_\theta}{\widehat{U}_z}$, $\circ \frac{u'_r}{\widehat{U}_z}$, $\Delta \frac{u'_z}{\widehat{U}_z}$; $\widehat{U}_z$ = 23.1 m/s. 101

8 30° fixed vane swirl generator; $\theta = -90°$, z=10 mm; $\square \frac{\overline{u_\theta u_z}}{\widehat{U}_z^2}$, $\circ \frac{\overline{u_r u_z}}{\widehat{U}_z^2}$, $\Delta \frac{\overline{u_r u_\theta}}{\widehat{U}_z^2}$, $+ \frac{g^2}{\widehat{U}_z^2}$; $\widehat{U}_z$ = 23.1 m/s. 102

9 30° fixed vane swirl generator; y=-33 mm, z=10 mm; $\square \frac{\overline{U_\theta}}{\widehat{U}_z}$, $\circ \frac{\overline{U_r}}{\widehat{U}_z}$, $\Delta \frac{\overline{U_z}}{\widehat{U}_z}$; $\widehat{U}_z$ = 23.1 m/s. 103

10 30° fixed vane swirl generator; y=-33 mm, z=10 mm; $\square \frac{u'_\theta}{\widehat{U}_z}$, $\circ \frac{u'_r}{\widehat{U}_z}$, $\Delta \frac{u'_z}{\widehat{U}_z}$; $\widehat{U}_z$ = 23.1 m/s. 104

11 30° fixed vane swirl generator; y=-33 mm, z=10 mm; $\square \frac{\overline{u_\theta u_z}}{\widehat{U}_z^2}$, $\circ \frac{\overline{u_r u_z}}{\widehat{U}_z^2}$, $\Delta \frac{\overline{u_r u_\theta}}{\widehat{U}_z^2}$, $+ \frac{g^2}{\widehat{U}_z^2}$; $\widehat{U}_z$ = 23.1 m/s. 105

12 30° fixed vane swirl generator; $\theta = -90°$, z=5 mm; $\square \frac{\overline{U_\theta}}{\hat{U}_z}$, $\circ \frac{\overline{U_r}}{\hat{U}_z}$, $\triangle \frac{\overline{U_z}}{\hat{U}_z}$; $\hat{U}_z$ = 12.2 m/s. 106

13 30° fixed vane swirl generator; $\theta = -90°$, z=5 mm; $\square \frac{u'_\theta}{\hat{U}_z}$, $\circ \frac{u'_r}{\hat{U}_z}$, $\triangle \frac{u'_z}{\hat{U}_z}$; $\hat{U}_z$ = 12.2 m/s. 107

14 30° fixed vane swirl generator; $\theta = -90°$, z=5 mm; $\square \frac{\overline{u_\theta u_z}}{\hat{U}_z^2}$, $\circ \frac{\overline{u_r u_z}}{\hat{U}_z^2}$, $\triangle \frac{\overline{u_r u_\theta}}{\hat{U}_z^2}$, $+ \frac{q^2}{\hat{U}_z^2}$; $\hat{U}_z$ = 12.2 m/s. 108

15 30° fixed vane swirl generator; y=-33 mm, z=5 mm; $\square \frac{\overline{U_\theta}}{\hat{U}_z}$, $\circ \frac{\overline{U_r}}{\hat{U}_z}$, $\triangle \frac{\overline{U_z}}{\hat{U}_z}$; $\hat{U}_z$ = 12.2 m/s. 109

16 30° fixed vane swirl generator; y=-33 mm, z=5 mm; $\square \frac{u'_\theta}{\hat{U}_z}$, $\circ \frac{u'_r}{\hat{U}_z}$, $\triangle \frac{u'_z}{\hat{U}_z}$; $\hat{U}_z$ = 12.2 m/s. 110

17 30° fixed vane swirl generator; y=-33 mm, z=5 mm; $\square \frac{\overline{u_\theta u_z}}{\hat{U}_z^2}$, $\circ \frac{\overline{u_r u_z}}{\hat{U}_z^2}$, $\triangle \frac{\overline{u_r u_\theta}}{\hat{U}_z^2}$, $+ \frac{q^2}{\hat{U}_z^2}$; $\hat{U}_z$ = 12.2 m/s. 111

18 45° fixed vane swirl generator; $\theta = -90°$, z=10 mm; $\square \frac{\overline{U_\theta}}{\hat{U}_z}$, $\circ \frac{\overline{U_r}}{\hat{U}_z}$, $\triangle \frac{\overline{U_z}}{\hat{U}_z}$; $\hat{U}_z$ = 22.5 m/s. 112

19 45° fixed vane swirl generator; $\theta = -90°$, z=10 mm; $\square \frac{u'_\theta}{\hat{U}_z}$, $\circ \frac{u'_r}{\hat{U}_z}$, $\triangle \frac{u'_z}{\hat{U}_z}$; $\hat{U}_z$ = 22.5 m/s. 113

20 45° fixed vane swirl generator; $\theta = -90°$, z=10 mm; $\square \frac{\overline{u_\theta u_z}}{\hat{U}_z^2}$, $\circ \frac{\overline{u_r u_z}}{\hat{U}_z^2}$, $\triangle \frac{\overline{u_r u_\theta}}{\hat{U}_z^2}$, $+ \frac{q^2}{\hat{U}_z^2}$; $\hat{U}_z$ = 22.5 m/s. 114

21 45° fixed vane swirl generator; y=-33 mm, z=10 mm; $\square \frac{\overline{U_\theta}}{\hat{U}_z}$, $\circ \frac{\overline{U_r}}{\hat{U}_z}$, $\triangle \frac{\overline{U_z}}{\hat{U}_z}$; $\hat{U}_z$ = 22.5 m/s. 115

22 45° fixed vane swirl generator; y=-33 mm, z=10 mm; $\square \frac{\overline{u_\theta'}}{U_z}$, $\circ \frac{\overline{u_r'}}{U_z}$, $\triangle \frac{\overline{u_z'}}{U_z}$; $\hat{U}_z = 22.5$ m/s. 116

23 45° fixed vane swirl generator; y=-33 mm, z=10 mm; $\square \frac{\overline{u_\theta u_z}}{U_z^2}$, $\circ \frac{\overline{u_r u_z}}{U_z^2}$, $\triangle \frac{\overline{u_r u_\theta}}{U_z^2}$, $+ \frac{q^2}{U_z^2}$; $\hat{U}_z = 22.5$ m/s. 117

24 45° fixed vane swirl generator; $\theta = -90°$, z=9 mm; $\square \frac{\overline{U_\theta}}{U_z}$, $\circ \frac{\overline{U_r}}{U_z}$, $\triangle \frac{\overline{U_z}}{U_z}$; $\hat{U}_z$ = 13.5 m/s. 118

25 45° fixed vane swirl generator; $\theta = -90°$, z=9 mm; $\square \frac{\overline{u_\theta'}}{U_z}$, $\circ \frac{\overline{u_r'}}{U_z}$, $\triangle \frac{\overline{u_z'}}{U_z}$; $\hat{U}_z$ = 13.5 m/s. 119

26 45° fixed vane swirl generator; $\theta = -90°$, z=9 mm; $\square \frac{\overline{u_\theta u_z}}{U_z^2}$, $\circ \frac{\overline{u_r u_z}}{U_z^2}$, $\triangle \frac{\overline{u_r u_\theta}}{U_z^2}$, $+ \frac{q^2}{U_z^2}$; $\hat{U}_z = 13.5$ m/s. 120

27 45° fixed vane swirl generator; y=-33 mm, z=9 mm; $\square \frac{\overline{U_\theta}}{U_z}$, $\circ \frac{\overline{U_r}}{U_z}$, $\triangle \frac{\overline{U_z}}{U_z}$; $\hat{U}_z$ = 13.5 m/s. 121

28 45° fixed vane swirl generator; y=-33 mm, z=9 mm; $\square \frac{\overline{u_\theta'}}{U_z}$, $\circ \frac{\overline{u_r'}}{U_z}$, $\triangle \frac{\overline{u_z'}}{U_z}$; $\hat{U}_z$ = 13.5 m/s. 122

29 45° fixed vane swirl generator; y=-33 mm, z=9 mm; $\square \frac{\overline{u_\theta u_z}}{U_z^2}$, $\circ \frac{\overline{u_r u_z}}{U_z^2}$, $\triangle \frac{\overline{u_r u_\theta}}{U_z^2}$, $+ \frac{q^2}{U_z^2}$; $\hat{U}_z = 13.5$ m/s. 123

30 60° fixed vane swirl generator; $\theta = -90°$, z=6 mm; $\square \frac{\overline{U_\theta}}{U_z}$, $\circ \frac{\overline{U_r}}{U_z}$, $\triangle \frac{\overline{U_z}}{U_z}$; $\hat{U}_z$ = 10.9 m/s. 124

31 60° fixed vane swirl generator; $\theta = -90°$, z=6 mm; $\square \frac{\overline{u_\theta'}}{U_z}$, $\circ \frac{\overline{u_r'}}{U_z}$, $\triangle \frac{\overline{u_z'}}{U_z}$; $\hat{U}_z$ = 10.9 m/s. 125

32 60° fixed vane swirl generator; $\theta = -90°$, z=6 mm; $\square \frac{\overline{u_\theta u_z}}{\hat{U}_z^2}$, $\circ \frac{\overline{u_r u_z}}{\hat{U}_z^2}$, $\triangle \frac{\overline{u_r u_\theta}}{\hat{U}_z^2}$, $+ \frac{q^2}{\hat{U}_z^2}$; $\hat{U}_z$ = 10.9 m/s. 126

33 60° fixed vane swirl generator; y=-33 mm, z=6 mm; $\square \frac{\overline{U_\theta}}{\hat{U}_z}$, $\circ \frac{\overline{U_r}}{\hat{U}_z}$, $\triangle \frac{\overline{U_z}}{\hat{U}_z}$; $\hat{U}_z$ = 10.9 m/s. 127

34 60° fixed vane swirl generator; y=-33 mm, z=6 mm; $\square \frac{u'_\theta}{\hat{U}_z}$, $\circ \frac{u'_r}{\hat{U}_z}$, $\triangle \frac{u'_z}{\hat{U}_z}$; $\hat{U}_z$ = 10.9 m/s. 128

35 60° fixed vane swirl generator; y=-33 mm, z=6 mm; $\square \frac{\overline{u_\theta u_z}}{\hat{U}_z^2}$, $\circ \frac{\overline{u_r u_z}}{\hat{U}_z^2}$, $\triangle \frac{\overline{u_r u_\theta}}{\hat{U}_z^2}$, $+ \frac{q^2}{\hat{U}_z^2}$; $\hat{U}_z$ = 10.9 m/s. 129

36 IFRF variable swirl generator primary flow; $\theta = 90°$, z=2.5 mm; $\square \frac{\overline{U_\theta}}{\hat{U}_z}$, $\circ \frac{\overline{U_r}}{\hat{U}_z}$, $\triangle \frac{\overline{U_z}}{\hat{U}_z}$; $\hat{U}_z$ = 8.2 m/s. 130

37 IFRF variable swirl generator primary flow; $\theta = 90°$, z=2.5 mm; $\square \frac{u'_\theta}{\hat{U}_z}$, $\circ \frac{u'_r}{\hat{U}_z}$, $\triangle \frac{u'_z}{\hat{U}_z}$; $\hat{U}_z$ = 8.2 m/s. 131

38 IFRF variable swirl generator primary flow; $\theta = 90°$, z=2.5 mm; $\square \frac{\overline{u_\theta u_z}}{\hat{U}_z^2}$, $\circ \frac{\overline{u_r u_z}}{\hat{U}_z^2}$, $\triangle \frac{\overline{u_r u_\theta}}{\hat{U}_z^2}$, $+ \frac{q^2}{\hat{U}_z^2}$; $\hat{U}_z$ = 8.2 m/s. 132

39 IFRF variable swirl generator primary flow; $\theta = \pm 90°$, z=2.5 mm; $\square \frac{\overline{U_\theta}}{\hat{U}_z}$, $\circ \frac{\overline{U_r}}{\hat{U}_z}$, $\triangle \frac{\overline{U_z}}{\hat{U}_z}$; $\hat{U}_z$ = 6.6 m/s. Open symbols for $\theta = +90°$, solid symbols for $\theta = -90°$. 133

40 IFRF variable swirl generator primary flow; $\theta = \pm 90°$, z=2.5 mm; $\square \frac{u'_\theta}{\hat{U}_z}$, $\circ \frac{u'_r}{\hat{U}_z}$, $\triangle \frac{u'_z}{\hat{U}_z}$; $\hat{U}_z$ = 6.6 m/s. Open symbols for $\theta = +90°$, solid symbols for $\theta = -90°$. 134

41 IFRF variable swirl generator primary flow; $\theta = \pm 90°$, z=2.5 mm; $\square \frac{\overline{u_\theta u_z}}{\hat{U}_z^2}$, $\circ \frac{\overline{u_r u_z}}{\hat{U}_z^2}$, $\Delta \frac{\overline{u_r u_\theta}}{\hat{U}_z^2}$, $+ \frac{q^2}{\hat{U}_z^2}$; $\hat{U}_z = 6.6$ m/s. Open symbols for $\theta = +90°$, solid symbols for $\theta = -90°$. 135

42 IFRF variable swirl generator secondary flow; S=0.0, $\theta = 90°$, z=2.5 mm; $\square \frac{\overline{U_\theta}}{\hat{U}_z}$, $\circ \frac{\overline{U_r}}{\hat{U}_z}$, $\Delta \frac{\overline{U_z}}{\hat{U}_z}$; $\hat{U}_z = 14.4$ m/s. 136

43 IFRF variable swirl generator secondary flow; S=0.0, $\theta = 90°$, z=2.5 mm; $\square \frac{u'_\theta}{\hat{U}_z}$, $\circ \frac{u'_r}{\hat{U}_z}$, $\Delta \frac{u'_z}{\hat{U}_z}$; $\hat{U}_z = 14.4$ m/s. 137

44 IFRF variable swirl generator secondary flow; S=0.0, $\theta = 90°$, z=2.5 mm; $\square \frac{\overline{u_\theta u_z}}{\hat{U}_z^2}$, $\circ \frac{\overline{u_r u_z}}{\hat{U}_z^2}$, $\Delta \frac{\overline{u_r u_\theta}}{\hat{U}_z^2}$, $+ \frac{q^2}{\hat{U}_z^2}$; $\hat{U}_z = 14.4$ m/s. 138

45 IFRF variable swirl generator secondary flow; S=1.0, $\theta = 90°$, z=4.0 mm; $\square \frac{\overline{U_\theta}}{\hat{U}_z}$, $\circ \frac{\overline{U_r}}{\hat{U}_z}$, $\Delta \frac{\overline{U_z}}{\hat{U}_z}$; $\hat{U}_z = 11.9$ m/s. 139

46 IFRF variable swirl generator secondary flow; S=1.0, $\theta = 90°$, z=4.0 mm; $\square \frac{u'_\theta}{\hat{U}_z}$, $\circ \frac{u'_r}{\hat{U}_z}$, $\Delta \frac{u'_z}{\hat{U}_z}$; $\hat{U}_z = 11.9$ m/s. 140

47 IFRF variable swirl generator secondary flow; S=1.0, $\theta = 90°$, z=4.0 mm; $\square \frac{\overline{u_\theta u_z}}{\hat{U}_z^2}$, $\circ \frac{\overline{u_r u_z}}{\hat{U}_z^2}$, $\Delta \frac{\overline{u_r u_\theta}}{\hat{U}_z^2}$, $+ \frac{q^2}{\hat{U}_z^2}$; $\hat{U}_z = 11.9$ m/s. 141

48 IFRF variable swirl generator secondary flow; S=1.0, $\theta = 90°$, z=4.0 mm; $\square \frac{\overline{U_\theta}}{\hat{U}_z}$, $\circ \frac{\overline{U_r}}{\hat{U}_z}$, $\Delta \frac{\overline{U_z}}{\hat{U}_z}$; $\hat{U}_z = 7.2$ m/s. 142

49 IFRF variable swirl generator secondary flow; S=1.0, $\theta = 90°$, z=4.0 mm; $\square \frac{u'_\theta}{\hat{U}_z}$, $\circ \frac{u'_r}{\hat{U}_z}$, $\Delta \frac{u'_z}{\hat{U}_z}$; $\hat{U}_z = 7.2$ m/s. 143

50 IFRF variable swirl generator secondary flow; S=1.0, $\theta = 90°$, z=4.0 mm; $\square \frac{\overline{u_\theta u_z}}{\hat{U}_z^2}$, $\circ \frac{\overline{u_r u_z}}{\hat{U}_z^2}$, $\Delta \frac{\overline{u_r u_\theta}}{\hat{U}_z^2}$, $+ \frac{q^2}{\hat{U}_z^2}$; $\hat{U}_z = 7.2$ m/s. 144

51 IFRF variable swirl generator secondary flow; S=2.0, $\theta = 90$, z=2.0 mm; $\square \frac{\overline{U_\theta}}{\hat{U}_z}$, $\circ \frac{\overline{U_r}}{\hat{U}_z}$, $\Delta \frac{\overline{U_z}}{\hat{U}_z}$; $\hat{U}_z = 16.5$ m/s. 145

52 IFRF variable swirl generator secondary flow; S=2.0, $\theta = 90°$, z=2.0 mm; $\square \frac{u'_\theta}{\hat{U}_z}$, $\circ \frac{u'_r}{\hat{U}_z}$, $\Delta \frac{u'_z}{\hat{U}_z}$; $\hat{U}_z = 16.5$ m/s. 146

53 IFRF variable swirl generator secondary flow; S=2.0, $\theta = 90°$, z=2.0 mm; $\square \frac{\overline{u_\theta u_z}}{\hat{U}_z^2}$, $\circ \frac{\overline{u_r u_z}}{\hat{U}_z^2}$, $\Delta \frac{\overline{u_r u_\theta}}{\hat{U}_z^2}$, $+ \frac{q^2}{\hat{U}_z^2}$; $\hat{U}_z = 16.5$ m/s. 147

54 IFRF variable swirl generator secondary flow; S=2.0, $\theta = 90°$, z=2.0 mm; $\square \frac{\overline{U_\theta}}{\hat{U}_z}$, $\circ \frac{\overline{U_r}}{\hat{U}_z}$, $\Delta \frac{\overline{U_z}}{\hat{U}_z}$; $\hat{U}_z = 8.2$ m/s. 148

55 IFRF variable swirl generator secondary flow; S=2.0, $\theta = 90°$, z=2.0 mm; $\square \frac{u'_\theta}{\hat{U}_z}$, $\circ \frac{u'_r}{\hat{U}_z}$, $\Delta \frac{u'_z}{\hat{U}_z}$; $\hat{U}_z = 8.2$ m/s. 149

56 IFRF variable swirl generator secondary flow; S=2.0, $\theta = 90°$, z=2.0 mm; $\square \frac{\overline{u_\theta u_z}}{\hat{U}_z^2}$, $\circ \frac{\overline{u_r u_z}}{\hat{U}_z^2}$, $\Delta \frac{\overline{u_r u_\theta}}{\hat{U}_z^2}$, $+ \frac{q^2}{\hat{U}_z^2}$; $\hat{U}_z = 8.2$ m/s. 150

57 IFRF variable swirl generator secondary flow; S=3.0, $\theta = 90°$, z=2.0 mm; $\square \frac{\overline{U_\theta}}{\hat{U}_z}$, $\circ \frac{\overline{U_r}}{\hat{U}_z}$, $\Delta \frac{\overline{U_z}}{\hat{U}_z}$; $\hat{U}_z = 15.9$ m/s. 151

58 IFRF variable swirl generator secondary flow; S=3.0, $\theta = 90°$, z=2.0 mm; $\square \frac{u'_\theta}{\hat{U}_z}$, $\circ \frac{u'_r}{\hat{U}_z}$, $\Delta \frac{u'_z}{\hat{U}_z}$; $\hat{U}_z = 15.9$ m/s. 152

59 IFRF variable swirl generator secondary flow; S=3.0, $\theta = 90°$, z=2.0 mm; $\square \frac{\overline{u_\theta u_z}}{\hat{U}_z^2}$, $\circ \frac{\overline{u_r u_z}}{\hat{U}_z^2}$, $\Delta \frac{\overline{u_r u_\theta}}{\hat{U}_z^2}$, $+ \frac{q^2}{\hat{U}_z^2}$; $\hat{U}_z = 15.9$ m/s. 153

60 IFRF variable swirl generator secondary flow; S=3.0, $\theta = 90°$, z=2.0 mm; $\square \frac{\overline{U_\theta}}{\hat{U}_z}$, $\circ \frac{\overline{U_r}}{\hat{U}_z}$, $\Delta \frac{\overline{U_z}}{\hat{U}_z}$; $\hat{U}_z = 7.9$ m/s. 154

61 IFRF variable swirl generator secondary flow; S=3.0, $\theta = 90°$, z=2.0 mm; $\square \frac{\overline{u_\theta'}}{\hat{U}_z}$, $\circ \frac{\overline{u_r'}}{\hat{U}_z}$, $\Delta \frac{\overline{u_z'}}{\hat{U}_z}$; $\hat{U}_z = 7.9$ m/s. 155

62 IFRF variable swirl generator secondary flow; S=3.0, $\theta = 90°$, z=2.0 mm; $\square \frac{\overline{u_\theta u_z}}{\hat{U}_z^2}$, $\circ \frac{\overline{u_r u_z}}{\hat{U}_z^2}$, $\Delta \frac{\overline{u_r u_\theta}}{\hat{U}_z^2}$, $+ \frac{q^2}{\hat{U}_z^2}$; $\hat{U}_z = 7.9$ m/s. 156

63 IFRF variable swirl generator secondary flow; S=4.0, $\theta = 90°$, z=2.0 mm; $\square \frac{\overline{U_\theta}}{\hat{U}_z}$, $\circ \frac{\overline{U_r}}{\hat{U}_z}$, $\Delta \frac{\overline{U_z}}{\hat{U}_z}$; $\hat{U}_z$ =19.6 m/s. 157

64 IFRF variable swirl generator secondary flow; S=4.0, $\theta = 90°$, z=2.0 mm; $\square \frac{\overline{u_\theta'}}{\hat{U}_z}$, $\circ \frac{\overline{u_r'}}{\hat{U}_z}$, $\Delta \frac{\overline{u_z'}}{\hat{U}_z}$; $\hat{U}_z$ =19.6 m/s. 158

65 IFRF variable swirl generator secondary flow; S=4.0, $\theta = 90°$, z=2.0 mm; $\square \frac{\overline{u_\theta u_z}}{\hat{U}_z^2}$, $\circ \frac{\overline{u_r u_z}}{\hat{U}_z^2}$, $\Delta \frac{\overline{u_r u_\theta}}{\hat{U}_z^2}$, $+ \frac{q^2}{\hat{U}_z^2}$; $\hat{U}_z$ =19.6 m/s. 159

66 IFRF variable swirl generator secondary flow; S=4.0, $\theta = 90°$, z=2.0 mm; $\square \frac{\overline{U_\theta}}{\hat{U}_z}$, $\circ \frac{\overline{U_r}}{\hat{U}_z}$, $\Delta \frac{\overline{U_z}}{\hat{U}_z}$; $\hat{U}_z$ =7.5 m/s. 160

67 IFRF variable swirl generator secondary flow; S=4.0, $\theta = 90°$, z=2.0 mm; $\square \frac{\overline{u_\theta'}}{\hat{U}_z}$, $\circ \frac{\overline{u_r'}}{\hat{U}_z}$, $\Delta \frac{\overline{u_z'}}{\hat{U}_z}$; $\hat{U}_z = 7.5$ m/s. 161

68 IFRF variable swirl generator secondary flow; S=4.0, $\theta = 90°$, z=2.0 mm; $\square \frac{\overline{u_\theta u_z}}{\hat{U}_z^2}$, $\circ \frac{\overline{u_r u_z}}{\hat{U}_z^2}$, $\Delta \frac{\overline{u_r u_\theta}}{\hat{U}_z^2}$, $+ \frac{q^2}{\hat{U}_z^2}$; $\hat{U}_z = 7.5$ m/s. 162

69 IFRF variable swirl generator secondary flow; S=4.5, $\theta = 90°$, z=4.0 mm; $\square \frac{\overline{U_\theta}}{\hat{U}_z}$, $\circ \frac{\overline{U_r}}{\hat{U}_z}$, $\Delta \frac{\overline{U_z}}{\hat{U}_z}$; $\hat{U}_z$ =17.4 m/s. 163

70 IFRF variable swirl generator secondary flow; S=4.5, $\theta = 90°$, z=4.0 mm; $\square \frac{\overline{u_\theta'}}{\hat{U}_z}$, $\circ \frac{\overline{u_r'}}{\hat{U}_z}$, $\Delta \frac{\overline{u_z'}}{\hat{U}_z}$; $\hat{U}_z = 17.4$ m/s. 164

71 IFRF variable swirl generator secondary flow; S=4.5, $\theta = 90°$, z=4.0 mm; $\square \frac{\overline{u_\theta u_z}}{\hat{U}_z^2}$, $\circ \frac{\overline{u_r u_z}}{\hat{U}_z^2}$, $\Delta \frac{\overline{u_r u_\theta}}{\hat{U}_z^2}$, $+ \frac{q^2}{\hat{U}_z^2}$; $\hat{U}_z$ =17.4 m/s. 165

72 IFRF variable swirl generator secondary flow; S=4.5, $\theta = 90°$, z=4.0 mm; $\square \frac{\overline{U_\theta}}{\hat{U}_z}$, $\circ \frac{\overline{U_r}}{\hat{U}_z}$, $\Delta \frac{\overline{U_z}}{\hat{U}_z}$; $\hat{U}_z = 8.3$ m/s. 166

73 IFRF variable swirl generator secondary flow; S=4.5, $\theta = 90°$, z=4.0 mm; $\square \frac{u'_\theta}{\hat{U}_z}$, $\circ \frac{u'_r}{\hat{U}_z}$, $\Delta \frac{u'_z}{\hat{U}_z}$; $\hat{U}_z = 8.3$ m/s. 167

74 IFRF variable swirl generator secondary flow; S=4.5, $\theta = 90°$, z=4.0 mm; $\square \frac{\overline{u_\theta u_z}}{\hat{U}_z^2}$, $\circ \frac{\overline{u_r u_z}}{\hat{U}_z^2}$, $\Delta \frac{\overline{u_r u_\theta}}{\hat{U}_z^2}$, $+ \frac{q^2}{\hat{U}_z^2}$; $\hat{U}_z = 8.3$ m/s. 168

1 Introduction

The CANMET/Combustion and Carbonization Research Laboratory (CCRL) tunnel furnace facility is used to test various coal based fuels. A computational model has been developed [1], which incorporates conservation laws and models of turbulence and combustion with the purpose to improve the understanding of the performance of these fuels and to allow prediction of the tunnel operation within ranges of the various flow and fuel parameters. The execution of this computational program requires as input the mean velocity and turbulence statistics at the entrance to the furnace. Measurements of the mean velocity field have already been conducted using a five hole probe [1], however no turbulence measurements have so far been available.

The objective of the present experimental study is to provide measurements of the mean velocity and turbulence stresses at the burner exit. Three fixed and one variable swirl generators were studied for various degrees of swirl and two different mass flowrates. The results can serve as a guide in the evaluation and possible redesign of the swirl generators as well as assist in the computational studies.

2 Experimental Facility

All experiments were performed at the Combustion and Carbonization Research Laboratory.

To make the flow more accessible to the measuring probes, the swirl generators were disconnected from the furnace and set up separately on supports. The swirling

(secondary) flow was provided by a blower, while the central (primary) flow was provided by a compressed air supply. The flowrate of the secondary stream was measured by an orifice plate meter, while that of the primary stream was measured by two rotameters in parallel.

Three fixed vane swirl generators were used, with vane angles of $30°, 45°$ and $60°$. Their dimensions and connection to the air supply system are shown in Figure 1.

The variable swirl generator and its air supply system are sketched in Figure 2. The original primary flow diffuser was found to produce a highly unsteady, separating flow and was therefore replaced by a new diffuser with an expansion angle of $6°$, which resulted in an improved air stream.

The primary air supply was relatively unstable. Because sudden velocity jumps of as much as 1 m/s occured ocasionally, measurements which were known to be affected by such jumps were discarded. Slow drifts in the air supply were also observed, but these were recorded and the data corrected accordingly. The primary temperature was monitored by a thermocouple, located in the primary supply line upstream of the rotameters. The reading of this thermocouple differed by less than $1K$ from the reading of a mercury thermometer located in the primary flow at the burner exit. The primary flowrate was estimated by integrating the axial component of mean velocity, $\widehat{U}_z$, across the exit plane of the burner.

The secondary air stream approached a stable flowrate and temperature after an one hour warm up period. The temperature of this stream was monitored by a a thermocouple, located near the upstream side of the orifice plate in the secondary supply

line. The temperature indicated by this thermocouple was checked against the reading of a mercury thermometer placed in the secondary flow at the burner exit, and was found to differ from that reading by less than $1K$. The secondary flowrate was estimated by integrating the axial component of mean velocity across the exit plane of the burner.

3 Instrumentation and Experimental Procedure

All measurements were taken using conventional hot wire anemometry. A TSI model 1241 cross wire array with wires .005 mm in diameter and 3 mm long was operated by constant temperature bridges (TSI model 1050a). The wires were heated to a temperature of about 463 K.

The electrical signals from the hot wire anemometers were offset by 3.5 V, low pass filtered to 10kHz and amplified by a factor of 5. The resulting rms signals were typically 100 mV. The conditioned signals were digitized simultaneously with a 12 bit A/D converter at a rate of 1 kHz for the velocity measurements and 8 kHz for the integral length scale measurements. Continuous digitized records of 40 000 points for each channel were stored on magnetic tape.

The hot-wire cooling was assumed to be sensitive only to normal velocity components [2]. The cross wire probes were calibrated with the probe axis aligned with the axial direction of the primary stream. The interference effects of the prongs and the thermal wakes of one wire on the other were kept low by maintaining, when possible, the angle between the probe axis and the mean flow direction to less than 20°. The direction of the mean velocity in the present swirling flows varied considerably and in some cases was

inclined by as much as 60° with respect to the mean axial direction. By mounting the probe such that the center of the measuring volume was on the vertical axis of rotation (see Figure 3) it was possible to roughly align its axis with the flow for all measurments. The probe-oriented and burner-oriented coordinate systems are defined in Figure 4.

The hot wires were calibrated versus pitot tube measurements by positioning each instrument along the axis of the primary stream of the corresponding burner. The turbulence intensity on the axis of the primary stream for the fixed vane swirl generator was acceptably low (about 3%). Because the high turbulence intensity of the primary stream of the variable swirl generator was very high (up to 40%) a piece of pipe with 19 mm diameter was inserted into the throat of the diffuser for the calibration and removed after calibration; the resulting flow also had a low turbulence intensity (about 3%). The pitot tube and hot wires were placed in the flow separately to reduce blockage and interference effects. Typical calibration curves for hot wires are shown in Figure 5. The anemometer bridge voltage was correlated with the air velocity by using a modified form of King's Law [2]

$$\tilde{E}_1^2 = A_1 + B_1 \tilde{U}_{eff1}^{n_1} \tag{1}$$

$$\tilde{E}_2^2 = A_2 + B_2 \tilde{U}_{eff2}^{n_2} \tag{2}$$

where the subscripts 1 and 2 refer to the two wires of the cross wire array and U_{eff} is the effective cooling velocity. The coefficients A, B and n for each wire were found by using least squares fitting techniques.

At each measuring position, two sets of measurements were taken, with the wires positioned succesively parallel to the horizontal and to a vertical plane. This was achieved

by rolling the probe about its axis by 90°. For the present cross-wire configuration with wires inclined by ±45° with respect to the probe axis, the effective cooling velocities are related to the velocity components in the probe oriented frame by

$$\tilde{U}_b = \frac{1}{2}(\tilde{U}_{eff1} + \tilde{U}_{eff2})/\cos\frac{\pi}{4} \quad (3)$$

$$\tilde{U}_n = \frac{1}{2}(\tilde{U}_{eff1} - \tilde{U}_{eff2})/\cos\frac{\pi}{4} \quad (4)$$

when the hot wires are in the n, b (horizontal) plane and

$$\tilde{U}_b = \frac{1}{2}(\tilde{U}_{eff1} + \tilde{U}_{eff2})/\cos\frac{\pi}{4} \quad (5)$$

$$\tilde{U}_y = \frac{1}{2}(\tilde{U}_{eff1} - \tilde{U}_{eff2})/\cos\frac{\pi}{4} \quad (6)$$

when the hot wires are in the y, b (vertical) plane.

The resulting simultaneous records of $\tilde{U}_b$ and $\tilde{U}_n$ and the simultaneous records of $\tilde{U}_b$ and $\tilde{U}_y$ were analyzed to provide the mean velocities U_b, U_n and U_y and the turbulence stresses $\overline{u_b u_n}$, $\overline{u_b u_y}$, $\overline{u_b^2}$, $\overline{u_n^2}$ and $\overline{u_y^2}$ (the term stress will be used loosely to designate velocity variances and covariances). Because the components $\tilde{U}_n$ and $\tilde{U}_y$ could not be measured simultaneously, the stress $\overline{u_n u_y}$ could not be calculated. The above mean velocities and stresses were then transformed to the cartesian, burner-oriented coordinate system (Figure 4) using the relations

$$U_x = U_n \cos\phi + U_b \sin\phi \quad (7)$$

$$U_y = U_y \quad (8)$$

$$U_z = U_b \cos\phi - U_n \sin\phi \quad (9)$$

$$\overline{u_x^2} = \overline{u_n^2}\cos^2\phi + \overline{u_b^2}\sin^2\phi + 2\overline{u_n u_b}\cos\phi\sin\phi \quad (10)$$

$$\overline{u_y^2} = \overline{u_y^2} \quad (11)$$

$$\overline{u_x^2} = \overline{u_b^2}\cos^2\phi + \overline{u_n^2}\sin^2\phi - 2\overline{u_n u_b}\cos\phi\sin\phi \tag{12}$$

$$\overline{u_x u_z} = \overline{u_n u_b}\cos^2\phi - \overline{u_n u_b}\sin^2\phi + \overline{u_b^2}\cos\phi\sin\phi - \overline{u_n^2}\cos\phi\sin\phi \tag{13}$$

$$\overline{u_x u_y} = \overline{u_b u_y}\cos\phi - \overline{u_n u_y}\sin\phi \tag{14}$$

$$\overline{u_x u_y} = \overline{u_n u_y}\cos\phi + \overline{u_b u_y}\sin\phi \tag{15}$$

The stress $\overline{u_x u_z}$ could be evaluated directly from the measurements. However, because the stress $\overline{u_n u_y}$ could not be measured, it would not be possible to calculate the stresses $\overline{u_x u_y}$ and $\overline{u_z u_y}$ without further assumptions. Finally, the mean velocities and stresses were transformed to the cylindrical coordinate sytem shown in Figure 4, using the relations

$$U_r = U_x\cos\theta + U_y\sin\theta \tag{16}$$

$$U_\theta = U_y\cos\theta - U_x\sin\theta \tag{17}$$

$$U_z = U_z \tag{18}$$

$$\overline{u_r^2} = \overline{u_x^2}\cos^2\theta + \overline{u_y^2}\sin^2\theta + 2\overline{u_x u_y}\cos\theta\sin\theta \tag{19}$$

$$\overline{u_z^2} = \overline{u_z^2} \tag{20}$$

$$\overline{u_\theta^2} = \overline{u_y^2}\cos^2\theta + \overline{u_x^2}\sin^2\theta - 2\overline{u_x u_y}\cos\theta\sin\theta \tag{21}$$

$$\overline{u_r u_\theta} = \overline{u_x u_y}\cos^2\theta - \overline{u_x u_y}\sin^2\theta - \overline{u_x^2}\cos\theta\sin\theta + \overline{u_y^2}\cos\theta\sin\theta \tag{22}$$

$$\overline{u_r u_z} = \overline{u_x u_z}\cos\theta + \overline{u_y u_z}\sin\theta \tag{23}$$

$$\overline{u_\theta u_z} = \overline{u_z u_y}\cos\theta - \overline{u_x u_z}\sin\theta \tag{24}$$

In general, the stresses in cylindrical coordinates cannot be calculated without the stresses $\overline{u_x u_y}$ and $\overline{u_z u_y}$. However, in the present study most measurements were taken along the vertical axes of the burners where $\theta = \pm 90°$. In these cases equations (19) to

(24) reduce to

$$\overline{u_r^2} = \overline{u_y^2} \tag{25}$$

$$\overline{u_x^2} = \overline{u_z^2} \tag{26}$$

$$\overline{u_\theta^2} = \overline{u_x^2} \tag{27}$$

$$\overline{u_r u_\theta} = -\overline{u_x u_y} \tag{28}$$

$$\overline{u_r u_x} = \pm\overline{u_x u_y} \tag{29}$$

$$\overline{u_x u_\theta} = \pm\overline{u_x u_x} \tag{30}$$

Under this condition the stresses $\overline{u_r^2}$, $\overline{u_x^2}$, $\overline{u_\theta^2}$ and $\overline{u_\theta u_x}$ can be calculated directly, but the other stresses cannot. The sum of the normal stresses is the same in all the coordinate systems and is denoted by q^2.

On the other hand, it is possible to calculate approximately all the stresses in all the coordinate systems when the stress $\overline{u_n u_y}$ is small compared to $\overline{u_b u_y}$ and $\overline{u_b u_n}$. To examine this possibility consider the flow in the probe-oriented system, such that the velocity vector is nearly parallel to the b direction. In such a case the stress $\overline{u_n u_y}$ might be approximated by a gradient transport model as

$$\overline{u_n u_y} = -\nu_T\left(\frac{\partial U_n}{\partial y} + \frac{\partial U_y}{\partial n}\right) \tag{31}$$

where ν_T is the isotropic eddy viscosity [4]. For a flow exactly parallel to the b axis, the velocities U_n and U_y and their gradients are zero and hence the stress $\overline{u_n u_y}$ is zero. The validity of this assumption will be evaluated in Section 4.1.

The temperature of either the primary or secondary flows differed from the temperature of the air used for calibration by up to $30K$. The mean velocity was corrected to

first order using the relation [2]

$$\frac{U - U_i}{U_i} = \frac{1}{n}\left(\frac{A}{BU_i^n} + 1\right)\left(\frac{T - T_c}{T_w - T_c}\right) \tag{32}$$

where U_i is the indicated velocity, T is the mean flow temperature, T_c is the calibration temperature and T_w is the temperature of the hot wire. The turbulence stresses were not corrected for temperature variation effects. Such effects are not expected to be substantial in most cases, because the main sensitivity of turbulence parameters is not on mean temperature but on the temperature fluctuations [2] and such fluctuations were mainly confined to the mixing layers of the two streams.

4 Measurements

4.1 General Description

The experimental conditions for the different sets of measurements and a directory of the related tables and figures are presented in in Tables 1 and 2.

At the burner exit plane, the primary and secondary streams are essentially independent. In the case of the IFRF swirl generator, it was possible to position the probe within 2 mm of the exit plane and the two streams were studied seperately. In the case of the fixed vane swirl generators, it was impossible to place the probe any closer than 6 mm to the exit plane without risking damage to the delicate hot wires. At this distance there may be some interaction of the two streams and for this reason both primary and secondary flows were measured for each case.

The uncorrected data in the probe oriented system are provided in Tables 3 to 20.

In most cases the mean flow was at a small angle to the probe axis (this is indicated by the fact that the velocity components normal to the probe axis were small compared to the component parallel to the probe axis).

The measured values of U_n and U_y are generally less than 15% of U_b and the gradients $\frac{\partial U_n}{\partial y}$ and $\frac{\partial U_y}{\partial n}$ are small compared to $\frac{\partial U_b}{\partial n}$ or $\frac{\partial U_b}{\partial y}$. On this basis it is reasonable to assume that the stress $\overline{u_n u_y}$ is small in comparison with $\overline{u_b u_n}$ or $\overline{u_b u_y}$. The stresses have been transformed to cylindrical cooordinates for presentation under the assumption that $\overline{u_n u_y} = 0$.

The radius weighted average velocity is defined as

$$\widehat{U_z} = \frac{\Sigma_i U_{zi} r_i}{\Sigma_i r_i} \tag{33}$$

where the subscript i indicates the measurements at different radial positions, r_i. For axisymmetric flows this quantity would be equal to the bulk velocity.

The data were analyzed to determine the three components of mean velocity, the six components of the turbulence stress tensor and the turbulent length scales. The velocity statistics are presented in three forms: a) tables (Tables 21, 23, 25, 27, 29, 31, 33, 35, 37, 39, 41, 43, 45, 47, 49, 51, 53 and 55) in S.I. units b) tables (Tables 22, 24, 26, 28, 30, 32, 34, 36, 38, 40, 42, 44, 46, 48, 50, 52, 54 and 56) where the velocities have been normalized with the radius weighted average velocity, corresponding to either the primary or the secondary flow region c) plots of mean velocity (Figures 6, 9, 12, 15, 18, 21, 24, 27, 30, 33, 36, 39, 42, 45, 48, 51, 54, 57, 60, 63, 66, 69 and 72), rms velocity (Figures 7, 10, 13, 16, 19, 22, 25, 28, 31, 34, 37, 40, 43, 46, 49, 52, 55, 58, 61, 64, 67, 70 and 73) shear stress and turbulent kinetic energy (Figures 8, 11, 14, 17, 20, 23, 26, 29,

32, 35, 38, 41, 44, 47, 50, 51, 56, 59, 62, 65, 68, 71 and 74) where all values have been normalized with the radius weighted average velocity over the entire region covered by the plot. Attention is drawn to the fact that, i) for the fixed vane swirl generators plots cover both primary and secondary flows; hence, quantities in these plots are normalized by velocity different from the value used in the tables, where quantities are normalized with respect to either the average primary or average secondary velocity, depending on whether the point is in the primary or secondary flow as defined below, ii) for the IFRF swirl generator the primary and secondary flows are plotted seperately; therefore, the radius weighted average velocity in these plots is the same as in the corresponding tables. An example of how these results can be used to estimate velocity components etc. at mass flow rates different from the present ones is included in section 4.3.

The streamwise integral time scale, defined by [2]

$$T_{bb} = \int_0^{\tau_o} \frac{\overline{u_b(0)u_b(\tau)}}{\overline{u_b^2}} d\tau \tag{34}$$

(35)

where τ is the time difference beween two measurements of velocity and τ_o is the first zero of the corresponding correlation, was measured at selected positions for each configuration at a relatively low flow rate (note that the digitizing rate of the data acquisition system did not permit the measurement of scales at high flow rates. The corresponding streamwise integral length scale was estimated using Taylor's "frozen flow" approximation [2], as

$$L_{bb} = U_b T_{bb} \tag{36}$$

(37)

These results are shown in Table 57. Because integral length scales are mainly a function of the geometrical shape and dimensions of the apparatus, they are not expected to change substantially as the flow rate changes.

4.2 Sources of Errors

The main sources of error in the present measurements are likely due to:

1. large turbulence intensities, which imply that the instantaneous velocity could be at a large angle to the probe axis and may occasionally be reversed; in such cases the mean velocity and the turbulence stresses would generally be overestimated.
2. the relatively large size of the probe, especially compared to the size of the fixed vane swirl generators. This effect will lead to spatial averaging of the flow statistics as well as cause possible flow distortion.

Where the turbulence intensity is less than 20%, the errors in the measurements of mean velocity are estimated to be less than 5% and those in the turbulence stresses less than 20%. Measurements indicating turbulence intensity higher than 20% should be used with reservation and for qualitative comparisons only.

4.3 Scaling of the Results

Properly nondimensionalized variables are expected to approach asymptotically constant values at large Reynolds numbers. The velocity statistics can be nondimensionalized using a reference velocity such as the radius weighted average axial mean velocity,

$\hat{U}_z$, at the exit of the burner. $\hat{U}_z$ is ideally related to the mass flow rate by $\dot{m} = \rho \hat{U}_z A$.

The present velocity measurements can be scaled by the mass flow rate to provide estimates of the various quantities at different flow rates. For example, let us estimate the mean axial velocity component in the secondary flow of the 30° fixed vane swirl generator, at the position with $\phi = -90°$ and $r = 27$ mm, at a secondary mass flow rate of $\dot{m} = 300$ kg/hr. Disregarding variations in air density and using Table 1, one finds that the equivalent radius weighted average velocity in the secondary flow is

$$\hat{U}_z = 22.7 \times (300/236) = 28.9 m/s \tag{38}$$

From Table 5, at the position of interest, one finds that

$$U_z/\hat{U}_z = 1.38 \tag{39}$$

Therefore, the estimated value of the mean axial velocity is

$$U_z = 1.38 \times 28.9 = 39.9 m/s \tag{40}$$

The integral length scales can be nondimensionalized by a dimension of the burner geometry, such as the primary diameter or the width of the secondary flow annulus.

4.4 The Fixed Vane Swirl Generators

Measurements for the fixed vane swirl generator were made along a radial line at $\theta = -90°$ with a 3 mm radial spacing. Due to the presence of the wakes of the guide vanes the flow is not axisymetric, although it should be roughly periodic. To provide additional information about the spatial variation of the measured quantities, a horizontal traverse

(y=0.0) was made along a line 33 mm away from the centre (see Figures 9, 10, 11, 15, 16, 17, 21, 22, 23, 27, 28, 29, 33, 34 and 35).

The plots of q^2 show a very high turbulence intensity in the mixing region between the primary and secondary flow, which suggests that this may be a region of recirculation. Therefore, the measurements in this region could be excessively inaccurate and should be at most used as qualitative information. For purposes of calculating the radius weighted average velocities for the primary and secondary streams, the primary flow is defined as ranging from r= 0 to 12 mm and the secondary flow from r=21 to 42 mm. This excludes the mixing region between the primary and secondary streams.

4.4.1 The Primary Flow

The primary flow is typical of fully developed pipe flow with a unidirectional mean velocity and a turbulence intensity between 3% and 5% in the core region. The turbulence and mean velocity profiles at different flow rates scale well with $\hat{U}_z$.

4.4.2 The Secondary Flow

The mean velocity direction for the 30° and 45° swirl generators was roughly tangential to the guide vanes. The velocity statistics at different flow rates scale well with $\hat{U}_z$ for the 30° swirl generator and less well for the 45° swirl generator.

The flow direction for the 60° swirl generator was surveyed visually using tufts before any hot wire measurements were made. This indicated that the secondary flow at the exit was nearly parallel to the face of the burner. As a result the secondary flow did

not seem to interact with the primary flow and an essentially stagnant region developed between the primary and secondary flows. The hot wire measurements also show a very strong radial flow component, consistent with the results of the flow visualization. In view of this abnormality, measurements of the flow from the 60° swirl generator were not pursued.

4.5 The IFRF Swirl Generator

Measurements for the variable swirl generator were made along a radial line at $\theta = 90°$ with a 5 mm radial spacing in all cases with the exception of the primary flow with $\Re = 39000$, where a full vertical traverse was made to evaluate the flow symmetry.

4.5.1 The Primary Flow

The mean velocity was essentially in the axial direction, although somewhat asymmetric (Figure 39). The local turbulence intensity was as high as 40% near the outer edge of the flow, which confirms the presence of recirculation previously detected using flow visualization. As a result, the mean velocity would be overestimated in these regions. The velocity statistics appear to scale well with $\hat{U}_s$.

4.5.2 The Secondary Flow

The mean velocity profiles scale well with $\hat{U}_s$ for all swirl settings. The turbulence scales well for swirl settings of 1,2,and 3, but for swirl settings of 4 and 4.5 there is an appreciable increase in turbulence level with $\Re$. There is also a trend of increasing

turbulence level with increasing swirl setting.

5 Using the Measurements in Turbulence Models

Because one of the main purposes of the present experiments is to assist in the computation of the furnace flow characteristics, it was considered appropriate to include in this report some guiding comments concerning the applicability of these measurements as input to turbulence models. The discussion will focus upon the standard, two-equation $k-\epsilon$ model [4], which is widely used in computational codes and has already been included in attempts to model the present flow. This model utilizes two differential equations, one for the turbulent kinetic energy per unit mass, k, and another for the kinetic energy dissipation rate, ϵ. The various terms in these equations are modelled in terms of the mean velocity field and contain a number of empirical constants, whose values have been based on experimental results in relatively "simple" flows.

The parameter k can be evaluated directly from the present measurements as $k = \frac{1}{2}q^2$. Its accuracy should be reasonably high, except perhaps in the mixing regions of the primary and secondary streams and near the wall of the primary stream of the variable swirl generator. The parameter ϵ has not been measured, because it involves extremely tedious measurements of mean squared spatial velocity derivatives in different directions. Alternatively, ϵ can be estimated as follows a) From the balance of all other terms in the turbulent kinetic energy equations; strong inhomogeneity and lack of measurements of various terms yield this approach impractical in the present case. b) From measurements of the mean squared temporal derivative of the streamwise velocity by assuming validity

of Taylor's approximation (i.e. proportionality of streamwise and temporal derivatives) and local isotropy (i.e. directional independence of the fine structure) of the flow. Although attemped, such measurements would be highly inaccurate in the present flow, due to the large size of the probe and the inadequate sampling rate capabilities of the data acquisition system. c) from the empirical relation

$$\epsilon = q^3/L_\epsilon \tag{41}$$

where L_ϵ is the dissipation length scale [3]. L_ϵ should be proportional to the presently measured integral length scales L_{bb}. As a rough estimate [3], one could use the relationship

$$L_\epsilon \approx 3L_{bb} \tag{42}$$

Such estimates of the dissipation have been included in Table 57.

The $k-\epsilon$ model utilizes the concept of an isotropic eddy viscosity, ν_T. This quantity could be estimated from direct measurements of shear stress and mean shear at regions of strongly sheared flow. For example,

$$\nu_T \approx \frac{-\overline{u_r u_z}}{\frac{\partial U_z}{\partial r}} \tag{43}$$

in regions where both terms on the right hand side are relatively large and where the mean shear is expected to be in the radial direction. Alternatively, ν_T could be estimated from the empirical relation [4]

$$\nu_T \approx 0.09 k^{\frac{1}{2}} L_\epsilon \tag{44}$$

Estimates based on equation (41) have also been included in Table 57.

6 Conclusions

1. By orienting a cross-wire probe such that its axis would be roughly aligned with the mean flow direction it has been possible to measure all the mean velocity components and the dominent turbulence stresses in the swirling flow at the exit of various swirl generators.

2. In the range of Reynolds number covered by the present experiments the mean velocity profiles and turbulence stresses can be scaled by the mass flowrate.

3. Typical esimates of quantities used in simple turbulence models have been based upon measurements as well as simplifying assumptions.

References

[1] P. J. Hughes. (1988) *A data package for the validation of a computer model of the tunnel furnace facility*, Energy Research Laboratories, CANMET REPORT 87-4E.

[2] S. Tavoularis (1986) *Encyclopedia of Fluid Mechanics, Vol. 1, Chapter 36: Techniques for turbulence measurement*, N. P. Cheremisinoff (editor),Gulf Publishing Company, Houston.

[3] A. A. Townsend (1976) *The Structure of Turbulent Shear Flow*, Second Edition, Cambridge University Press, Cambridge.

[4] W. Rodi, *Turbulence Models and their Application in Hydraulics*, Intern. Assoc. for Hydr. Research, Delft.

vane angle	primary			secondary			tables	figures
	$\widehat{U_z}$ (m/s)	$\Re$	$\dot{m}$ (kg/hr)	$\widehat{U_z}$ (m/s)	$\Re$	$\dot{m}$ (kg/hr)		
30°	31.4	53 000	57.2	22.7	26 000	236.	3,21,22	6 to 11
	15.2	26 000	27.7	12.1	14 000	126.	4,23,24	12 to 17
45°	28.9	49 000	52.7	21.0	24 000	218.	5,25,26	18 to 23
	19.3	33 000	35.2	13.2	15 000	137.	6,27,28	24 to 29
60°	—	—	—	—	—	—	—	—
	15.4	26 000	28.1	10.9	12 000	113.	7,29,30	30 to 35

Table 1: The experimental conditions for the fixed vane swirl generators

Stream	S	$\widehat{U_z}$(m/s)	$\Re$	$\dot{m}$ (kg/hr)	tables	figures
primary	n.a.	8.2	47 000	183	8,31,32	36,37,38
		6.6	39 000	147	9,33,34	39,40,41
secondary	0.0	14.3	41 000	935	10,35,36	42,43,44
		—	—	—		
secondary	1.0	11.9	34 000	778	11,37,38	45,46,47
		7.2	21 000	471	12,39,40	48,49,50
secondary	2.0	16.4	47 000	1070	13,41,42	51,52,53
		8.2	24 000	538	14,43,44	54,55,56
secondary	3.0	15.1	43 000	987	15,45,46	57,58,59
		7.9	23 000	516	16,47,48	60,61,62
secondary	4.0	19.6	56 000	1280	17,49,50	63,64,65
		7.5	22 000	490	18,51,52	66,67,68
secondary	4.5	17.4	50 000	1140	19,53,54	69,70,71
		8.3	24 000	545	20,55,56	72,73,74

Table 2: The experimental conditions for the IFRF swirl generator

x (mm)	y (mm)	$T_a(°C)$	plane	ϕ (deg)	U_b (m/s)	U_+(m/s)	u'_b (m/s)	u'_+ (m/s)	$\overline{u_b u_+}(m^2/s^2)$
0.0	0.0	17.6	zy	0.0	33.56	-0.85	1.06	0.69	-0.01436
0.0	-3.0	17.5	zy	0.0	33.43	-1.21	1.17	0.74	-0.20844
0.0	-6.0	17.4	zy	0.0	32.17	-1.57	1.61	0.87	-0.55632
0.0	-9.0	17.3	zy	0.0	29.71	-2.10	2.08	1.11	-0.89960
0.0	-12.0	17.3	zy	0.0	25.35	-3.29	2.66	1.77	-1.14300
0.0	-15.0	17.3	zy	0.0	13.72	-1.39	3.40	2.33	-2.52591
0.0	-18.0	17.2	zy	0.0	18.82	2.14	6.12	2.14	-0.75570
0.0	-21.0	17.2	zy	30.0	22.02	5.15	4.12	3.89	11.41039
0.0	-24.0	17.2	zy	30.0	35.41	3.80	2.13	1.54	-1.53624
0.0	-27.0	17.2	zy	30.0	33.79	2.31	2.42	1.88	-1.91707
0.0	-30.0	22.9	zy	30.0	32.67	1.94	2.63	2.58	-3.02429
0.0	-33.0	22.9	zy	30.0	26.93	2.30	5.04	3.93	-9.98098
0.0	-36.0	22.9	zy	30.0	20.61	3.22	5.71	4.00	-4.91794
0.0	-39.0	22.9	zy	30.0	13.89	1.62	5.58	3.47	-6.20280
0.0	-42.0	22.9	zy	30.0	4.85	0.57	2.24	1.36	-0.40284
-5.0	-33.0	22.9	zy	30.0	31.98	0.05	2.54	2.21	-2.54558
-10.0	-33.0	22.9	zy	30.0	30.63	-3.68	3.12	2.97	3.77561
5.0	-33.0	22.7	zy	30.0	20.91	2.34	5.22	3.70	-7.81230
10.0	-33.0	22.2	zy	30.0	17.28	3.34	4.36	2.98	-3.25696
10.0	-33.0	22.2	zx	30.0	18.22	-3.65	3.71	3.57	-3.42247
5.0	-33.0	22.2	zx	30.0	20.14	-4.35	4.32	3.69	-4.24608
0.0	-33.0	22.2	zx	30.0	26.76	-2.39	4.93	3.32	0.94302
-5.0	-33.0	22.2	zx	30.0	32.32	0.35	2.46	2.21	1.07902
-10.0	-33.0	22.2	zx	30.0	32.89	-0.23	2.33	1.98	1.62551
0.0	-42.0	22.2	zx	30.0	5.48	-1.08	2.06	1.20	-1.06124
0.0	-39.0	22.2	zx	30.0	13.77	-3.17	5.46	3.29	-9.02791
0.0	-36.0	22.2	zx	30.0	20.08	-2.10	5.62	3.51	-4.27921
0.0	-33.0	22.2	zx	30.0	26.60	-2.47	4.87	3.32	1.29529
0.0	-30.0	22.2	zx	30.0	32.77	-1.30	2.75	2.45	0.70839
0.0	-27.0	22.2	zx	30.0	33.70	-0.80	2.63	2.30	-1.51944
0.0	-24.0	22.2	zx	30.0	35.75	-0.87	2.21	2.10	-0.70919
0.0	-21.0	22.2	zx	30.0	25.83	8.60	3.51	3.27	-3.30972
0.0	-18.0	22.2	zx	0.0	11.35	-0.24	2.97	2.77	-0.32771
0.0	-15.0	22.2	zx	0.0	13.47	-0.74	3.74	3.38	0.89376
0.0	-12.0	22.2	zx	0.0	24.50	-3.13	3.22	2.09	2.78490
0.0	-9.0	22.2	zx	0.0	29.47	-1.41	2.27	1.21	0.35972
0.0	-6.0	17.5	zx	0.0	32.01	-1.10	1.77	0.92	0.14087
0.0	-3.0	17.5	zx	0.0	32.92	-0.89	1.29	0.76	-0.05162
0.0	0.0	17.5	zx	0.0	33.34	-0.71	1.06	0.68	-0.10720

Table 3: Data in the probe oriented system (uncorrected for temperature) for the 30° degree fixed vane swirl generator. When the wires are in the "zx" plane the subscript "+" is to be taken as "n" and when in the "zy" plane as "y"; z=10 mm.

x (mm)	y (mm)	$T_a(°C)$	plane	ϕ (deg)	U_b (m/s)	U_+(m/s)	u'_b (m/s)	u'_+ (m/s)	$\overline{u_b u_+}(m^2/s^2)$
0.0	0.0	25.6	zx	0.0	16.64	0.00	0.61	0.42	0.02622
0.0	-3.0	25.4	zx	0.0	16.53	0.12	0.75	0.47	0.01975
0.0	-6.0	25.3	zx	0.0	15.82	0.25	0.98	0.55	0.01187
0.0	-9.0	25.4	zx	0.0	14.46	0.41	1.15	0.69	-0.04170
0.0	-12.0	25.4	zx	0.0	12.25	0.96	1.59	1.01	-0.47457
0.0	-18.0	25.4	zx	0.0	5.75	-0.51	1.69	1.72	0.24176
0.0	-21.0	29.1	zx	30.0	14.13	-2.47	3.04	2.52	3.05383
0.0	-24.0	29.1	zx	30.0	19.29	0.21	0.98	1.09	-0.07540
0.0	-27.0	29.1	zx	30.0	18.43	-0.01	1.14	0.99	-0.14615
0.0	-30.0	29.2	zx	30.0	17.86	-0.16	1.31	1.06	-0.23731
0.0	-33.0	29.2	zx	30.0	16.24	0.06	2.03	1.62	-0.11536
0.0	-36.0	29.2	zx	30.0	13.82	0.02	2.91	2.03	1.79443
0.0	-39.0	29.2	zx	30.0	10.83	1.85	3.00	2.04	2.08883
0.0	-42.0	29.2	zx	30.0	4.21	0.68	1.90	1.10	0.67144
-5.0	-33.0	29.2	zx	30.0	17.30	-0.09	1.22	1.13	-0.23550
-10.0	-33.0	29.2	zx	30.0	11.12	0.51	2.75	2.36	-3.59715
5.0	-33.0	29.3	zx	30.0	12.74	1.37	2.81	2.05	0.94000
10.0	-33.0	29.3	zx	30.0	9.53	1.54	2.36	2.06	1.80005
10.0	-33.0	28.0	zy	30.0	7.61	2.10	2.23	1.52	-0.02963
5.0	-33.0	28.0	zy	30.0	8.69	1.81	2.82	1.87	-0.92871
0.0	-33.0	28.1	zy	30.0	12.83	1.78	3.05	2.28	-2.82867
-5.0	-33.0	28.1	zy	30.0	16.59	0.74	1.64	1.47	-1.33807
-10.0	-33.0	28.1	zy	30.0	16.70	-0.60	1.36	1.26	0.00424
0.0	-42.0	28.1	zy	30.0	2.44	0.25	1.27	0.62	-0.05083
0.0	-39.0	28.2	zy	30.0	6.60	0.74	2.83	1.88	-1.69799
0.0	-36.0	28.2	zy	30.0	10.36	1.98	3.05	2.21	-0.70505
0.0	-33.0	28.2	zy	30.0	12.86	1.74	3.08	2.20	-2.73139
0.0	-30.0	28.2	zy	30.0	16.79	1.68	1.86	1.67	-1.57257
0.0	-27.0	28.2	zy	30.0	17.60	1.79	1.65	1.25	-0.70271
0.0	-24.0	28.2	zy	30.0	18.47	2.55	1.41	1.03	-0.62073
0.0	-21.0	28.2	zy	30.0	14.90	3.58	2.45	2.27	3.45213
0.0	-18.0	24.3	zy	0.0	12.71	1.71	4.54	2.38	5.37158
0.0	-15.0	24.3	zy	0.0	6.66	-0.24	2.55	1.66	0.81914
0.0	-12.0	24.3	zy	0.0	11.54	-1.32	1.95	1.48	-0.16703
0.0	-9.0	24.3	zy	0.0	14.81	-0.55	1.39	0.87	-0.15323
0.0	-6.0	24.3	zy	0.0	15.67	-0.24	1.09	0.68	-0.08312
0.0	-3.0	24.3	zy	0.0	16.53	-0.04	0.89	0.59	0.01488
0.0	0.0	24.3	zy	0.0	16.09	0.12	0.70	0.55	0.10247

Table 4: Data in the probe oriented system (uncorrected for temperature) for the 30° degree fixed vane swirl generator. When the wires are in the "zx" plane the subscript "+" is to be taken as "n" and when in the "zy" plane as "y"; z=5 mm.

x (mm)	y (mm)	$T_a(°C)$	plane	ϕ (deg)	U_b (m/s)	U_+(m/s)	u'_b (m/s)	u'_+ (m/s)	$\overline{u_b u_+}(m^2/s^2)$
0.0	0.0	21.2	zx	0.0	33.01	-0.24	1.05	0.73	0.00243
-3.0	0.0	21.2	zx	0.0	32.74	-0.51	1.22	0.75	-0.20044
-6.0	0.0	21.2	zx	0.0	31.12	-0.78	1.61	0.86	-0.51663
-9.0	0.0	21.2	zx	0.0	28.83	-1.04	2.03	1.07	-0.91496
-12.0	0.0	21.3	zx	0.0	24.19	-1.46	3.10	1.85	-2.29763
-15.0	0.0	21.3	zx	0.0	13.43	-2.42	4.05	2.87	-6.57072
-18.0	0.0	21.6	zx	0.0	16.26	-0.96	5.44	2.30	0.46286
0.0	-3.0	21.6	zx	0.0	32.47	-0.04	1.34	0.79	-0.20502
0.0	-6.0	21.6	zx	0.0	30.86	0.11	1.81	0.92	-0.34949
0.0	-9.0	21.6	zx	0.0	28.25	0.24	2.29	1.20	-0.39709
0.0	-12.0	21.6	zx	0.0	23.55	1.05	3.67	2.01	-2.05049
0.0	-15.0	21.6	zx	0.0	13.10	1.79	4.15	2.94	1.76293
0.0	-18.0	21.6	zx	0.0	16.48	-1.61	6.48	3.04	0.56630
0.0	-21.0	26.4	zx	45.0	35.28	-2.84	6.17	4.55	-7.22569
0.0	-24.0	26.4	zx	45.0	37.38	-4.00	4.44	4.35	-6.96273
0.0	-27.0	26.4	zx	45.0	33.69	-1.62	4.65	4.22	-11.22416
0.0	-30.0	26.4	zx	45.0	30.84	0.52	4.92	4.20	-12.88359
0.0	-33.0	26.4	zx	45.0	30.70	0.36	5.05	4.66	-15.60949
0.0	-36.0	26.3	zx	45.0	33.53	-2.12	4.40	4.08	-11.24923
0.0	-39.0	26.3	zx	45.0	29.38	0.52	5.48	3.98	-9.75875
0.0	-42.0	26.3	zx	45.0	12.63	2.22	5.67	2.65	3.37575
-5.0	-33.0	26.3	zx	45.0	22.61	3.70	4.53	4.14	-1.17587
5.0	-33.0	26.3	zx	45.0	36.61	1.65	3.06	2.87	1.45466
10.0	-33.0	26.3	zx	45.0	34.90	3.18	3.77	2.94	1.33021
15.0	-33.0	26.3	zx	45.0	30.39	3.53	5.52	3.31	6.04036
20.0	-33.0	26.3	zx	45.0	15.75	1.92	5.60	3.20	7.51665
20.0	-33.0	26.3	zy	45.0	16.11	-4.89	6.57	3.46	-7.96443
15.0	-33.0	26.3	zx	45.0	28.51	-9.78	5.68	3.13	-1.23509
10.0	-33.0	26.3	zx	45.0	33.55	-6.53	3.99	3.14	2.19289
5.0	-33.0	26.3	zx	45.0	36.73	-1.40	3.10	2.76	1.29395
0.0	-33.0	26.3	zx	45.0	31.74	0.99	4.64	3.74	-0.87904
-5.0	-33.0	26.3	zx	45.0	21.61	-3.27	5.22	3.35	2.90513
0.0	-42.0	26.3	zx	45.0	11.77	0.40	6.13	3.34	11.16981
0.0	-39.0	26.3	zx	45.0	29.50	1.09	6.07	4.29	7.49038
0.0	-36.0	26.3	zx	45.0	33.13	1.19	4.66	3.75	-4.95090
0.0	-33.0	26.3	zx	45.0	30.60	0.81	4.83	3.74	-0.19219
0.0	-30.0	26.4	zy	45.0	30.56	-1.92	4.88	3.58	0.68538
0.0	-27.0	26.4	zy	45.0	32.93	-5.06	5.63	3.37	-0.38788
0.0	-24.0	26.4	zy	45.0	34.84	-7.97	5.87	3.42	-3.02631
0.0	-21.0	26.4	zy	45.0	29.43	-9.60	4.95	4.39	-12.27956
0.0	-18.0	26.4	zy	0.0	19.75	0.77	7.28	2.73	-1.65783
0.0	-15.0	26.4	zy	0.0	13.15	2.16	4.00	2.80	5.37845
0.0	-12.0	26.4	zy	0.0	24.88	0.71	3.51	2.05	2.51731
0.0	-9.0	26.4	zy	0.0	29.29	0.24	2.33	1.26	1.03675
0.0	-6.0	26.4	zy	0.0	29.30	0.05	1.69	0.93	0.44270
0.0	-3.0	26.4	zy	0.0	32.49	-0.33	1.22	0.77	0.16121
0.0	0.0	27.1	zy	0.0	33.01	-0.57	1.08	0.75	-0.05874
-3.0	0.0	27.1	zy	0.0	32.72	-0.44	1.19	0.78	-0.20402
-6.0	0.0	27.4	zy	0.0	29.10	-0.22	1.49	0.84	-0.31078
-9.0	0.0	27.4	zy	0.0	28.98	-0.22	2.07	1.06	-0.46411
-12.0	0.0	27.4	zy	0.0	25.51	0.13	2.77	1.55	-1.20502
-15.0	0.0	27.4	zy	0.0	14.42	2.45	4.28	2.55	-0.69644

Table 5: Data in the probe oriented system (uncorrected for temperature) for the 45° degree fixed vane swirl generator. When the wires are in the "zx" plane the subscript "+" is to be taken as "n" and when in the "zy" plane as "y"; z=10 mm.

x (mm)	y (mm)	$T_a(°C)$	plane	ϕ (deg)	U_b (m/s)	U_+ (m/s)	u'_b (m/s)	u'_+ (m/s)	$\overline{u_b u_+}(m^2/s^2)$
0.0	0.0	19.6	zx	0.0	20.53	0.78	0.78	0.53	0.07317
0.0	-3.0	19.6	zx	0.0	22.00	2.27	0.90	0.58	0.04703
0.0	-6.0	19.6	zx	0.0	19.59	1.61	1.12	0.62	0.01574
0.0	-9.0	19.6	zx	0.0	17.73	1.03	1.37	0.75	0.04040
0.0	-12.0	19.6	zx	0.0	17.64	1.59	1.96	1.13	0.21447
0.0	-15.0	19.6	zx	0.0	9.90	2.93	2.89	2.03	2.22581
0.0	-18.0	19.6	zx	0.0	6.73	-2.06	2.26	1.75	-1.40925
0.0	-21.0	24.2	zx	45.0	16.70	-0.05	4.66	2.51	-1.77288
0.0	-24.0	24.2	zx	45.0	23.52	-3.72	2.94	2.93	-0.74169
0.0	-27.0	24.2	zx	45.0	22.92	-2.85	2.40	2.37	-0.82147
0.0	-30.0	24.2	zx	45.0	22.33	-1.10	2.52	2.26	-0.67242
0.0	-33.0	24.2	zx	45.0	22.62	0.45	2.49	2.08	-0.64766
0.0	-36.0	24.3	zx	45.0	21.68	-0.37	1.94	1.57	0.09342
0.0	-39.0	24.3	zx	45.0	18.99	0.59	2.99	2.14	-1.68277
0.0	-42.0	24.3	zx	45.0	7.72	1.04	3.31	1.77	1.54597
0.0	-44.0	24.3	zx	45.0	4.29	0.12	2.31	1.16	1.10261
-5.0	-33.0	24.3	zx	45.0	15.47	-0.04	3.00	3.01	-4.09205
5.0	-33.0	24.3	zx	45.0	20.26	1.57	2.67	2.01	2.21838
10.0	-33.0	24.6	zx	45.0	20.30	2.12	3.02	1.77	0.52062
15.0	-33.0	24.6	zx	4.5	17.43	1.34	3.76	1.97	3.00252
20.0	-33.0	24.6	zx	45.0	6.91	0.10	2.76	1.62	1.31788
20.0	-33.0	24.6	zy	45.0	8.12	1.72	3.35	2.01	2.18009
15.0	-33.0	24.6	zy	45.0	15.93	5.31	3.47	2.10	1.51353
10.0	-33.0	24.6	zy	45.0	19.44	3.81	2.39	2.13	0.56979
5.0	-33.0	24.6	zy	45.0	20.98	0.19	2.22	1.80	0.13396
0.0	-33.0	24.6	zy	45.0	20.96	-1.88	2.27	2.01	0.09127
-5.0	-33.0	24.6	zy	45.0	12.92	1.11	3.02	2.33	-0.27058
0.0	-42.0	24.6	zy	45.0	7.85	-0.95	3.67	2.40	-4.55441
0.0	-39.0	24.6	zy	45.0	15.90	-1.25	3.92	2.72	-4.35758
0.0	-36.0	24.6	zy	45.0	20.57	-1.37	2.24	2.12	0.61295
0.0	-33.0	24.6	zy	45.0	20.60	-1.96	2.42	2.02	0.42584
0.0	-30.0	24.6	zy	45.0	21.27	-0.93	2.65	2.17	0.18205
0.0	-27.0	24.6	zy	45.0	22.32	0.66	2.83	2.13	-0.37576
0.0	-24.0	24.6	zy	45.0	22.87	2.61	3.05	2.18	1.33017
0.0	-21.0	24.6	zy	45.0	18.20	4.36	3.23	3.08	5.90910
0.0	-18.0	24.6	zy	0.0	12.89	-0.95	4.18	1.95	2.15746
0.0	-15.0	20.1	zy	0.0	6.97	-1.90	2.39	1.71	-1.59535
0.0	-12.0	19.9	zy	0.0	13.77	-1.46	2.30	1.36	-1.32080
0.0	-9.0	19.9	zy	0.0	16.61	-1.24	1.40	0.83	-0.42789
0.0	-6.0	19.9	zy	0.0	16.88	-1.16	1.11	0.64	-0.26835
0.0	-3.0	19.9	zy	0.0	17.82	-1.01	0.82	0.53	-0.10799
0.0	0.0	20.0	zy	0.0	19.53	-0.85	0.74	0.51	0.00395

Table 6: Data in the probe oriented system (uncorrected for temperature) for the 45° degree fixed vane swirl generator. When the wires are in the "zx" plane the subscript "+" is to be taken as "n" and when in the "zy" plane as "y"; z=9 mm.

x (mm)	y (mm)	T_a(°C)	plane	ϕ (deg)	U_b (m/s)	U_+(m/s)	u'_b (m/s)	u'_+ (m/s)	$\overline{u_b u_+}(m^2/s^2)$
0.0	0.0	24.4	zy	0.0	17.70	0.04	0.69	0.56	0.07968
0.0	-3.0	24.4	zy	0.0	17.20	-0.05	0.88	0.69	-0.08873
0.0	-6.0	24.4	zy	0.0	16.13	-0.23	1.12	0.82	-0.23693
0.0	-9.0	24.4	zy	0.0	14.70	-0.31	1.41	1.05	-0.43044
0.0	-12.0	24.4	zy	0.0	11.00	-0.75	2.39	1.71	-1.30605
0.0	-15.0	24.4	zy	0.0	5.25	-0.44	2.22	1.55	-0.97702
0.0	-18.0	24.4	zy	0.0	4.53	-0.16	2.04	1.23	0.29016
0.0	-21.0	28.6	zy	60.0	7.05	0.10	2.72	1.60	0.99091
0.0	-24.0	28.6	zy	60.0	8.72	-0.30	4.07	2.28	2.09102
0.0	-27.0	28.6	zy	60.0	10.87	-1.79	4.28	3.03	-1.53558
0.0	-30.0	28.7	zy	60.0	11.77	-2.80	3.70	2.87	-4.34908
0.0	-33.0	28.7	zy	60.0	13.73	-4.29	3.83	2.82	-4.15110
0.0	-36.0	28.7	zy	60.0	19.30	-8.30	4.18	3.10	-5.22179
0.0	-39.0	28.7	zy	60.0	24.63	-12.78	4.17	3.22	-5.51936
0.0	-41.0	28.7	zy	60.0	24.55	-13.55	4.53	3.75	-9.96045
5.0	-33.0	28.7	zy	60.0	14.20	-4.34	3.93	3.10	-3.63222
10.0	-33.0	28.7	zy	60.0	16.12	-4.26	4.23	3.38	-3.23053
-5.0	-33.0	28.7	zy	60.0	20.50	-9.06	4.77	3.85	-10.82356
-5.0	-33.0	28.7	zy	60.0	17.79	-6.91	4.13	3.63	-8.99151
-5.0	-33.0	28.7	zx	60.0	17.82	-1.44	5.00	3.42	3.31154
10.0	-33.0	28.7	zx	60.0	16.94	-0.33	4.70	3.08	2.34136
-5.0	-33.0	28.7	zx	60.0	23.55	1.57	5.14	3.09	0.61812
-10.0	-33.0	28.7	zx	60.0	25.08	-0.42	7.23	2.58	8.72148
0.0	-41.0	28.7	zx	60.0	31.43	-0.52	7.23	3.38	14.46436
0.0	-39.0	28.7	zx	60.0	32.22	0.72	6.07	3.65	13.80378
0.0	-36.0	28.7	zx	60.0	26.32	1.75	4.92	3.59	6.26961
0.0	-33.0	28.7	zx	60.0	18.14	1.27	4.53	3.02	1.92490
0.0	-30.0	28.7	zx	60.0	13.18	0.33	4.29	2.55	1.99678
0.0	-27.0	28.7	zx	60.0	10.95	0.73	4.00	2.74	4.72405
0.0	-24.0	28.7	zx	60.0	8.23	0.98	3.68	2.60	5.32566
0.0	-21.0	28.7	zx	60.0	6.43	0.74	3.18	1.61	0.82069
0.0	-18.0	24.3	zx	0.0	4.82	0.14	2.00	1.09	-0.04144
0.0	-15.0	24.3	zx	0.0	5.48	-0.52	2.42	1.50	-0.85532
0.0	-12.0	24.3	zx	0.0	10.67	-1.40	2.82	1.84	0.62528
0.0	-9.0	24.3	zx	0.0	14.24	-0.38	1.49	1.13	0.10190
0.0	-6.0	24.3	zx	0.0	16.90	-0.26	1.17	0.89	0.00418
0.0	-3.0	24.2	zx	0.0	17.14	-0.13	0.88	0.71	-0.02519
0.0	0.0	24.2	zx	0.0	17.86	-0.01	0.70	0.66	-0.05056

Table 7: Data in the probe oriented system (uncorrected for temperature) for the 60° degree fixed vane swirl generator. When the wires are in the "zx" plane the subscript "+" is to be taken as "n" and when in the "zy" plane as "y"; z=6 mm.

x (mm)	y (mm)	$T_a(°C)$	plane	ϕ (deg)	U_b (m/s)	U_+(m/s)	u'_b (m/s)	u'_+ (m/s)	$\overline{u_b u_+}(m^2/s^2)$
0.0	0.0	21.4	zy	0.0	19.69	-0.30	6.71	4.05	0.32908
0.0	5.0	21.8	zy	0.0	17.81	0.08	6.29	3.81	3.24566
0.0	10.0	21.8	zy	0.0	15.38	0.33	6.15	3.41	5.37505
0.0	15.0	21.8	zy	0.0	13.01	0.44	5.64	3.18	5.00493
0.0	20.0	21.9	zy	0.0	10.57	0.47	4.89	2.69	4.06563
0.0	25.0	21.9	zy	0.0	8.57	0.37	4.16	2.28	3.02316
0.0	30.0	21.9	zy	0.0	6.88	0.20	3.69	1.87	2.16612
0.0	35.0	22.2	zy	0.0	5.68	0.00	2.87	1.43	0.95326
0.0	40.0	22.3	zy	0.0	4.77	-0.19	2.44	1.24	0.33976
0.0	40.0	22.9	zx	0.0	4.71	-0.16	2.61	1.22	-0.32751
0.0	35.0	23.0	zx	0.0	5.56	-0.24	3.14	1.35	-0.38127
0.0	30.0	23.0	zx	0.0	6.92	-0.31	3.76	1.75	-0.94011
0.0	25.0	23.0	zx	0.0	8.39	-0.41	4.66	2.19	-1.40217
0.0	20.0	23.1	zx	0.0	10.27	-0.47	5.39	2.78	-2.01847
0.0	15.0	23.2	zx	0.0	12.55	-0.55	5.66	3.20	-2.30068
0.0	10.0	23.0	zx	0.0	14.81	-0.61	6.14	3.37	-2.78149
0.0	5.0	23.1	zx	0.0	16.89	-0.70	6.22	3.63	-3.48145
0.0	0.0	23.1	zx	0.0	18.13	-0.88	5.95	3.89	-2.21897

Table 8: Data in the probe oriented system (uncorrected for temperature) for the primary flow of the IFRF variable swirl generator. When the wires are in the "zx" plane the subscript "+" is to be taken as "n" and when in the "zy" plane as "y"; z=2.5 mm.

x (mm)	y (mm)	$T_a(°C)$	plane	ϕ (deg)	U_b (m/s)	U_+ (m/s)	u'_b (m/s)	u'_+ (m/s)	$\overline{u_b u_+}(m^2/s^2)$
0.0	0.0	25.6	zy	0.0	10.60	-0.37	3.83	2.30	-0.35057
0.0	5.0	25.4	zy	0.0	9.88	-0.11	3.86	2.27	0.87496
0.0	10.0	25.3	zy	0.0	8.64	0.03	3.58	2.14	1.55363
0.0	15.0	25.3	zy	0.0	7.22	0.13	3.46	1.88	2.02586
0.0	20.0	25.3	zy	0.0	5.84	0.14	3.15	1.59	1.34813
0.0	25.0	25.2	zy	0.0	4.48	0.11	2.71	1.36	1.04973
0.0	30.0	25.1	zy	0.0	3.50	0.06	2.08	0.99	0.34794
0.0	35.0	25.1	zy	0.0	2.63	0.00	1.90	0.84	0.39031
0.0	40.0	25.2	zy	0.0	1.99	-0.07	1.46	0.55	0.00664
0.0	-5.0	25.3	zy	0.0	10.66	-0.64	3.71	2.36	-1.44970
0.0	-10.0	25.2	zy	0.0	10.02	-0.83	3.71	2.29	-2.73066
0.0	-15.0	25.3	zy	0.0	8.76	-0.91	3.67	2.14	-3.22552
0.0	-20.0	25.4	zy	0.0	7.32	-0.92	3.38	2.06	-3.41119
0.0	-25.0	25.5	zy	0.0	5.86	-0.83	3.04	1.69	-2.65512
0.0	-30.0	25.5	zy	0.0	4.53	-0.67	2.64	1.41	-1.77653
0.0	-35.0	25.4	zy	0.0	3.50	-0.51	2.30	1.15	-1.36381
0.0	-40.0	25.6	zy	0.0	2.64	-0.34	1.96	0.94	-0.83551
0.0	-40.0	21.7	zx	0.0	4.25	-0.20	2.67	1.10	-0.65526
0.0	-35.0	21.7	zx	0.0	5.39	-0.30	3.06	1.36	-0.81884
0.0	-30.0	21.8	zx	0.0	6.66	-0.41	3.60	1.77	-1.12706
0.0	-25.0	22.2	zx	0.0	8.17	-0.50	3.92	2.05	-0.94139
0.0	-20.0	22.2	zx	0.0	9.92	-0.63	4.26	2.35	-1.22030
0.0	-15.0	22.2	zx	0.0	11.63	-0.69	4.48	2.64	-1.44382
0.0	-10.0	22.2	zx	0.0	12.97	-0.69	4.37	2.70	-2.38090
0.0	-5.0	22.2	zx	0.0	13.48	-0.63	4.62	2.76	-2.08669
0.0	0.0	22.2	zx	0.0	13.18	-0.54	4.50	2.68	-1.89137
0.0	5.0	22.3	zx	0.0	12.10	-0.46	4.60	2.62	-1.55717
0.0	10.0	22.3	zx	0.0	10.62	-0.37	4.19	2.46	-1.41026
0.0	15.0	22.2	zx	0.0	8.88	-0.33	3.86	2.23	-1.44940
0.0	20.0	22.4	zx	0.0	7.39	-0.31	3.63	1.90	-0.81234
0.0	25.0	22.4	zx	0.0	5.99	-0.24	3.28	1.58	-0.55014
0.0	30.0	22.5	zx	0.0	4.72	-0.20	2.71	1.22	-0.37597
0.0	35.0	22.4	zx	0.0	3.84	-0.16	2.04	0.97	-0.01991
0.0	40.0	22.6	zx	0.0	3.10	-0.16	1.96	0.85	-0.21572

Table 9: Data in the probe oriented system (uncorrected for temperature) for the primary flow of the IFRF variable swirl generator. When the wires are in the "zx" plane the subscript "+" is to be taken as "n" and when in the "zy" plane as "y"; z=2.5 mm.

x (mm)	y (mm)	$T_a(°C)$	plane	ϕ (deg)	U_b (m/s)	U_+(m/s)	u'_b (m/s)	u'_+ (m/s)	$\overline{u_b u_+}(m^2/s^2)$
0.0	50.0	31.6	zy	0.0	14.13	-1.04	1.86	1.12	0.09680
0.0	55.0	31.6	zy	0.0	13.51	-0.93	1.93	1.56	0.58821
0.0	60.0	31.6	zy	0.0	12.77	-0.95	1.88	1.78	0.77628
0.0	65.0	31.6	zy	0.0	12.22	-0.95	1.94	1.82	0.58696
0.0	70.0	32.2	zy	0.0	11.81	-0.96	1.86	1.74	0.39949
0.0	75.0	32.4	zy	0.0	11.61	-0.92	1.85	1.63	0.19720
0.0	80.0	32.6	zy	0.0	11.49	-0.82	1.82	1.45	0.15978
0.0	85.0	32.7	zy	0.0	11.17	-0.64	1.90	1.02	0.11229
0.0	85.0	33.0	zx	0.0	10.34	-0.02	1.95	2.43	-0.93977
0.0	80.0	33.0	zx	0.0	10.95	-0.21	1.83	2.27	-0.63709
0.0	75.0	33.0	zx	0.0	11.28	-0.39	1.80	1.99	-0.45998
0.0	70.0	33.0	zx	0.0	11.53	-0.54	1.86	1.90	-0.40742
0.0	65.0	33.0	zx	0.0	11.94	-0.67	1.82	1.84	-0.35716
0.0	60.0	33.0	zx	0.0	12.40	-0.75	1.90	1.88	-0.30400
0.0	55.0	33.0	zx	0.0	12.96	-0.77	1.79	1.88	-0.17540
0.0	50.0	33.1	zx	0.0	13.48	-0.90	1.87	2.13	-0.24614

Table 10: Data in the probe oriented system (uncorrected for temperature) for the secondary flow of the IFRF variable swirl generator. When the wires are in the "zx" plane the subscript "+" is to be taken as "n" and when in the "zy" plane as "y"; θ=0.0, z=2.5 mm.

x (mm)	y (mm)	$T_a(°C)$	plane	ϕ (deg)	U_b (m/s)	U_+(m/s)	u'_b (m/s)	u'_+ (m/s)	$\overline{u_b u_+}(m^2/s^2)$
0.0	50.0	35.6	zx	30.0	9.17	2.11	2.67	2.42	0.19228
0.0	55.0	35.6	zx	30.0	10.44	2.23	2.49	2.31	-0.41110
0.0	60.0	35.6	zx	30.0	10.69	1.28	2.53	2.21	-0.11419
0.0	65.0	35.6	zx	30.0	11.01	0.59	2.53	2.26	0.66649
0.0	70.0	35.6	zx	30.0	11.46	0.10	2.47	2.36	0.40593
0.0	75.0	35.6	zx	30.0	12.02	-0.12	2.57	2.55	-0.12849
0.0	80.0	35.6	zx	30.0	12.50	-0.08	2.85	2.95	-1.46845
0.0	85.0	35.5	zy	30.0	12.72	0.19	3.31	3.23	-2.57362
0.0	80.0	35.5	zy	30.0	13.42	-0.80	3.17	1.62	-0.91626
0.0	75.0	35.5	zy	30.0	12.81	-0.89	2.90	1.91	-0.80963
0.0	70.0	35.4	zy	30.0	12.06	-0.93	2.60	2.17	-0.50757
0.0	65.0	35.4	zy	30.0	11.40	-0.87	2.65	2.33	-0.32128
0.0	60.0	35.4	zy	30.0	11.00	-0.80	2.58	2.29	0.01133
0.0	55.0	35.4	zy	30.0	10.97	-0.73	2.65	2.04	0.05202
0.0	50.0	35.4	zy	30.0	11.43	-0.71	2.67	1.58	0.19038
					7.56	-1.23	2.74	1.45	-2.22089

Table 11: Data in the probe oriented system (uncorrected for temperature) for the secondary flow of the IFRF variable swirl generator. When the wires are in the "zx" plane the subscript "+" is to be taken as "n" and when in the "zy" plane as "y"; S=1.0, z=4.0 mm.

x (mm)	y (mm)	T_a(°C)	plane	ϕ (deg)	U_b (m/s)	U_+(m/s)	u'_b (m/s)	u'_+ (m/s)	$\overline{u_b u_+}$(m^2/s^2)
0.0	50.0	32.6	zx	30.0	6.19	1.22	1.75	1.75	0.14261
0.0	55.0	32.2	zx	30.0	7.18	1.59	1.58	1.62	-0.09218
0.0	60.0	32.2	zx	30.0	7.30	1.20	1.58	1.57	0.12672
0.0	65.0	32.3	zx	30.0	7.49	0.92	1.60	1.58	0.26456
0.0	70.0	32.3	zx	30.0	7.72	0.79	1.62	1.55	0.38641
0.0	75.0	32.3	zx	30.0	7.93	0.80	1.67	1.75	0.09175
0.0	80.0	32.4	zx	30.0	8.08	0.96	1.82	1.89	-0.31163
0.0	85.0	32.4	zx	30.0	8.03	1.09	2.02	1.99	-0.40203
0.0	85.0	32.4	zy	30.0	8.78	-0.42	2.10	1.07	-0.21718
0.0	80.0	32.5	zy	30.0	8.50	-0.44	1.90	1.31	-0.15863
0.0	75.0	32.5	zy	30.0	8.16	-0.46	1.81	1.43	-0.01570
0.0	70.0	32.6	zy	30.0	7.88	-0.46	1.74	1.50	-0.10361
0.0	65.0	32.6	zy	30.0	7.71	-0.45	1.66	1.49	0.01351
0.0	60.0	32.6	zy	30.0	7.71	-0.44	1.68	1.28	0.23099
0.0	55.0	32.6	zy	30.0	7.93	-0.45	1.72	1.03	0.14702
0.0	50.0	32.6	zy	30.0	3.95	-0.61	1.63	1.04	-0.98742

Table 12: Data in the probe oriented system (uncorrected for temperature) for the secondary flow of the IFRF variable swirl generator. When the wires are in the "zx" plane the subscript "+" is to be taken as "n" and when in the "zy" plane as "y"; S=1.0, z=4.0 mm.

x (mm)	y (mm)	$T_a(°C)$	plane	ϕ (deg)	U_b (m/s)	U_+(m/s)	u'_h (m/s)	u'_+ (m/s)	$\overline{u_b u_+}(m^2/s^2)$
0.0	50.0	34.7	zx	45.0	10.53	-0.17	4.46	3.03	3.57063
0.0	55.0	34.7	zx	45.0	14.22	-0.62	4.61	3.34	2.91332
0.0	60.0	34.7	zx	45.0	16.95	-1.23	4.60	3.34	2.77118
0.0	65.0	34.7	zx	45.0	19.07	-1.42	3.99	3.26	1.95348
0.0	70.0	34.7	zx	45.0	20.78	-1.19	3.48	3.35	1.73420
0.0	75.0	34.8	zx	45.0	21.99	-0.65	3.06	3.01	-0.24695
0.0	80.0	34.8	zx	45.0	22.69	-0.04	3.18	3.14	-1.10738
0.0	85.0	34.8	zx	45.0	22.80	0.54	3.09	2.89	-0.93232
0.0	80.0	34.9	zy	45.0	22.90	0.94	3.15	1.92	0.73456
0.0	75.0	35.1	zy	45.0	22.77	0.90	2.97	2.38	-0.70778
0.0	70.0	35.2	zy	45.0	22.12	0.79	3.01	2.68	-0.68524
0.0	65.0	35.2	zy	45.0	21.06	0.64	3.39	2.78	-0.52919
0.0	60.0	35.2	zy	45.0	19.36	-1.33	3.90	2.76	-2.09506
0.0	55.0	35.2	zy	45.0	17.21	-1.44	4.54	2.77	-3.87853
0.0	50.0	35.2	zz	45.0	14.65	-1.66	5.03	2.92	-5.89668
0.0	70.0	35.2	zx	45.0	11.07	-0.76	4.71	2.61	-5.14755
					20.85	0.61	3.40	2.68	-1.08367

Table 13: Data in the probe oriented system (uncorrected for temperature) for the secondary flow of the IFRF variable swirl generator. When the wires are in the "zx" plane the subscript "+" is to be taken as "n" and when in the "zy" plane as "y"; S=2.0, z=2.0 mm.

x (mm)	y (mm)	$T_a(°C)$	plane	ϕ (deg)	U_b (m/s)	U_+(m/s)	u'_b (m/s)	u'_+ (m/s)	$\overline{u_b u_+}(m^2/s^2)$
0.0	50.0	33.0	zy	45.0	5.87	-0.19	2.39	0.95	-0.33734
0.0	55.0	32.7	zy	45.0	7.38	0.03	2.29	1.14	-0.21572
0.0	60.0	32.6	zy	45.0	8.51	0.10	2.24	1.28	-0.05324
0.0	65.0	32.6	zy	45.0	9.49	0.16	2.00	1.33	-0.14504
0.0	70.0	32.2	zy	45.0	10.32	0.22	1.69	1.41	-0.19173
0.0	75.0	32.2	zy	45.0	10.91	0.30	1.64	1.33	-0.24679
0.0	80.0	32.2	zy	45.0	11.33	0.33	1.58	1.21	-0.18118
0.0	85.0	31.8	zx	45.0	11.47	0.38	1.63	1.02	0.14922
0.0	80.0	31.8	zx	45.0	11.41	0.07	1.57	1.47	-0.26721
0.0	75.0	31.7	zx	45.0	11.34	-0.22	1.50	1.41	-0.29270
0.0	70.0	31.6	zx	45.0	10.94	-0.49	1.54	1.60	-0.12622
0.0	65.0	31.5	zx	45.0	10.29	-0.67	1.81	1.65	0.23535
0.0	60.0	31.5	zx	45.0	9.46	-0.68	2.07	1.71	0.63159
0.0	55.0	31.4	zx	45.0	8.47	-0.48	2.26	1.67	0.88891
0.0	50.0	31.4	zx	45.0	7.22	-0.11	2.33	1.75	0.85530
					5.48	-0.02	2.08	1.57	0.80453

Table 14: Data in the probe oriented system (uncorrected for temperature) for the secondary flow of the IFRF variable swirl generator. When the wires are in the "zx" plane the subscript "+" is to be taken as "n" and when in the "zy" plane as "y"; S=2.0, z=2.0 mm.

x (mm)	y (mm)	$T_a(°C)$	plane	ϕ (deg)	U_b (m/s)	U_+ (m/s)	u'_b (m/s)	u'_+ (m/s)	$\overline{u_b u_+}(m^2/s^2)$
0.0	50.0	33.6	zy	55.0	10.61	-0.56	4.46	2.69	-1.61763
0.0	55.0	33.9	zy	55.0	13.58	-0.59	5.29	3.07	-2.31438
0.0	60.0	34.0	zy	55.0	18.17	-0.03	6.17	3.89	-2.32830
0.0	65.0	34.2	zy	55.0	22.98	0.94	6.13	4.05	-2.35242
0.0	70.0	34.2	zy	55.0	26.96	1.83	5.34	4.06	-2.83870
0.0	75.0	34.6	zy	55.0	28.96	2.33	4.63	3.65	-2.63596
0.0	80.0	34.8	zy	55.0	29.77	2.36	4.34	3.27	-2.83761
0.0	85.0	34.9	zy	55.0	29.82	2.10	4.02	2.62	-1.08656
0.0	90.0	35.0	zx	55.0	29.31	4.24	4.16	2.92	-1.36008
0.0	75.0	35.1	zx	55.0	29.59	2.92	4.33	3.08	-2.26749
0.0	70.0	35.2	zx	55.0	28.87	0.94	4.73	3.81	-1.05469
0.0	65.0	35.3	zx	55.0	26.50	-0.99	5.19	4.06	1.29602
0.0	60.0	35.4	zx	55.0	22.31	-2.16	5.93	3.98	2.54546
0.0	55.0	35.4	zx	55.0	17.21	-2.20	6.12	3.65	1.44589
0.0	50.0	35.4	zx	55.0	12.96	-1.48	5.33	3.18	0.43834
					10.85	-0.75	4.90	2.41	0.95317

Table 15: Data in the probe oriented system (uncorrected for temperature) for the secondary flow of the IFRF variable swirl generator. When the wires are in the "zx" plane the subscript "+" is to be taken as "n" and when in the "zy" plane as "y"; S=3.0, z=2.0 mm.

x (mm)	y (mm)	$T_a(^oC)$	plane	ϕ (deg)	U_b (m/s)	U_+(m/s)	u'_b (m/s)	u'_+ (m/s)	$\overline{u_b u_+}(m^2/s^2)$
0.0	50.0	31.0	zx	55.0	5.61	-0.36	2.55	1.25	0.09914
0.0	55.0	31.1	zx	55.0	6.69	-0.77	2.71	1.65	0.05913
0.0	60.0	31.1	zx	55.0	8.86	-1.17	3.11	1.89	0.35401
0.0	65.0	31.1	zx	55.0	11.51	-1.19	3.26	2.08	0.68543
0.0	70.0	31.0	zx	55.0	13.80	-0.61	2.74	2.13	0.47684
0.0	75.0	31.0	zx	55.0	15.09	0.40	2.52	2.03	-0.32680
0.0	80.0	31.0	zx	55.0	15.43	1.43	2.22	1.67	-0.56312
0.0	85.0	31.2	zx	55.0	15.26	2.13	2.18	1.48	-0.32497
0.0	85.0	31.1	zy	55.0	15.47	1.14	2.13	1.36	-0.30493
0.0	80.0	31.1	zy	55.0	15.46	1.22	2.17	1.67	-0.60386
0.0	75.0	31.1	zy	55.0	15.05	1.20	2.54	1.95	-0.93273
0.0	70.0	31.1	zy	55.0	13.88	0.89	2.66	2.06	-0.71259
0.0	65.0	31.1	zy	55.0	11.82	0.42	3.12	2.08	-0.86251
0.0	60.0	31.1	zy	55.0	9.23	-0.08	3.03	1.98	-0.73675
0.0	55.0	31.1	zy	55.0	6.93	-0.35	2.67	1.51	-0.65937
0.0	50.0	31.1	zy	55.0	5.39	-0.28	2.19	1.32	-0.56459

Table 16: Data in the probe oriented system (uncorrected for temperature) for the secondary flow of the IFRF variable swirl generator. When the wires are in the "zx" plane the subscript "+" is to be taken as "n" and when in the "zy" plane as "y"; S=3.0, z=2.0 mm.

x (mm)	y (mm)	$T_o(°C)$	plane	ϕ (deg)	U_b (m/s)	U_+ (m/s)	u'_b (m/s)	u'_+ (m/s)	$\overline{u_b u_+}$ (m^2/s^2)
0.0	50.0	35.6	zx	55.0	13.46	-0.66	6.18	2.74	1.55116
0.0	55.0	35.6	zx	55.0	14.62	-1.35	6.02	3.47	0.52580
0.0	60.0	35.6	zx	55.0	17.87	-2.40	7.06	3.86	0.50134
0.0	65.0	35.6	zx	55.0	23.05	-3.18	7.61	4.25	2.12809
0.0	70.0	35.6	zx	55.0	28.50	-3.03	7.18	4.47	3.34893
0.0	75.0	35.6	zx	55.0	32.97	-1.67	6.72	4.73	0.39203
0.0	80.0	35.6	zx	55.0	35.47	0.61	6.18	4.33	-4.46885
0.0	85.0	35.6	zx	55.0	36.07	2.87	5.88	3.84	-5.46988
0.0	80.0	35.7	zy	55.0	35.73	3.69	6.22	3.10	-5.85595
0.0	75.0	35.6	zy	55.0	35.04	3.51	6.34	3.69	-7.18605
0.0	70.0	35.7	zy	55.0	32.96	2.77	7.09	4.26	-6.47655
0.0	65.0	35.7	zy	55.0	29.01	1.49	7.11	4.47	-5.19377
0.0	60.0	35.7	zy	55.0	23.83	0.19	6.94	4.41	-3.97751
0.0	55.0	35.7	zy	55.0	18.74	-0.83	6.60	3.91	-3.57306
0.0	50.0	35.7	zy	55.0	15.15	-1.30	5.68	3.31	-2.31143
					12.69	-1.12	4.92	2.85	-1.60589

Table 17: Data in the probe oriented system (uncorrected for temperature) for the secondary flow of the IFRF variable swirl generator. When the wires are in the "zx" plane the subscript "+" is to be taken as "n" and when in the "zy" plane as "y"; S=4., z=2.0 mm.

x (mm)	y (mm)	$T_a(°C)$	plane	ϕ (deg)	U_b (m/s)	U_+ (m/s)	u'_b (m/s)	u'_+ (m/s)	$\overline{u_b u_+}$ (m^2/s^2)
0.0	50.0	29.8	zx	55.0	5.30	-0.15	2.47	1.12	0.44272
0.0	55.0	29.8	zx	55.0	5.86	-0.31	2.76	1.32	0.43589
0.0	60.0	29.8	zx	55.0	7.09	-0.61	3.12	1.66	0.35871
0.0	65.0	29.8	zx	55.0	9.20	-0.92	3.35	1.85	0.60631
0.0	70.0	29.8	zx	55.0	11.84	-0.95	3.65	2.11	0.92860
0.0	75.0	29.8	zx	55.0	14.20	-0.46	3.37	2.29	0.37294
0.0	80.0	29.8	zx	55.0	15.62	0.32	3.07	2.18	-0.55004
0.0	85.0	29.8	zx	55.0	16.08	1.25	2.87	1.77	-0.91735
0.0	80.0	29.8	zy	55.0	15.37	1.75	3.00	1.73	-1.89174
0.0	75.0	29.8	zy	55.0	14.43	1.34	3.34	1.85	-1.67560
0.0	70.0	30.8	zy	55.0	12.77	0.78	3.47	2.06	-1.95865
0.0	65.0	30.0	zy	55.0	10.50	0.21	3.55	1.99	-1.07696
0.0	60.0	30.0	zy	55.0	8.12	-0.28	3.20	1.88	-1.19014
0.0	55.0	30.1	zy	55.0	6.28	-0.53	2.49	1.56	-0.70553
0.0	50.0	30.1	zy	55.0	5.12	-0.47	2.22	1.42	-0.73784
					4.30	-0.18	1.89	1.28	-0.41294

Table 18: Data in the probe oriented system (uncorrected for temperature) for the secondary flow of the IFRF variable swirl generator. When the wires are in the "zx" plane the subscript "+" is to be taken as "n" and when in the "zy" plane as "y"; S=4.0, z=2.0 mm.

x (mm)	y (mm)	$T_a(°C)$	plane	ϕ (deg)	U_h (m/s)	U_+(m/s)	u'_h (m/s)	u'_+ (m/s)	$\overline{u_h u_+}(m^2/s^2)$
0.0	50.0	34.4	zx	55.0	11.29	-0.72	5.51	2.11	0.42614
0.0	55.0	34.4	zx	55.0	12.32	-1.15	5.70	2.74	0.82681
0.0	60.0	34.6	zx	55.0	14.75	-2.02	6.23	3.30	0.38407
0.0	65.0	34.7	zx	55.0	18.89	-2.95	6.90	3.68	0.30539
0.0	70.0	34.7	zx	55.0	23.93	-3.32	6.90	4.16	0.73468
0.0	75.0	34.9	zx	55.0	28.56	-2.51	6.90	4.43	-0.03674
0.0	80.0	35.1	zx	55.0	31.63	-0.67	6.18	4.18	-3.63556
0.0	85.0	35.1	zx	55.0	32.82	1.53	5.63	3.63	-5.27817
0.0	80.0	35.1	zy	55.0	31.70	3.79	6.36	3.36	-9.61467
0.0	75.0	35.2	zy	55.0	29.89	3.00	6.81	3.83	-9.39978
0.0	70.0	35.3	zy	55.0	26.32	1.99	7.00	4.09	-6.52525
0.0	65.0	35.4	zy	55.0	21.71	0.76	7.05	3.98	-4.51672
0.0	60.0	35.4	zy	55.0	16.68	-0.40	6.28	3.77	-3.86557
0.0	55.0	35.4	zy	55.0	13.03	-0.98	5.15	3.06	-2.63523
0.0	50.0	35.6	zy	55.0	10.83	-0.88	4.50	2.82	-1.68332
					9.29	-0.32	4.17	2.67	-0.85091

Table 19: Data in the probe oriented system (uncorrected for temperature) for the secondary flow of the IFRF variable swirl generator. When the wires are in the "zx" plane the subscript "+" is to be taken as "n" and when in the "zy" plane as "y"; S=4.5, z=2.0 mm.

x (mm)	y (mm)	$T_a(°C)$	plane	ϕ (deg)	U_b (m/s)	U_+ (m/s)	u'_b (m/s)	u'_+ (m/s)	$\overline{u_b u_+}(m^2/s^2)$
0.0	50.0	30.2	zy	55.0	4.66	-0.18	2.08	1.25	-0.43062
0.0	55.0	30.1	zy	55.0	5.48	-0.46	2.26	1.37	-0.46236
0.0	60.0	30.2	zy	55.0	6.59	-0.50	2.60	1.61	-0.81586
0.0	65.0	30.3	zy	55.0	8.42	-0.25	3.20	1.96	-0.90926
0.0	70.0	30.3	zy	55.0	10.97	0.29	3.58	2.10	-1.20411
0.0	75.0	30.3	zy	55.0	13.39	0.94	3.75	2.17	-1.49674
0.0	80.0	30.3	zy	55.0	15.27	1.61	3.66	2.02	-2.16929
0.0	85.0	30.3	zy	55.0	16.26	2.02	3.44	1.85	-2.40738
0.0	90.0	30.3	zy	55.0	16.32	2.22	3.06	1.73	-1.43100
0.0	85.0	30.3	zx	55.0	16.85	0.72	3.12	2.08	-1.82796
0.0	80.0	30.3	zx	55.0	16.17	-0.43	3.36	2.25	-1.20083
0.0	75.0	30.3	zx	55.0	14.51	-1.37	3.56	2.24	-0.26034
0.0	70.0	30.3	zx	55.0	12.15	-1.75	3.71	2.14	-0.16076
0.0	65.0	30.4	zx	55.0	9.50	-1.55	3.51	1.89	-0.20960
0.0	60.0	30.4	zx	55.0	7.39	-1.04	3.19	1.72	-0.34013
0.0	55.0	30.4	zx	55.0	6.19	-0.61	2.74	1.43	0.09714
0.0	50.0	30.4	zx	55.0	5.67	-0.36	2.72	1.16	-0.04087

Table 20: Data in the probe oriented system (uncorrected for temperature) for the secondary flow of the IFRF variable swirl generator. When the wires are in the "zx" plane the subscript "+" is to be taken as "n" and when in the "zy" plane as "y"; S=4.5, z=4.5 mm.

θ (deg)	r (mm)	T_a(°C)	U_θ (m/s)	U_r(m/s)	U_z (m/s)	u'_θ (m/s)	u'_r (m/s)	u'_z (m/s)	$\overline{u_\theta u_z}(m^2/s^2)$	$\overline{u_r u_z}(m^2/s^2)$	$\overline{u_r u_\theta}(m^2/s^2)$	$q^2(m^2/s^2)$	q/Q
-90.	0.0	17.5	-0.7	0.8	32.5	0.68	0.69	1.06	-0.107	0.014	0.000	2.06	0.04
-90.	3.0	17.5	-0.9	1.2	32.1	0.76	0.74	1.29	-0.052	0.206	0.000	2.80	0.05
-90.	6.0	17.5	-1.1	1.5	31.2	0.92	0.87	1.77	0.141	0.556	0.000	4.73	0.07
-90.	9.0	22.2	-1.5	2.0	31.2	1.21	1.11	2.27	0.360	0.900	0.000	7.85	0.09
-90.	12.0	22.2	-3.3	3.2	26.0	2.09	1.77	3.22	2.785	1.143	0.000	17.85	0.16
-90.	15.0	22.2	-0.8	1.4	14.3	3.36	2.33	3.74	0.804	2.526	0.000	30.85	0.39
-90.	18.0	22.2	-0.3	-2.1	12.1	2.77	2.14	2.97	-0.328	0.756	0.000	21.12	0.37
-90.	21.0	22.2	21.6	-5.0	19.2	2.67	3.89	3.85	-0.949	-9.882	-5.705	38.20	0.21
-90.	24.0	22.2	18.1	-3.7	33.2	1.96	1.54	2.32	-0.159	1.330	0.768	11.65	0.09
-90.	27.0	22.2	17.1	-2.2	31.3	2.10	1.86	2.80	-0.068	1.660	0.969	15.73	0.11
-90.	30.0	22.2	16.2	-2.1	30.7	2.65	2.56	2.56	1.047	2.619	1.512	20.21	0.13
-90.	33.0	22.2	12.0	-2.5	25.8	3.89	3.93	4.49	6.236	8.644	4.990	50.76	0.25
-91.	33.4	22.2	11.9	-2.5	25.7	3.91	3.93	4.41	6.164	8.644	4.990	50.18	0.25
-99.	33.4	22.2	7.0	-1.5	20.8	3.17	3.85	4.59	-0.945	6.700	3.355	45.93	0.31
-73.	34.5	22.2	17.2	-2.7	29.5	2.54	2.13	2.20	1.376	2.021	1.035	15.81	0.12
-107.	34.5	22.2	7.1	-1.5	18.7	3.00	3.14	4.06	-2.029	2.332	1.669	35.33	0.30
-90.	36.0	22.2	17.6	-1.3	30.3	2.22	3.10	1.91	0.444	-3.551	-0.713	18.14	0.12
-90.	39.0	22.2	8.7	-3.4	19.6	3.67	4.00	5.52	6.212	4.259	2.459	59.93	0.36
-90.	42.0	22.2	4.4	-1.7	14.4	2.79	3.47	5.73	3.699	5.372	3.101	52.71	0.48
			1.9	-0.6	5.7	1.11	1.36	2.11	0.690	0.349	0.201	7.53	0.46

Table 21: Data for the 30° fixed vane swirl generator presented in cylindrical coordinates; z=10 mm.

θ (deg)	r (mm)	T_a(°C)	$\frac{U_\theta}{U_z}$	$\frac{U_r}{U_z}$	$\frac{U_z}{U_z}$	$\frac{u'_\theta}{U_z}$	$\frac{u'_r}{U_z}$	$\frac{u'_z}{U_z}$	$\frac{\overline{u_\theta u_r}}{U_z^2}$	$\frac{\overline{u_\theta u_z}}{U_z^2}$	$\frac{\overline{u_r u_z}}{U_z^2}$	$\frac{k^2}{U_z^2}$	q/Q
-90.	0.0	17.5	-0.02	0.03	1.04	0.022	0.022	0.034	-0.000109	0.000015	0.000000	0.002098	0.044
-90.	3.0	17.5	-0.03	0.04	1.02	0.024	0.024	0.041	-0.000052	0.000212	0.000000	0.002845	0.052
-90.	6.0	17.5	-0.03	0.05	1.00	0.029	0.028	0.056	0.000143	0.000566	0.000000	0.004807	0.070
-90.	9.0	22.2	-0.05	0.07	1.00	0.039	0.036	0.072	0.000366	0.000915	0.000000	0.007979	0.089
-90.	12.0	22.2	-0.05	0.07	1.00	0.039	0.036	0.072	0.000366	0.000915	0.000000	0.007979	0.160
-90.	15.0	22.2	-0.03	0.06	0.63	0.149	0.103	0.165	0.001740	0.004918	0.000000	0.060060	0.385
-90.	18.0	22.2	-0.01	-0.09	0.53	0.122	0.095	0.131	-0.000638	0.001471	0.000000	0.041116	0.375
-90.	21.0	22.2	0.95	-0.22	0.85	0.127	0.172	0.170	-0.001849	-0.019239	-0.011108	0.074369	0.211
-90.	24.0	22.2	0.80	-0.16	1.47	0.067	0.068	0.102	-0.000310	0.002590	0.001496	0.022687	0.090
-90.	27.0	22.2	0.76	-0.10	1.36	0.092	0.083	0.123	-0.000132	0.003232	0.001866	0.030626	0.111
-90.	30.0	22.2	0.71	-0.09	1.36	0.117	0.114	0.113	0.002038	0.005099	0.002944	0.039345	0.129
-90.	33.0	22.2	0.53	-0.11	1.14	0.172	0.173	0.198	0.012141	0.016829	0.009716	0.096819	0.249
-81.	33.4	22.2	0.52	-0.11	1.13	0.173	0.173	0.194	0.012002	0.016829	0.009716	0.097695	0.249
-99.	33.4	22.2	0.31	-0.06	0.92	0.140	0.170	0.202	-0.001841	0.013044	0.006532	0.069429	0.308
-73.	34.5	22.2	0.76	-0.12	1.30	0.112	0.094	0.097	0.002678	0.003935	0.002014	0.030786	0.116
-107.	34.5	22.2	0.31	-0.07	0.82	0.132	0.139	0.179	-0.003961	0.004541	0.003250	0.068787	0.297
-90.	36.0	22.2	0.78	-0.06	1.34	0.098	0.137	0.094	0.000864	-0.006914	-0.001389	0.035322	0.122
-90.	39.0	22.2	0.30	-0.15	0.86	0.162	0.176	0.244	0.012098	0.008292	0.004788	0.116683	0.357
-90.	42.0	22.2	0.20	-0.06	0.63	0.123	0.153	0.253	0.007183	0.010459	0.006038	0.102619	0.480
-90.	42.0	22.2	0.09	-0.03	0.25	0.049	0.060	0.093	0.001344	0.000679	0.000392	0.014661	0.456

Table 22: Normalized data for the 30° fixed vane swirl generator; $\hat{U}_z = 31.4$ m/s for the primary flow and $\hat{U}_z = 22.7$ m/s for the secondary flow; z=10 mm.

θ (deg)	r (mm)	T_g(°C)	U_θ (m/s)	U_r(m/s)	U_z (m/s)	u'_θ (m/s)	u'_r (m/s)	u'_z (m/s)	$\overline{u_\theta u_z}(m^2/s^2)$	$\overline{u_r u_z}(m^2/s^2)$	$\overline{u_r u_\theta}(m^2/s^2)$	$q^2(m^2/s^2)$	q/Q
-90.	0.0	25.6	0.0	-0.1	16.7	0.42	0.55	0.61	0.026	-0.102	0.000	0.85	0.06
-90.	3.0	25.4	0.1	0.0	16.5	0.47	0.59	0.75	0.020	-0.015	0.000	1.13	0.06
-90.	6.0	25.3	0.2	0.2	15.8	0.55	0.68	0.98	0.012	0.083	0.000	1.74	0.08
-90.	9.0	25.4	0.4	0.5	14.4	0.69	0.87	1.15	-0.042	0.153	0.000	2.56	0.11
-90.	12.0	25.4	1.0	1.3	12.2	1.01	1.48	1.59	-0.475	0.167	0.000	5.72	0.19
-90.	18.0	25.4	-0.5	-1.7	5.7	1.72	2.38	1.69	0.242	-5.372	0.000	11.45	0.56
-90.	21.0	29.1	5.3	-3.8	14.4	3.12	2.27	2.43	2.793	-2.990	-1.726	20.75	0.29
-90.	24.0	29.1	10.5	-2.7	17.8	1.03	1.03	1.04	-0.133	0.538	0.310	3.21	0.09
-90.	27.0	29.1	9.9	-1.9	17.1	0.97	1.25	1.16	0.064	0.609	0.351	3.86	0.10
-90.	30.0	29.2	9.4	-1.8	16.7	1.03	1.67	1.33	0.145	1.362	0.786	5.65	0.12
-99.	33.4	29.2	8.8	-1.9	15.0	1.70	2.20	1.96	0.593	2.365	1.366	11.58	0.19
-81.	33.4	29.3	9.0	-2.2	16.1	1.16	1.39	1.28	0.152	1.149	0.793	4.92	0.12
-107.	34.5	29.2	8.3	-0.7	11.1	2.40	1.92	2.48	1.926	1.105	0.806	15.61	0.28
-73.	34.5	29.3	6.4	-1.3	10.1	1.69	1.30	3.19	-0.892	0.267	-0.386	14.73	0.32
-90.	36.0	29.2	6.9	-0.2	8.1	2.41	1.62	1.92	1.397	0.450	1.080	12.11	0.33
-90.	39.0	29.2	7.4	-2.1	12.8	2.60	2.21	2.42	2.785	0.611	0.353	17.47	0.28
-90.	42.0	29.2	7.5	-0.8	9.1	2.66	1.88	2.44	3.138	1.471	0.849	16.70	0.34
			2.9	-0.3	3.6	1.54	0.62	1.56	1.386	0.044	0.025	5.21	0.49

Table 23: Data for the 30° fixed vane swirl generator presented in cylindrical coordinates; z=5 mm.

θ (deg)	r (mm)	T_a(°C)	$\frac{U_\theta}{\hat{U}_z}$	$\frac{U_r}{\hat{U}_z}$	$\frac{U_z}{\hat{U}_z}$	$\frac{u'_\theta}{\hat{U}_z}$	$\frac{u'_r}{\hat{U}_z}$	$\frac{u'_z}{\hat{U}_z}$	$\frac{\overline{u_\theta u_z}}{\hat{U}_z^2}$	$\frac{\overline{u_\theta u_r}}{\hat{U}_z^2}$	$\frac{\overline{u_r u_z}}{\hat{U}_z^2}$	$\frac{q^2}{\hat{U}_z^2}$	q/Q
-90.	0.0	25.6	0.00	-0.01	1.10	0.028	0.036	0.040	0.000113	-0.000443	0.000000	0.003679	0.055
-90.	3.0	25.4	0.01	0.00	1.08	0.031	0.039	0.049	0.000085	-0.000064	0.000000	0.004890	0.065
-90.	6.0	25.3	0.02	0.02	1.04	0.036	0.045	0.065	0.000051	0.000359	0.000000	0.007504	0.084
-90.	9.0	25.4	0.03	0.04	0.95	0.046	0.057	0.076	-0.000180	0.000662	0.000000	0.011071	0.111
-90.	12.0	25.4	0.03	0.04	0.95	0.046	0.057	0.076	-0.000180	0.000662	0.000000	0.011071	0.194
-90.	18.0	25.4	-0.04	-0.14	0.47	0.142	0.197	0.139	0.001652	-0.036710	0.000000	0.078220	0.563
-90.	21.0	29.1	0.44	-0.31	1.19	0.258	0.188	0.200	0.019088	-0.020431	-0.011796	0.141791	0.288
-90.	24.0	29.1	0.87	-0.22	1.47	0.085	0.085	0.086	-0.000906	0.003674	0.002121	0.021959	0.086
-90.	27.0	29.1	0.82	-0.16	1.41	0.080	0.104	0.096	0.000435	0.004159	0.002401	0.026352	0.099
-90.	30.0	29.2	0.78	-0.15	1.38	0.085	0.138	0.110	0.000989	0.009307	0.005374	0.038623	0.124
-99.	33.4	29.2	0.73	-0.15	1.24	0.141	0.182	0.162	0.004055	0.016166	0.009333	0.079105	0.194
81.	33.4	29.2	0.74	-0.18	1.33	0.096	0.115	0.106	0.001040	0.007852	0.005420	0.033605	0.119
-107.	34.5	29.3	0.69	-0.06	0.92	0.196	0.159	0.205	0.013165	0.007554	0.005511	0.106703	0.284
-73.	34.5	29.2	0.53	-0.11	0.83	0.139	0.108	0.264	-0.006099	0.001822	-0.002636	0.100633	0.320
-90.	36.0	29.2	0.57	-0.02	0.67	0.199	0.134	0.159	0.009546	0.003076	0.007377	0.082791	0.327
-90.	39.0	29.2	0.62	-0.17	1.06	0.215	0.183	0.200	0.019031	0.004173	0.002409	0.119412	0.279
-90.	42.0	29.2	0.62	-0.07	0.75	0.221	0.156	0.202	0.021443	0.010050	0.005802	0.114101	0.345
			0.24	-0.02	0.30	0.128	0.051	0.129	0.009469	0.000301	0.000174	0.035598	0.491

Table 24: Normalized data for the 30° fixed vane swirl generator; $\hat{U}_z = 15.2$ m/s for the primary flow and $\hat{U}_z = 12.1$ m/s for the secondary flow; z=5 mm.

θ (deg)	r (mm)	T_a(°C)	U_θ (m/s)	U_r(m/s)	U_z (m/s)	u'_θ (m/s)	u'_r (m/s)	u'_z (m/s)	$\overline{u_\theta u_z}(m^2/s^2)$	$\overline{u_r u_z}(m^2/s^2)$	$\overline{u_r u_\theta}(m^2/s^2)$	$q^2(m^2/s^2)$	q/Q
-90.	3.0	21.6	0.0	0.4	32.9	0.79	0.77	1.34	-0.205	-0.161	0.000	3.00	0.05
-90.	6.0	21.6	0.1	-0.1	31.3	0.92	0.93	1.81	-0.349	-0.443	0.000	4.97	0.07
-90.	9.0	21.6	0.2	-0.3	28.7	1.20	1.26	2.29	-0.397	-1.037	0.000	8.28	0.10
-90.	12.0	21.6	1.1	-0.8	23.9	2.01	2.05	3.67	-2.050	-2.517	0.000	21.67	0.19
-180.	15.0	21.3	-2.7	2.4	13.6	2.55	2.87	4.05	0.696	6.571	0.000	31.12	0.40
-90.	15.0	21.6	1.8	-2.4	13.3	2.94	2.80	4.15	1.763	-5.378	0.000	33.68	0.43
-180.	18.0	21.6	0.0	1.0	16.5	0.00	2.30	5.44	0.000	-0.463	0.000	34.83	0.36
-90.	18.0	21.6	-1.6	-0.9	16.7	3.04	2.73	6.48	0.566	1.658	0.000	58.62	0.45
-90.	21.0	26.4	25.3	10.5	29.6	4.71	4.39	6.05	8.721	8.683	8.683	78.01	0.22
-90.	24.0	26.4	26.0	8.7	32.2	3.51	3.42	5.12	0.413	2.140	2.140	50.29	0.17
-90.	27.0	26.4	25.0	5.5	27.5	2.91	3.37	5.56	1.902	0.274	0.274	50.71	0.19
-90.	30.0	26.4	24.4	2.1	23.6	2.84	3.58	5.82	3.295	-0.485	-0.485	54.68	0.22
-90.	33.0	26.4	24.2	0.0	23.6	2.83	0.00	6.26	1.871	0.000	0.000	47.19	0.20
-90.	33.0	26.3	25.5	0.0	23.9	4.11	0.00	4.32	3.783	0.000	0.000	35.57	0.17
-90.	33.0	26.3	24.4	0.0	23.2	4.30	0.00	4.34	4.703	0.000	0.000	37.32	0.18
-99.	33.4	26.3	20.3	-3.1	14.8	4.15	0.63	4.47	1.695	-0.257	-2.615	37.66	0.24
-81.	33.4	26.3	29.4	4.5	27.2	3.17	0.48	2.71	0.558	0.085	1.520	17.62	0.10
-81.	33.4	26.3	27.1	4.1	29.6	3.11	0.47	2.70	0.977	0.148	1.466	17.21	0.10
-99.	33.4	26.3	14.2	-2.1	19.4	4.65	0.71	4.04	7.942	-1.203	-3.283	38.51	0.26
-73.	34.5	26.3	28.3	8.6	24.7	3.42	1.04	3.18	2.657	0.805	3.544	22.88	0.12
-73.	34.5	26.3	20.1	6.1	31.1	3.72	1.13	3.27	2.924	0.886	4.189	25.80	0.14
-90.	36.0	26.3	24.4	0.0	27.7	2.60	0.00	5.41	1.388	0.000	0.000	36.00	0.16
-90.	36.0	26.3	26.7	0.0	24.8	3.60	0.00	4.78	3.842	0.000	0.000	35.78	0.16
-66.	36.2	26.3	24.0	10.9	20.9	4.71	2.14	3.83	8.909	4.049	10.084	41.46	0.19
-66.	36.2	26.3	13.3	6.1	29.7	4.05	1.84	4.72	10.208	4.640	7.447	42.01	0.20
-59.	38.6	26.3	9.0	11.7	10.8	4.35	4.62	3.64	6.108	10.287	9.850	53.53	0.40
-90.	39.0	26.3	23.3	0.0	22.4	3.63	0.00	5.72	7.076	0.000	0.000	45.86	0.21
-90.	39.0	26.3	23.8	0.0	22.1	5.93	0.00	4.49	9.237	0.000	0.000	55.26	0.23
-90.	42.0	26.3	11.6	0.0	8.2	4.79	0.00	4.03	12.565	0.000	0.000	39.21	0.44
-90.	42.0	26.3	9.5	0.0	8.9	5.96	0.00	3.64	13.242	0.000	0.000	48.79	0.53

Table 25: Data for the 45° fixed vane swirl generator presented in cylindrical coordinates; z=10 mm.

θ (deg)	r (mm)	T_a(°C)	$\frac{U_\theta}{U_z}$	$\frac{U_r}{U_z}$	$\frac{U_z}{U_z}$	$\frac{u'}{U_z}$	$\frac{v'}{U_z}$	$\frac{w'}{U_z}$	$\frac{\overline{u_\theta u_z}}{U_z^2}$	$\frac{\overline{u_r u_z}}{U_z^2}$	$\frac{\overline{u_z u_z}}{U_z^2}$	$\frac{k^2}{U_z^2}$	q/Q
-90.	3.0	21.6	0.00	0.01	1.09	0.026	0.025	0.044	-0.000224	-0.000176	0.000000	0.003278	0.053
-90.	6.0	21.6	0.00	0.00	1.03	0.030	0.031	0.060	-0.000382	-0.000484	0.000000	0.005430	0.071
-90.	9.0	21.6	0.01	-0.01	0.95	0.040	0.042	0.076	-0.000434	-0.001132	0.000000	0.009048	0.100
-90.	12.0	21.6	0.01	-0.01	0.95	0.040	0.042	0.076	-0.000434	-0.001132	0.000000	0.009048	0.195
-180.	15.0	21.3	-0.12	0.11	0.61	0.114	0.128	0.181	0.001394	0.013150	0.000000	0.062280	0.397
-90.	15.0	21.6	0.08	-0.11	0.60	0.131	0.125	0.186	0.003528	-0.010764	0.000000	0.067411	0.426
-180.	18.0	21.6	0.00	0.04	0.74	0.000	0.103	0.243	0.000000	-0.000926	0.000000	0.069698	0.357
-90.	18.0	21.6	-0.07	-0.04	0.75	0.136	0.122	0.290	0.001133	0.003318	0.000000	0.117320	0.455
-90.	21.0	26.4	1.13	0.47	1.33	0.211	0.196	0.271	0.017453	0.017377	0.017377	0.156116	0.219
-90.	24.0	26.4	1.16	0.39	1.44	0.157	0.153	0.229	0.000826	0.004282	0.004282	0.100638	0.168
-90.	27.0	26.4	1.12	0.25	1.23	0.130	0.151	0.249	0.003806	0.000549	0.000549	0.101478	0.190
-90.	30.0	26.4	1.09	0.09	1.06	0.127	0.160	0.260	0.006593	-0.000970	-0.000970	0.109432	0.217
-90.	33.0	26.4	1.08	0.00	1.06	0.126	0.000	0.280	0.003743	0.000000	0.000000	0.094428	0.203
-90.	33.0	26.3	1.14	0.00	1.07	0.184	0.000	0.193	0.007571	0.000000	0.000000	0.071184	0.171
-99.	33.4	26.3	1.09	0.00	1.04	0.192	0.000	0.194	0.009412	0.000000	0.000000	0.074676	0.181
-81.	33.4	26.3	0.91	-0.14	0.66	0.186	0.028	0.200	0.003391	-0.000514	-0.005234	0.075376	0.243
-81.	33.4	26.3	1.31	0.20	1.21	0.142	0.021	0.121	0.001117	0.000169	0.003042	0.035258	0.104
-99.	33.4	26.3	1.21	0.18	1.32	0.139	0.021	0.121	0.001954	0.000296	0.002934	0.034434	0.103
-73.	34.5	26.3	0.63	-0.10	0.87	0.208	0.032	0.181	0.015894	-0.002408	-0.006569	0.077075	0.257
-73.	34.5	26.3	1.27	0.38	1.10	0.153	0.046	0.142	0.005318	0.001612	0.007092	0.045784	0.124
-90.	36.0	26.3	0.90	0.27	1.39	0.166	0.050	0.146	0.005851	0.001773	0.008383	0.051632	0.135
-90.	36.0	26.3	1.09	0.00	1.24	0.116	0.000	0.242	0.002778	0.000000	0.000000	0.072050	0.162
-66.	36.2	26.3	1.19	0.00	1.11	0.161	0.000	0.214	0.007688	0.000000	0.000000	0.071613	0.164
-66.	36.2	26.3	1.07	0.49	0.94	0.211	0.096	0.171	0.017828	0.008104	0.020180	0.082961	0.191
-59.	38.6	26.3	0.60	0.27	1.33	0.181	0.082	0.211	0.020429	0.009286	0.014904	0.084069	0.196
-90.	39.0	26.3	0.40	0.52	0.48	0.195	0.207	0.163	0.012224	0.020587	0.019712	0.107120	0.399
-90.	39.0	26.3	1.04	0.00	1.00	0.162	0.000	0.256	0.014161	0.000000	0.000000	0.091772	0.209
-90.	42.0	26.3	1.06	0.00	0.99	0.265	0.000	0.201	0.018485	0.000000	0.000000	0.110588	0.229
-90.	42.0	26.3	0.52	0.00	0.37	0.214	0.000	0.180	0.025145	0.000000	0.000000	0.078464	0.440
			0.43	0.00	0.40	0.267	0.000	0.163	0.026501	0.000000	0.000000	0.097630	0.535

Table 26: Normalized data for the 45° fixed vane swirl generator; $\hat{U}_z = 30.3$ m/s for the primary flow and $\hat{U}_z = 22.4$ m/s for the secondary flow: z=10 mm

θ (deg)	r (mm)	T_a(°C)	U_θ (m/s)	U_r(m/s)	U_z (m/s)	u'_θ (m/s)	u'_r (m/s)	u'_z (m/s)	$\overline{u_\theta u_z}(m^2/s^2)$	$\overline{u_r u_z}(m^2/s^2)$	$\overline{u_r u_\theta}(m^2/s^2)$	$q^2(m^2/s^2)$	q/Q
-90.	0.0	19.6	0.8	0.8	20.8	0.53	0.51	0.78	0.073	-0.004	0.000	1.16	0.05
-90.	3.0	19.6	2.3	1.0	22.3	0.56	0.53	0.90	0.047	0.108	0.000	1.42	0.05
-90.	6.0	19.6	1.6	1.2	19.9	0.62	0.64	1.12	0.016	0.268	0.000	2.04	0.07
-90.	9.0	19.6	1.1	1.2	18.0	0.75	0.83	1.37	0.040	0.428	0.000	3.14	0.10
-90.	12.0	19.6	1.6	1.5	17.9	1.13	1.36	1.96	0.214	1.321	0.000	6.96	0.15
-90.	15.0	19.6	3.0	1.9	10.0	2.03	1.71	2.89	2.226	1.595	0.000	15.40	0.37
-90.	18.0	19.6	-2.1	0.9	6.8	1.75	1.95	2.26	-1.409	-2.157	0.000	11.95	0.48
-90.	21.0	24.2	13.1	-4.9	13.0	3.50	3.08	3.97	7.712	-4.178	-4.178	37.48	0.32
-90.	24.0	24.2	15.5	-3.0	21.1	2.81	2.18	3.06	0.022	-0.941	-0.941	21.99	0.18
-90.	27.0	24.2	15.7	-0.9	19.9	2.21	2.13	2.55	0.068	0.266	0.266	15.92	0.16
-90.	30.0	24.2	16.6	0.9	18.2	2.25	2.17	2.53	0.624	-0.129	-0.129	16.17	0.16
-90.	33.0	24.2	18.1	2.0	17.2	2.15	2.02	2.43	0.943	-0.301	-0.301	14.60	0.15
-81.	33.4	24.3	11.8	-3.1	12.1	2.24	2.32	3.62	-0.026	0.197	0.258	23.50	0.28
-73.	34.5	24.6	18.2	2.2	14.5	2.78	1.82	1.84	1.552	0.139	0.584	14.42	0.17
-90.	36.0	24.3	16.7	1.0	14.2	2.59	2.12	2.37	3.002	0.489	0.247	16.82	0.18
-66.	36.2	24.6	5.3	1.4	17.1	1.79	2.12	1.74	0.663	-0.433	-0.433	10.73	0.14
-59.	38.6	24.6	5.8	-4.1	19.2	2.28	1.90	3.69	3.874	0.585	-0.711	22.45	0.23
-90.	39.0	24.3	15.4	1.2	5.4	2.68	1.82	1.95	2.942	-0.019	0.355	14.28	0.47
-90.	42.0	24.3	7.0	1.3	14.3	2.26	2.72	2.91	2.191	3.081	3.081	20.96	0.22
-90.	44.0	24.3	3.6	1.0	5.2	2.93	2.40	2.35	3.908	3.220	3.220	19.89	0.51
				0.0	3.3	2.11	0.00	1.49	1.997	0.000	0.000	6.68	0.53

Table 27: Data for the 45° fixed vane swirl generator presented in cylindrical coordinates; z=9 mm.

θ (deg)	r (mm)	T_a(°C)	$\frac{U_a}{\hat{U}_z}$	$\frac{V_a}{\hat{U}_z}$	$\frac{W_a}{\hat{U}_z}$	$\frac{u'_a}{\hat{U}_z}$	$\frac{v'_a}{\hat{U}_z}$	$\frac{w'_a}{\hat{U}_z}$	$\frac{\overline{u_a v_a}}{\hat{U}^2}$	$\frac{\overline{u_a w_a}}{\hat{U}^2}$	$\frac{\overline{v_a w_a}}{\hat{U}^2}$	$\frac{q^2}{\hat{U}^2}$	q/Q
-90.	0.0	19.6	0.04	0.04	1.08	0.027	0.027	0.041	0.000196	-0.000011	0.000000	0.003099	0.052
-90.	3.0	19.6	0.12	0.06	1.15	0.030	0.027	0.046	0.000126	0.000289	0.000000	0.003801	0.053
-90.	6.0	19.6	0.09	0.06	1.03	0.032	0.033	0.058	0.000042	0.000719	0.000000	0.005468	0.072
-90.	9.0	19.6	0.05	0.06	0.93	0.039	0.043	0.071	0.000108	0.001146	0.000000	0.008413	0.098
-90.	12.0	19.6	0.05	0.06	0.93	0.039	0.043	0.071	0.000108	0.001146	0.000000	0.008413	0.147
-90.	15.0	19.6	0.23	0.15	0.76	0.154	0.129	0.218	0.012705	0.009106	0.000000	0.087910	0.368
-90.	18.0	19.6	-0.16	0.07	0.52	0.132	0.147	0.171	-0.008044	-0.012315	0.000000	0.068206	0.480
-90.	21.0	24.2	0.99	-0.37	0.98	0.264	0.232	0.300	0.044022	-0.023850	-0.023850	0.213941	0.320
-90.	24.0	24.2	1.17	-0.23	1.59	0.212	0.164	0.231	0.000123	-0.005369	-0.005369	0.125533	0.178
-90.	27.0	24.2	1.19	-0.07	1.51	0.167	0.161	0.193	0.000386	0.001517	0.001517	0.090857	0.157
-90.	30.0	24.2	1.26	0.07	1.37	0.170	0.164	0.191	0.003559	-0.000735	-0.000735	0.092309	0.163
-90.	33.0	24.2	1.36	0.15	1.30	0.162	0.153	0.184	0.005385	-0.001719	-0.001719	0.083315	0.153
-99.	33.4	24.3	0.89	-0.24	0.91	0.169	0.175	0.274	-0.000149	0.001127	0.001475	0.134151	0.282
-81.	33.4	24.3	1.28	0.17	1.10	0.210	0.138	0.139	0.008861	0.000796	0.003333	0.082326	0.169
-73.	34.5	24.6	1.37	0.08	1.07	0.196	0.160	0.179	0.017133	0.002789	0.001411	0.096005	0.178
-90.	36.0	24.3	1.26	0.10	1.29	0.135	0.160	0.131	0.003786	-0.002474	-0.002474	0.061267	0.137
-66.	36.2	24.6	0.40	-0.31	1.45	0.173	0.144	0.279	0.022112	0.003341	-0.004060	0.128164	0.233
-59.	38.6	24.6	0.44	0.09	0.41	0.202	0.138	0.147	0.016793	-0.000111	0.002024	0.081499	0.471
-90.	39.0	24.3	1.16	0.10	1.08	0.171	0.206	0.220	0.012505	0.017588	0.017588	0.119623	0.218
-90.	42.0	24.3	0.53	0.07	0.40	0.222	0.182	0.177	0.022308	0.018382	0.018382	0.113536	0.509
-90.	44.0	24.3	0.27	0.00	0.25	0.159	0.000	0.113	0.011399	0.000000	0.000000	0.038101	0.533

Table 28: Normalized data for the 45° fixed vane swirl generator; $\hat{U}_z = 19.3$ m/s for the primary flow and $\hat{U}_z = 13.2$ m/s for the secondary flow; z=9 mm.

θ (deg)	r (mm)	T_a(°C)	U_θ (m/s)	U_r(m/s)	U_z (m/s)	u'_θ (m/s)	u'_r (m/s)	u'_z (m/s)	$\overline{u_\theta u_z}(m^2/s^2)$	$\overline{u_r u_z}(m^2/s^2)$	$\overline{u_r u_\theta}(m^2/s^2)$	$q^2(m^2/s^2)$	q/Q
-90.	0.0	24.2	0.0	0.0	17.6	0.66	0.56	0.70	-0.051	-0.080	0.000	1.23	0.06
-90.	3.0	24.2	-0.1	0.1	16.9	0.71	0.69	0.88	-0.025	0.089	0.000	1.77	0.08
-90.	6.0	24.3	-0.3	0.2	16.7	0.89	0.82	1.17	0.004	0.237	0.000	2.82	0.10
-90.	9.0	24.3	-0.4	0.3	14.1	1.13	1.05	1.49	0.102	0.430	0.000	4.59	0.15
-90.	12.0	24.3	-1.4	0.7	10.6	1.84	1.71	2.82	0.625	1.306	0.000	14.25	0.35
-90.	15.0	24.3	-0.5	0.4	5.4	1.50	1.55	2.42	-0.855	0.977	0.000	10.49	0.59
-90.	18.0	24.3	0.1	0.2	4.8	1.09	1.23	2.00	-0.041	-0.290	0.000	6.72	0.54
-90.	21.0	28.7	6.4	-0.1	2.8	2.99	1.60	1.94	2.848	-0.495	-0.858	15.25	0.56
-90.	24.0	28.7	8.2	0.3	3.5	4.06	2.28	1.96	0.287	-1.046	-1.811	25.50	0.56
-90.	27.0	28.7	10.6	1.9	5.2	4.24	3.03	2.35	1.300	0.768	1.330	32.69	0.48
-90.	30.0	28.7	12.5	3.0	6.8	4.14	2.87	2.78	4.152	2.175	3.766	33.10	0.40
-90.	33.0	28.7	17.6	4.6	8.6	4.39	2.82	3.21	3.955	2.076	3.595	37.55	0.20
-99.	33.4	28.7	16.8	4.9	10.9	5.15	3.34	3.48	4.734	3.830	5.759	49.52	0.34
-99.	33.4	28.7	23.6	3.9	11.2	4.98	3.33	3.64	7.590	3.397	6.023	49.14	0.27
-73.	34.5	28.7	13.6	8.9	9.4	4.31	3.71	3.26	3.648	2.793	4.981	42.98	0.35
-107.	34.5	28.7	22.1	-6.7	13.8	6.66	2.02	3.24	14.732	-4.464	-13.436	58.90	0.29
-90.	36.0	28.7	25.4	8.9	12.5	5.18	3.10	3.21	1.761	2.611	4.522	46.70	0.23
-90.	39.0	28.7	30.3	13.7	16.6	6.55	3.22	2.69	3.313	2.760	4.780	60.54	0.21
-90.	41.0	28.7	28.9	14.5	17.3	7.39	3.75	3.01	10.441	4.980	8.626	77.72	0.24

Table 29: Data for the 60° fixed vane swirl generator presented in cylindrical coordinates;

z=6 mm.

θ (deg)	r (mm)	T_a(°C)	$\frac{U_\theta}{U_s}$	$\frac{U_r}{U_s}$	$\frac{U_z}{U_s}$	$\frac{u'_\theta}{U_s}$	$\frac{u'_r}{U_s}$	$\frac{u'_z}{U_s}$	$\frac{\overline{u_\theta u_z}}{U_s^2}$	$\frac{\overline{u_r u_z}}{U_s^2}$	$\frac{\overline{u_r u_\theta}}{U_s^2}$	$\frac{k^2}{U_s^2}$	q/Q
-90.	0.0	24.2	0.00	0.00	1.14	0.042	0.036	0.045	-0.000212	-0.000334	0.000000	0.005156	0.063
-90.	3.0	24.2	-0.01	0.00	1.10	0.046	0.045	0.057	-0.000106	0.000372	0.000000	0.007423	0.079
-90.	6.0	24.3	-0.02	0.01	1.08	0.057	0.053	0.075	0.000018	0.000992	0.000000	0.011826	0.100
-90.	9.0	24.3	-0.02	0.02	0.91	0.073	0.068	0.096	0.000427	0.001803	0.000000	0.019224	0.152
-90.	12.0	24.3	-0.02	0.02	0.91	0.073	0.068	0.096	0.000427	0.001803	0.000000	0.019224	0.353
-90.	15.0	24.3	-0.05	0.04	0.51	0.140	0.145	0.227	-0.007544	0.008617	0.000000	0.092561	0.593
-90.	18.0	24.3	0.01	0.02	0.45	0.102	0.116	0.188	-0.000365	-0.002559	0.000000	0.059305	0.543
-90.	21.0	28.7	0.60	-0.01	0.26	0.281	0.150	0.182	0.025119	-0.004370	-0.007569	0.134474	0.556
-90.	24.0	28.7	0.77	0.03	0.33	0.381	0.214	0.184	0.002528	-0.009221	-0.015972	0.224902	0.562
-90.	27.0	28.7	1.00	0.18	0.49	0.398	0.285	0.221	0.011464	0.006772	0.011729	0.288300	0.476
-90.	30.0	28.7	1.17	0.28	0.64	0.389	0.269	0.261	0.036617	0.019179	0.033220	0.291942	0.396
-90.	33.0	28.7	1.65	0.43	0.81	0.413	0.264	0.301	0.034883	0.018306	0.031708	0.331154	0.305
-99.	33.4	28.7	1.57	0.46	1.02	0.484	0.313	0.327	0.041753	0.033779	0.050790	0.439449	0.343
-90.	33.4	28.7	2.21	0.36	1.05	0.468	0.313	0.342	0.066946	0.029962	0.053119	0.433450	0.266
-73.	34.5	28.7	1.28	0.84	0.88	0.405	0.348	0.306	0.032180	0.024638	0.043933	0.379041	0.349
-107.	34.5	28.7	2.07	-0.63	1.30	0.625	0.189	0.304	0.129941	-0.039376	-0.118501	0.519498	0.285
-90.	36.0	28.7	2.38	0.84	1.17	0.486	0.291	0.301	0.015529	0.023028	0.039886	0.411851	0.230
-90.	39.0	28.7	2.84	1.28	1.56	0.615	0.303	0.253	0.029216	0.024340	0.042159	0.533993	0.210
-90.	41.0	28.7	2.71	1.36	1.63	0.694	0.353	0.283	0.092086	0.043926	0.076081	0.685484	0.240

Table 30: Normalized data for the 60° fixed vane swirl generator; $\hat{U}_s = 15.4$ m/s for the primary flow and $\hat{U}_s = 10.6$ m/s for the secondary flow; z=6 mm.

θ (deg)	r (mm)	T_s(°C)	U_θ (m/s)	U_r(m/s)	U_z (m/s)	u'_θ (m/s)	u'_r (m/s)	u'_z (m/s)	$\overline{u_\theta u_z}(m^2/s^2)$	$\overline{u_r u_z}(m^2/s^2)$	$\overline{u_r u_\theta}(m^2/s^2)$	$q^2(m^2/s^2)$	q/Q
-90.	0.0	23.1	-0.9	0.3	18.7	3.89	4.05	5.95	-2.219	-0.329	0.000	66.97	0.44
90.	5.0	23.1	0.7	0.1	17.4	3.63	3.81	6.22	3.481	3.246	0.000	66.48	0.47
90.	10.0	23.0	0.6	0.3	15.3	3.37	3.41	6.14	2.781	5.375	0.000	60.68	0.51
90.	15.0	23.2	0.6	0.4	13.0	3.20	3.18	5.66	2.301	5.005	0.000	52.39	0.56
90.	20.0	23.1	0.5	0.5	10.6	2.78	2.69	5.39	2.018	4.060	0.000	43.99	0.62
90.	25.0	23.0	0.4	0.4	8.7	2.19	2.28	4.66	1.402	3.023	0.000	31.66	0.65
90.	30.0	23.0	0.3	0.2	7.2	1.75	1.87	3.76	0.940	2.166	0.000	20.69	0.63
90.	35.0	23.0	0.2	0.0	5.7	1.35	1.43	3.14	0.381	0.953	0.000	13.75	0.64
90.	40.0	22.9	0.2	-0.2	4.9	1.22	1.24	2.61	0.328	0.340	0.000	9.87	0.64

Table 31: Data for the primary flow of the IFRF variable swirl generator presented in cylindrical coordinates; z=2.5 mm.

θ (deg)	r (mm)	T_s(°C)	$\frac{U_\theta}{U_s}$	$\frac{U_r}{U_s}$	$\frac{U_z}{U_s}$	$\frac{u'_\theta}{U_s}$	$\frac{u'_r}{U_s}$	$\frac{u'_z}{U_s}$	$\frac{\overline{u_\theta u_z}}{U_s^2}$	$\frac{\overline{u_r u_z}}{U_s^2}$	$\frac{\overline{u_r u_\theta}}{U_s^2}$	$\frac{q^2}{U_s^2}$	q/Q
-90.	0.0	23.1	-0.11	0.04	2.29	0.476	0.494	0.727	-0.033096	-0.004908	0.000000	0.998869	0.437
90.	5.0	23.1	0.09	0.01	2.13	0.444	0.465	0.760	0.051925	0.048409	0.000000	0.991592	0.467
90.	10.0	23.0	0.08	0.04	1.86	0.411	0.417	0.750	0.041456	0.080168	0.000000	0.905051	0.510
90.	15.0	23.2	0.07	0.05	1.59	0.391	0.388	0.691	0.034314	0.074648	0.000000	0.781397	0.557
90.	20.0	23.1	0.06	0.06	1.30	0.339	0.329	0.658	0.030105	0.060638	0.000000	0.656108	0.623
90.	25.0	23.0	0.05	0.05	1.06	0.267	0.278	0.569	0.020913	0.045090	0.000000	0.472207	0.648
90.	30.0	23.0	0.04	0.03	0.87	0.214	0.228	0.459	0.014022	0.032307	0.000000	0.308555	0.635
90.	35.0	23.0	0.03	0.00	0.70	0.164	0.175	0.384	0.005687	0.014218	0.000000	0.205039	0.645
90.	40.0	22.9	0.02	-0.02	0.59	0.149	0.152	0.319	0.004885	0.005067	0.000000	0.147199	0.645

Table 32: Normalized data for the primary flow of the IFRF variable swirl generator;

$\bar{U}_s$ = 15.4 m/s, z=2.5 mm.

θ (deg)	r (mm)	T_a(°C)	U_θ (m/s)	U_r(m/s)	U_z (m/s)	u'_θ (m/s)	u'_r (m/s)	u'_z (m/s)	$\overline{u_\theta u_z}(m^2/s^2)$	$\overline{u_r u_z}(m^2/s^2)$	$\overline{u_r u_\theta}(m^2/s^2)$	$q^2(m^2/s^2)$	q/Q
-90.	0.0	22.2	-0.5	0.4	13.4	2.68	2.30	4.50	-1.891	0.351	0.000	32.70	0.43
90.	5.0	22.3	0.5	-0.1	12.3	2.62	2.27	4.60	1.557	0.875	0.000	33.21	0.47
-90.	5.0	22.2	-0.6	0.7	13.7	2.76	2.36	4.62	-2.087	1.450	0.000	34.52	0.43
90.	10.0	22.3	0.4	0.0	10.8	2.46	2.14	4.19	1.410	1.554	0.000	28.17	0.49
-90.	10.0	22.2	-0.7	0.9	13.2	2.70	2.29	4.37	-2.381	2.731	0.000	31.64	0.43
90.	15.0	22.2	0.3	0.1	9.0	2.23	1.88	3.86	1.449	2.026	0.000	23.43	0.54
-90.	15.0	22.2	-0.7	0.9	11.8	2.64	2.14	4.48	-1.444	3.226	0.000	31.67	0.47
90.	20.0	22.4	0.3	0.1	7.5	1.90	1.59	3.63	0.812	1.348	0.000	19.35	0.58
-90.	20.0	22.2	-0.6	1.0	10.1	2.35	2.06	4.26	-1.220	3.411	0.000	27.86	0.52
90.	25.0	22.4	0.2	0.1	6.1	1.58	1.36	3.28	0.550	1.050	0.000	15.12	0.64
-90.	25.0	22.2	-0.5	0.9	8.3	2.05	1.69	3.92	-0.941	2.655	0.000	22.45	0.57
90.	30.0	22.5	0.2	0.1	4.8	1.22	0.99	2.71	0.376	0.348	0.000	9.79	0.65
-90.	30.0	21.8	-0.4	0.7	6.7	1.77	1.41	3.60	-1.127	1.777	0.000	18.10	0.63
90.	35.0	22.4	0.2	0.0	3.9	0.97	0.84	2.04	0.020	0.390	0.000	5.79	0.61
-90.	35.0	21.7	-0.3	0.5	5.4	1.36	1.15	3.06	-0.819	1.364	0.000	12.54	0.65
90.	40.0	22.6	0.2	-0.1	3.2	0.85	0.55	1.96	0.216	0.007	0.000	4.88	0.69
-90.	40.0	21.7	-0.2	0.4	4.3	1.10	0.94	2.67	-0.655	0.836	0.000	9.26	0.71

Table 33: Data for the primary flow of the IFRF variable swirl generator presented in cylindrical coordinates; z=2.5 mm.

θ (deg)	r (mm)	T_a(°C)	$\frac{U_\theta}{U_z}$	$\frac{U_r}{U_z}$	$\frac{U_z}{U_z}$	$\frac{u'_\theta}{U_z}$	$\frac{u'_r}{U_z}$	$\frac{u'_z}{U_z}$	$\frac{\overline{u_\theta u_z}}{U_z^2}$	$\frac{\overline{u_r u_z}}{U_z^2}$	$\frac{\overline{u_r u_\theta}}{U_z^2}$	$\frac{q^2}{U_z^2}$	q/Q
-90.	0.0	22.2	-0.06	0.06	2.03	0.407	0.349	0.684	-0.043686	0.008097	0.000000	0.755326	0.427
90.	5.0	22.3	0.07	-0.02	1.87	0.396	0.346	0.700	0.035967	0.020210	0.000000	0.767140	0.468
-90.	5.0	22.2	-0.10	0.10	2.08	0.419	0.358	0.702	-0.048198	0.033485	0.000000	0.797219	0.428
90.	10.0	22.3	0.06	0.01	1.64	0.374	0.325	0.637	0.032574	0.035885	0.000000	0.650576	0.491
-90.	10.0	22.2	-0.11	0.13	2.00	0.411	0.348	0.664	-0.054993	0.063072	0.000000	0.730798	0.425
90.	15.0	22.2	0.05	0.02	1.37	0.340	0.286	0.587	0.033478	0.046793	0.000000	0.541086	0.536
-90.	15.0	22.2	-0.11	0.14	1.80	0.402	0.326	0.681	-0.033349	0.074502	0.000000	0.731586	0.474
90.	20.0	22.4	0.05	0.02	1.15	0.289	0.242	0.552	0.018763	0.031139	0.000000	0.447025	0.582
-90.	20.0	22.2	-0.10	0.14	1.53	0.357	0.313	0.647	-0.028186	0.078791	0.000000	0.643496	0.520
90.	25.0	22.4	0.04	0.02	0.93	0.240	0.207	0.499	0.012707	0.024246	0.000000	0.349303	0.635
-90.	25.0	22.2	-0.08	0.13	1.26	0.312	0.256	0.596	-0.021744	0.061327	0.000000	0.518432	0.566
90.	30.0	22.5	0.03	0.01	0.74	0.186	0.150	0.411	0.009684	0.008037	0.000000	0.226136	0.646
-90.	30.0	21.8	-0.06	0.10	1.02	0.269	0.214	0.548	-0.026032	0.041034	0.000000	0.418162	0.629
90.	35.0	22.4	0.03	0.00	0.60	0.147	0.128	0.310	0.000460	0.009015	0.000000	0.133764	0.611
-90.	35.0	21.7	-0.05	0.08	0.82	0.207	0.175	0.465	-0.018913	0.031501	0.000000	0.289585	0.648
90.	40.0	22.4	0.02	-0.01	0.48	0.130	0.084	0.298	0.004983	0.000153	0.000000	0.112767	0.692
-90.	40.0	21.7	-0.03	0.05	0.65	0.168	0.143	0.407	-0.015135	0.019296	0.000000	0.213805	0.707

Table 34: Normalized data for the primary flow of the IFRF variable swirl generator; $\bar{U}_z$ = 6.6 m/s, z=10 mm.

θ (deg)	r (mm)	T_s(°C)	U_θ (m/s)	U_r(m/s)	U_z (m/s)	u'_θ (m/s)	u'_r (m/s)	u'_z (m/s)	$\overline{u_\theta u_z}(m^2/s^2)$	$\overline{u_r u_z}(m^2/s^2)$	$\overline{u_r u_\theta}(m^2/s^2)$	$q^2(m^2/s^2)$	q/Q
90.	50.0	33.1	1.1	-1.2	16.5	2.13	1.12	1.87	0.246	0.097	0.000	9.29	0.18
90.	55.0	33.0	0.9	-1.1	15.9	1.88	1.56	1.79	0.175	0.588	0.000	9.16	0.19
90.	60.0	33.0	0.9	-1.1	15.2	1.88	1.78	1.90	0.304	0.776	0.000	10.28	0.21
90.	65.0	33.0	0.8	-1.1	14.6	1.84	1.82	1.82	0.357	0.587	0.000	10.00	0.22
90.	70.0	33.0	0.6	-1.1	14.2	1.90	1.74	1.86	0.407	0.399	0.000	10.07	0.22
90.	75.0	33.0	0.4	-1.1	13.8	1.99	1.63	1.80	0.460	0.197	0.000	9.84	0.23
90.	80.0	33.0	0.2	-1.0	13.5	2.27	1.45	1.83	0.637	0.160	0.000	10.60	0.24
90.	85.0	33.0	0.0	-0.7	12.7	2.43	1.02	1.95	0.940	0.112	0.000	10.75	0.26

Table 35: Data for the secondary flow of the IFRF variable swirl generator presented in cylindrical coordinates; S=0.0, z=2.5 mm.

θ (deg)	r (mm)	$T_a(°C)$	$\frac{U_\theta}{U_x}$	$\frac{U_r}{U_x}$	$\frac{U_x}{U_x}$	$\frac{u'_\theta}{U_x}$	$\frac{u'_r}{U_x}$	$\frac{u'_x}{U_x}$	$\frac{\overline{u_\theta u_x}}{U_x^2}$	$\frac{\overline{u_r u_x}}{U_x^2}$	$\frac{\overline{u_r u_\theta}}{U_x^2}$	$\frac{q^2}{U_x^2}$	q/Q
90.	50.0	33.1	0.07	-0.08	1.15	0.149	0.078	0.130	0.001195	0.000470	0.000000	0.045110	0.184
90.	55.0	33.0	0.06	-0.07	1.11	0.131	0.108	0.124	0.000852	0.002856	0.000000	0.044471	0.190
90.	60.0	33.0	0.06	-0.08	1.06	0.131	0.124	0.132	0.001476	0.003769	0.000000	0.049917	0.210
90.	65.0	33.0	0.05	-0.08	1.02	0.128	0.127	0.127	0.001734	0.002850	0.000000	0.048548	0.215
90.	70.0	33.0	0.04	-0.08	0.99	0.132	0.121	0.130	0.001978	0.001939	0.000000	0.048894	0.223
90.	80.0	33.0	0.02	-0.07	0.97	0.139	0.114	0.125	0.002233	0.000957	0.000000	0.047758	0.226
90.	85.0	33.0	0.00	-0.05	0.89	0.169	0.071	0.136	0.004562	0.000776	0.000000	0.051468	0.241
										0.000545	0.000000	0.052168	0.257

Table 36: Normalized data for the secondary flow of the IFRF variable swirl generator; S=0.0, $\bar{U}_x = 14.4$ m/s, z=2.5 mm.

θ (deg)	r (mm)	$T_a(°C)$	U_θ (m/s)	U_r(m/s)	U_z (m/s)	u'_θ (m/s)	u'_r (m/s)	u'_z (m/s)	$\overline{u_\theta u_z}(m^2/s^2)$	$\overline{u_r u_z}(m^2/s^2)$	$\overline{u_r u_\theta}(m^2/s^2)$	$q^2(m^2/s^2)$	q/Q
90.	50.0	35.6	-8.0	-1.5	8.6	2.52	1.45	2.58	-0.650	-1.923	1.110	15.13	0.33
90.	55.0	35.6	-8.9	-0.8	9.9	2.28	1.58	2.52	-0.166	0.165	-0.095	14.03	0.28
90.	60.0	35.6	-8.0	-0.9	10.7	2.28	2.04	2.48	-0.594	0.045	-0.026	15.46	0.29
90.	65.0	35.6	-7.5	-0.9	11.5	2.45	2.29	2.34	-0.891	0.010	-0.006	16.73	0.30
90.	70.0	35.6	-7.2	-1.0	12.2	2.46	2.33	2.37	-0.444	-0.278	0.161	17.11	0.29
90.	75.0	35.6	-7.4	-1.1	13.0	2.54	2.17	2.59	0.022	-0.440	0.254	17.86	0.28
90.	80.0	35.6	-7.7	-1.0	13.4	2.70	1.91	3.09	0.991	-0.701	0.405	20.51	0.29
90.	85.0	35.6	-8.1	-0.9	13.5	2.89	1.62	3.61	1.065	-0.794	0.458	24.03	0.31

Table 37: Data for the secondary flow of the IFRF variable swirl generator presented in cylindrical coordinates; S=1.0, z=4.0 mm.

θ (deg)	r (mm)	$T_o(°C)$	$\frac{U_\theta}{U_z}$	$\frac{U_r}{U_z}$	$\frac{U_z}{U_z}$	$\frac{u'_\theta}{U_z}$	$\frac{u'_r}{U_z}$	$\frac{u'_z}{U_z}$	$\frac{\overline{u_\theta u_z}}{U_z^2}$	$\frac{\overline{u_r u_z}}{U_z^2}$	$\frac{\overline{u_r u_\theta}}{U_z^2}$	$\frac{k}{U_z^2}$	q/Q
90.	50.0	35.6	-0.67	-0.12	0.72	0.212	0.122	0.217	-0.004606	-0.013620	0.007863	0.107179	0.329
90.	55.0	35.6	-0.75	-0.07	0.83	0.192	0.133	0.212	-0.001176	0.001168	-0.000674	0.099356	0.282
90.	60.0	35.6	-0.68	-0.07	0.90	0.192	0.171	0.208	-0.004209	0.000319	-0.000184	0.109512	0.293
90.	65.0	35.6	-0.63	-0.08	0.97	0.206	0.193	0.197	-0.006312	0.000069	-0.000040	0.118473	0.298
90.	70.0	35.6	-0.61	-0.09	1.03	0.207	0.196	0.200	-0.003146	-0.001970	0.001138	0.121177	0.290
90.	75.0	35.6	-0.62	-0.09	1.09	0.213	0.183	0.218	0.000157	-0.003113	0.001797	0.126454	0.283
90.	80.0	35.6	-0.65	-0.09	1.13	0.227	0.161	0.260	0.007017	-0.004967	0.002868	0.145233	0.292
90.	85.0	35.6	-0.68	-0.08	1.14	0.243	0.136	0.304	0.007545	-0.005620	0.003244	0.170209	0.311

Table 38: Normalized data for the secondary flow of the IFRF variable swirl generator; S=1.0, $\hat{U}_z = 11.9$ m/s, z=4.0 mm.

θ (deg)	r (mm)	$T_a(°C)$	U_θ (m/s)	U_r(m/s)	U_z (m/s)	u'_θ (m/s)	u'_r (m/s)	u'_z (m/s)	$\overline{u_\theta u_z}(m^2/s^2)$	$\overline{u_r u_z}(m^2/s^2)$	$\overline{u_r u_\theta}(m^2/s^2)$	$q^2(m^2/s^2)$	q/Q
90.	50.0	32.6	-5.0	-0.7	5.7	1.78	1.04	1.71	-0.076	-0.855	0.494	7.19	0.35
90.	55.0	32.2	-5.9	-0.5	6.4	1.59	1.03	1.61	0.104	0.127	-0.074	6.19	0.29
90.	60.0	32.2	-5.5	-0.5	6.8	1.61	1.28	1.55	-0.075	0.200	-0.115	6.61	0.29
90.	65.0	32.3	-5.4	-0.5	7.1	1.65	1.49	1.52	-0.171	0.012	-0.007	7.27	0.30
90.	70.0	32.3	-5.4	-0.5	7.5	1.67	1.50	1.50	-0.294	-0.090	0.052	7.30	0.29
90.	75.0	32.3	-5.5	-0.5	7.7	1.75	1.43	1.66	0.085	-0.014	0.008	7.90	0.30
90.	80.0	32.4	-5.8	-0.5	7.7	1.80	1.31	1.91	0.262	-0.137	0.079	8.60	0.30
90.	85.0	32.4	-5.9	-0.5	7.6	1.91	1.07	2.10	0.139	-0.188	0.109	9.19	0.32

Table 39: Data for the secondary flow of the IFRF variable swirl generator presented in cylindrical coordinates; S=1.0, z=4.0 mm.

θ (deg)	r (mm)	T_∞(°C)	$\frac{U_\theta}{\hat{U}_z}$	$\frac{U_r}{\hat{U}_z}$	$\frac{U_z}{\hat{U}_z}$	$\frac{u'_\theta}{\hat{U}_z}$	$\frac{u'_r}{\hat{U}_z}$	$\frac{u'_z}{\hat{U}_z}$	$\frac{\overline{u_\theta u_r}}{\hat{U}_z^2}$	$\frac{\overline{u_\theta u_z}}{\hat{U}_z^2}$	$\frac{\overline{u_r u_z}}{\hat{U}_z^2}$	$\frac{k}{\hat{U}_z^2}$	q/Q
90.	50.0	32.6	-0.69	-0.10	0.79	0.249	0.145	0.239	-0.001487	-0.016651	0.009614	0.140099	0.354
90.	55.0	32.2	-0.82	-0.07	0.90	0.221	0.144	0.225	0.002031	0.002479	-0.001431	0.120485	0.285
90.	60.0	32.2	-0.77	-0.07	0.95	0.225	0.178	0.216	-0.001461	0.003895	-0.002249	0.128790	0.293
90.	65.0	32.3	-0.75	-0.07	1.00	0.231	0.208	0.213	-0.003328	0.000228	-0.000132	0.141606	0.301
90.	70.0	32.3	-0.75	-0.07	1.04	0.233	0.210	0.209	-0.005732	-0.001751	0.001011	0.142114	0.293
90.	75.0	32.3	-0.77	-0.07	1.07	0.245	0.200	0.232	0.001647	-0.000265	0.000153	0.153765	0.297
90.	80.0	32.4	-0.81	-0.07	1.08	0.251	0.182	0.267	0.005101	-0.002675	0.001544	0.167416	0.304
90.	85.0	32.4	-0.82	-0.06	1.06	0.266	0.150	0.293	0.002707	-0.003862	0.002114	0.178881	0.315

Table 40: Normalized data for the secondary flow of the IFRF variable swirl generator; S=1.0, $\hat{U}_z$ = 7.2 m/s, z=4.0 mm.

θ (deg)	r (mm)	T_a(°C)	U_θ (m/s)	U_r(m/s)	U_z (m/s)	u'_θ (m/s)	u'_r (m/s)	u'_z (m/s)	$\overline{u_\theta u_z}(m^2/s^2)$	$\overline{u_r u_z}(m^2/s^2)$	$\overline{u_r u_\theta}(m^2/s^2)$	$q^2(m^2/s^2)$	q/Q
90.	50.0	34.7	-9.0	0.0	9.3	4.26	0.00	3.31	-5.355	0.000	0.000	29.11	0.42
90.	50.0	35.2	-9.0	0.0	10.3	3.06	0.00	4.43	-7.691	0.000	0.000	29.00	0.39
90.	55.0	34.7	-11.8	-2.0	12.7	4.37	2.92	3.64	-5.027	-4.170	4.170	40.89	0.37
90.	60.0	34.7	-13.5	-1.7	15.6	4.35	2.77	3.66	-5.000	-2.743	2.743	40.04	0.31
90.	65.0	34.7	-15.2	-1.6	17.5	3.90	2.76	3.37	-2.631	-1.481	1.481	34.19	0.25
90.	70.0	34.7	-16.8	0.8	18.8	3.66	2.78	3.15	-0.450	-0.374	0.374	31.02	0.22
90.	70.0	35.2	-18.5	0.8	17.4	2.88	2.78	3.23	-2.169	-0.374	0.374	26.48	0.20
90.	75.0	34.8	-18.3	1.0	19.3	3.00	2.68	3.08	-0.156	-0.485	0.485	25.63	0.19
90.	80.0	34.8	-19.4	1.1	19.4	2.98	2.36	3.33	-0.116	-0.500	0.500	25.63	0.18
90.	85.0	34.8	-20.0	1.2	19.0	2.83	1.92	3.14	-0.593	0.519	-0.519	21.59	0.17

Table 41: Data for the secondary flow of the IFRF variable swirl generator presented in cylindrical coordinates; S=2.0, z=2.0 mm.

θ (deg)	r (mm)	T_o(°C)	$\frac{U_\theta}{U_x}$	$\frac{U_r}{U_x}$	$\frac{U_x}{U_x}$	$\frac{u'_\theta}{U_x}$	$\frac{u'_r}{U_x}$	$\frac{u'_x}{U_x}$	$\frac{\overline{u_\theta u_x}}{U_x^2}$	$\frac{\overline{u_r u_x}}{U_x^2}$	$\frac{\overline{u_r u_\theta}}{U_x^2}$	$\frac{k^2}{U_x^2}$	q/Q
90.	50.0	34.7	-0.54	0.00	0.56	0.258	0.000	0.201	-0.019614	0.000000	0.000000	0.106609	0.418
90.	50.0	35.2	-0.55	0.00	0.62	0.185	0.000	0.268	-0.028171	0.000000	0.000000	0.106224	0.393
90.	55.0	34.7	-0.71	-0.12	0.77	0.265	0.176	0.221	-0.018414	-0.015272	0.015272	0.149768	0.366
90.	60.0	34.7	-0.82	-0.10	0.94	0.264	0.168	0.222	-0.018315	-0.010045	0.010045	0.146671	0.306
90.	65.0	34.7	-0.92	-0.09	1.06	0.236	0.167	0.204	-0.009637	-0.005426	0.005426	0.125218	0.252
90.	70.0	34.7	-1.02	0.05	1.14	0.221	0.168	0.191	-0.001648	-0.001371	0.001371	0.113622	0.221
90.	70.0	35.2	-1.12	0.05	1.06	0.174	0.168	0.196	-0.007944	-0.001371	0.001371	0.096999	0.202
90.	75.0	34.8	-1.11	0.06	1.17	0.181	0.162	0.186	-0.000570	-0.001775	0.001775	0.093863	0.190
90.	80.0	34.8	-1.18	0.07	1.18	0.180	0.144	0.202	-0.000423	-0.001833	0.001833	0.093871	0.184
90.	85.0	34.8	-1.21	0.07	1.15	0.171	0.116	0.190	-0.002170	0.001903	-0.001903	0.079068	0.168

Table 42: Normalized data for the secondary flow of the IFRF variable swirl generator; S=2.0, $\bar{U}_x = 16.5$ m/s, z=2.0 mm.

θ (deg)	r (mm)	T_s(°C)	U_θ (m/s)	U_r(m/s)	U_z (m/s)	u'_θ (m/s)	u'_r (m/s)	u'_z (m/s)	$\overline{u_\theta u_z}(m^2/s^2)$	$\overline{u_r u_z}(m^2/s^2)$	$\overline{u_r u_\theta}(m^2/s^2)$	$q^2(m^2/s^2)$	q/Q
90.	50.0	31.4	-4.5	-0.2	4.5	2.05	0.95	1.61	-0.936	-0.239	0.239	7.68	0.43
90.	55.0	31.4	-5.9	0.1	6.0	2.26	1.14	1.84	-1.175	-0.153	0.153	9.77	0.37
90.	60.0	31.5	-6.6	0.1	7.4	2.20	1.26	1.75	-1.147	-0.038	0.038	9.54	0.31
90.	65.0	31.5	-7.2	0.2	8.3	2.06	1.33	1.73	-0.671	-0.103	0.103	8.99	0.27
90.	70.0	31.6	-7.9	0.3	9.0	1.79	1.41	1.66	-0.276	-0.136	0.136	7.96	0.24
90.	75.0	31.7	-8.6	0.4	9.4	1.53	1.33	1.61	0.091	-0.175	0.175	6.70	0.20
90.	80.0	31.8	-9.2	0.4	9.5	1.35	1.21	1.55	-0.139	-0.128	0.128	5.71	0.18
90.	85.0	31.8	-9.5	0.5	9.3	1.43	1.02	1.61	-0.148	0.106	-0.106	5.68	0.18

Table 43: Data for the secondary flow of the IFRF variable swirl generator presented in cylindrical coordinates; S=2.0, z=2.0 mm.

θ (deg)	r (mm)	$T_a(°C)$	$\frac{U_\theta}{U_z}$	$\frac{U_r}{U_z}$	$\frac{U_z}{U_z}$	$\frac{u'_\theta}{U_z}$	$\frac{u'_r}{U_z}$	$\frac{u'_z}{U_z}$	$\frac{\overline{u_\theta u_z}}{U_z^2}$	$\frac{\overline{u_r u_z}}{U_z^2}$	$\frac{\overline{u_r u_\theta}}{U_z^2}$	$\frac{q^2}{U_z^2}$	q/Q
90.	50.0	31.4	-0.55	-0.03	0.55	0.250	0.116	0.196	-0.013908	-0.003545	0.003545	0.114128	0.431
90.	55.0	31.4	-0.72	0.01	0.74	0.275	0.139	0.224	-0.017464	-0.002267	0.002267	0.145235	0.371
90.	60.0	31.5	-0.81	0.02	0.90	0.268	0.156	0.213	-0.017042	-0.000560	0.000560	0.141754	0.312
90.	65.0	31.5	-0.88	0.03	1.01	0.251	0.162	0.210	-0.009973	-0.001524	0.001524	0.133672	0.272
90.	70.0	31.6	-0.97	0.03	1.10	0.219	0.172	0.202	-0.004097	-0.002015	0.002015	0.118331	0.235
90.	75.0	31.7	-1.05	0.05	1.14	0.186	0.162	0.196	0.001358	-0.002594	0.002594	0.099509	0.203
90.	80.0	31.8	-1.12	0.05	1.16	0.165	0.148	0.189	-0.002061	-0.001904	0.001904	0.084868	0.181
90.	85.0	31.8	-1.16	0.06	1.14	0.175	0.125	0.196	-0.002205	0.001568	-0.001568	0.084461	0.179

Table 44: Normalized data for the secondary flow of the IFRF variable swirl generator; S=2.0, $\hat{U}_z = 8.2$ m/s, z=2.0 mm.

θ (deg)	r (mm)	T_a(°C)	U_θ (m/s)	U_r(m/s)	U_z (m/s)	u'_θ (m/s)	u'_r (m/s)	u'_z (m/s)	$\overline{u_\theta u_z}(m^2/s^2)$	$\overline{u_r u_z}(m^2/s^2)$	$\overline{u_r u_\theta}(m^2/s^2)$	$q^2(m^2/s^2)$	q/Q
90.	50.0	35.4	-10.5	-0.6	8.4	4.35	2.69	3.31	-8.227	-0.928	1.325	37.11	0.45
90.	55.0	35.4	-12.1	-0.7	10.6	4.77	3.07	3.96	-8.449	-1.327	1.896	47.90	0.43
90.	60.0	35.4	-15.8	0.0	14.3	5.55	3.89	4.46	-10.808	-1.335	1.907	65.88	0.38
90.	65.0	35.4	-20.9	1.2	17.7	5.59	4.05	4.45	-8.227	-1.349	1.927	67.40	0.30
90.	70.0	35.3	-25.8	2.2	19.4	4.97	4.06	4.32	-4.463	-1.628	2.325	59.85	0.24
90.	75.0	35.2	-29.4	2.8	19.1	4.34	3.65	4.25	-4.062	-1.512	2.159	50.25	0.20
90.	80.0	35.1	-31.4	2.9	17.7	3.69	3.27	3.83	-5.139	-1.628	2.324	38.99	0.17
90.	85.0	35.0	-32.0	2.6	16.1	3.63	2.62	3.56	-4.609	-0.623	0.890	32.68	0.16

Table 45: Data for the secondary flow of the IFRF variable swirl generator presented in cylindrical coordinates; S=3.0, z=2.0 mm.

θ (deg)	r (mm)	T_o(°C)	$\frac{U_\theta}{U_s}$	$\frac{U_r}{U_s}$	$\frac{U_z}{U_s}$	$\frac{u'_\theta}{U_s}$	$\frac{u'_r}{U_s}$	$\frac{u'_z}{U_s}$	$\frac{\overline{u_\theta u_z}}{U_s^2}$	$\frac{\overline{u_r u_z}}{U_s^2}$	$\frac{\overline{u_r u_\theta}}{U_s^2}$	$\frac{q^2}{U_s^2}$	q/Q
90.	50.0	35.4	-0.66	-0.04	0.53	0.274	0.169	0.206	-0.032505	-0.003666	0.005236	0.146642	0.452
90.	55.0	35.4	-0.76	-0.04	0.67	0.300	0.193	0.249	-0.033383	-0.005245	0.007491	0.189262	0.430
90.	60.0	35.4	-0.99	0.00	0.90	0.349	0.244	0.280	-0.042707	-0.005277	0.007536	0.260324	0.381
90.	65.0	35.4	-1.31	0.07	1.11	0.351	0.255	0.280	-0.032505	-0.005331	0.007614	0.266303	0.300
90.	70.0	35.3	-1.62	0.14	1.22	0.312	0.255	0.272	-0.017635	-0.006433	0.009188	0.236480	0.239
90.	75.0	35.2	-1.85	0.18	1.20	0.273	0.229	0.267	-0.016051	-0.005974	0.008532	0.198540	0.202
90.	80.0	35.1	-1.97	0.18	1.11	0.232	0.206	0.241	-0.020307	-0.006431	0.009184	0.154040	0.173
90.	85.0	35.0	-2.01	0.16	1.01	0.228	0.165	0.224	-0.018211	-0.002463	0.003517	0.129119	0.159

Table 46: Normalized data for the secondary flow of the IFRF variable swirl generator; S=3.0, $\hat{U}_s$ = 15.9 m/s, z=2.0 mm.

θ (deg)	r (mm)	T_s(°C)	U_θ (m/s)	U_r(m/s)	U_z (m/s)	u'_θ (m/s)	u'_r (m/s)	u'_z (m/s)	$\overline{u_\theta u_z}(m^2/s^2)$	$\overline{u_r u_z}(m^2/s^2)$	$\overline{u_r u_\theta}(m^2/s^2)$	$q^2(m^2/s^2)$	q/Q
90.	50.0	31.0	-5.1	-0.3	4.1	2.23	1.32	1.76	-2.284	-0.324	0.462	9.83	0.48
90.	55.0	31.1	-5.9	-0.4	5.2	2.43	1.51	2.05	-2.156	-0.376	0.540	12.35	0.45
90.	60.0	31.1	-7.6	-0.1	7.0	2.82	1.98	2.29	-2.734	-0.423	0.604	17.12	0.40
90.	65.0	31.1	-10.1	0.5	8.7	3.04	2.05	2.40	-2.743	-0.495	0.707	19.19	0.33
90.	70.0	31.0	-12.6	1.0	9.6	2.64	2.06	2.25	-1.231	-0.409	0.584	16.31	0.25
90.	75.0	31.0	-14.4	1.4	9.5	2.30	1.95	2.27	-1.145	-0.535	0.764	14.27	0.22
90.	80.0	31.0	-15.4	1.4	8.8	1.92	1.67	2.00	-1.199	-0.346	0.495	10.50	0.18
90.	85.0	31.2	-15.8	1.3	8.1	1.90	1.36	1.82	-1.320	-0.175	0.250	8.77	0.17

Table 47: Data for the secondary flow of the IFRF variable swirl generator, presented in cylindrical coordinates; S=3.0, z=2.0 mm.

θ (deg)	r (mm)	T_s(°C)	$\frac{U_\theta}{U_s}$	$\frac{U_r}{U_s}$	$\frac{U_z}{U_s}$	$\frac{u'_\theta}{U_s}$	$\frac{u'_r}{U_s}$	$\frac{u'_z}{U_s}$	$\frac{\overline{u_\theta u_r}}{U_s^2}$	$\frac{\overline{u_\theta u_z}}{U_s^2}$	$\frac{\overline{u_r u_z}}{U_s^2}$	$\frac{q^2}{U_s^2}$	q/Q
90.	50.0	31.0	-0.65	-0.04	0.52	0.284	0.168	0.224	-0.036936	-0.005237	0.007479	0.159016	0.479
90.	55.0	31.1	-0.75	-0.05	0.66	0.309	0.192	0.260	-0.034866	-0.006116	0.008735	0.199785	0.449
90.	60.0	31.1	-0.97	-0.01	0.88	0.359	0.252	0.291	-0.044212	-0.006834	0.009760	0.276908	0.401
90.	65.0	31.1	-1.28	0.06	1.11	0.386	0.261	0.306	-0.044354	-0.006000	0.011425	0.310253	0.326
90.	70.0	31.0	-1.60	0.13	1.22	0.336	0.262	0.286	-0.019908	-0.006610	0.009440	0.263757	0.254
90.	75.0	31.0	-1.84	0.18	1.21	0.293	0.248	0.289	-0.018517	-0.005652	0.012356	0.230729	0.218
90.	80.0	31.0	-1.96	0.18	1.12	0.244	0.212	0.255	-0.019392	-0.005601	0.007999	0.169827	0.182
90.	85.0	31.2	-2.00	0.17	1.02	0.241	0.173	0.232	-0.021339	-0.002826	0.004039	0.141903	0.167

Table 48: Normalized data for the secondary flow of the IFRF variable swirl generator; S=3.0, $\hat{U}_s$ = 7.9 m/s, z=2.0 mm.

θ (deg)	r (mm)	T_a(°C)	U_θ (m/s)	U_r(m/s)	U_z (m/s)	u'_θ (m/s)	u'_r (m/s)	u'_z (m/s)	$\overline{u_\theta u_z}(m^2/s^2)$	$\overline{u_r u_z}(m^2/s^2)$	$\overline{u_r u_\theta}(m^2/s^2)$	$q^2(m^2/s^2)$	q/Q
90.	50.0	35.6	-13.2	-1.3	10.2	5.43	2.85	4.02	-13.858	-0.921	1.315	53.78	0.44
90.	55.0	35.6	-13.9	-1.5	11.7	5.37	3.31	4.42	-11.177	-1.326	1.893	59.28	0.42
90.	60.0	35.6	-16.4	-1.0	14.9	6.23	3.91	5.09	-16.241	-2.049	2.927	80.04	0.40
90.	65.0	35.6	-21.0	0.3	19.3	6.84	4.41	5.40	-17.969	-2.281	3.258	95.38	0.34
90.	70.0	35.6	-26.4	1.8	22.9	6.66	4.47	5.22	-13.670	-2.979	4.254	91.59	0.27
90.	75.0	35.6	-31.8	3.4	24.6	6.17	4.26	5.43	-10.585	-3.715	5.305	85.79	0.23
90.	80.0	35.6	-35.8	4.3	24.1	5.25	3.69	5.42	-10.635	-4.122	5.886	70.55	0.19
90.	85.0	35.6	-37.9	4.5	22.3	4.78	3.10	5.14	-11.183	-3.359	4.797	58.89	0.17

Table 49: Data for the secondary flow of the IFRF variable swirl generator presented in cylindrical coordinates; S=4.0, z=10 mm.

θ (deg)	r (mm)	T_a(°C)	$\frac{U_\theta}{U_s}$	$\frac{U_r}{U_s}$	$\frac{U_z}{U_s}$	$\frac{u'_\theta}{U_s}$	$\frac{u'_r}{U_s}$	$\frac{u'_z}{U_s}$	$\frac{\overline{u_\theta u_z}}{U_s^2}$	$\frac{\overline{u_r u_z}}{U_s^2}$	$\frac{\overline{u_r u_\theta}}{U_s^2}$	$\frac{k^2}{U_s^2}$	q/Q
90.	50.0	35.6	-0.67	-0.07	0.52	0.278	0.145	0.205	-0.036145	-0.002402	0.003431	0.140263	0.438
90.	55.0	35.6	-0.71	-0.06	0.60	0.274	0.169	0.226	-0.029153	-0.003458	0.004939	0.154611	0.423
90.	60.0	35.6	-0.84	-0.05	0.76	0.318	0.200	0.260	-0.042361	-0.005345	0.007634	0.208774	0.403
90.	65.0	35.6	-1.07	0.01	0.99	0.349	0.225	0.276	-0.046920	-0.005951	0.008498	0.248783	0.343
90.	70.0	35.6	-1.35	0.09	1.17	0.340	0.229	0.267	-0.035656	-0.007770	0.011097	0.238890	0.273
90.	75.0	35.6	-1.62	0.17	1.26	0.315	0.218	0.278	-0.027609	-0.009689	0.013838	0.223767	0.230
90.	80.0	35.6	-1.83	0.22	1.23	0.268	0.188	0.277	-0.027740	-0.010751	0.015354	0.184023	0.194
90.	85.0	35.6	-1.94	0.23	1.14	0.244	0.158	0.262	-0.029080	-0.008761	0.012512	0.153605	0.173

Table 50: Normalized data for the secondary flow of the IFRF variable swirl generator;

S=4.0, $\hat{U}_s$ = 19.6 m/s, z=2 mm.

θ (deg)	r (mm)	T_a(°C)	U_θ (m/s)	U_r(m/s)	U_z (m/s)	u'_θ (m/s)	u'_r (m/s)	u'_z (m/s)	$\overline{u_\theta u_z}(m^2/s^2)$	$\overline{u_r u_z}(m^2/s^2)$	$\overline{u_r u_\theta}(m^2/s^2)$	$q^2(m^2/s^2)$	q/Q
90.	50.0	29.8	-4.9	-0.2	3.6	2.22	1.28	1.56	-2.122	-0.237	0.338	9.00	0.50
90.	55.0	29.8	-5.3	-0.5	4.1	2.47	1.42	1.81	-2.604	-0.423	0.604	11.36	0.50
90.	60.0	29.8	-6.2	-0.6	5.2	2.79	1.56	2.17	-3.154	-0.405	0.578	14.89	0.48
90.	65.0	29.8	-7.9	-0.3	6.8	3.03	1.88	2.33	-3.442	-0.683	0.975	18.18	0.41
90.	70.0	29.8	-10.3	0.3	8.5	3.36	1.99	2.55	-3.839	-0.618	0.882	21.70	0.35
90.	75.0	29.8	-12.8	0.9	9.5	3.12	2.06	2.63	-2.748	-1.123	1.604	20.89	0.29
90.	80.0	29.8	-14.6	1.5	9.7	2.71	1.85	2.60	-2.378	-0.961	1.373	17.55	0.24
90.	85.0	29.8	-15.6	2.0	9.2	2.39	1.73	2.39	-2.711	-1.085	1.550	14.38	0.21

Table 51: Data for the secondary flow of the IFRF variable swirl generator presented in cylindrical coordinates; S=4.0, z=2.0 mm.

θ (deg)	r (mm)	T_o(°C)	$\frac{U_\theta}{U_s}$	$\frac{U_r}{U_s}$	$\frac{U_z}{U_s}$	$\frac{u'_\theta}{U_s}$	$\frac{u'_r}{U_s}$	$\frac{u'_z}{U_s}$	$\frac{\overline{u_\theta u_r}}{U_s^2}$	$\frac{\overline{u_\theta u_z}}{U_s^2}$	$\frac{\overline{u_r u_z}}{U_s^2}$	$\frac{q^2}{U_s^2}$	q/Q
90.	50.0	29.8	-0.65	-0.03	0.48	0.298	0.172	0.209	-0.038163	-0.004260	0.006084	0.161933	0.496
90.	55.0	29.8	-0.71	-0.07	0.55	0.331	0.190	0.242	-0.046847	-0.007612	0.010872	0.204389	0.504
90.	60.0	29.8	-0.83	-0.08	0.69	0.374	0.209	0.291	-0.056741	-0.007279	0.010396	0.267778	0.477
90.	65.0	29.8	-1.06	-0.04	0.91	0.407	0.253	0.312	-0.061921	-0.012279	0.017536	0.326980	0.408
90.	70.0	29.8	-1.38	0.04	1.14	0.450	0.266	0.342	-0.069058	-0.011111	0.015868	0.390343	0.348
90.	80.0	29.8	-1.71	0.12	1.28	0.418	0.277	0.353	-0.049430	-0.020208	0.028860	0.375771	0.286
90.	85.0	29.8	-1.95	0.20	1.31	0.364	0.248	0.349	-0.042769	-0.017288	0.024689	0.315722	0.238
90.	85.0	29.8	-2.09	0.26	1.23	0.320	0.232	0.320	-0.048765	-0.019518	0.027874	0.258701	0.208

Table 52: Normalized data for the secondary flow of the IFRF variable swirl generator; S=4.0, $\hat{U}_s$ = 7.5 m/s, z=2.0 mm.

θ (deg)	r (mm)	$T_o(^oC)$	U_θ (m/s)	U_r(m/s)	U_z (m/s)	u'_θ (m/s)	u'_r (m/s)	u'_z (m/s)	$\overline{u_\theta u_z}(m^2/s^2)$	$\overline{u_r u_z}(m^2/s^2)$	$\overline{u_r u_\theta}(m^2/s^2)$	$q^2(m^2/s^2)$	q/Q
90.	50.0	34.4	-10.8	-0.4	8.6	4.71	2.67	3.55	-12.003	-0.488	0.697	41.90	0.47
90.	55.0	34.4	-11.5	-1.0	9.7	5.00	2.82	3.86	-11.437	-0.966	1.379	47.88	0.46
90.	60.0	34.6	-13.3	-1.1	12.2	5.48	3.06	4.44	-12.996	-1.512	2.159	59.08	0.42
90.	65.0	34.7	-16.8	-0.4	16.0	6.06	3.77	4.95	-15.932	-2.218	3.167	75.36	0.37
90.	70.0	34.7	-21.4	1.0	19.8	6.19	3.98	5.16	-13.992	-2.591	3.700	80.86	0.31
90.	75.0	34.9	-26.6	2.4	22.2	6.20	4.09	5.38	-13.159	-3.743	5.345	83.99	0.26
90.	80.0	35.1	-30.9	3.6	22.6	5.29	3.83	5.26	-11.001	-5.391	7.700	70.37	0.22
90.	85.0	35.1	-33.6	4.6	21.2	4.54	3.36	4.92	-10.492	-5.515	7.876	56.15	0.19

Table 53: Data for the secondary flow of the IFRF variable swirl generator presented in cylindrical coordinates; S=4.5, z=2.0 mm.

θ (deg)	r (mm)	T_a(°C)	$\frac{U_\theta}{U_x}$	$\frac{U_r}{U_x}$	$\frac{U_x}{U_x}$	$\frac{u'_\theta}{U_x}$	$\frac{u'_r}{U_x}$	$\frac{u'_x}{U_x}$	$\frac{\overline{u_\theta u_x}}{U_x^2}$	$\frac{\overline{u_r u_x}}{U_x^2}$	$\frac{\overline{u_r u_\theta}}{U_x^2}$	$\frac{k}{U_x^2}$	q/Q
90.	50.0	34.4	-0.62	-0.02	0.49	0.271	0.153	0.204	-0.039709	-0.001615	0.002306	0.138614	0.470
90.	55.0	34.4	-0.66	-0.06	0.56	0.288	0.162	0.222	-0.037836	-0.003194	0.004562	0.158392	0.459
90.	60.0	34.6	-0.77	-0.06	0.70	0.315	0.176	0.255	-0.042993	-0.005000	0.007141	0.195452	0.424
90.	65.0	34.7	-0.96	-0.03	0.92	0.348	0.217	0.284	-0.052707	-0.007337	0.010478	0.249315	0.375
90.	70.0	34.7	-1.23	0.06	1.14	0.356	0.229	0.297	-0.046290	-0.008570	0.012240	0.267493	0.308
90.	75.0	34.9	-1.53	0.14	1.28	0.356	0.235	0.309	-0.043532	-0.012382	0.017683	0.277840	0.264
90.	80.0	35.1	-1.78	0.21	1.30	0.304	0.220	0.303	-0.036394	-0.017836	0.025473	0.232795	0.218
90.	85.0	35.1	-1.93	0.26	1.22	0.261	0.193	0.283	-0.034709	-0.018244	0.026055	0.185758	0.187

Table 54: Normalized data for the secondary flow of the IFRF variable swirl generator; S=4.5, $\widehat{U}_x = 17.4$ m/s, z=2.0 mm.

θ (deg)	r (mm)	T_o(°C)	U_θ (m/s)	U_r(m/s)	U_z (m/s)	u'_θ (m/s)	u'_r (m/s)	u'_z (m/s)	$\overline{u_\theta u_z}(m^2/s^2)$	$\overline{u_r u_z}(m^2/s^2)$	$\overline{u_r u_\theta}(m^2/s^2)$	$q^2(m^2/s^2)$	q/Q
90.	50.0	30.4	-5.1	-0.2	4.1	2.32	1.25	1.84	-2.855	-0.247	0.353	10.32	0.49
90.	55.0	30.4	-5.4	-0.5	4.6	2.41	1.37	1.94	-2.544	-0.265	0.379	11.42	0.47
90.	60.0	30.4	-6.3	-0.6	5.8	2.74	1.61	2.38	-3.514	-0.468	0.668	15.78	0.46
90.	65.0	30.4	-7.9	-0.3	7.6	3.04	1.96	2.58	-4.164	-0.522	0.745	19.72	0.40
90.	70.0	30.3	-10.2	0.3	9.5	3.25	2.10	2.78	-4.362	-0.691	0.986	22.75	0.34
90.	75.0	30.3	-12.6	1.1	10.7	3.16	2.17	2.80	-3.730	-0.858	1.226	22.52	0.29
90.	80.0	30.3	-14.7	1.8	10.9	2.85	2.02	2.87	-3.340	-1.244	1.777	20.44	0.25
90.	85.0	30.3	-16.1	2.3	10.2	2.50	1.85	2.80	-3.153	-1.381	1.972	17.47	0.22

Table 55: Data for the secondary flow of the IFRF variable swirl generator presented in cylindrical coordinates; S=4.5, z=4.0 mm.

θ (deg)	r (mm)	T_a(°C)	$\frac{U_\theta}{U_s}$	$\frac{U_r}{U_s}$	$\frac{U_x}{U_s}$	$\frac{u'_\theta}{U_s}$	$\frac{u'_r}{U_s}$	$\frac{u'_x}{U_s}$	$\frac{\overline{u_\theta u_x}}{U_s^2}$	$\frac{\overline{u_r u_x}}{U_s^2}$	$\frac{\overline{u_r u_\theta}}{U_s^2}$	$\frac{q^2}{U_s^2}$	q/Q
90.	50.0	30.4	-0.61	-0.02	0.49	0.278	0.150	0.220	-0.040972	-0.003545	0.005063	0.148158	0.491
90.	55.0	30.4	-0.65	-0.06	0.56	0.289	0.164	0.232	-0.036512	-0.003806	0.005436	0.163877	0.472
90.	60.0	30.4	-0.75	-0.07	0.69	0.328	0.193	0.285	-0.050442	-0.006716	0.009592	0.226435	0.464
90.	65.0	30.4	-0.94	-0.03	0.91	0.364	0.235	0.309	-0.059759	-0.007485	0.010690	0.283090	0.405
90.	70.0	30.3	-1.22	0.04	1.14	0.390	0.252	0.334	-0.062803	-0.009913	0.014157	0.326544	0.342
90.	75.0	30.3	-1.51	0.13	1.28	0.379	0.259	0.335	-0.053533	-0.012322	0.017597	0.323153	0.287
90.	80.0	30.3	-1.76	0.22	1.30	0.341	0.242	0.344	-0.047942	-0.017858	0.025504	0.293354	0.246
90.	85.0	30.3	-1.93	0.27	1.23	0.299	0.221	0.335	-0.045261	-0.019819	0.028304	0.250707	0.218

Table 56: Normalized data for the secondary flow of the IFRF variable swirl generator; S=4.5, $\hat{U}_s = 8.3$ m/s, z=4.0 mm.

		ϕ (deg)	x (mm)	y (mm)	z (mm)	$\tilde{U}_b$ (m/s)	L_{bb} (mm)	$k(m^2/s^2)$	$\epsilon(m^2/s^3)$	$\nu_T(m^2/s)$
fixed vane 30°	prim.	0	0.	0.	3.	8.5	2.21	.10	13.5	.0002
	sec.	30	0.	-33.	3.	7.0	7.71	.24	14.4	.0010
IFRF	prim.	0	0.	0.	3.	6.4	20.5	4.3	410.	.011
IFRF S=1.	sec.	30.	0.	70.	3.	8.1	33.2	2.9	140.	.015
IFRF S=2.	sec.	45.	0.	70.	3.	8.1	31.6	2.5	118.	.013
IFRF S=3.	sec.	55.	0.	70.	3.	10.8	35.3	5.5	345.	.022
IFRF S=4.	sec.	55.	0.	70.	3.	11.6	66.3	12.6	646.	.062

Table 57: The measured integral length scales and estimated quantities useful for turbulence models.

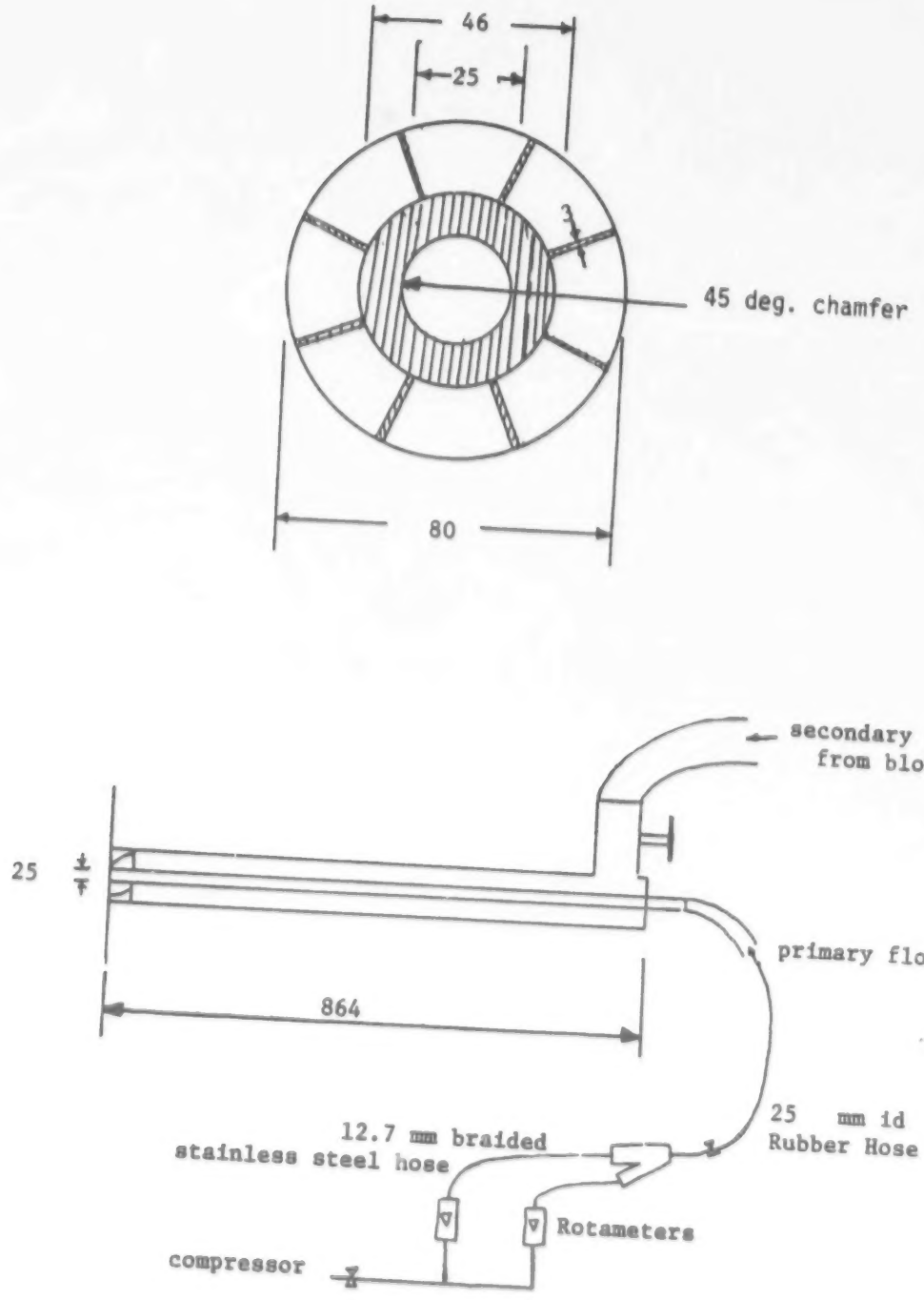

Figure 1: The fixed vane swirl generators.

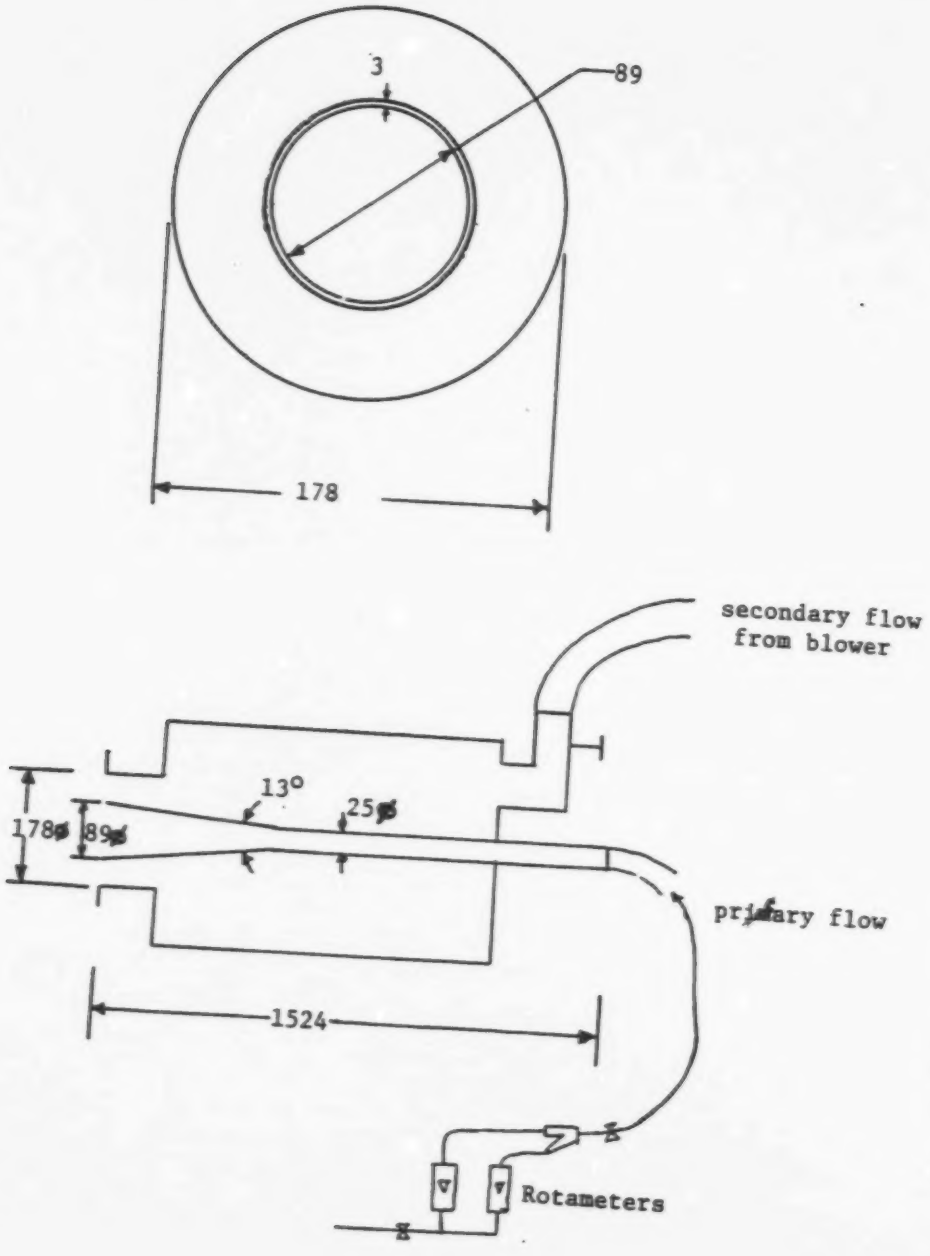

Figure 2: The IFRF variable swirl generator.

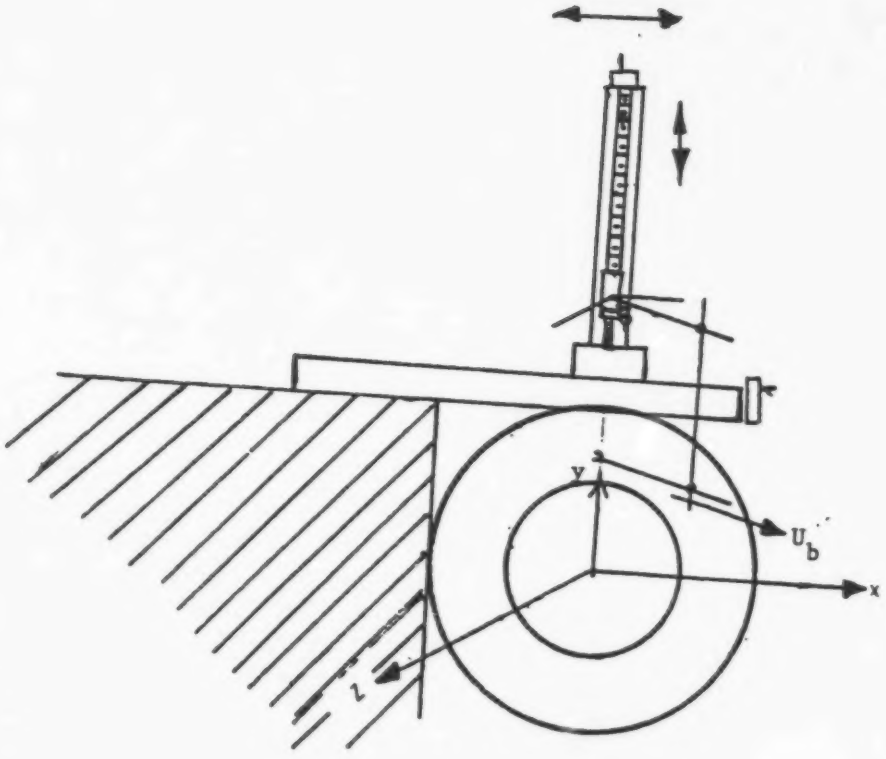

Figure 3: The traversing mechanism.

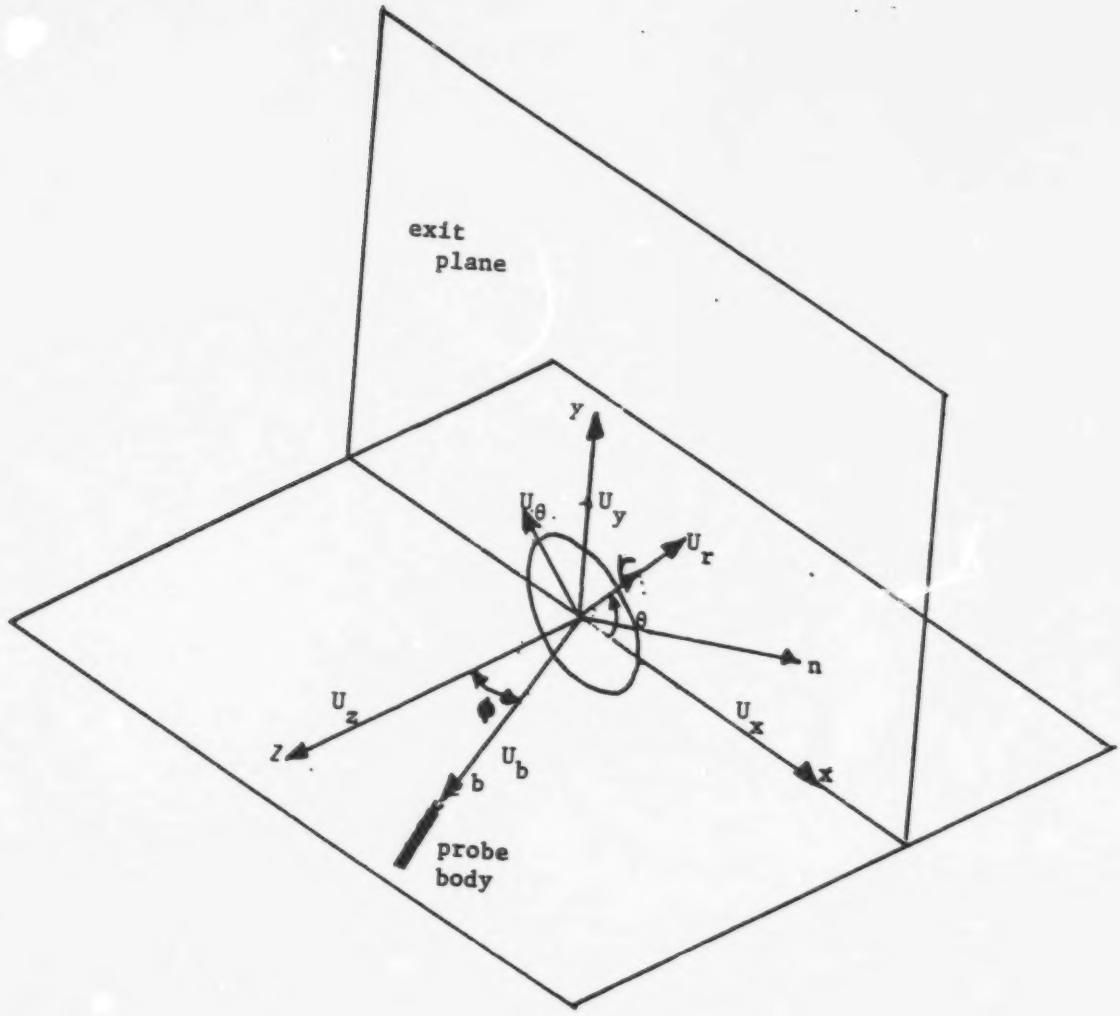

Figure 4: The coordinate systems and velocity components.

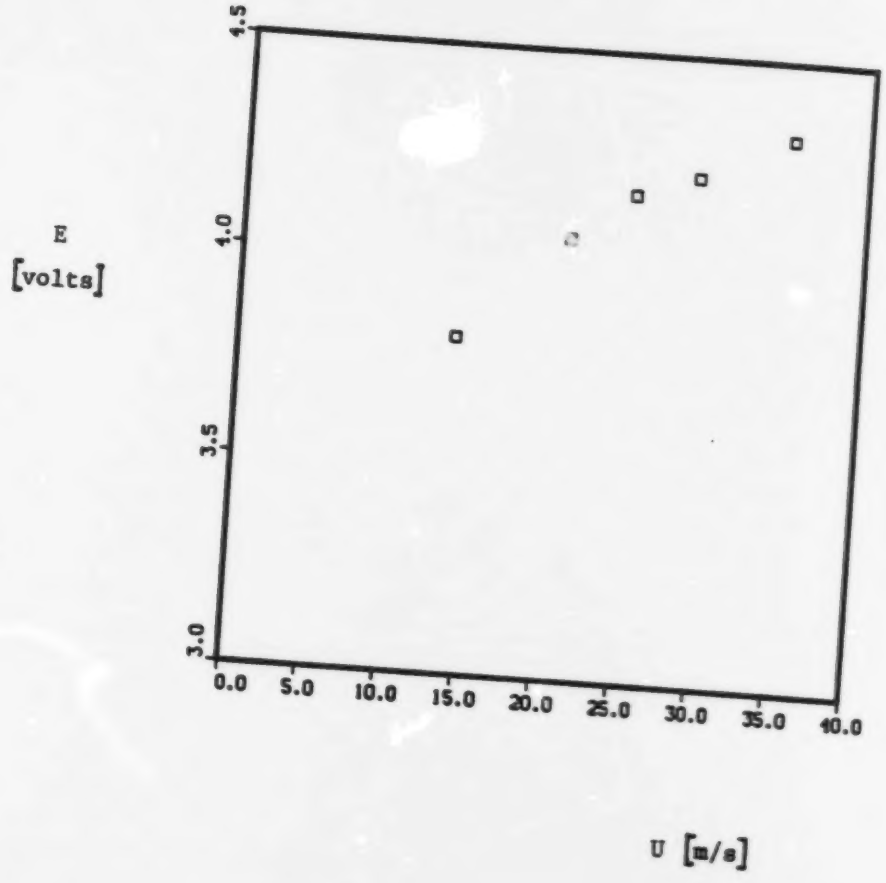

Figure 5: Typical hot wire calibration results.

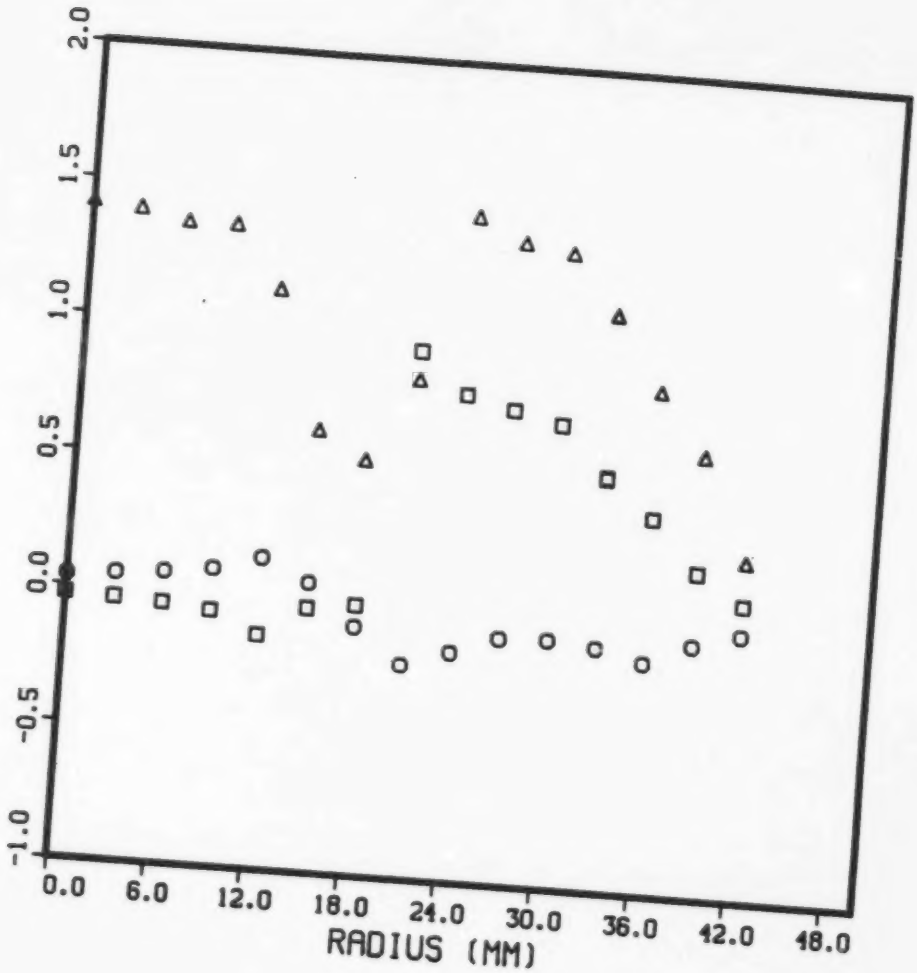

Figure 6: 30° fixed vane swirl generator; $\theta = -90°$, z=10 mm; $\square \frac{U_\theta}{\hat{U}_z}$, $\circ \frac{U_r}{\hat{U}_z}$, $\Delta \frac{U_z}{\hat{U}_z}$; $\hat{U}_z$ = 23.1 m/s.

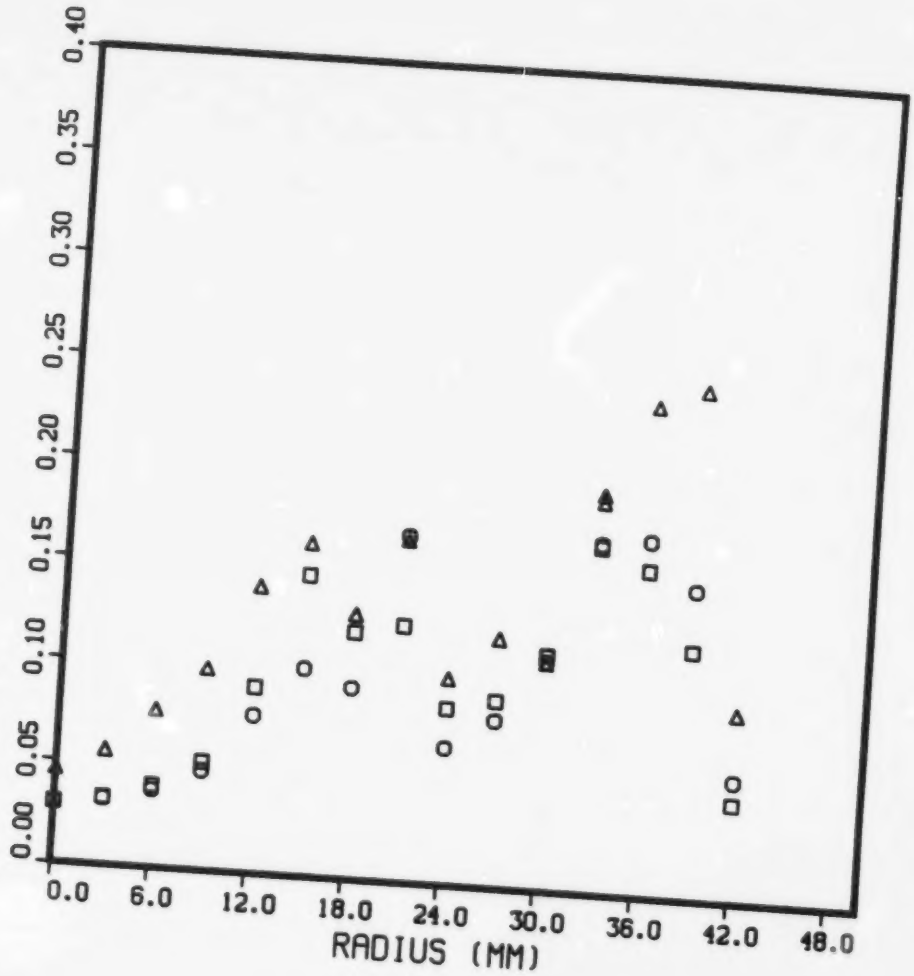

Figure 7: 30° fixed vane swirl generator; $\theta = -90°$, z=10 mm; $\Box \frac{u'}{U_z}$, $\circ \frac{w'}{U_z}$, $\triangle \frac{u'}{U_z}$; $\hat{U}_z =$ 23.1 m/s.

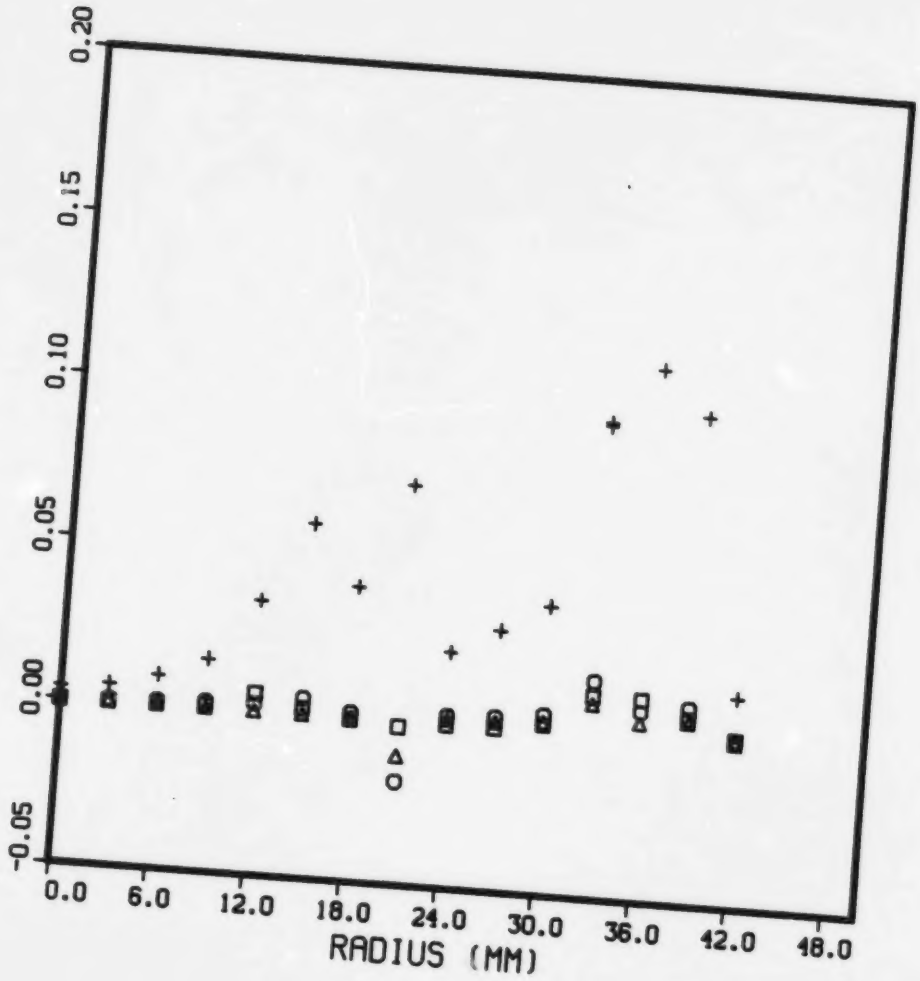

Figure 8: 30° fixed vane swirl generator; $\theta = -90°$, z=10 mm; $\square \frac{\overline{u_r u_z}}{U_z^2}$, $\circ \frac{\overline{u_r u_z}}{U_z^2}$, $\triangle \frac{\overline{u_r u_z}}{U_z^2}$, $+ \frac{q^2}{U_z^2}$; $\widehat{U}_z = 23.1$ m/s.

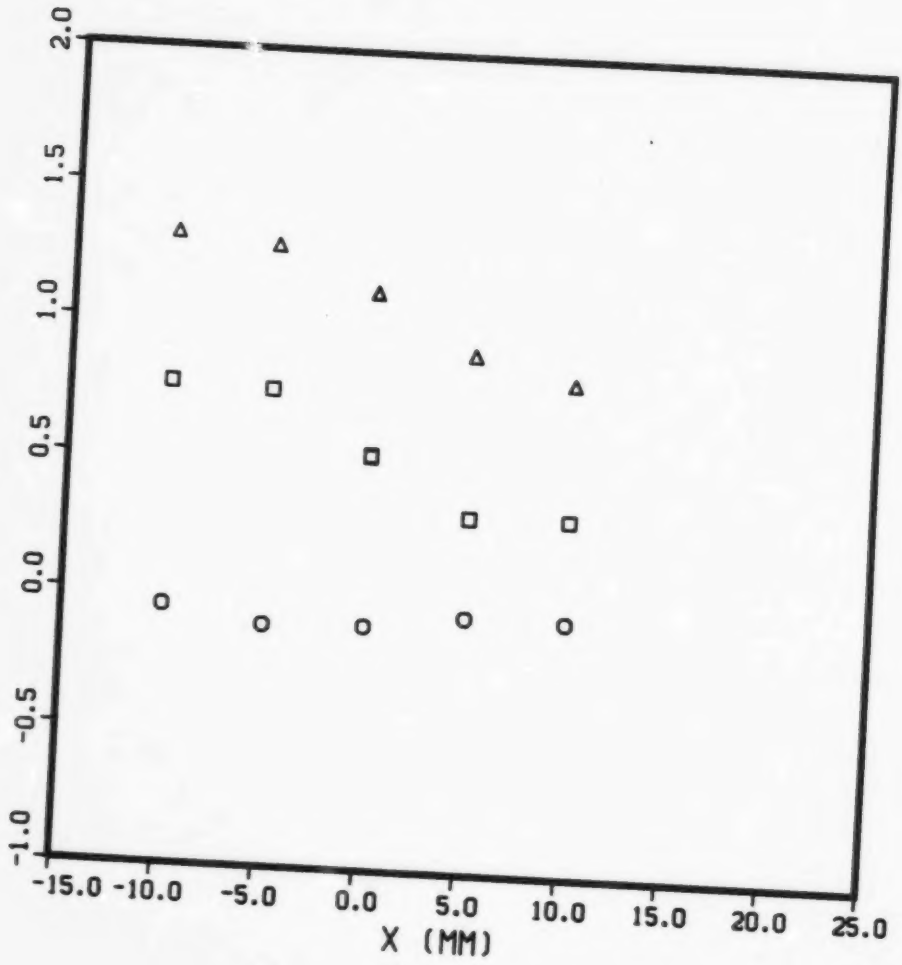

Figure 9: 30° fixed vane swirl generator; y=-33 mm, z=10 mm; $\square \frac{U_x}{\hat{U}_x}$, $\circ \frac{U_r}{\hat{U}_x}$, $\triangle \frac{U_\theta}{\hat{U}_x}$; $\hat{U}_x$ = 23.1 m/s.

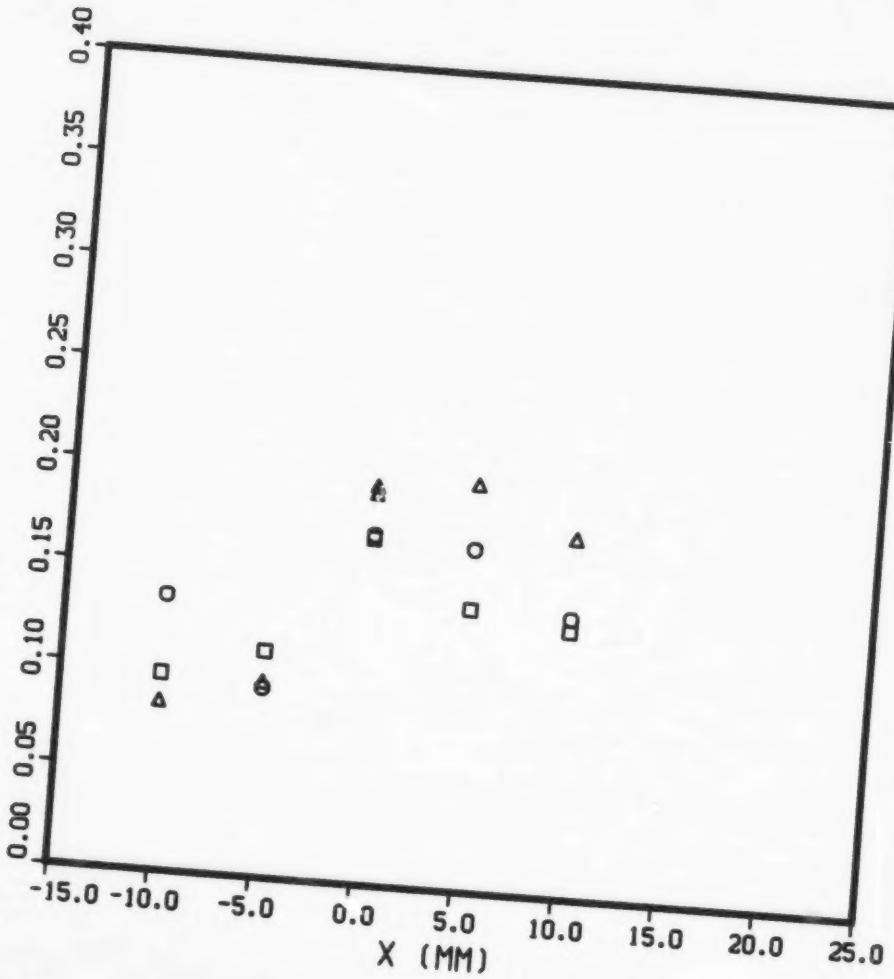

Figure 10: 30° fixed vane swirl generator; y=-33 mm, z=10 mm; □ $\frac{u'}{\hat{U}_z}$, ○ $\frac{u'}{\hat{U}_z}$, △ $\frac{u'}{\hat{U}_z}$; $\hat{U}_z$ = 23.1 m/s.

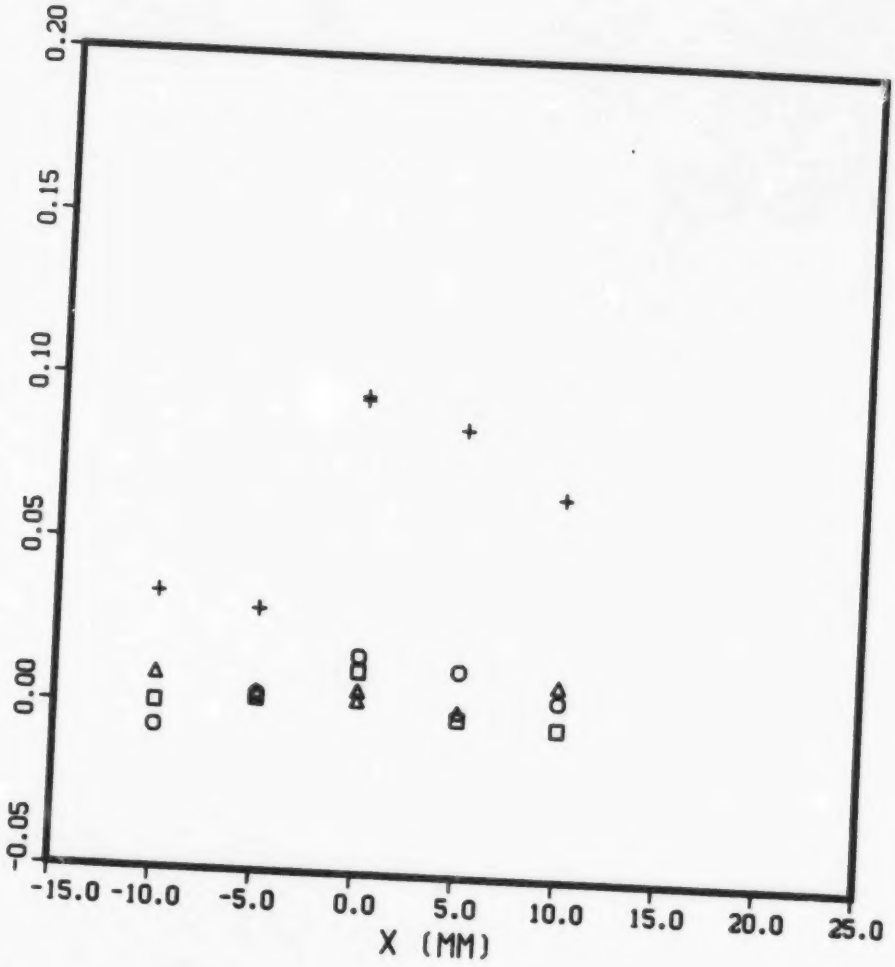

Figure 11: 30° fixed vane swirl generator; y=-33 mm, z=10 mm; $\square \frac{\overline{u_\theta u_x}}{U_z^2}$, $\circ \frac{\overline{u_r u_x}}{U_z^2}$, $\triangle \frac{\overline{u_r u_\theta}}{U_z^2}$, $+ \frac{q^2}{U_z^2}$; $\bar{U}_z = 23.1$ m/s.

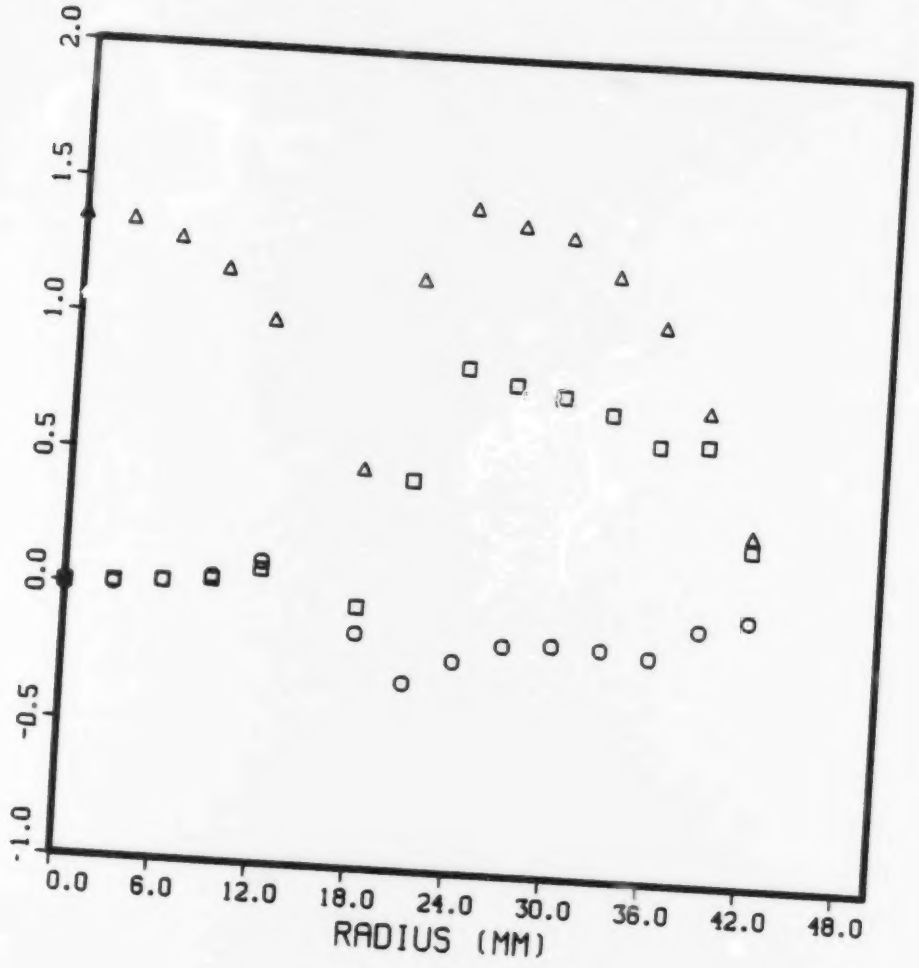

Figure 12: 30° fixed vane swirl generator; $\theta = -90°$, z=5 mm; $\square \frac{U_\theta}{U_z}$, $\circ \frac{U_r}{U_z}$, $\Delta \frac{U_z}{U_z}$; $\bar{U}_z$ = 12.2 m/s.

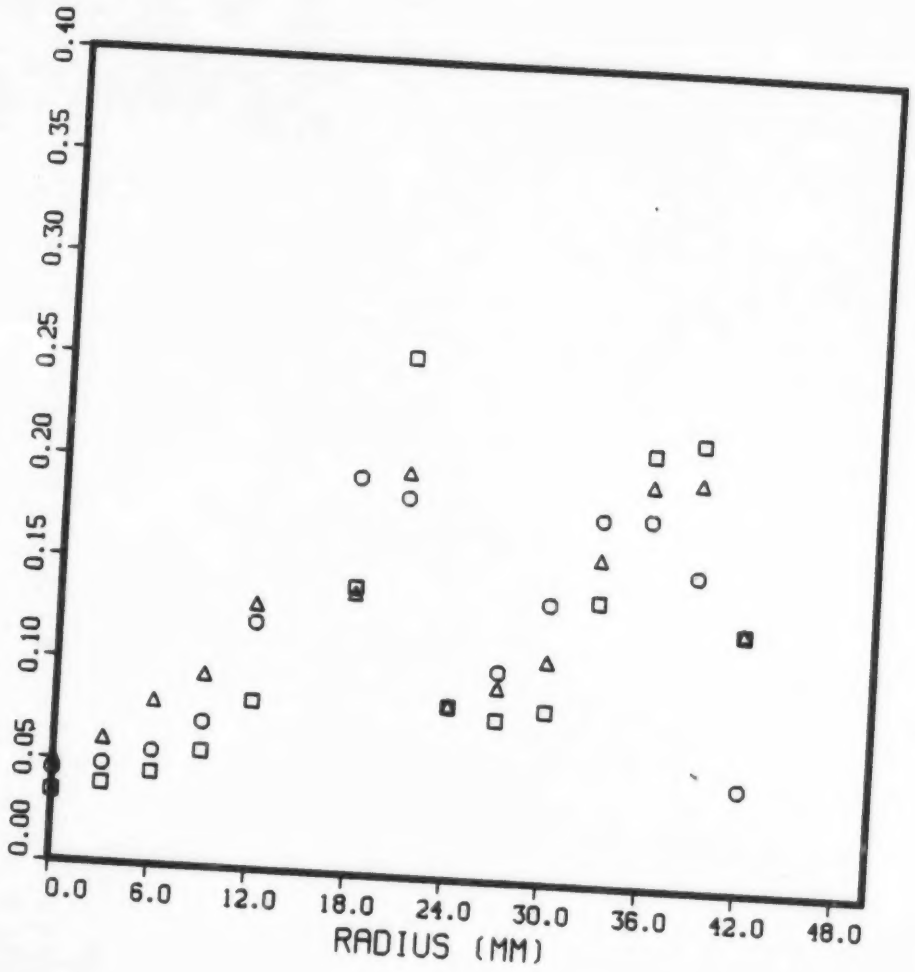

Figure 13: 30° fixed vane swirl generator; $\theta = -90°$, z=5 mm; $\square \frac{u'_\theta}{\hat{U}_z}$, $\circ \frac{u'_r}{\hat{U}_z}$, $\triangle \frac{u'_z}{\hat{U}_z}$; $\hat{U}_z$ = 12.2 m/s.

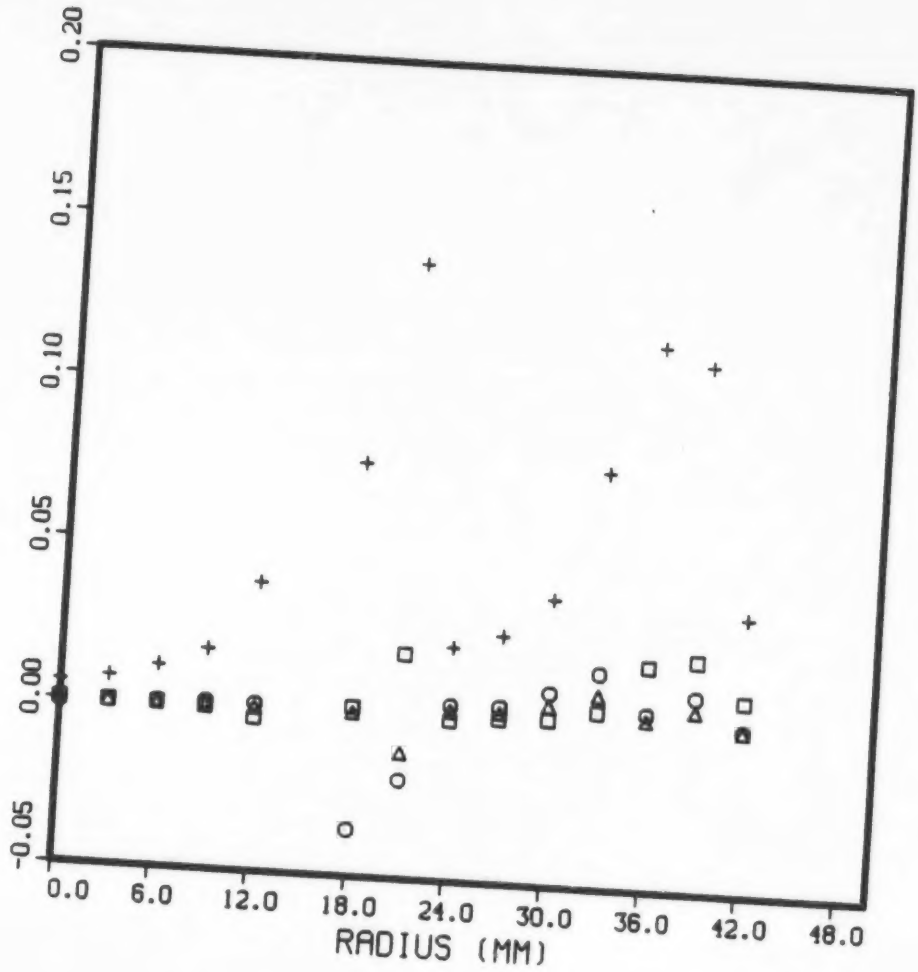

Figure 14: 30° fixed vane swirl generator; $\theta = -90°$, z=5 mm; $\square \frac{\overline{u_\theta u_z}}{U_z^2}$, $\circ \frac{\overline{u_r u_z}}{U_z^2}$, $\triangle \frac{\overline{u_r u_\theta}}{U_z^2}$, $+ \frac{q^2}{U_z^2}$; $\hat{U}_z = 12.2$ m/s.

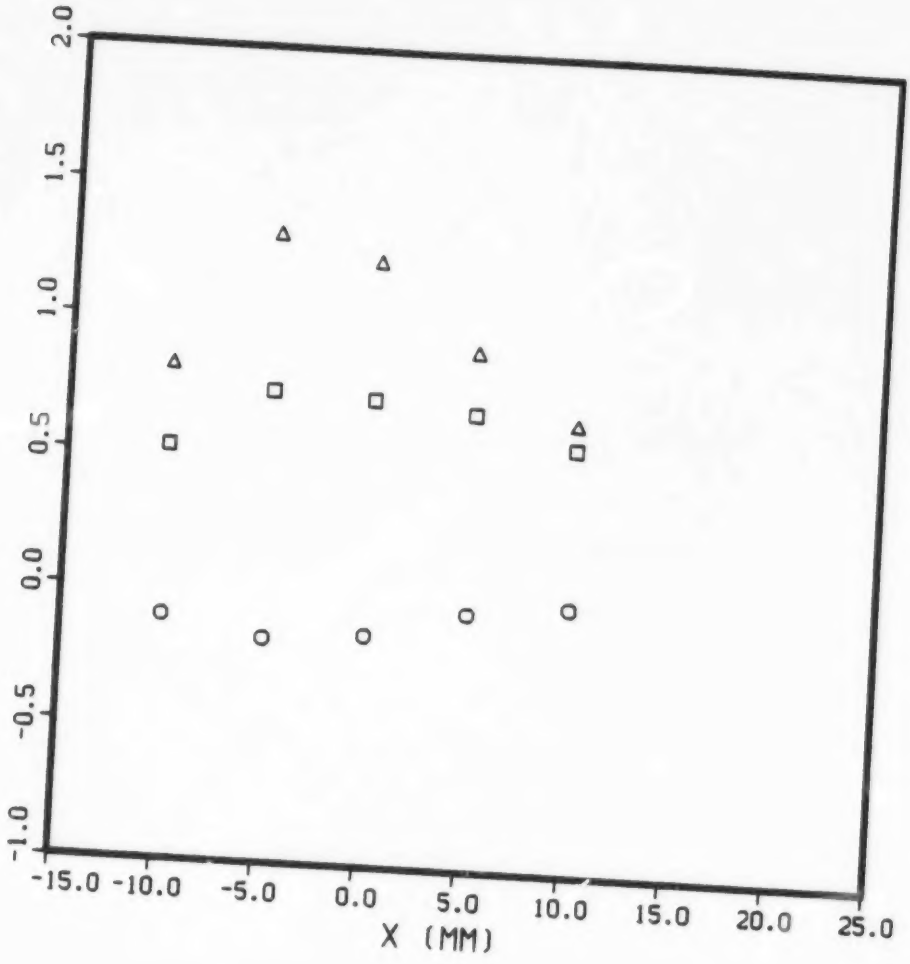

Figure 15: 30° fixed vane swirl generator; y=-33 mm, z=5 mm; $\square \frac{U_x}{\hat{U}_x}$, $\circ \frac{U_z}{\hat{U}_x}$, $\Delta \frac{U_r}{\hat{U}_x}$; $\hat{U}_z$ = 12.2 m/s.

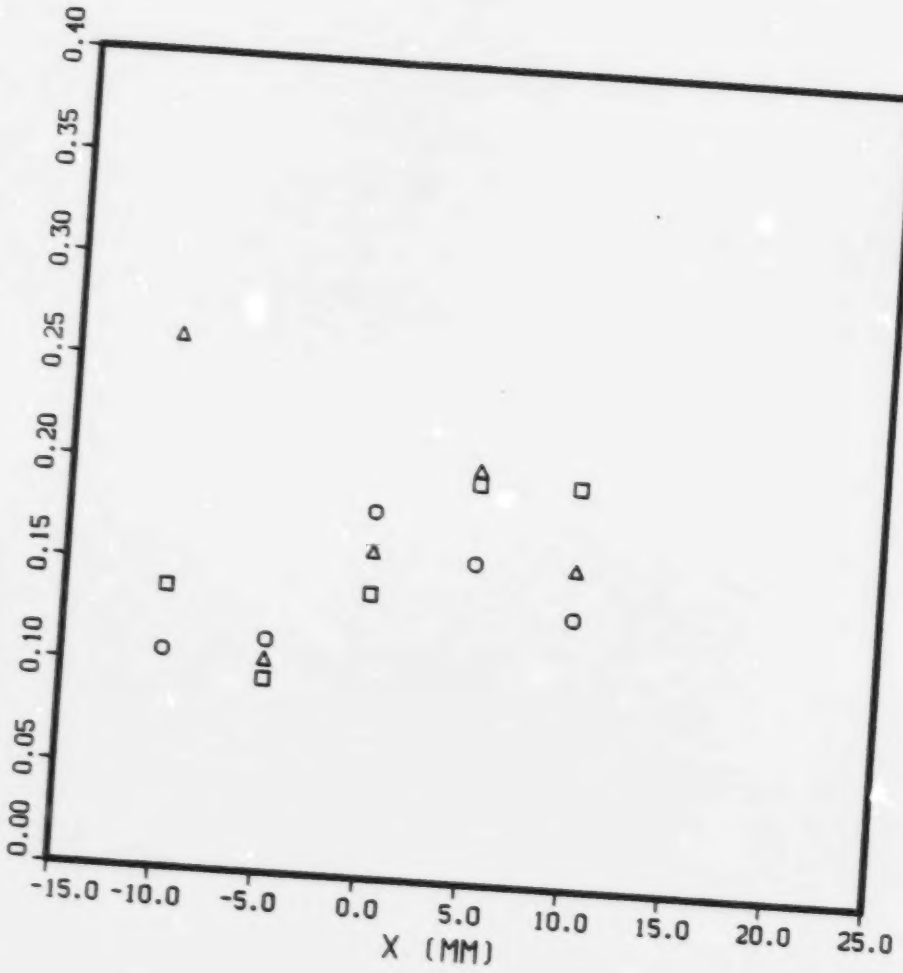

Figure 16: 30° fixed vane swirl generator; y=-33 mm, z=5 mm; □ $\frac{u'_\theta}{U_z}$, ○ $\frac{u'_r}{U_z}$, △ $\frac{u'_z}{U_z}$; U_z = 12.2 m/s.

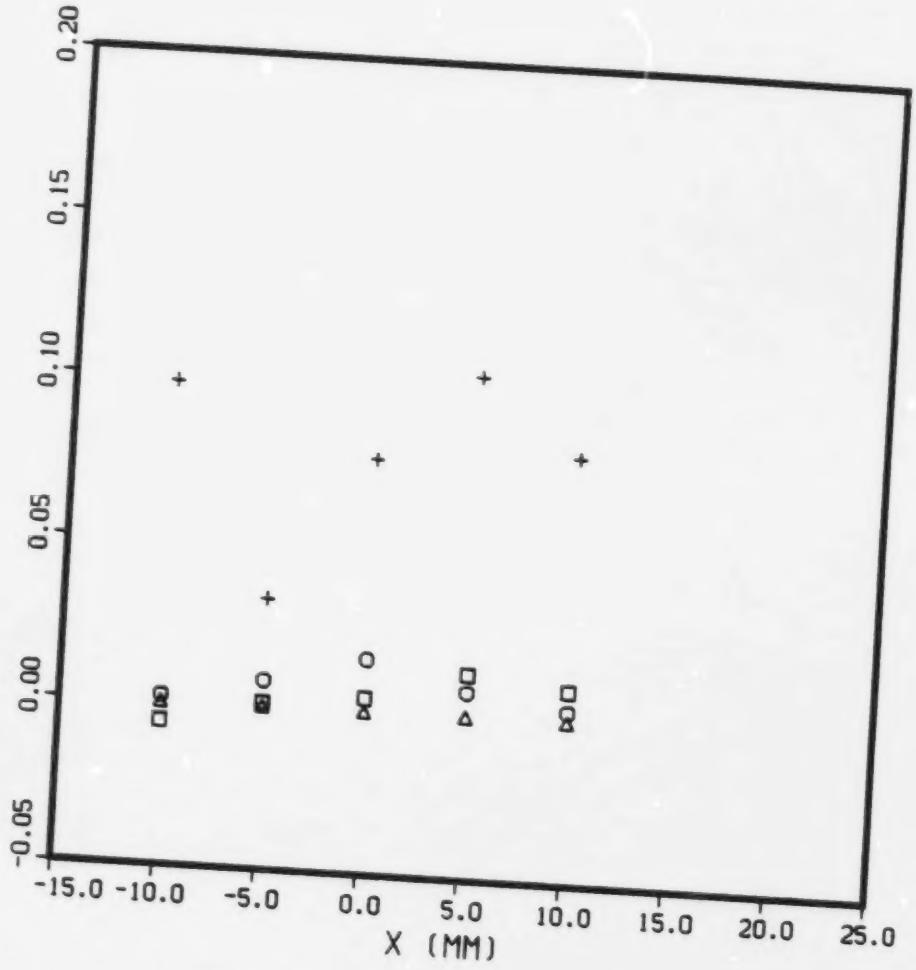

Figure 17: 30° fixed vane swirl generator; y=-33 mm, z=5 mm; $\square \frac{\overline{u_\theta u_\theta}}{U_z^2}$, $\circ \frac{\overline{u_r u_r}}{U_z^2}$, $\triangle \frac{\overline{u_z u_z}}{U_z^2}$, $+ \frac{q^2}{U_z^2}$; $\hat{U}_z = 12.2$ m/s.

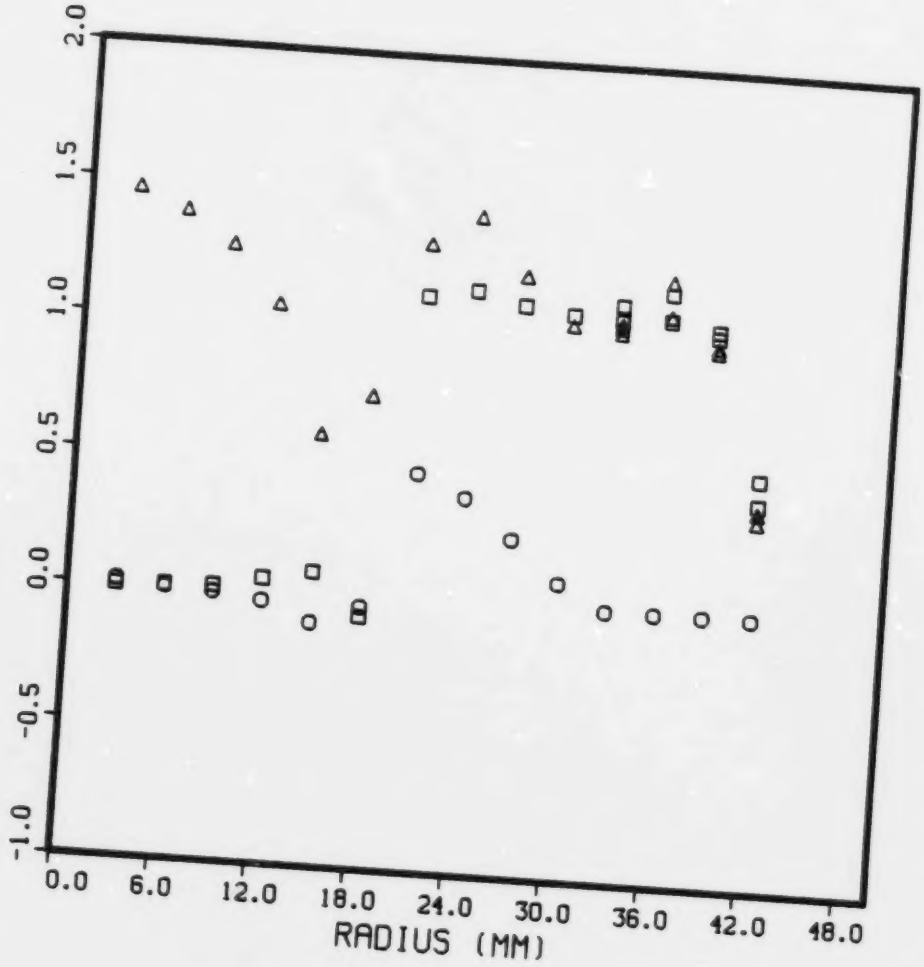

Figure 18: 45° fixed vane swirl generator; $\theta = -90°$, z=10 mm; $\square \frac{U_\theta}{\hat{U}_z}$, $\circ \frac{U_r}{\hat{U}_z}$, $\Delta \frac{U_z}{\hat{U}_z}$; $\hat{U}_z =$ 22.5 m/s.

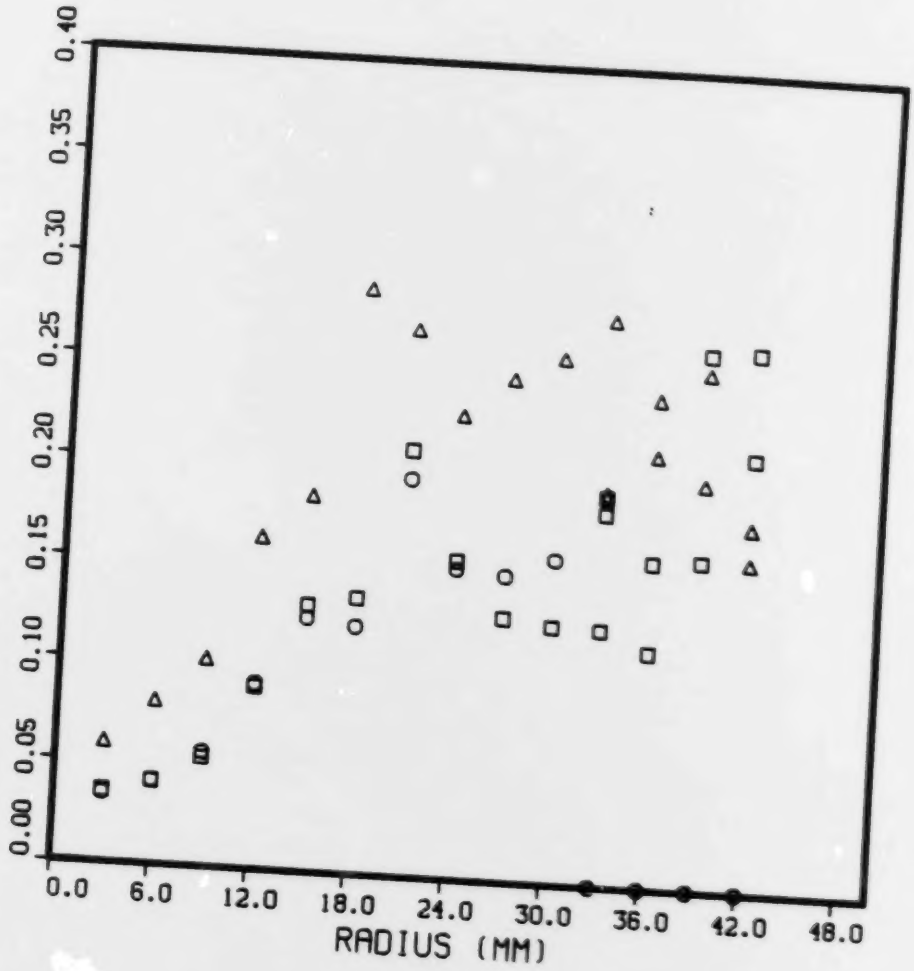

Figure 19: 45° fixed vane swirl generator; $\theta = -90°$, z=10 mm; $\square \frac{u'_\theta}{U_z}$, $\circ \frac{u'_z}{U_z}$, $\Delta \frac{u'_r}{U_z}$; $\hat{U}_z$ = 22.5 m/s.

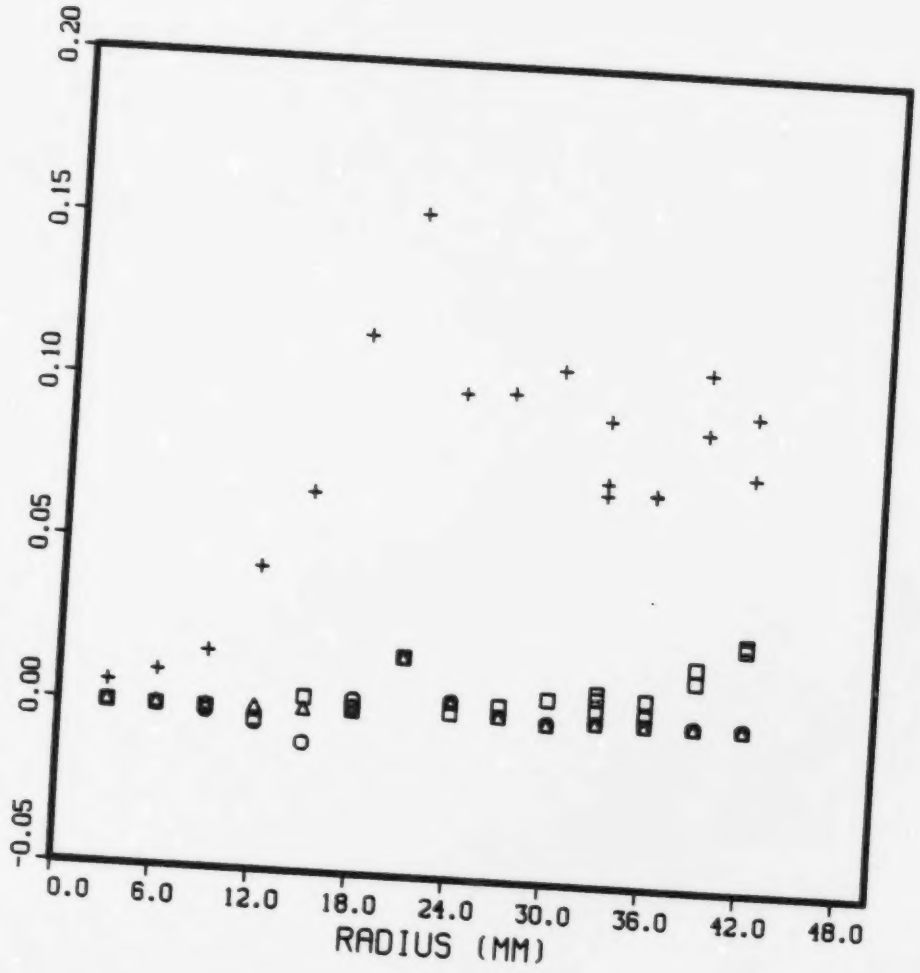

Figure 20: 45° fixed vane swirl generator; $\theta = -90°$, z=10 mm; $\square \frac{\overline{u_\theta u_\theta}}{U_z^2}$, $\circ \frac{\overline{u_r u_r}}{U_z^2}$, $\triangle \frac{\overline{u_z u_z}}{U_z^2}$, $+ \frac{q^2}{U_z^2}$; $\hat{U}_z = 22.5$ m/s.

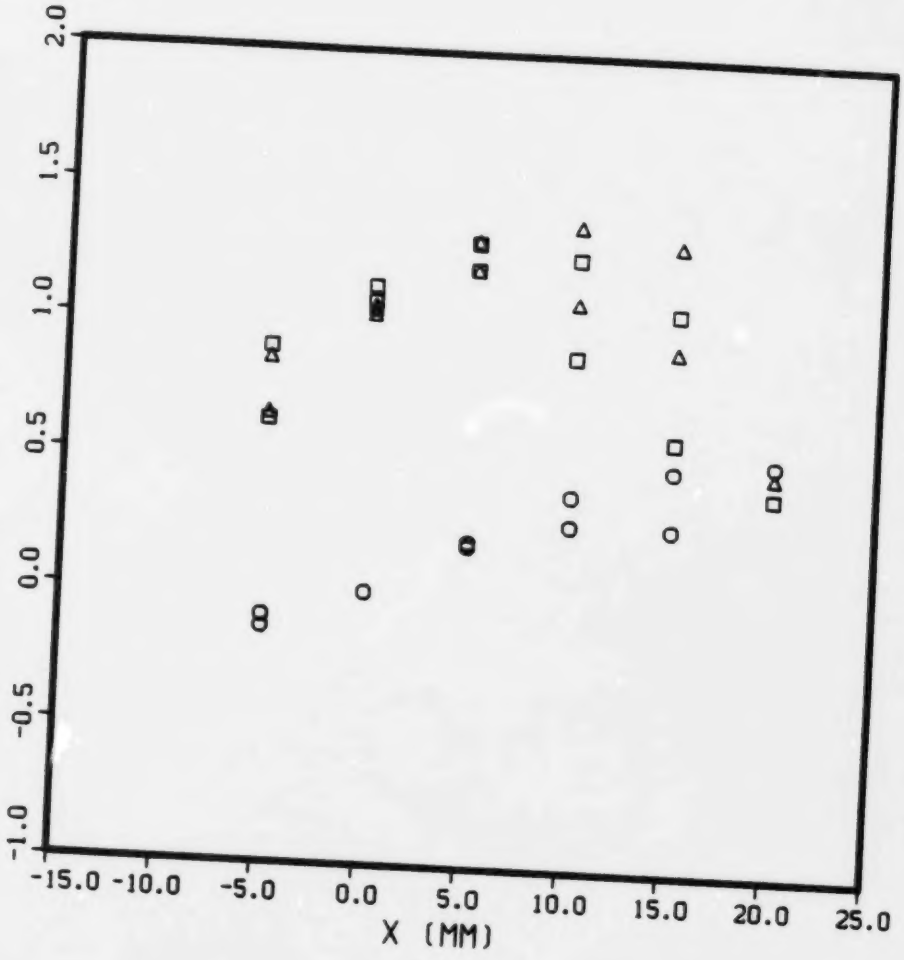

Figure 21: 45° fixed vane swirl generator; y=-33 mm, z=10 mm; $\square \frac{U_x}{\hat{U}_z}$, $\circ \frac{U_r}{\hat{U}_z}$, $\triangle \frac{U_\theta}{\hat{U}_z}$; $\hat{U}_z$ = 22.5 m/s.

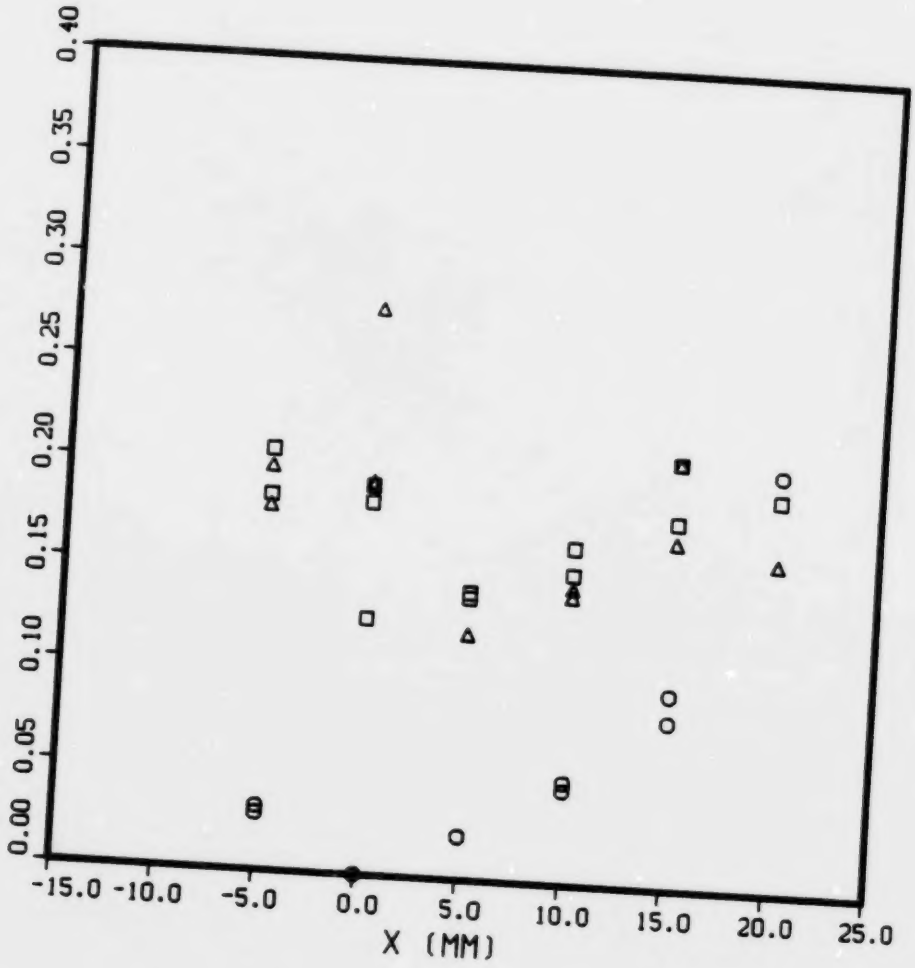

Figure 22: 45° fixed vane swirl generator; y=-33 mm, z=10 mm; $\square \frac{u'}{U_z}$, $\circ \frac{u'}{U_z}$, $\Delta \frac{u'}{U_z}$; $\hat{U}_z$ = 22.5 m/s.

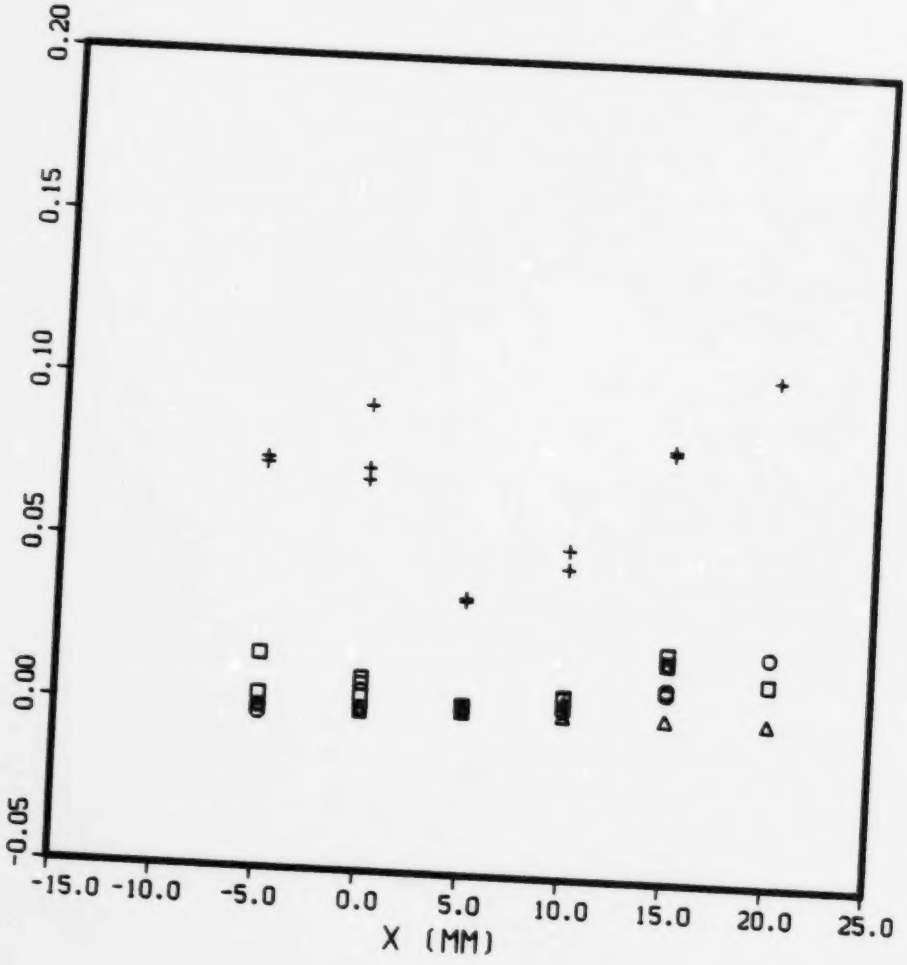

Figure 23: 45° fixed vane swirl generator; y=-33 mm, z=10 mm; □ $\frac{\overline{u_\theta u_\theta}}{U_z^2}$, ○ $\frac{\overline{u_r u_r}}{U_z^2}$, △ $\frac{\overline{u_r u_\theta}}{U_z^2}$, + $\frac{q^2}{U_z^2}$; $\hat{U}_z = 22.5$ m/s.

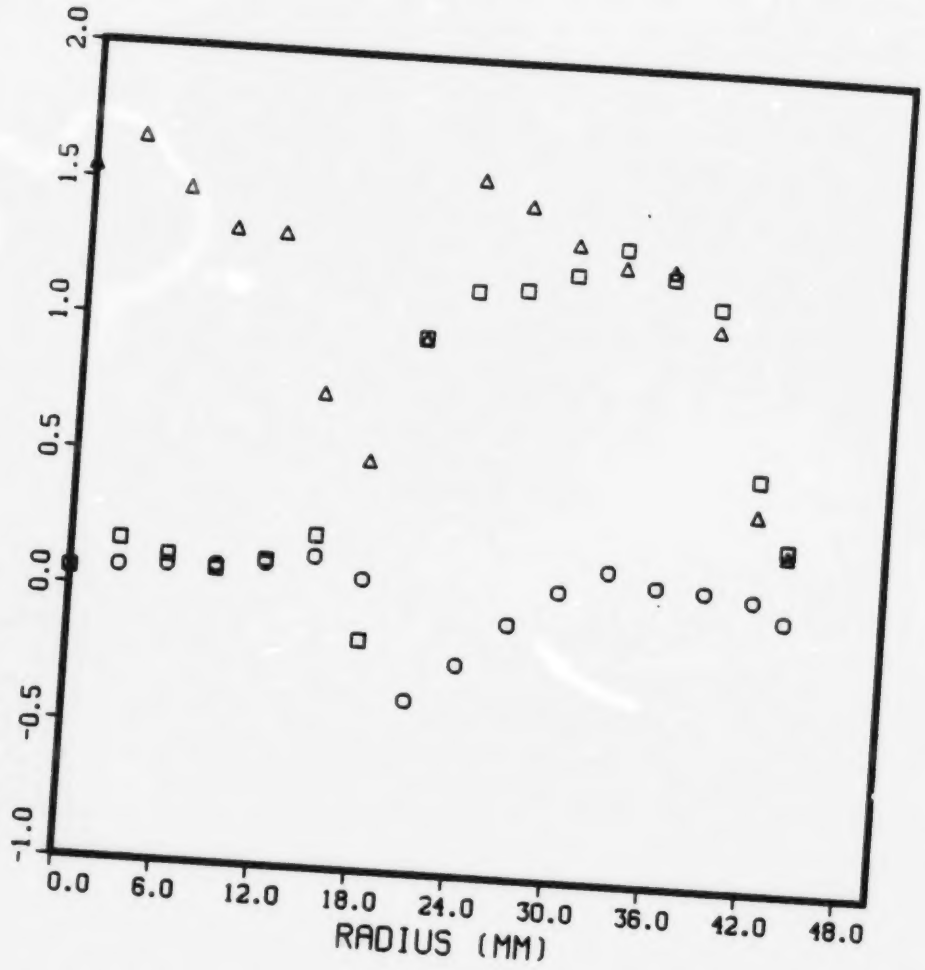

Figure 24: 45° fixed vane swirl generator; $\theta = -90°$, z=9 mm; $\square \frac{U_\theta}{U_z}$, $\circ \frac{U_r}{U_z}$, $\Delta \frac{U_z}{U_z}$; $\hat{U}_z =$ 13.5 m/s.

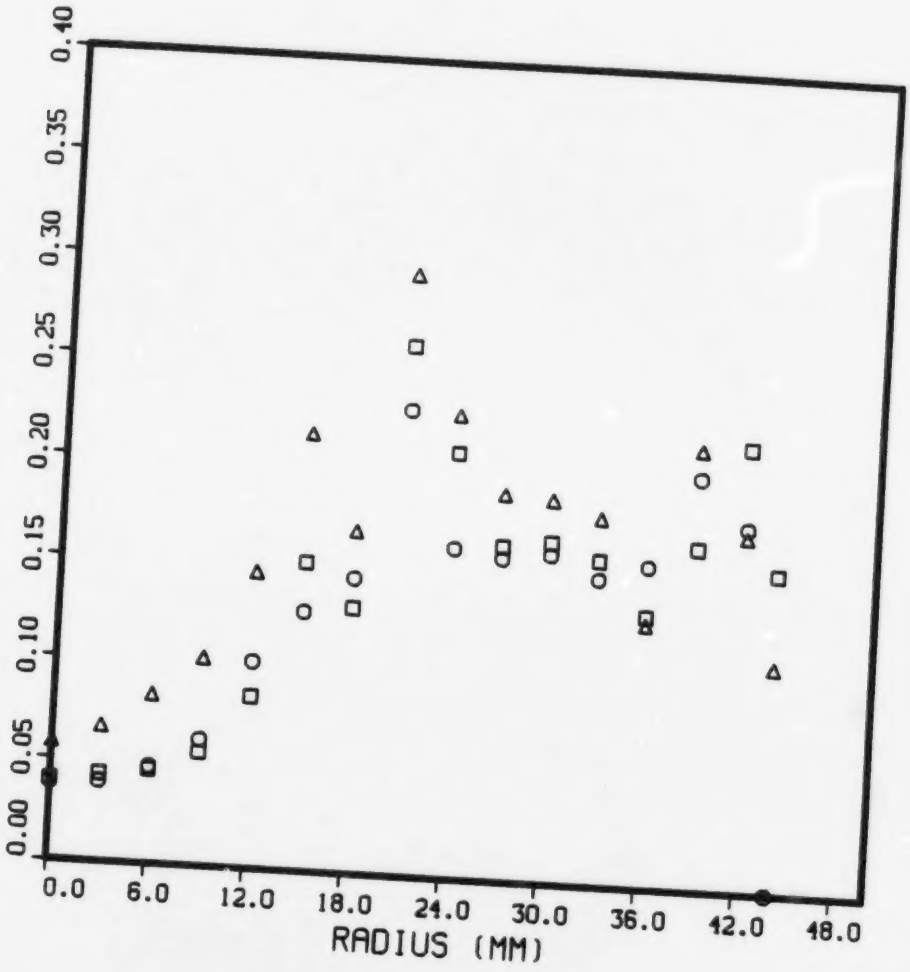

Figure 25: 45° fixed vane swirl generator; $\theta = -90°$, z=9 mm; $\square \frac{u'_z}{\hat{U}_z}$, $\circ \frac{u'_r}{\hat{U}_z}$, $\Delta \frac{u'_\theta}{\hat{U}_z}$; $\hat{U}_z$ = 13.5 m/s.

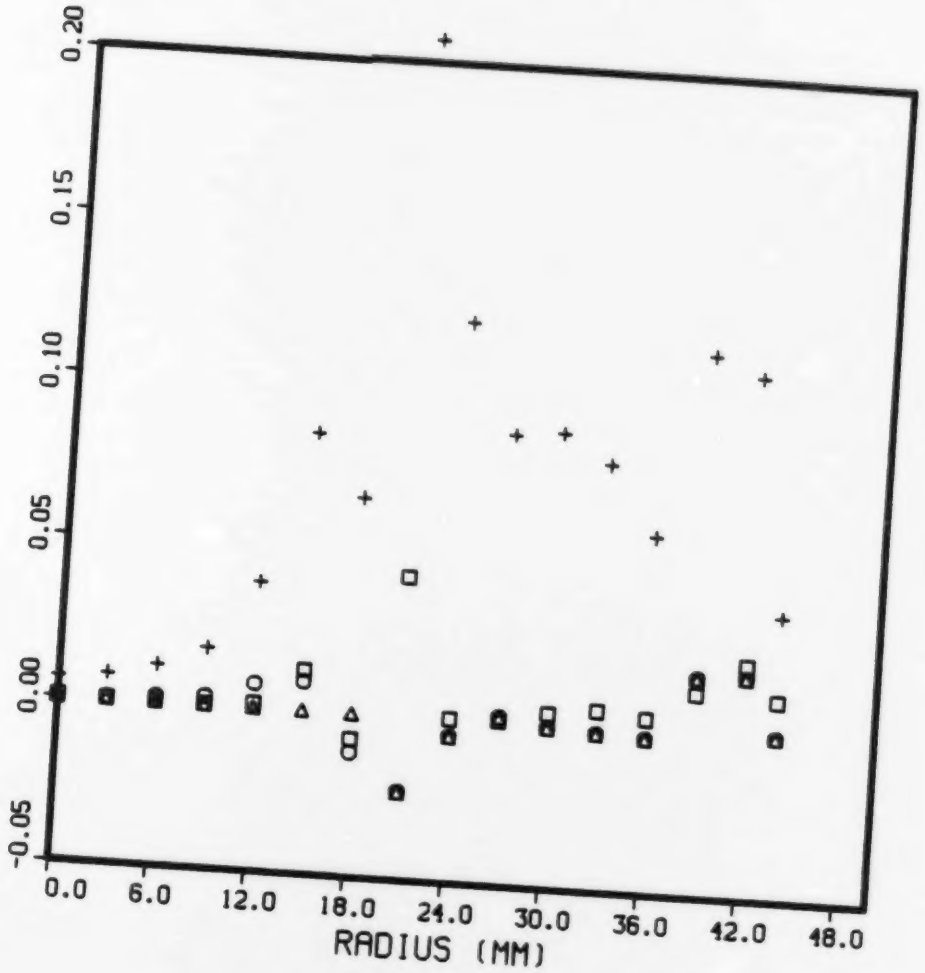

Figure 26: 45° fixed vane swirl generator; $\theta = -90°$, z=9 mm; $\square \frac{\overline{u_\theta u_z}}{U_z^2}$, $\circ \frac{\overline{u_r u_z}}{U_z^2}$, $\triangle \frac{\overline{u_r u_\theta}}{U_z^2}$, $+ \frac{q^2}{U_z^2}$; $\widehat{U}_z = 13.5$ m/s.

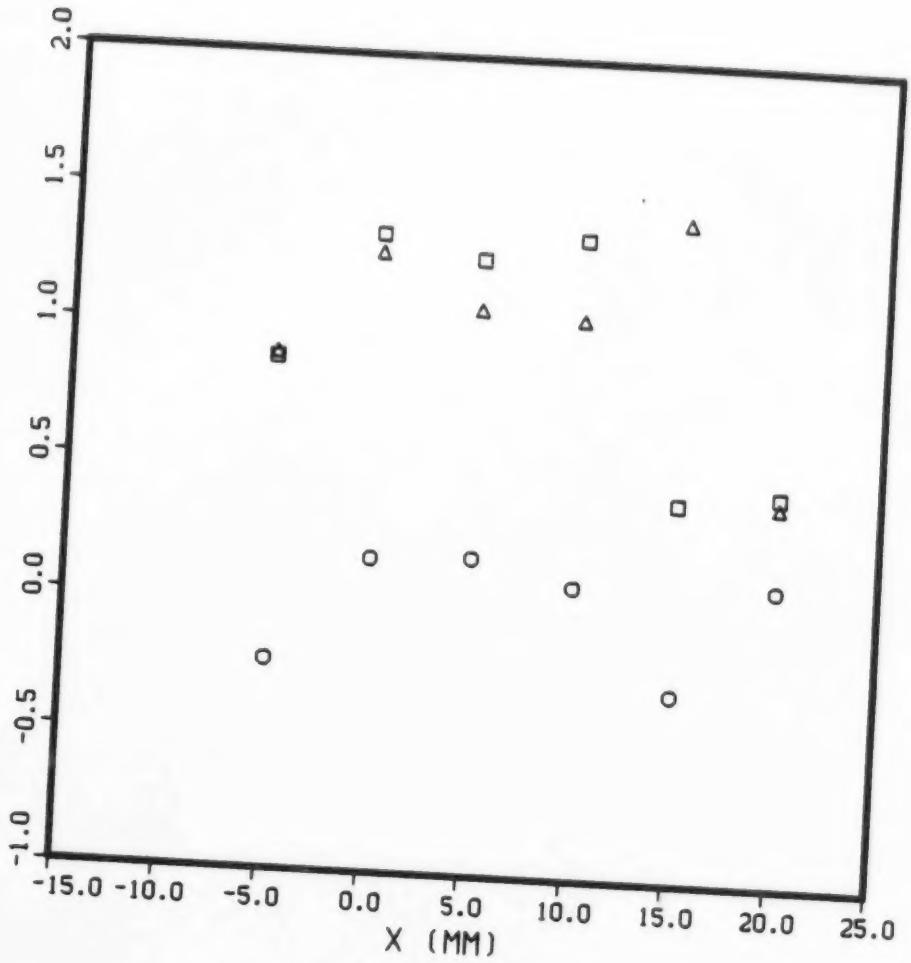

Figure 27: 45° fixed vane swirl generator; y=-33 mm, z=9 mm; $\square \frac{U_x}{U_z}$, $\circ \frac{U_r}{U_z}$, $\Delta \frac{U_\theta}{U_z}$; $\hat{U}_z$ = 13.5 m/s.

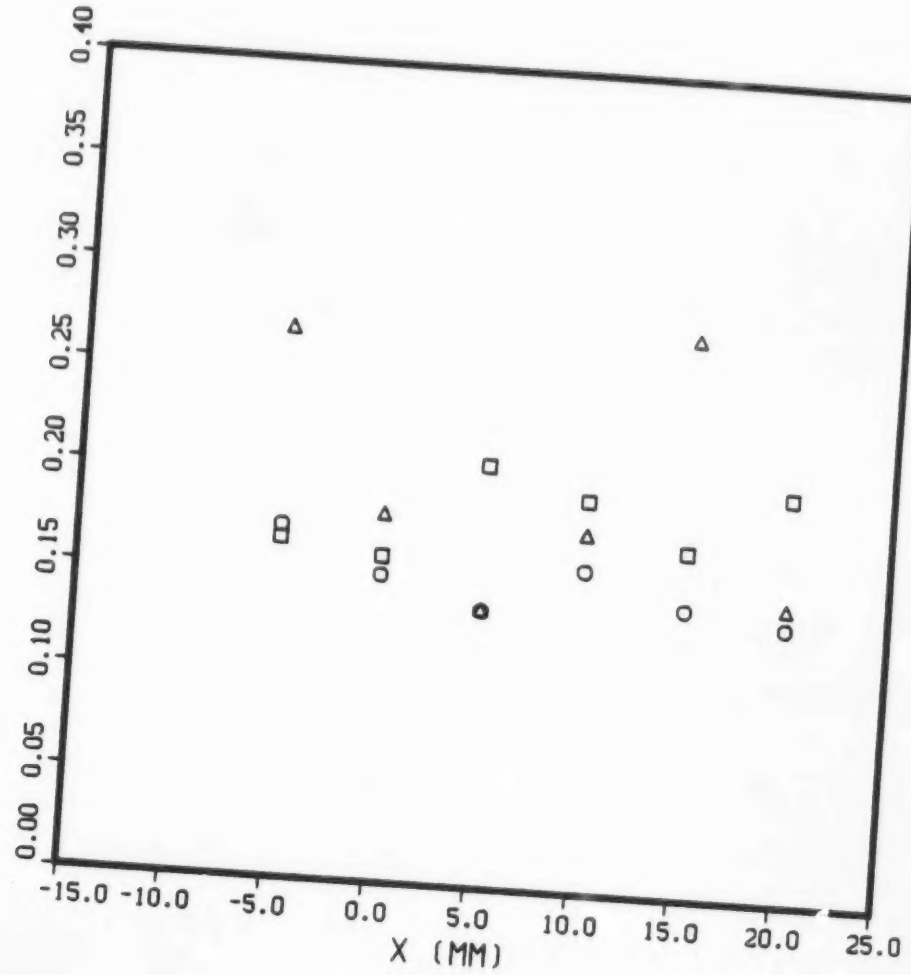

Figure 28: 45° fixed vane swirl generator; y=-33 mm, z=9 mm; $\square \frac{u'_x}{U_x}$, $\circ \frac{u'_z}{U_x}$, $\triangle \frac{u'_y}{U_x}$; $\hat{U}_z$ = 13.5 m/s.

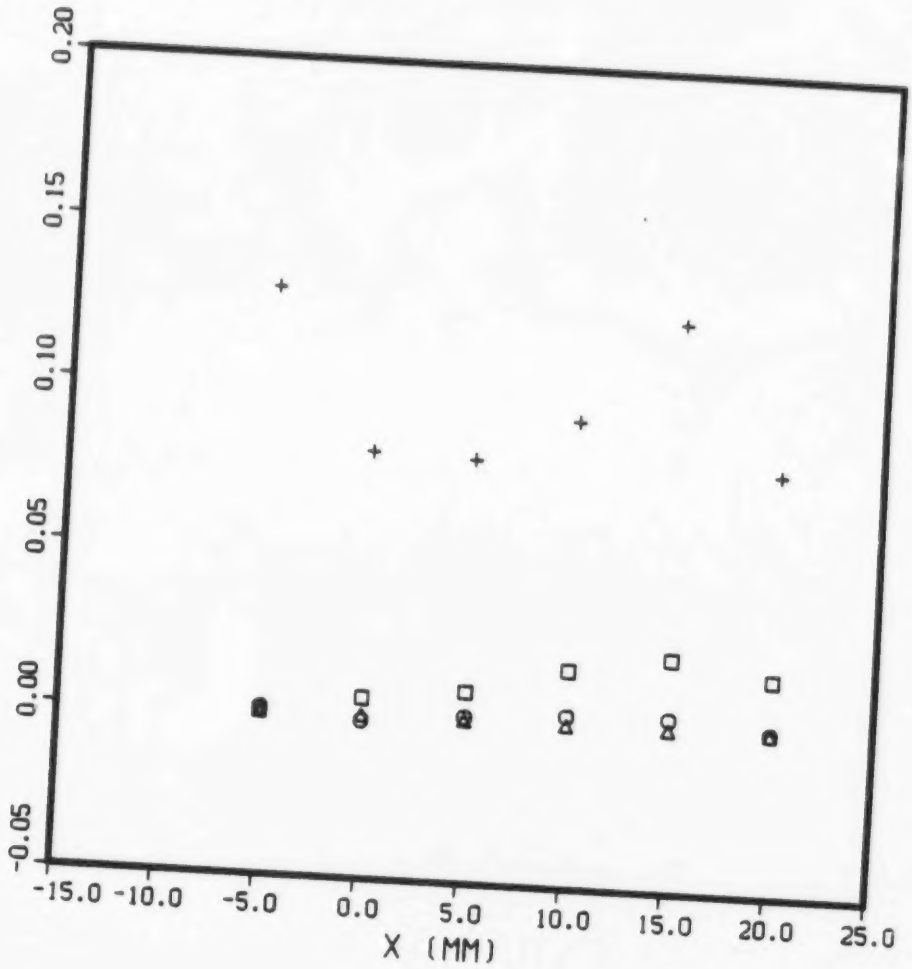

Figure 29: 45° fixed vane swirl generator; y=-33 mm, z=9 mm; □ $\frac{\overline{u_x u_x}}{\hat{U}_z^2}$, ○ $\frac{\overline{u_z u_z}}{\hat{U}_z^2}$, △ $\frac{\overline{u_y u_y}}{\hat{U}_z^2}$, + $\frac{q^2}{\hat{U}_z^2}$; $\hat{U}_z$ = 13.5 m/s.

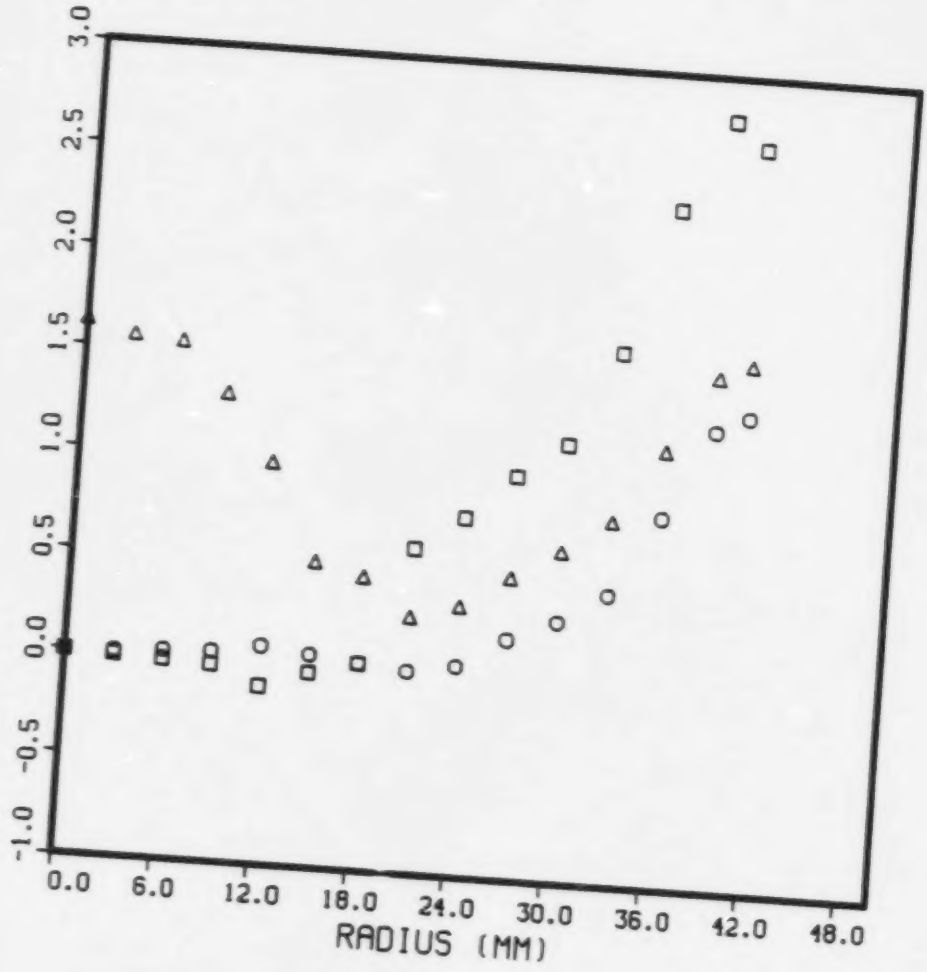

Figure 30: 60° fixed vane swirl generator; $\theta = -90°$, z=6 mm; $\square \frac{U_\theta}{U_z}$, $\circ \frac{U_r}{U_z}$, $\Delta \frac{U_z}{U_z}$; $\hat{U}_z =$ 10.9 m/s.

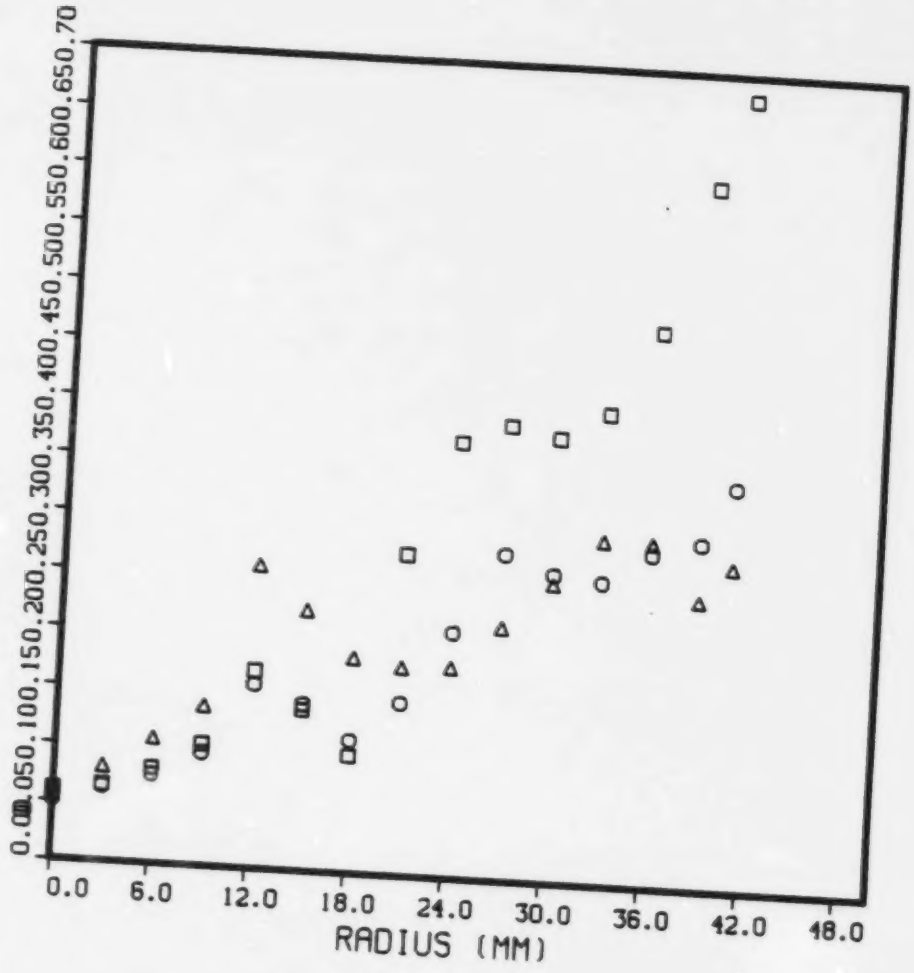

Figure 31: 45° fixed vane swirl generator; $\theta = -90°$, z=6 mm; $\square \frac{u'}{U_z}$, $\circ \frac{u'}{U_z}$, $\triangle \frac{u'}{U_z}$; $\hat{U}_z$ = 10.9 m/s.

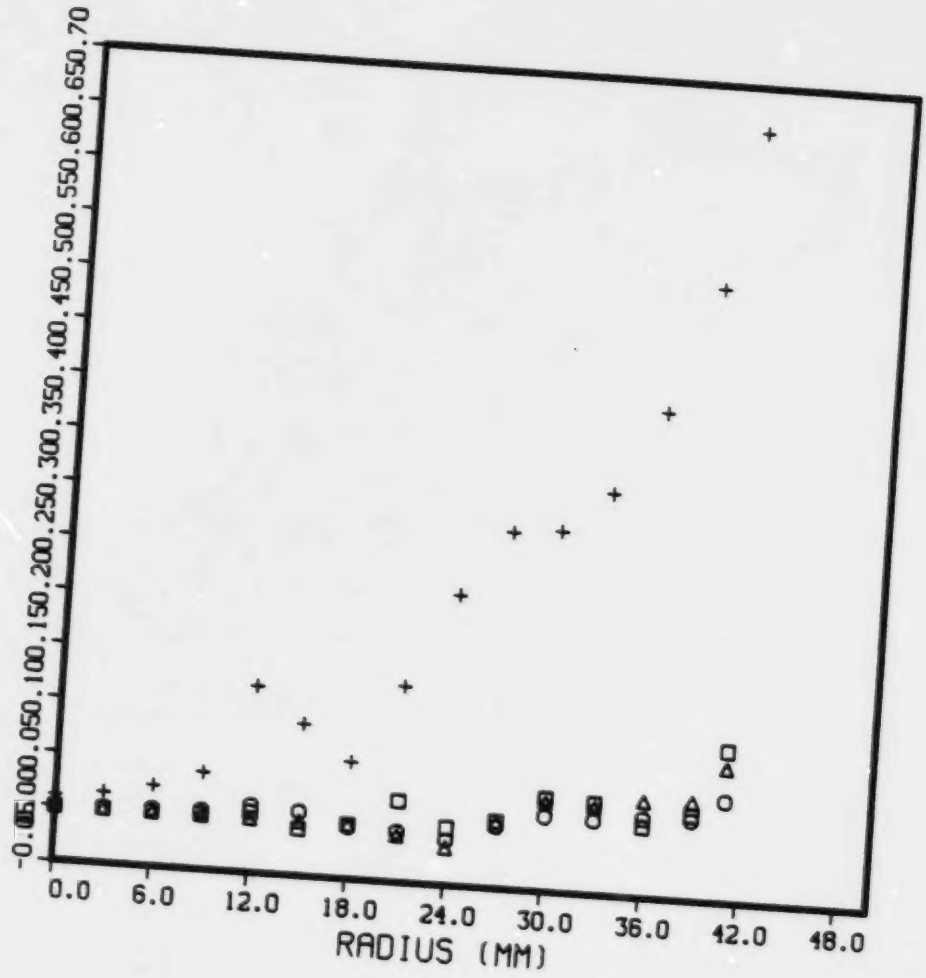

Figure 32: 60° fixed vane swirl generator; $\theta = -90°$, z=6 mm; $\square \frac{\overline{u_\theta u_\theta}}{U_z^2}$, $\circ \frac{\overline{u_r u_r}}{U_z^2}$, $\triangle \frac{\overline{u_r u_\theta}}{U_z^2}$, $+ \frac{q^2}{U_z^2}$; $\widehat{U}_z = 10.9$ m/s.

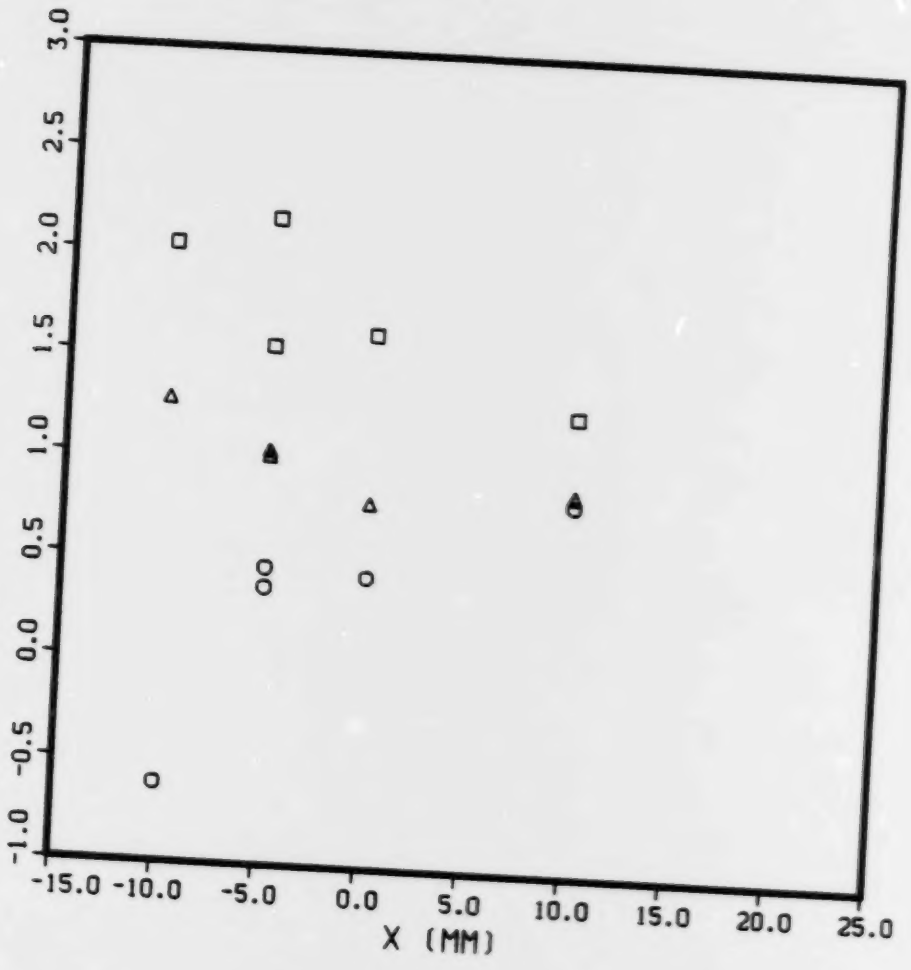

Figure 33: 60° fixed vane swirl generator; y=-33 mm, z=6 mm; $\square \frac{U_x}{U_x}$, $\circ \frac{U_r}{U_x}$, $\Delta \frac{U_\theta}{U_x}$; $\hat{U}_x$ = 10.9 m/s.

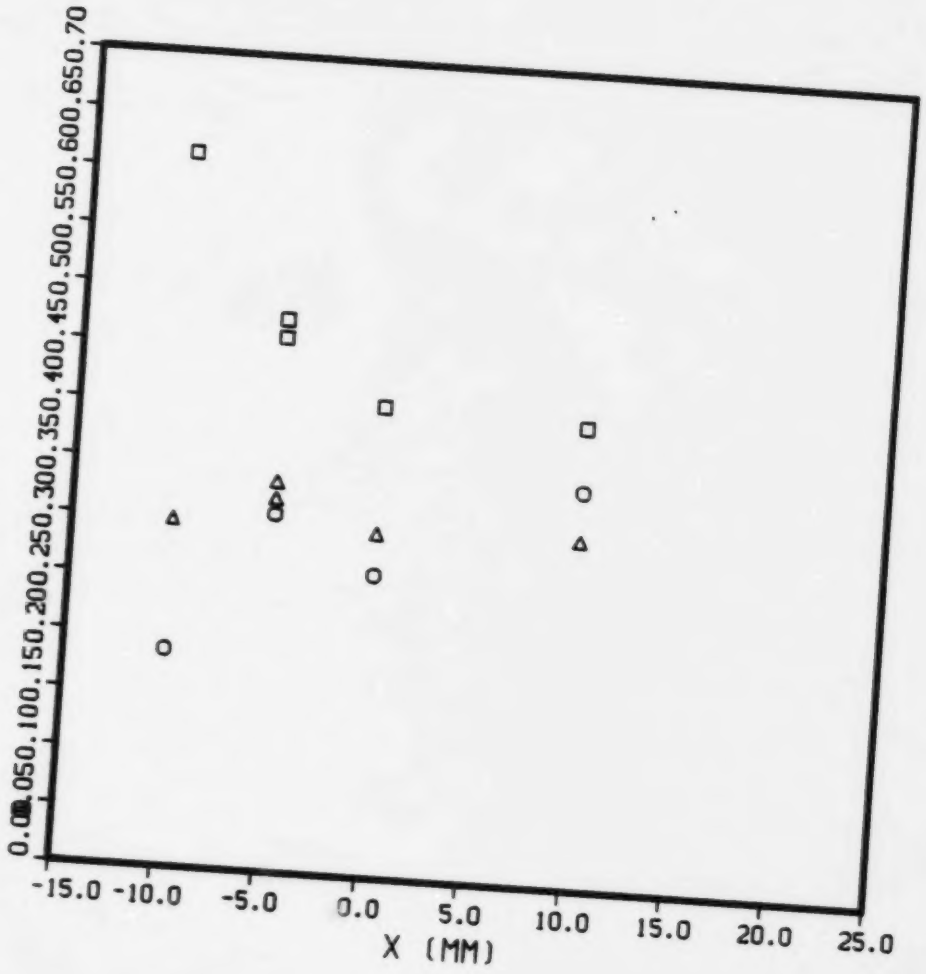

Figure 34: 45° fixed vane swirl generator; y=-33 mm, z=6 mm; $\square \frac{u'_x}{U_x}$, $\circ \frac{u'_r}{U_x}$, $\Delta \frac{u'_z}{U_z}$; $\hat{U}_z$ = 10.9 m/s.

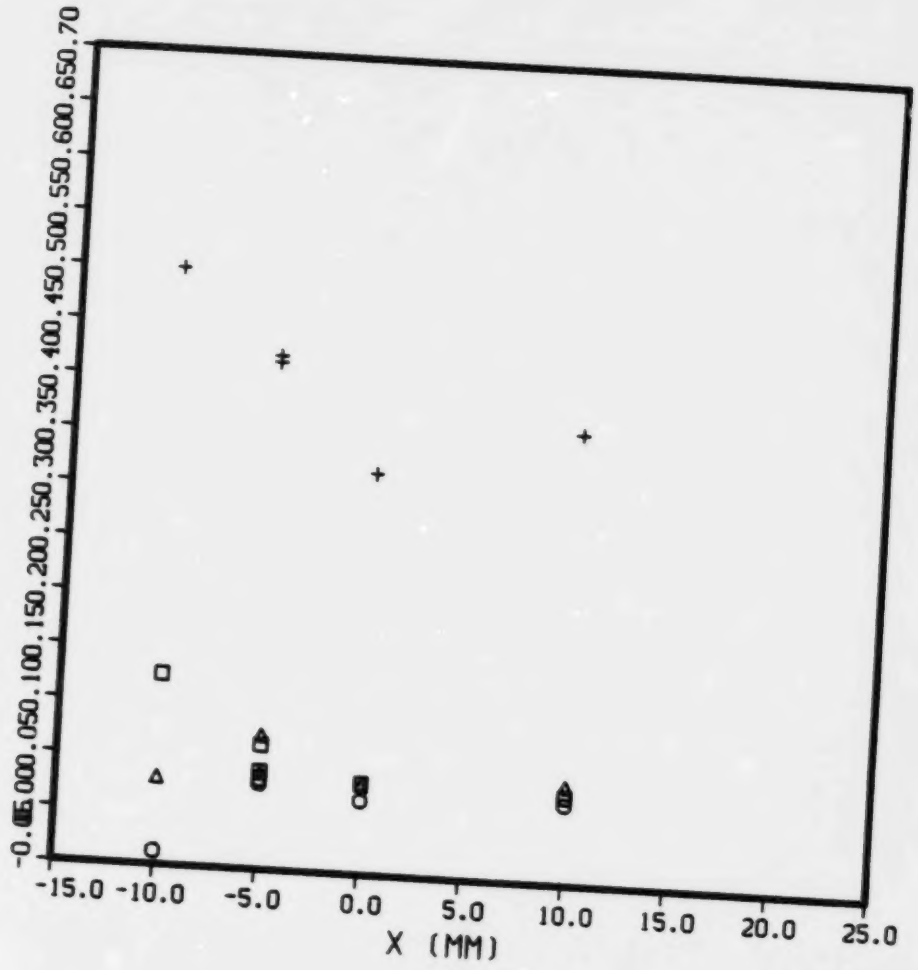

Figure 35: 60° fixed vane swirl generator; y=-33 mm, z=6 mm; □ $\frac{\overline{u_x u_x}}{U_z^2}$, ○ $\frac{\overline{u_y u_y}}{U_z^2}$, △ $\frac{\overline{u_z u_z}}{U_z^2}$, + $\frac{q^2}{U_z^2}$; $\hat{U}_z = 10.9$ m/s.

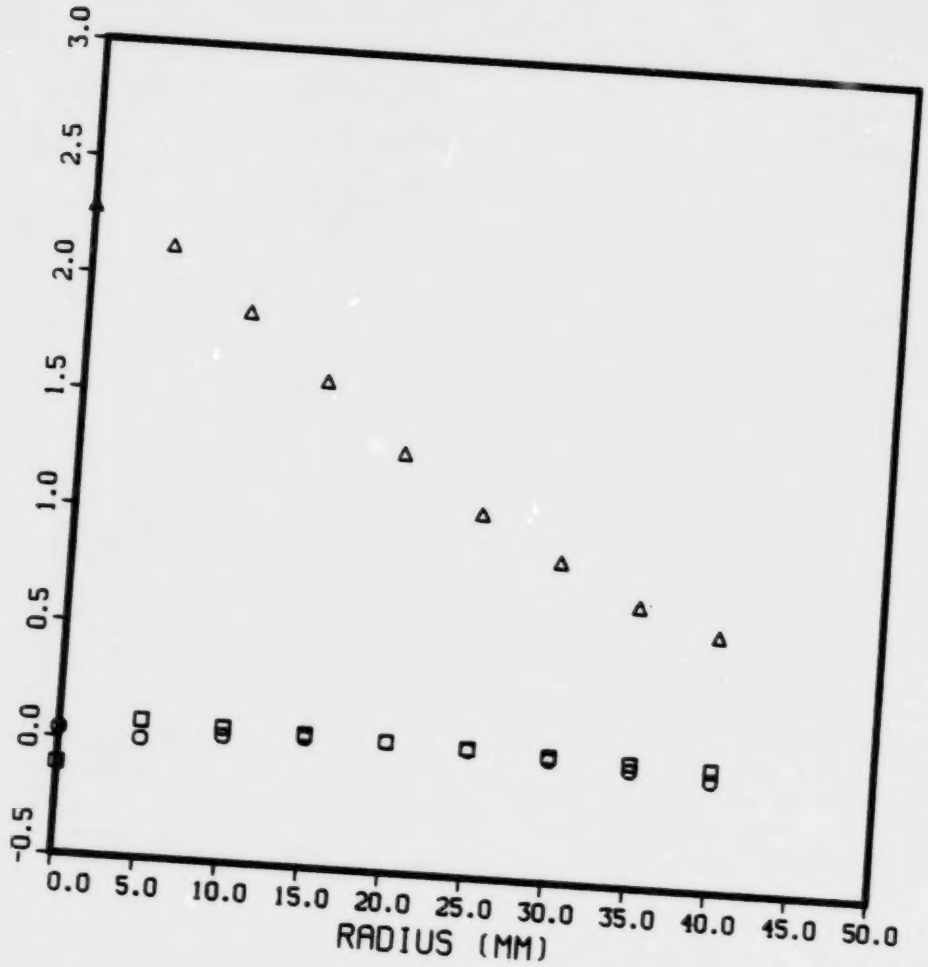

Figure 36: IFRF variable swirl generator primary flow; $\theta = 90°$, z=2.5 mm; $\square \frac{U_\theta}{U_z}$, $\circ \frac{U_r}{U_z}$, $\triangle \frac{U_z}{U_z}$; $\hat{U}_z = 8.2$ m/s.

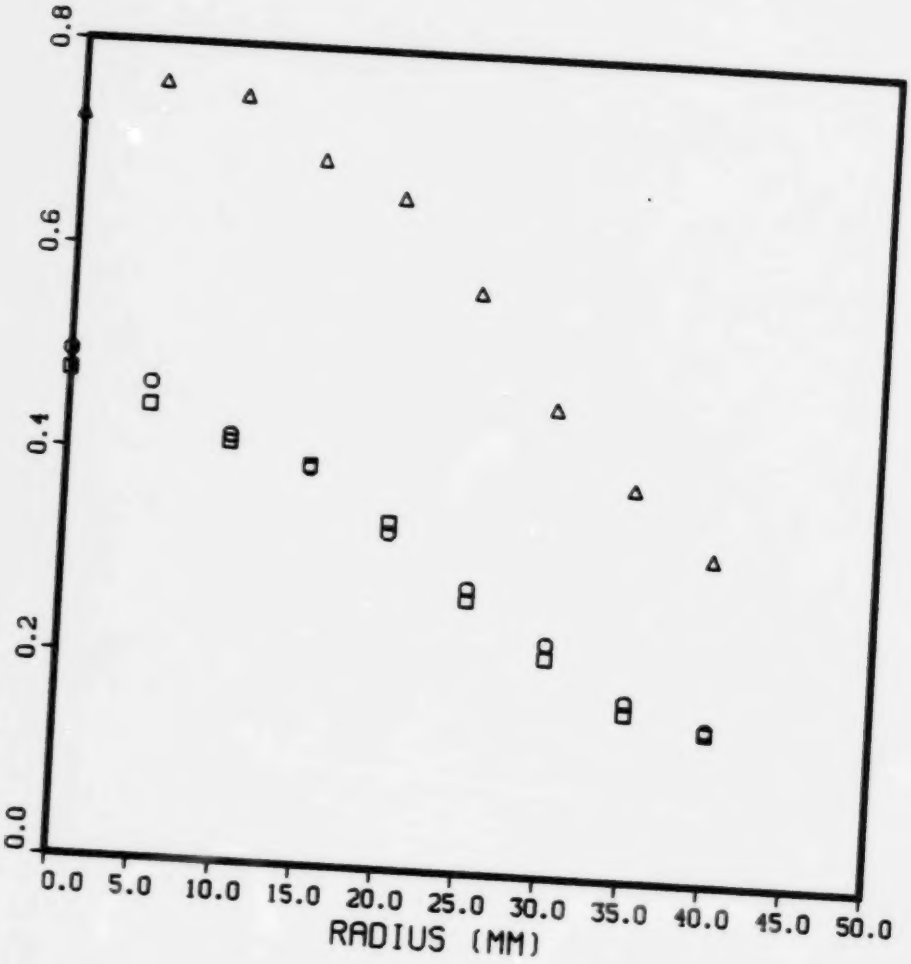

Figure 37: IFRF variable swirl generator primary flow; $\theta = 90°$, z=2.5 mm; $\Box \frac{u'}{\hat{U}_z}$, $\circ \frac{u'}{\hat{U}_z}$, $\Delta \frac{u'}{\hat{U}_z}$; $\hat{U}_z = 8.2$ m/s.

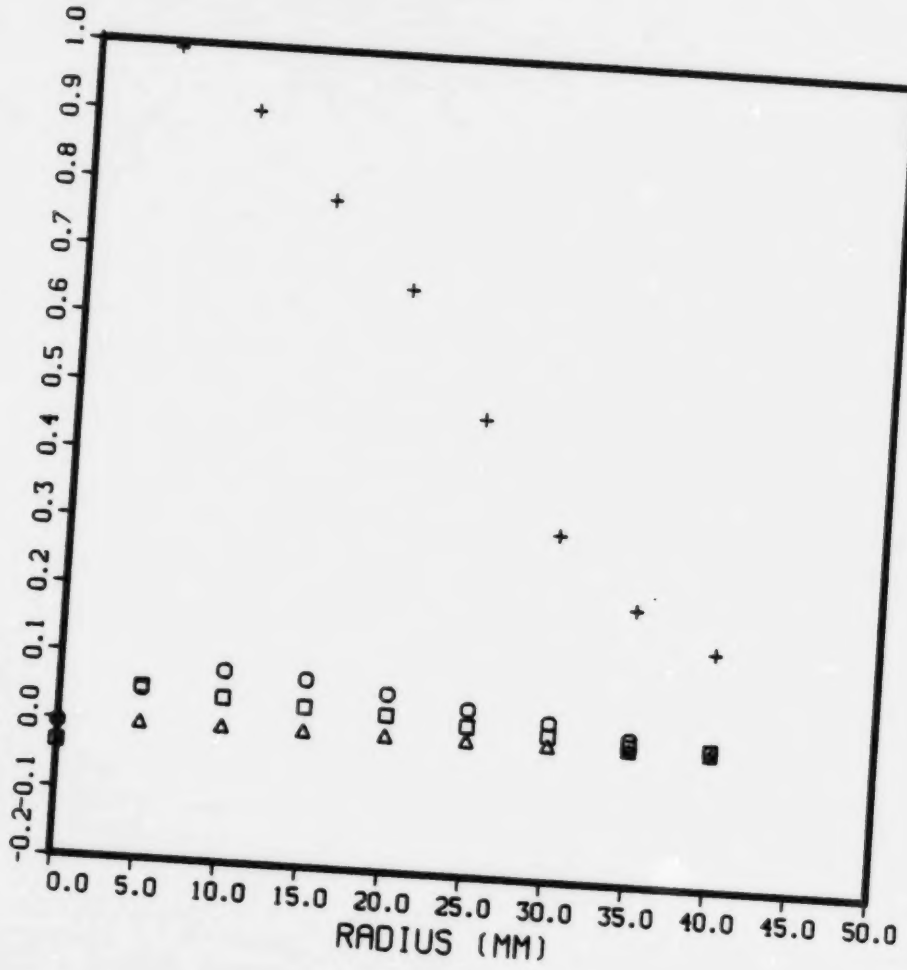

Figure 38: IFRF variable swirl generator primary flow; θ = 90°, z=2.5 mm; $\circ \frac{\overline{u_r u_z}}{\hat{U}_z^2}$, $\triangle \frac{\overline{u_r u_\theta}}{\hat{U}_z^2}$, $+ \frac{q^2}{\hat{U}_z^2}$; $\hat{U}_z = 8.2$ m/s.

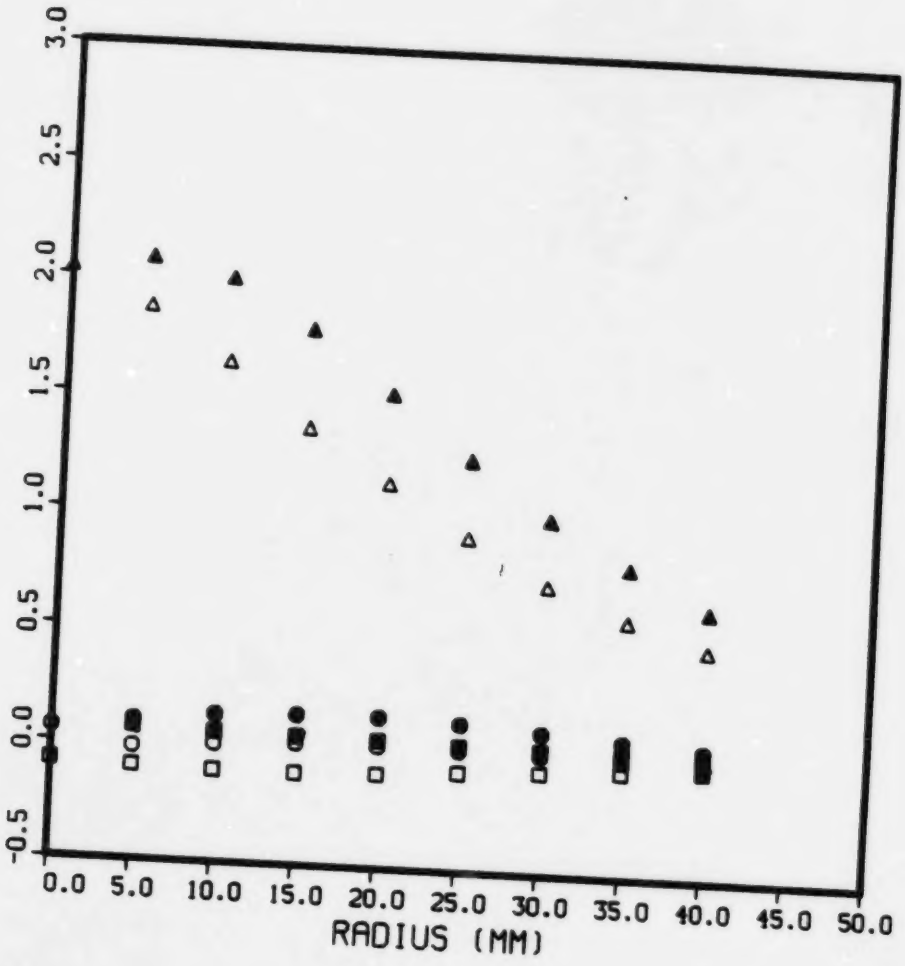

Figure 39: IFRF variable swirl generator primary flow; $\theta = \pm 90°$, z=2.5 mm; $\square \frac{U_z}{U_s}$, $\circ \frac{U_r}{U_s}$, $\triangle \frac{U_\theta}{U_s}$; $\hat{U}_s = 6.6$ m/s. Open symbols for $\theta = +90°$, solid symbols for $\theta = -90°$.

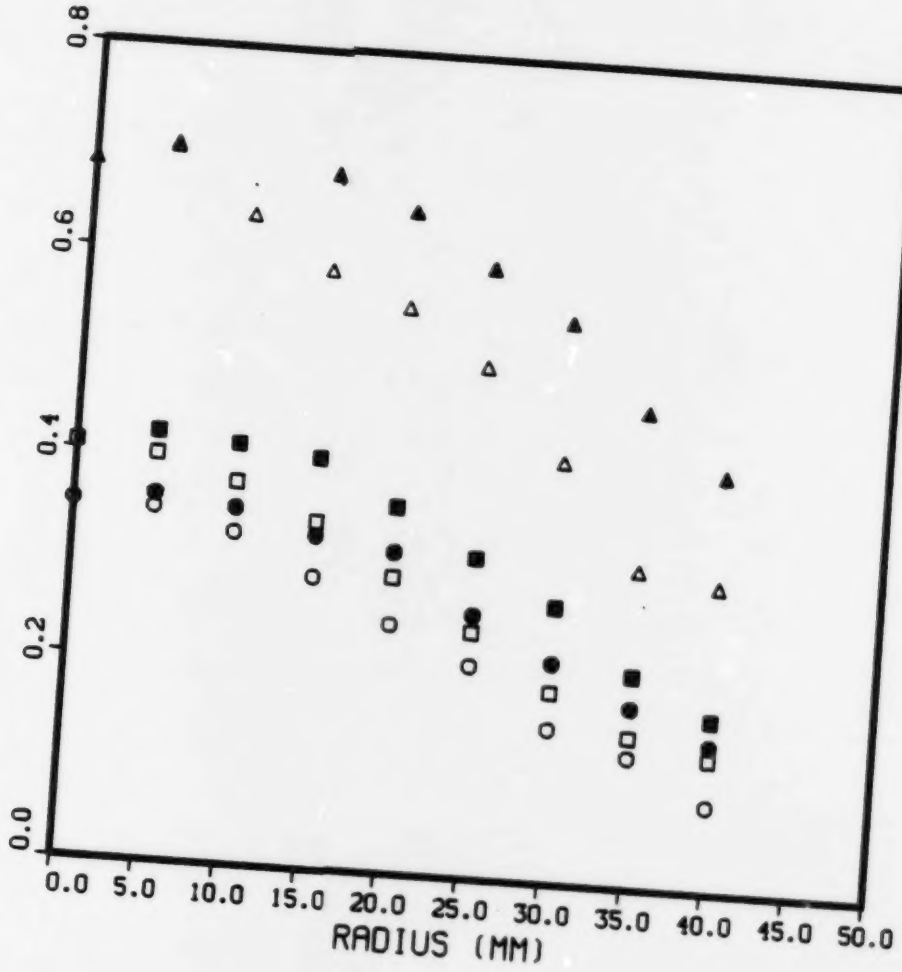

Figure 40: IFRF variable swirl generator primary flow; $\theta = \pm 90°$, z=2.5 mm; $\Box \frac{u'_z}{\hat{U}_z}$, $\circ \frac{u'_r}{\hat{U}_z}$, $\Delta \frac{u'_z}{\hat{U}_z}$; $\hat{U}_z = 6.6$ m/s. Open symbols for $\theta = +90°$, solid symbols for $\theta = -90°$.

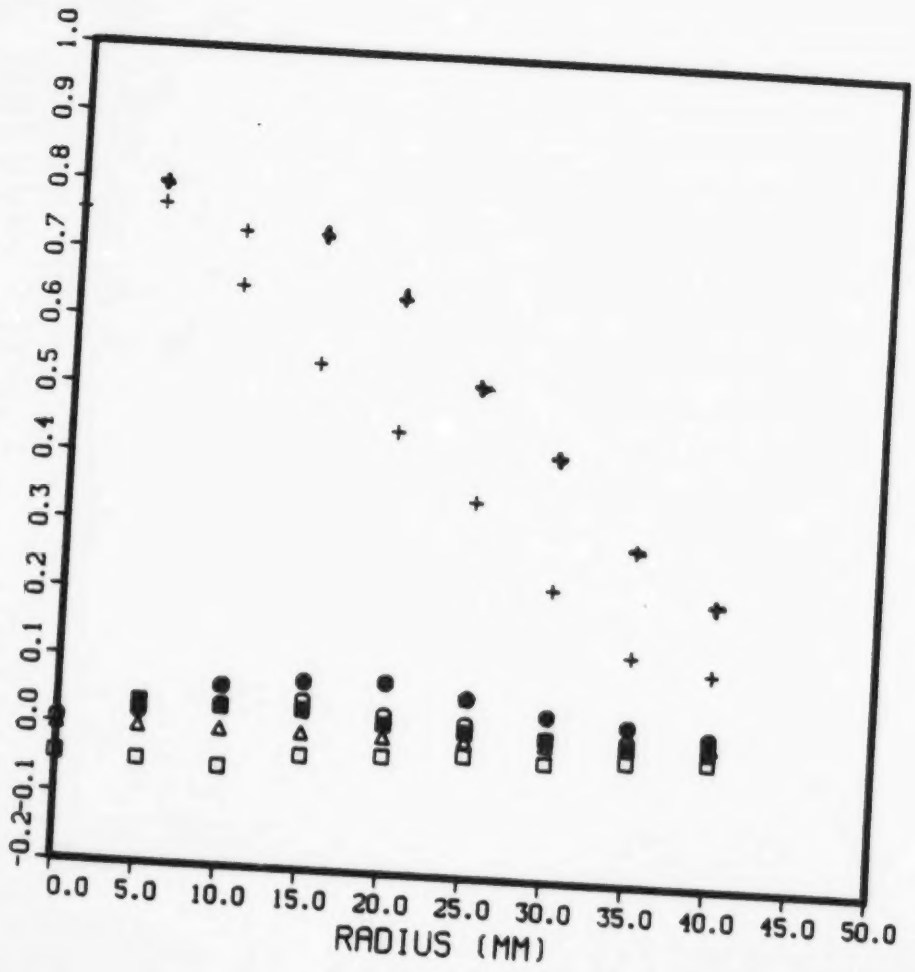

Figure 41: IFRF variable swirl generator primary flow; $\theta = \pm 90°$, z=2.5 mm; $\square \frac{\overline{u_\theta u_z}}{U_z^2}$, $\circ \frac{\overline{u_r u_z}}{U_z^2}$, $\triangle \frac{\overline{u_r u_\theta}}{U_z^2}$, $+ \frac{k^2}{U_z^2}$; $\hat{U}_z = 6.6$ m/s. Open symbols for $\theta = +90°$, solid symbols for $\theta = -90°$.

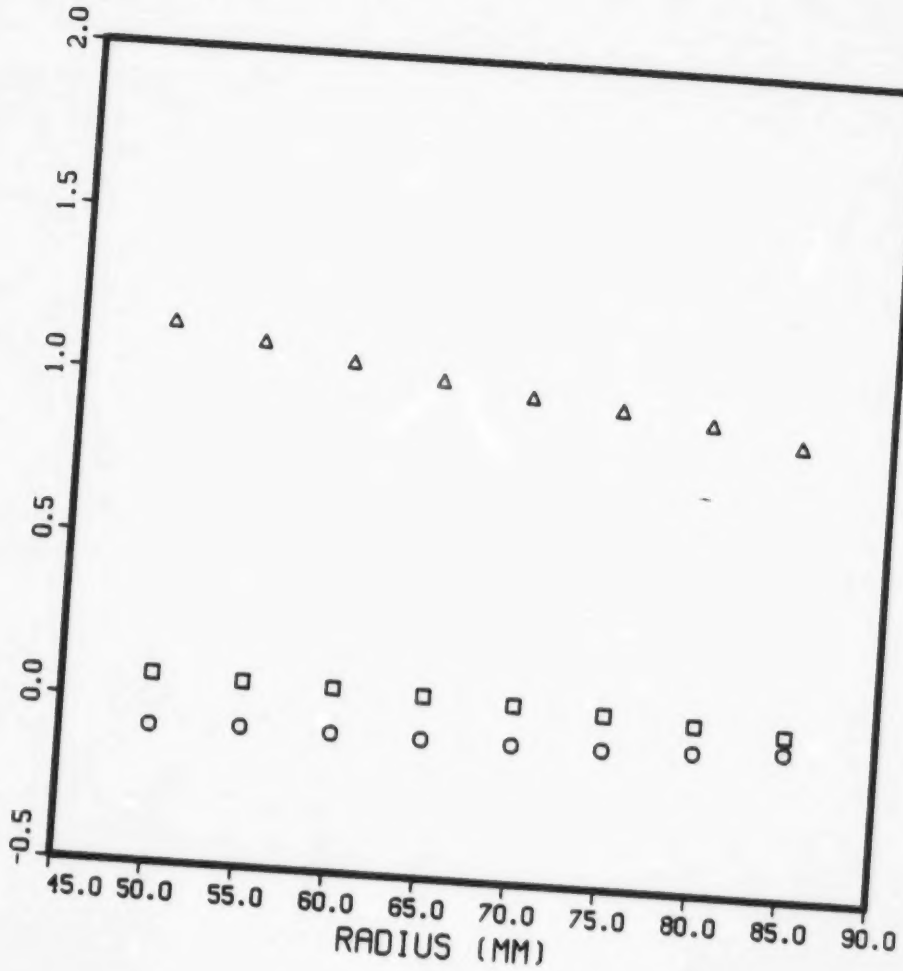

Figure 42: IFRF variable swirl generator secondary flow; S=0.0, $\theta = 90°$, z=2.5 mm; $\square \frac{U_\theta}{\hat{U}_z}$, $\circ \frac{U_r}{\hat{U}_z}$, $\triangle \frac{U_z}{\hat{U}_z}$; $\hat{U}_z = 14.4$ m/s.

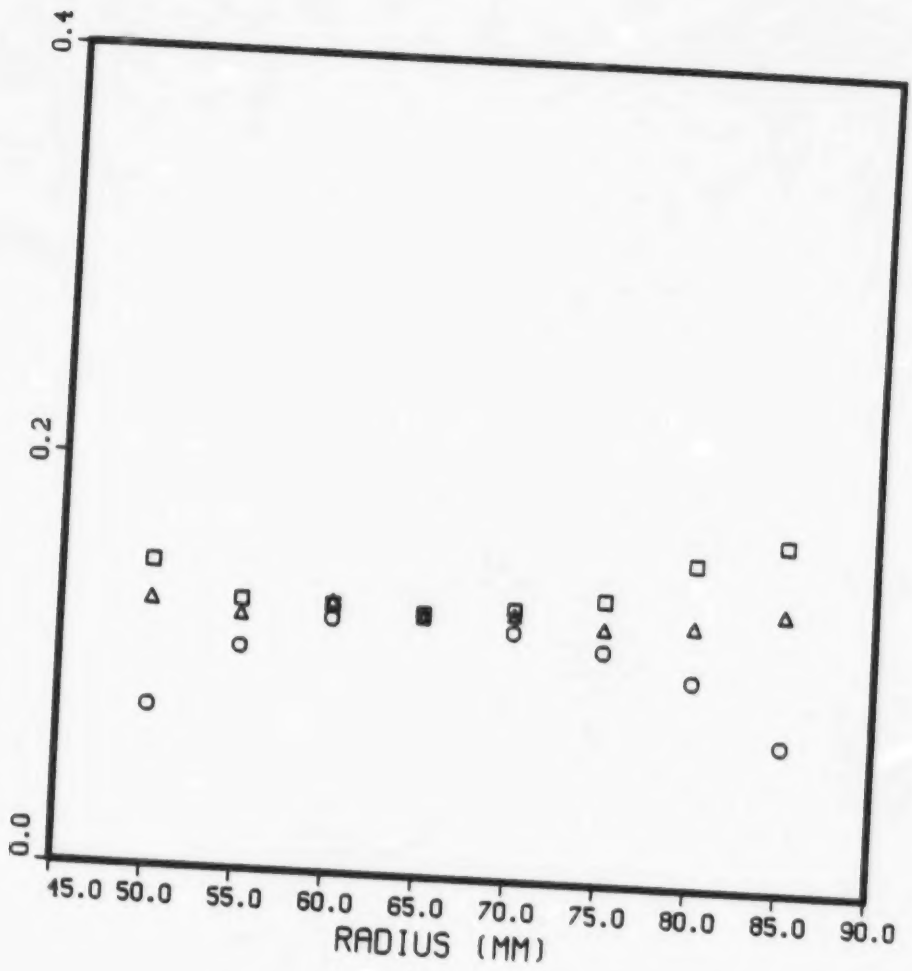

Figure 43: IFRF variable swirl generator secondary flow; S=0.0, $\theta = 90°$, z=2.5 mm; $\square \frac{u'_R}{\hat{U}_z}$, $\circ \frac{u'_z}{\hat{U}_z}$, $\Delta \frac{u'_\theta}{\hat{U}_z}$; $\hat{U}_z = 14.4$ m/s.

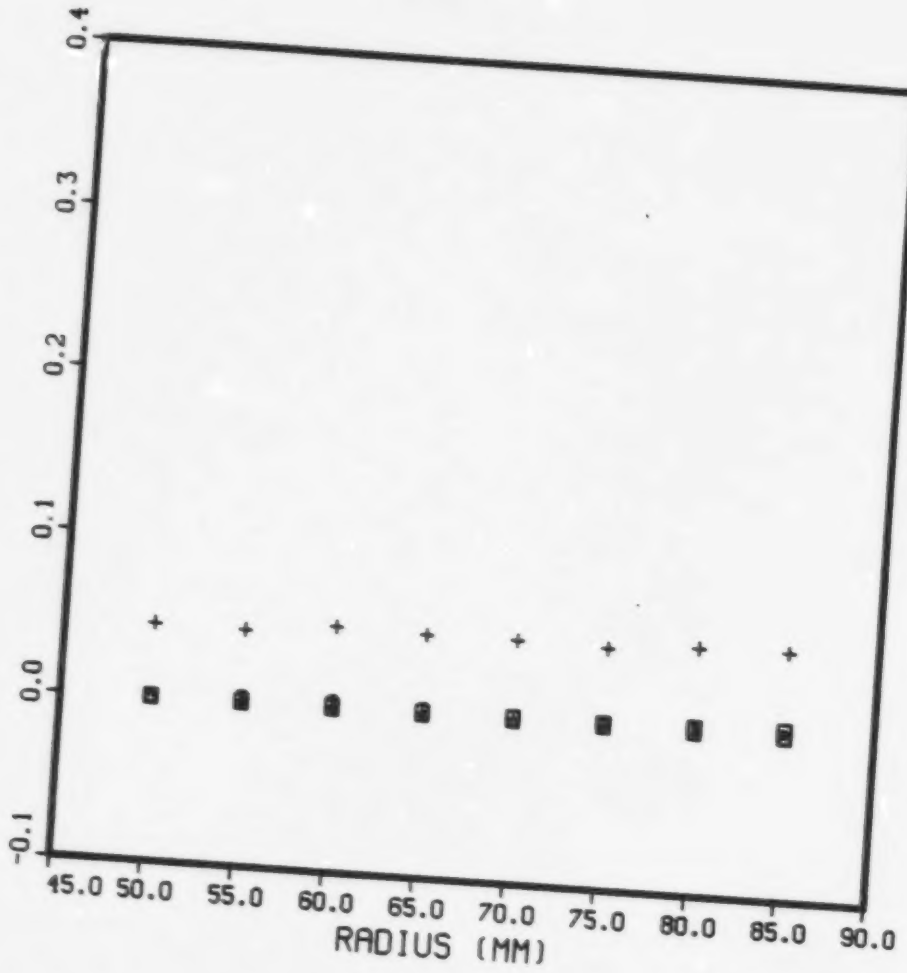

Figure 44: IFRF variable swirl generator secondary flow; S=0.0, $\theta = 90°$, z=2.5 mm; $\square \frac{\overline{u_\theta u_z}}{U_i^2}$, $\circ \frac{\overline{u_r u_z}}{U_i^2}$, $\triangle \frac{\overline{u_r u_\theta}}{U_i^2}$, $+ \frac{q^2}{U_i^2}$; $\widehat{U}_z = 14.4$ m/s.

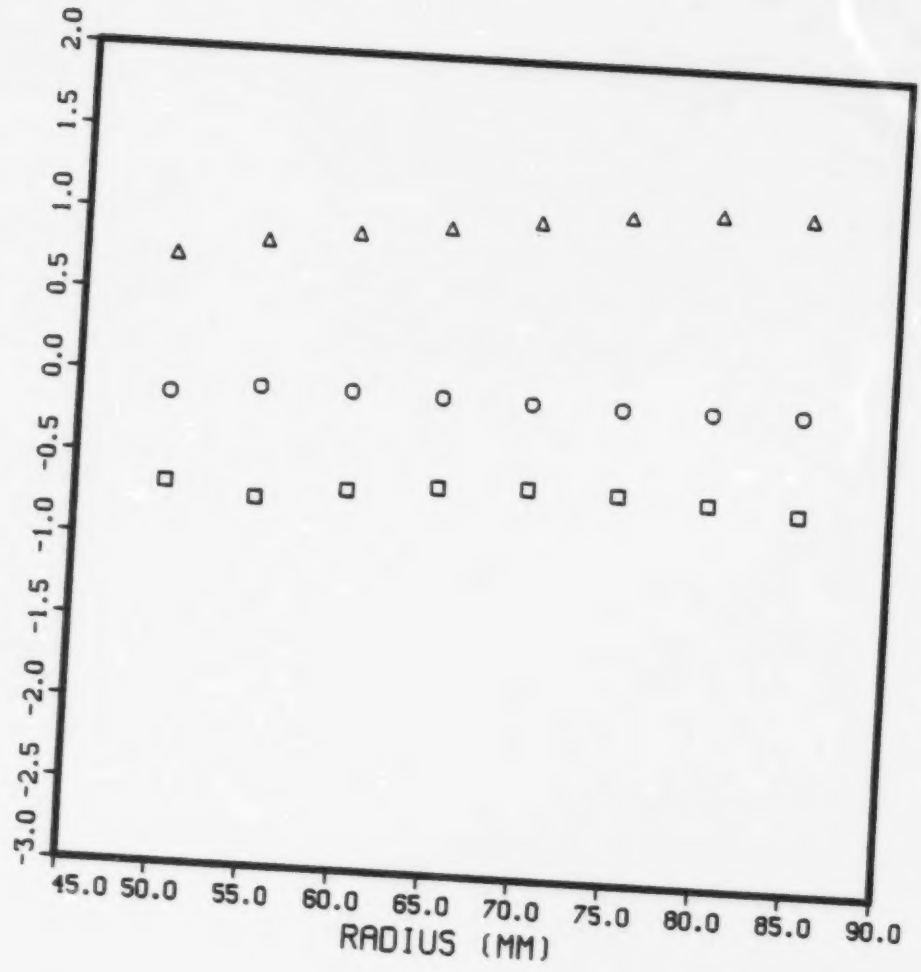

Figure 45: IFRF variable swirl generator secondary flow; S=1.0, $\theta = 90°$, z=4.0 mm; $\square \frac{U_a}{U_s}$, $\circ \frac{U_r}{U_s}$, $\triangle \frac{U_t}{U_s}$; $\hat{U}_s = 11.9$ m/s.

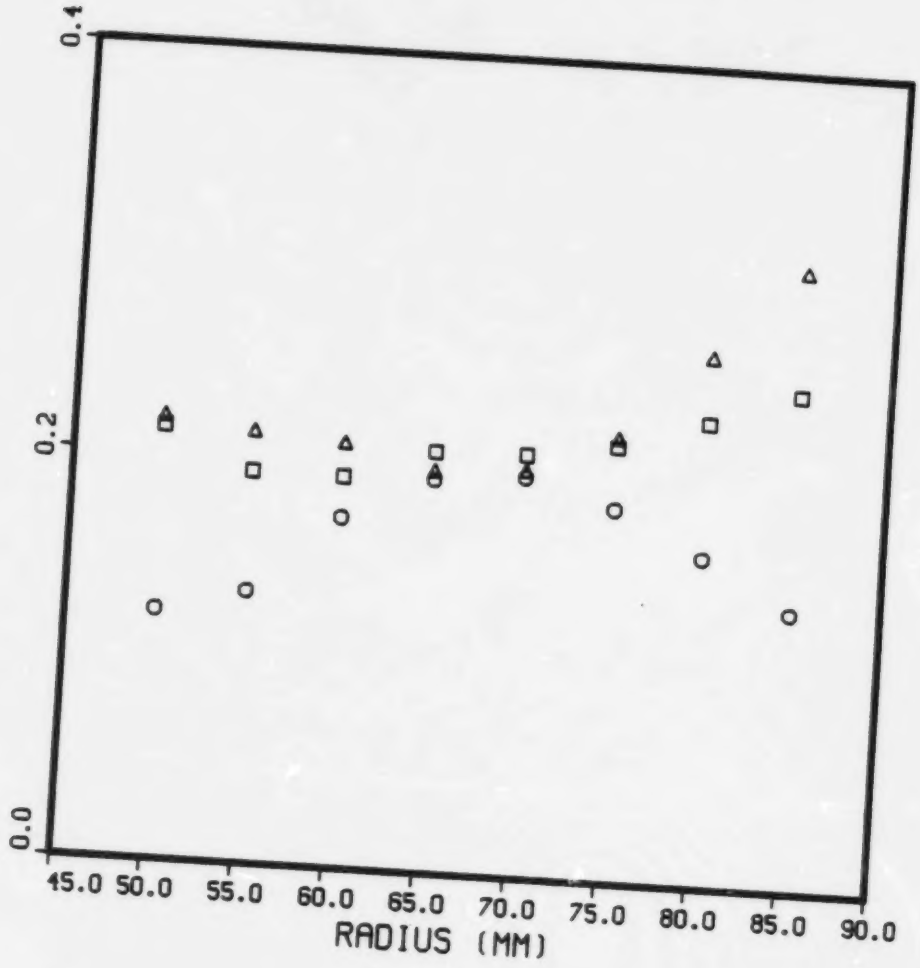

Figure 46: IFRF variable swirl generator secondary flow; S=1.0, $\theta = 90°$, z=4.0 mm; $\square \frac{u'_z}{\hat{U}_z}$, $\circ \frac{u'_r}{\hat{U}_z}$, $\triangle \frac{u'_\theta}{\hat{U}_z}$; $\hat{U}_z = 11.9$ m/s.

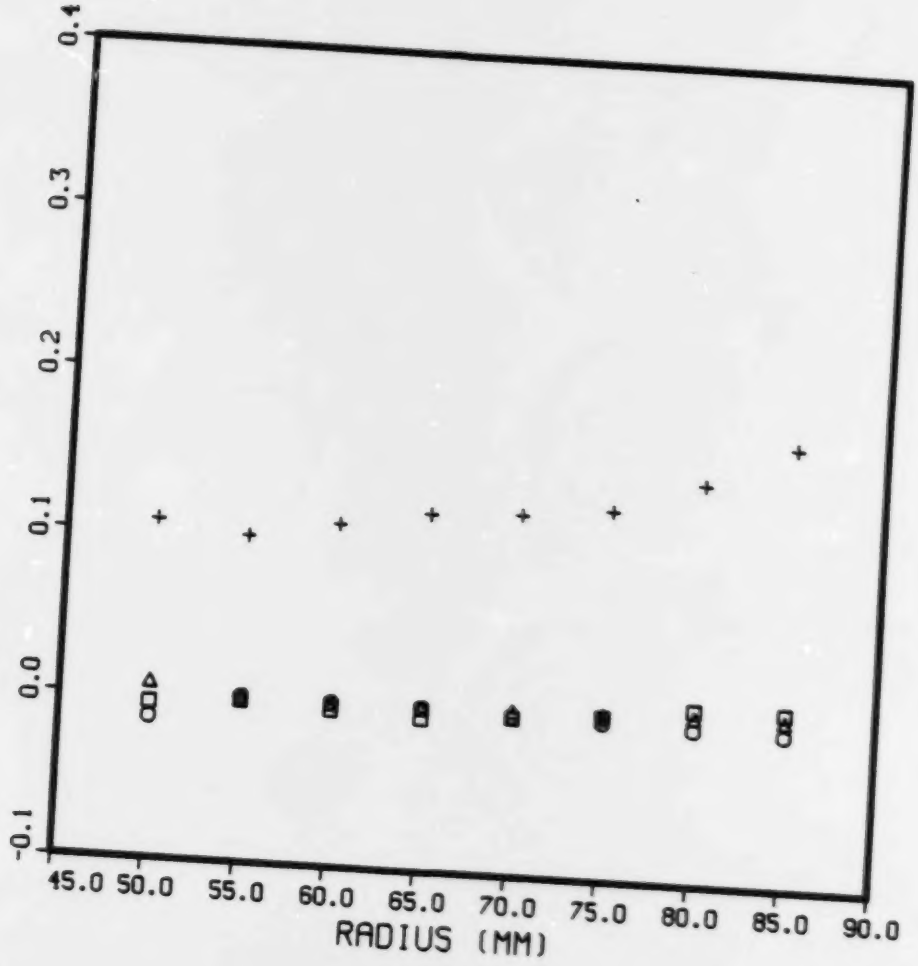

Figure 47: IFRF variable swirl generator secondary flow; S=1.0, $\theta = 90°$, z=4.0 mm; $\square \frac{\overline{u_\theta u_z}}{U_i^2}$, $\circ \frac{\overline{u_r u_z}}{U_i^2}$, $\triangle \frac{\overline{u_r u_\theta}}{U_i^2}$, $+ \frac{q^2}{U_i^2}$; $\widehat{U}_i = 11.9$ m/s.

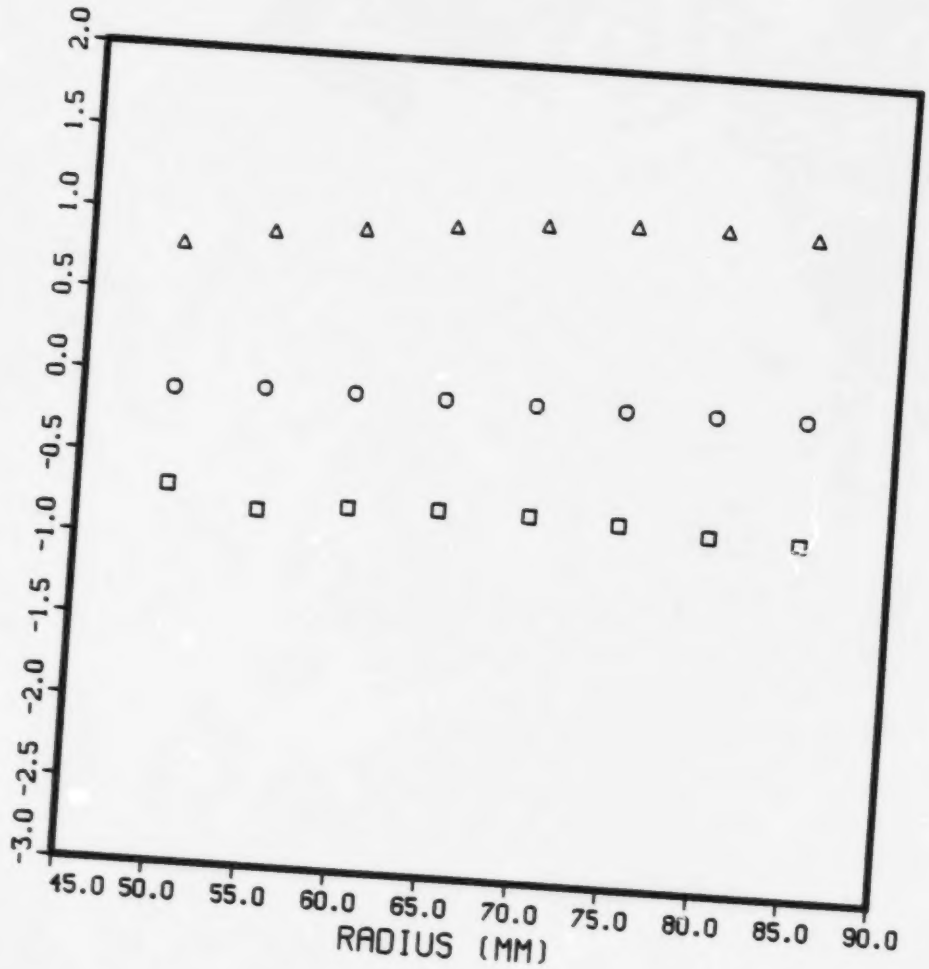

Figure 48: IFRF variable swirl generator secondary flow; S=1.0, $\theta = 90°$, z=4.0 mm; $\square \frac{U_\theta}{\hat{U}_z}$, $\circ \frac{U_r}{\hat{U}_z}$, $\Delta \frac{U_z}{\hat{U}_z}$; $\hat{U}_z = 7.2$ m/s.

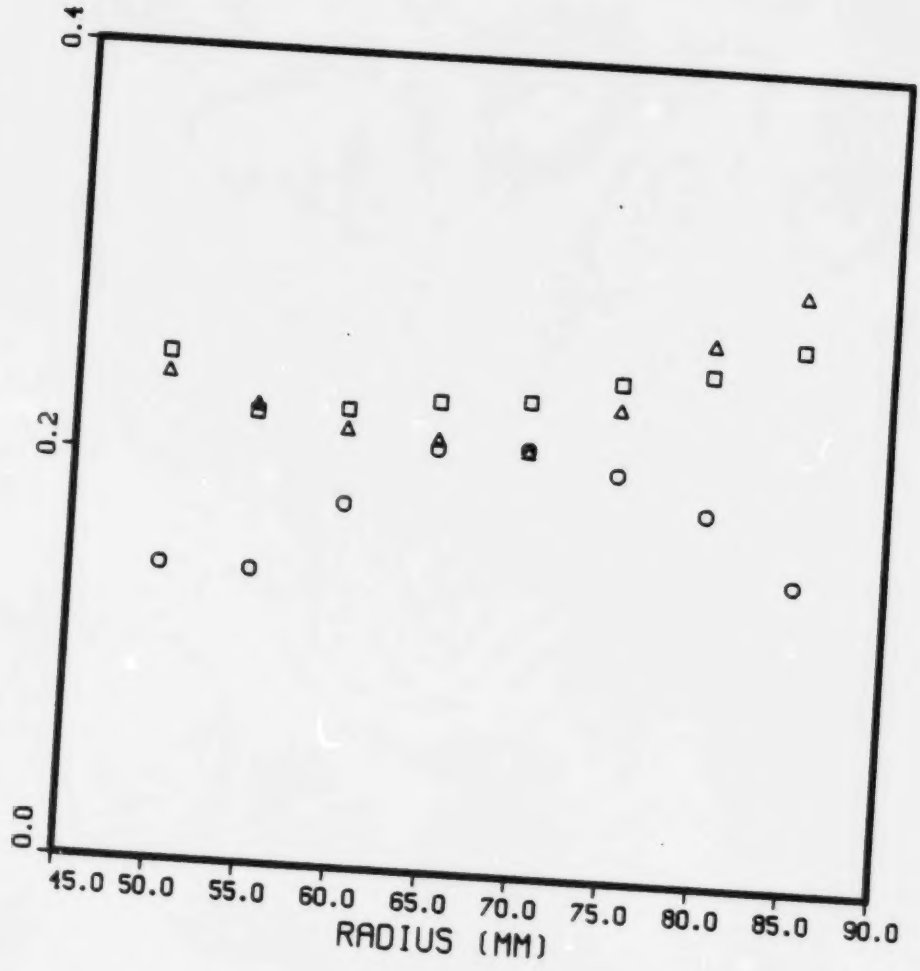

Figure 49: IFRF variable swirl generator secondary flow; S=1.0, $\theta = 90°$, z=4.0 mm; $\square \frac{u'_\theta}{\hat{U}_z}$, $\circ \frac{u'_r}{\hat{U}_z}$, $\triangle \frac{u'_z}{\hat{U}_z}$; $\hat{U}_z = 7.2$ m/s.

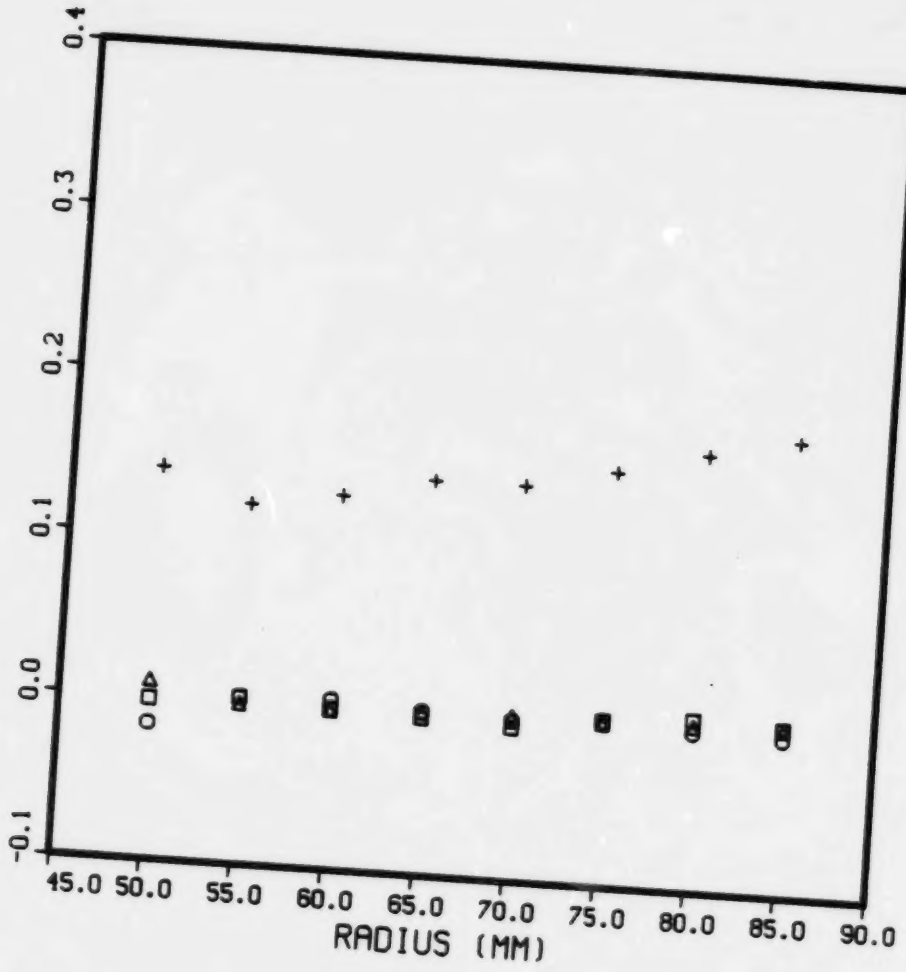

Figure 50: IFRF variable swirl generator secondary flow; S=1.0, $\theta = 90°$, z=4.0 mm; $\square \frac{\overline{u_\theta u_z}}{U_i^2}$, $\circ \frac{\overline{u_r u_z}}{U_i^2}$, $\Delta \frac{\overline{u_r u_\theta}}{U_i^2}$, $+ \frac{q^2}{U_i^2}$; $\hat{U}_z = 7.2$ m/s.

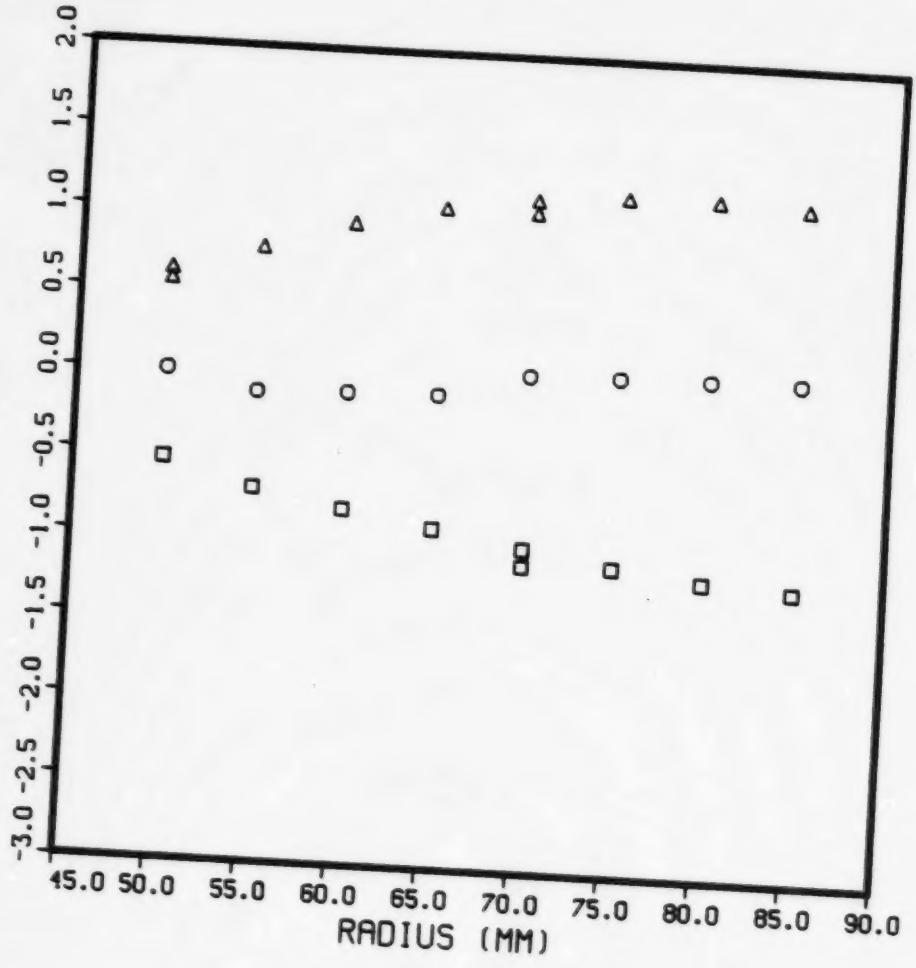

Figure 51: IFRF variable swirl generator secondary flow; S=2.0, $\theta = 90°$, z=2.0 mm; $\square \frac{U_\theta}{U_s}$, $\circ \frac{U_r}{U_s}$, $\Delta \frac{U_z}{U_s}$; $\hat{U}_s = 16.5$ m/s.

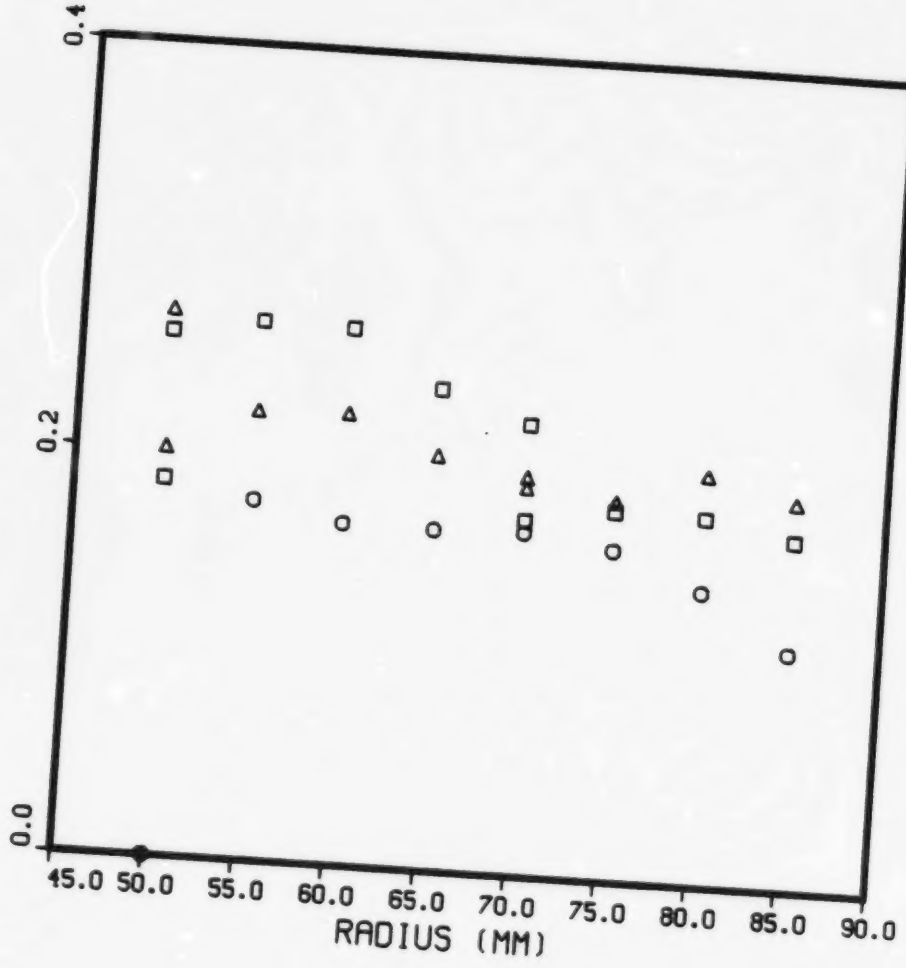

Figure 52: IFRF variable swirl generator secondary flow; S=2.0, $\theta = 90°$, z=2.0 mm; $\square \frac{u'}{\hat{U}_z}$, $\circ \frac{w'}{\hat{U}_z}$, $\triangle \frac{u'}{\hat{U}_z}$; $\hat{U}_z = 16.5$ m/s.

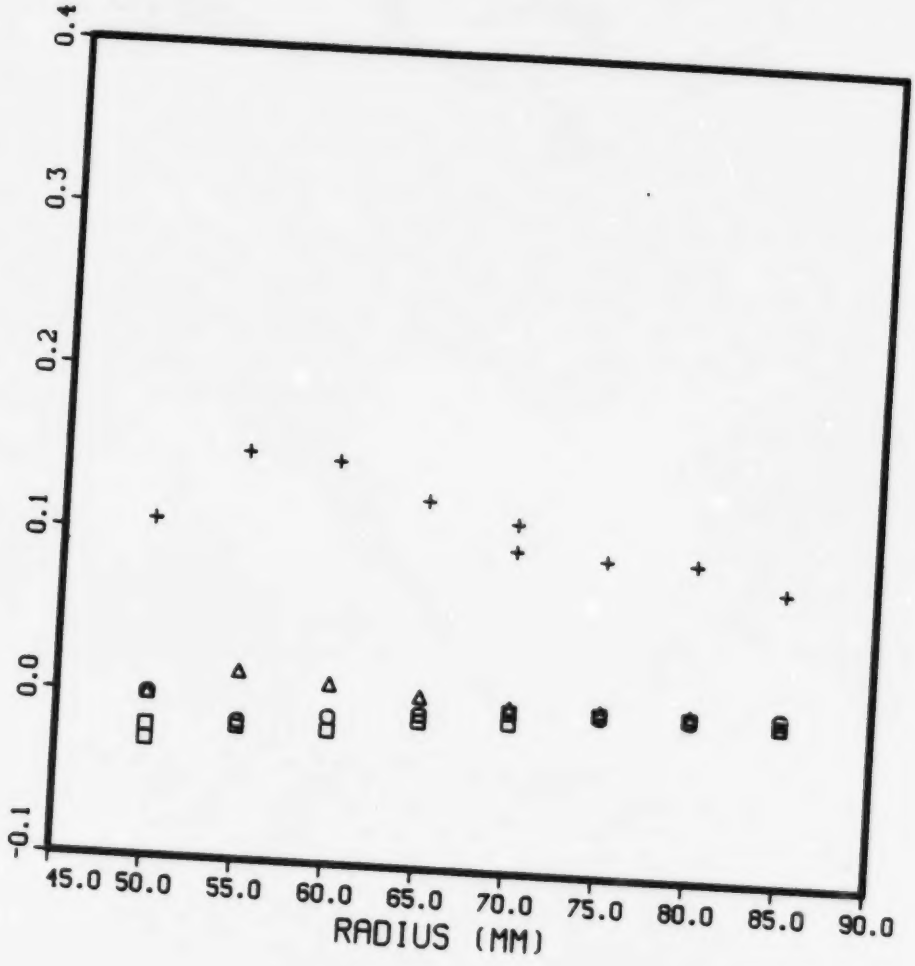

Figure 53: IFRF variable swirl generator secondary flow; S=2.0, $\theta = 90°$, z=2.0 mm; $\square \frac{\overline{u_\theta u_z}}{\hat{U}_z^2}$, $\circ \frac{\overline{u_r u_z}}{\hat{U}_z^2}$, $\triangle \frac{\overline{u_r u_\theta}}{\hat{U}_z^2}$, $+ \frac{q^2}{\hat{U}_z^2}$; $\hat{U}_z = 16.5$ m/s.

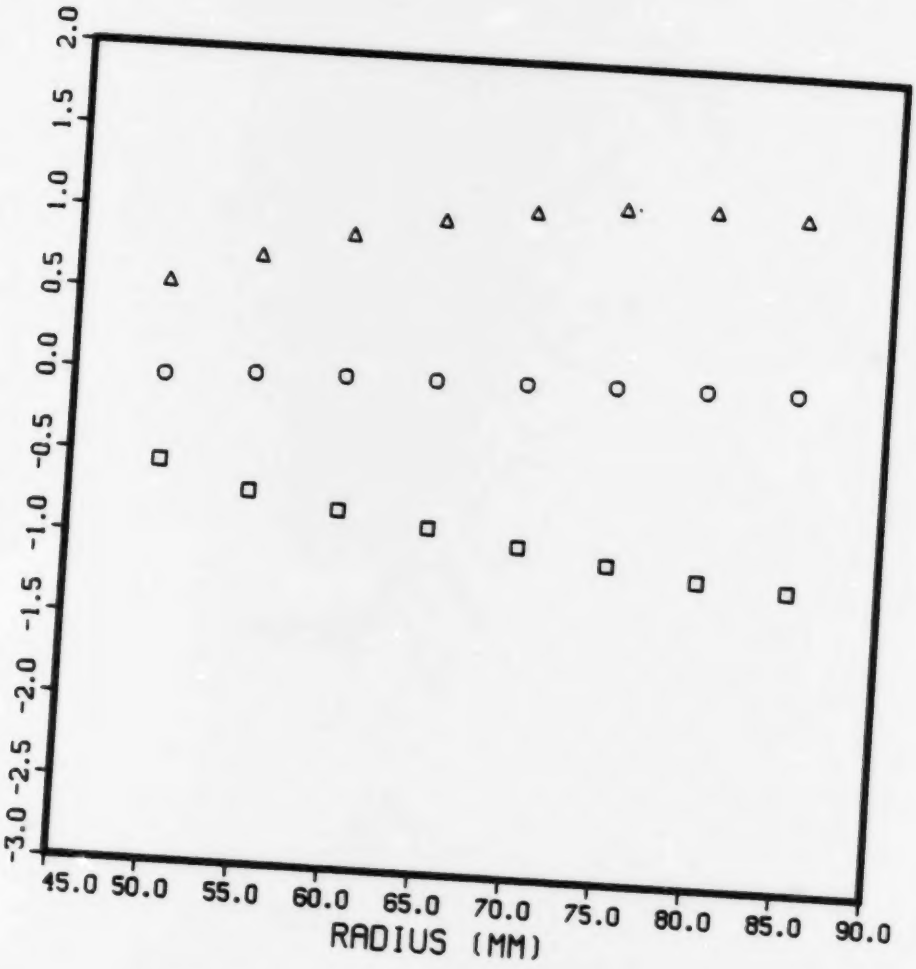

Figure 54: IFRF variable swirl generator secondary flow; S=2.0, $\theta = 90°$, z=2.0 mm; $\square \frac{U_\theta}{U_z}$, $\circ \frac{U_r}{U_z}$, $\triangle \frac{U_z}{U_z}$; $\hat{U}_z = 8.2$ m/s.

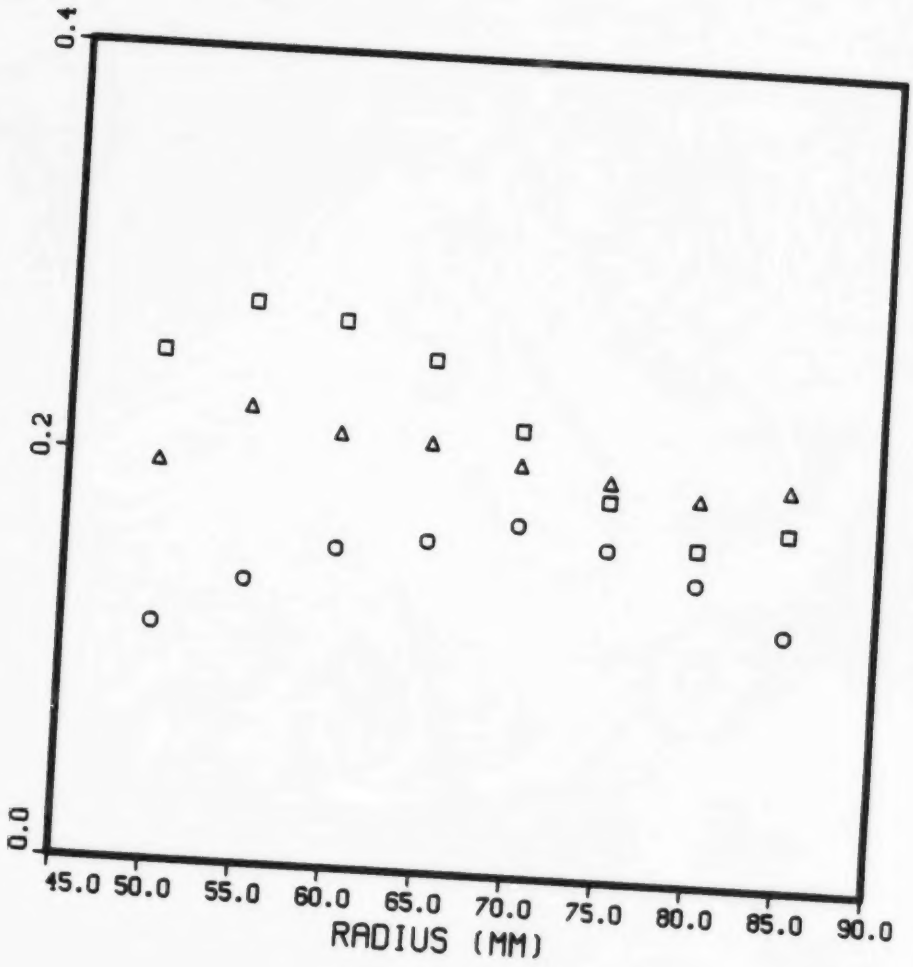

Figure 55: IFRF variable swirl generator secondary flow; S=2.0, $\theta = 90°$, z=2.0 mm; $\Box \frac{u'_z}{\hat{U}_z}$, $\circ \frac{u'_r}{\hat{U}_z}$, $\Delta \frac{u'_\theta}{\hat{U}_z}$; $\hat{U}_z = 8.2$ m/s.

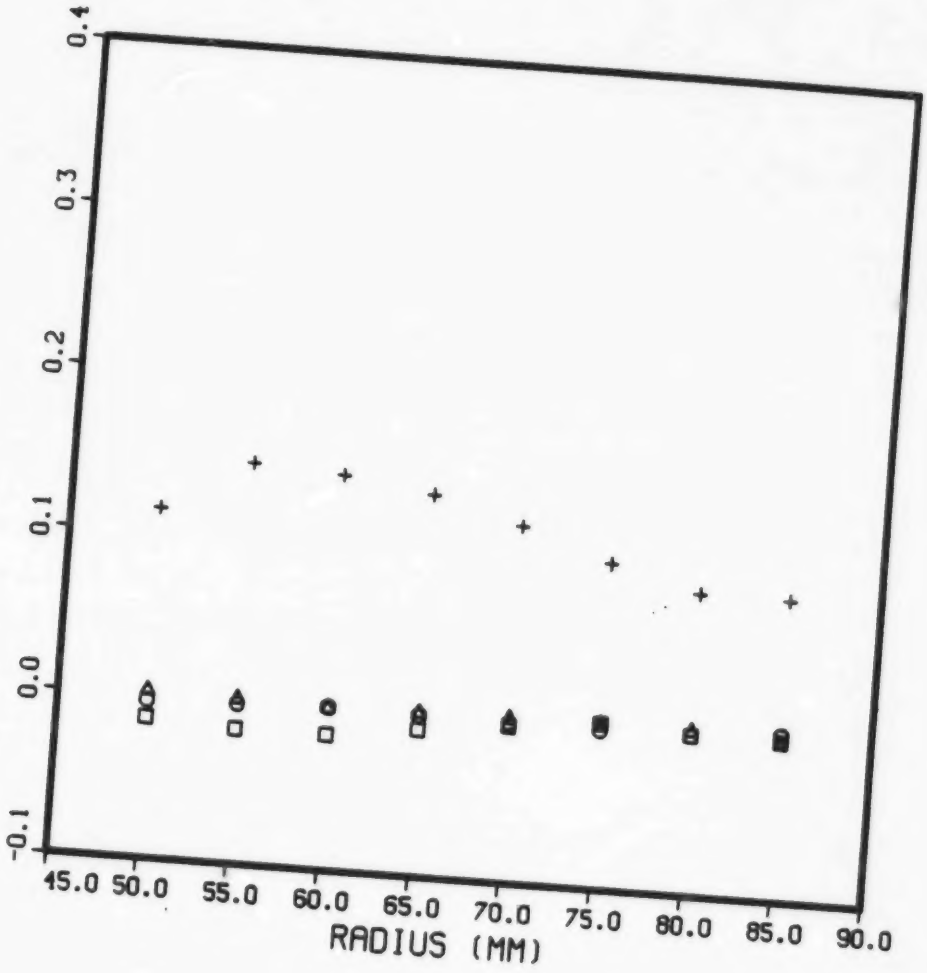

Figure 56: IFRF variable swirl generator secondary flow; S=2.0, $\theta = 90°$, z=2.0 mm; $\square \frac{\overline{u_\theta u_z}}{U_i^2}$, $\circ \frac{\overline{u_r u_z}}{U_i^2}$, $\triangle \frac{\overline{u_r u_\theta}}{U_i^2}$, $+ \frac{q^2}{U_i^2}$; $\hat{U}_z = 8.2$ m/s.

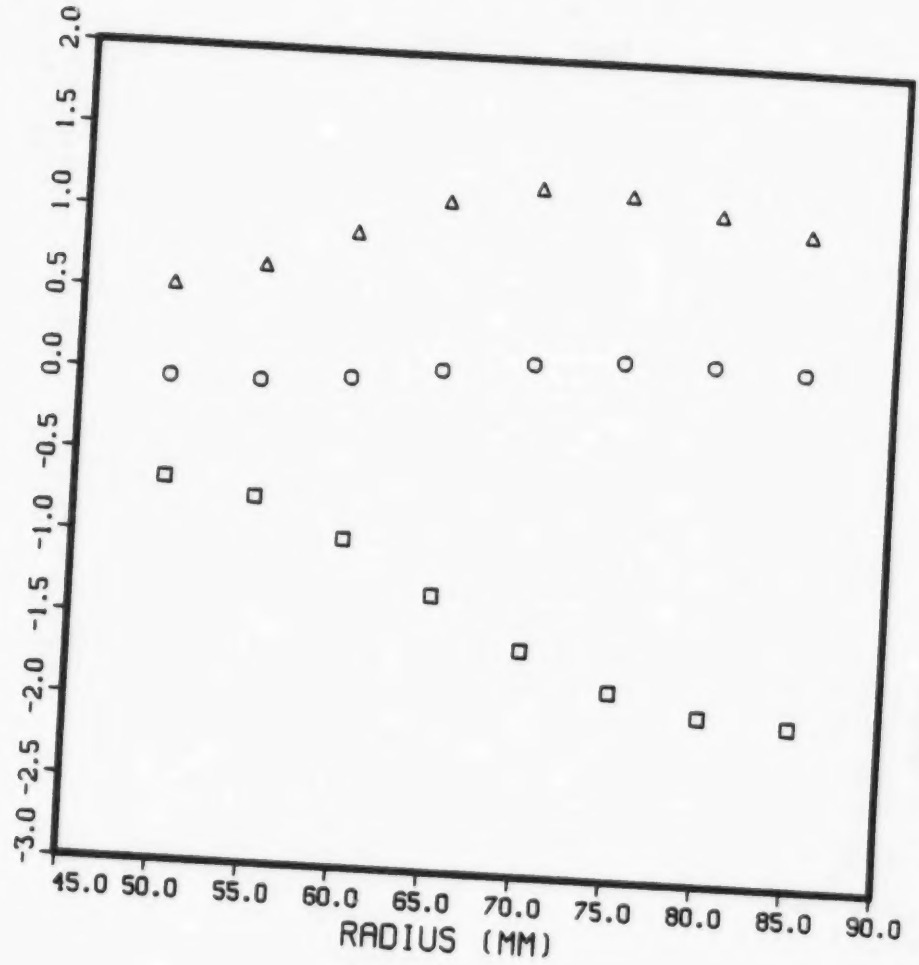

Figure 57: IFRF variable swirl generator secondary flow; S=3.0, $\theta = 90°$, z=2.0 mm; $\square \frac{U_\theta}{U_z}$, $\circ \frac{U_r}{U_z}$, $\triangle \frac{U_z}{U_z}$; $\hat{U}_z = 15.9$ m/s.

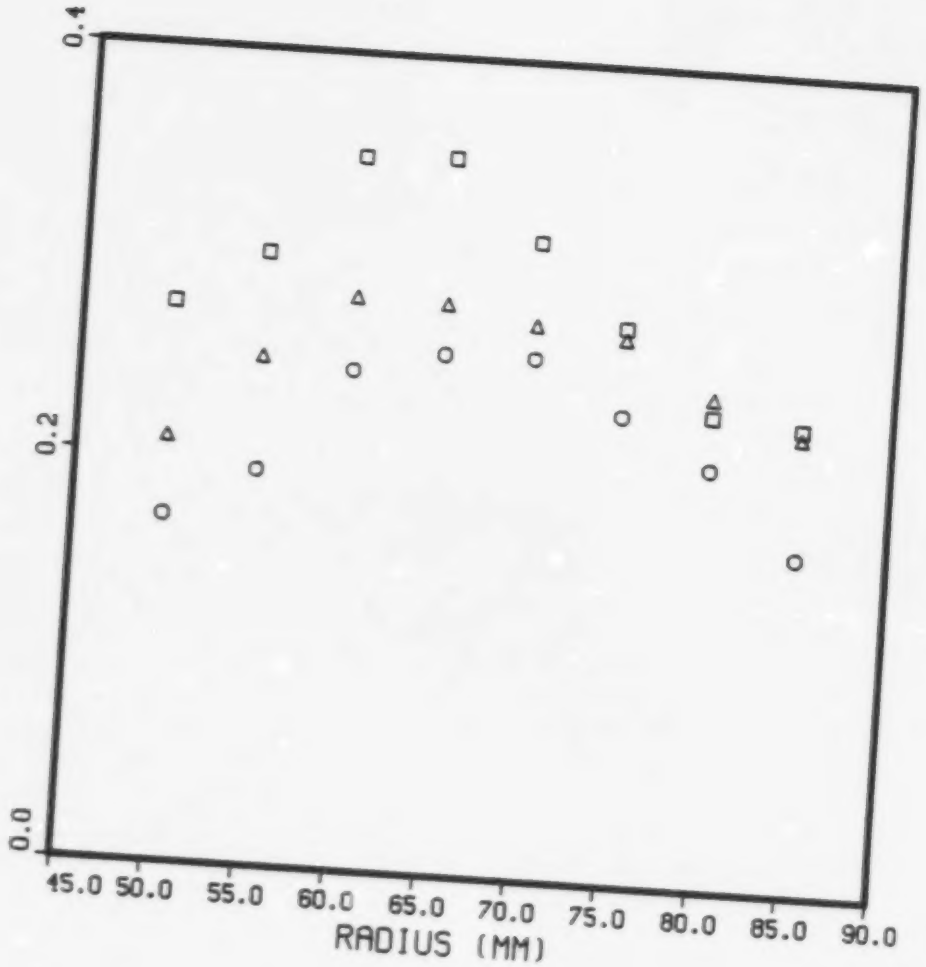

Figure 58: IFRF variable swirl generator secondary flow; S=3.0, $\theta = 90°$, z=2.0 mm; $\Box \frac{u'_R}{\hat{U}_z}$, $\circ \frac{u'_z}{\hat{U}_z}$, $\Delta \frac{u'_t}{\hat{U}_z}$; $\hat{U}_z = 15.9$ m/s.

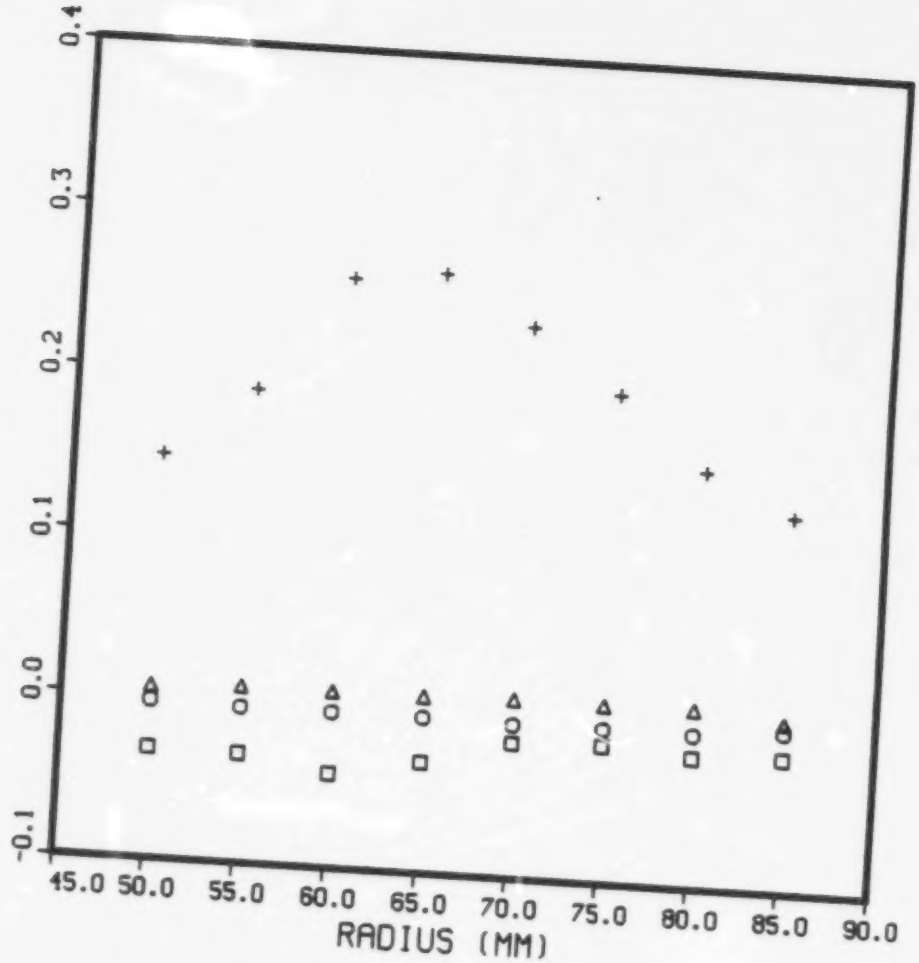

Figure 59: IFRF variable swirl generator secondary flow; S=3.0, $\theta = 90°$, z=2.0 mm; $\square \frac{\overline{u_\theta u_z}}{U_z^2}$, $\circ \frac{\overline{u_r u_z}}{U_z^2}$, $\triangle \frac{\overline{u_r u_\theta}}{U_z^2}$, $+ \frac{q^2}{U_z^2}$; $\widehat{U}_z = 15.9$ m/s.

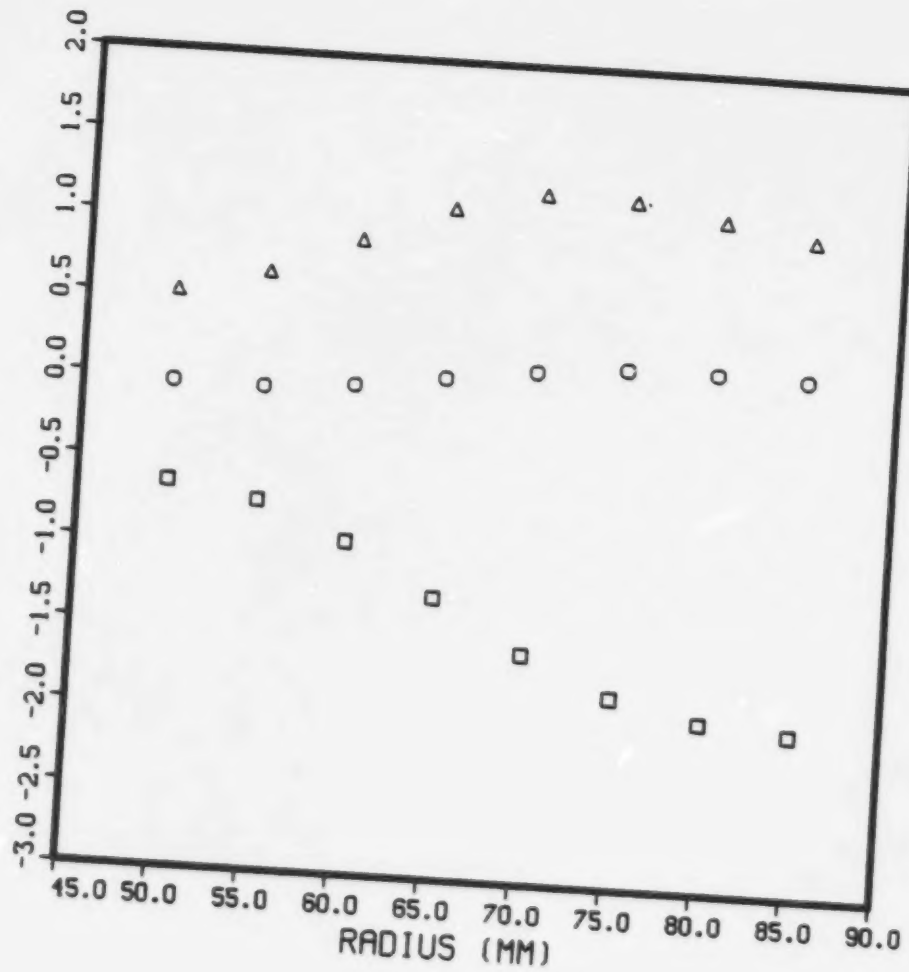

Figure 60: IFRF variable swirl generator secondary flow; S=3.0, $\theta = 90°$, z=2.0 mm; $\square \frac{U_\theta}{U_z}$, $\circ \frac{U_r}{U_z}$, $\triangle \frac{U_z}{U_z}$; $\hat{U}_z = 7.9$ m/s.

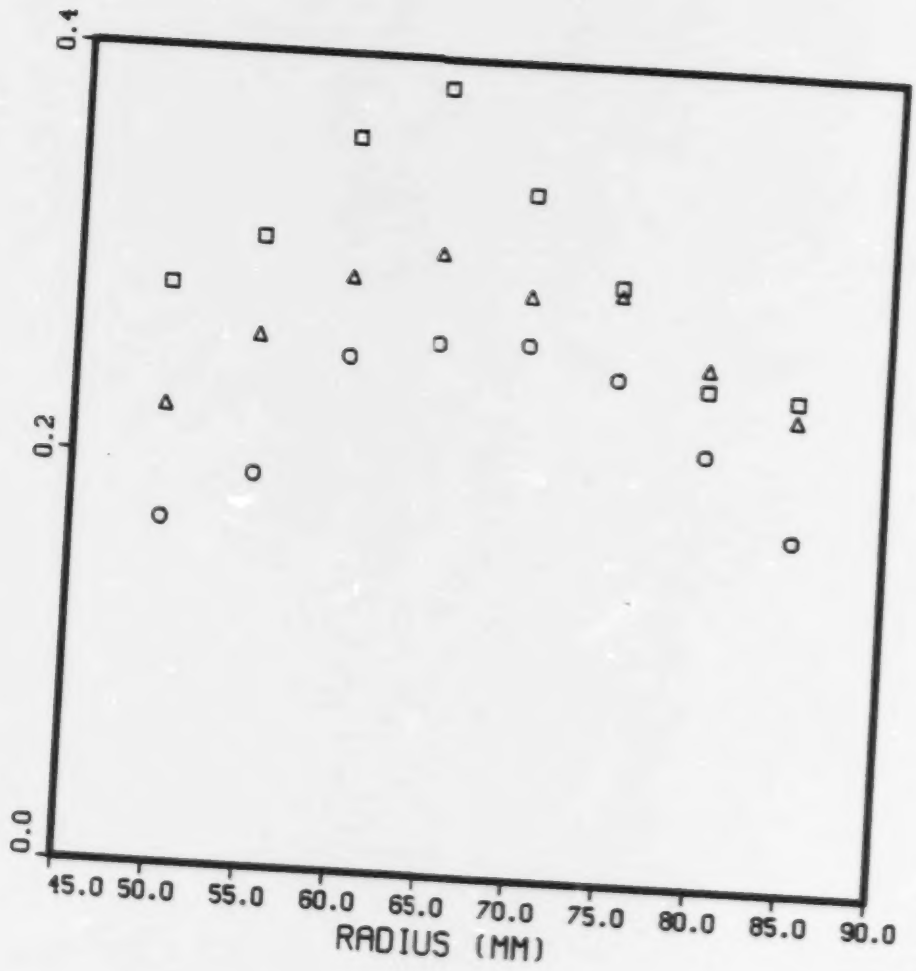

Figure 61: IFRF variable swirl generator secondary flow; S=3.0, $\theta = 90°$, z=2.0 mm; $\Box \frac{u'_R}{U_z}$, $\circ \frac{u'_\theta}{U_z}$, $\Delta \frac{u'_z}{U_z}$; $\hat{U}_z = 7.9$ m/s.

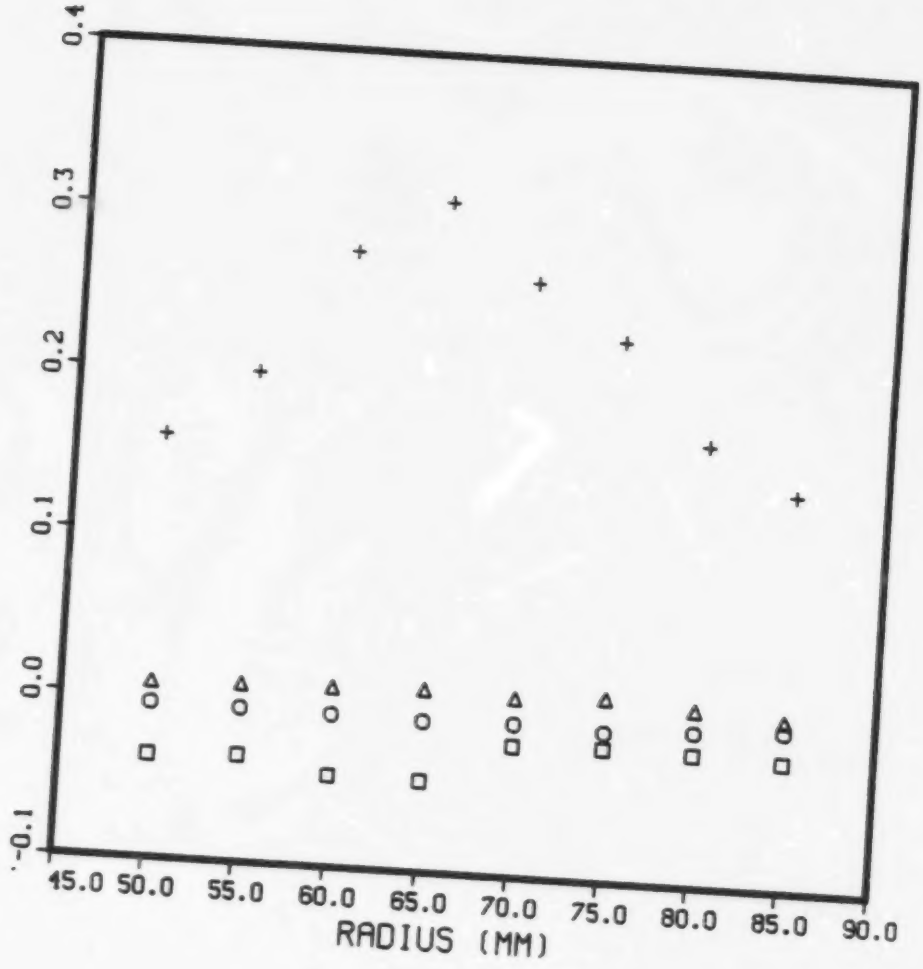

Figure 62: IFRF variable swirl generator secondary flow; S=3.0, $\theta = 90°$, z=2.0 mm; $\square \frac{\overline{u_\theta u_z}}{U_z^2}$, $\circ \frac{\overline{u_r u_z}}{U_z^2}$, $\triangle \frac{\overline{u_r u_\theta}}{U_z^2}$, $+ \frac{q^2}{U_z^2}$; $\widehat{U}_z = 7.0$ m/s.

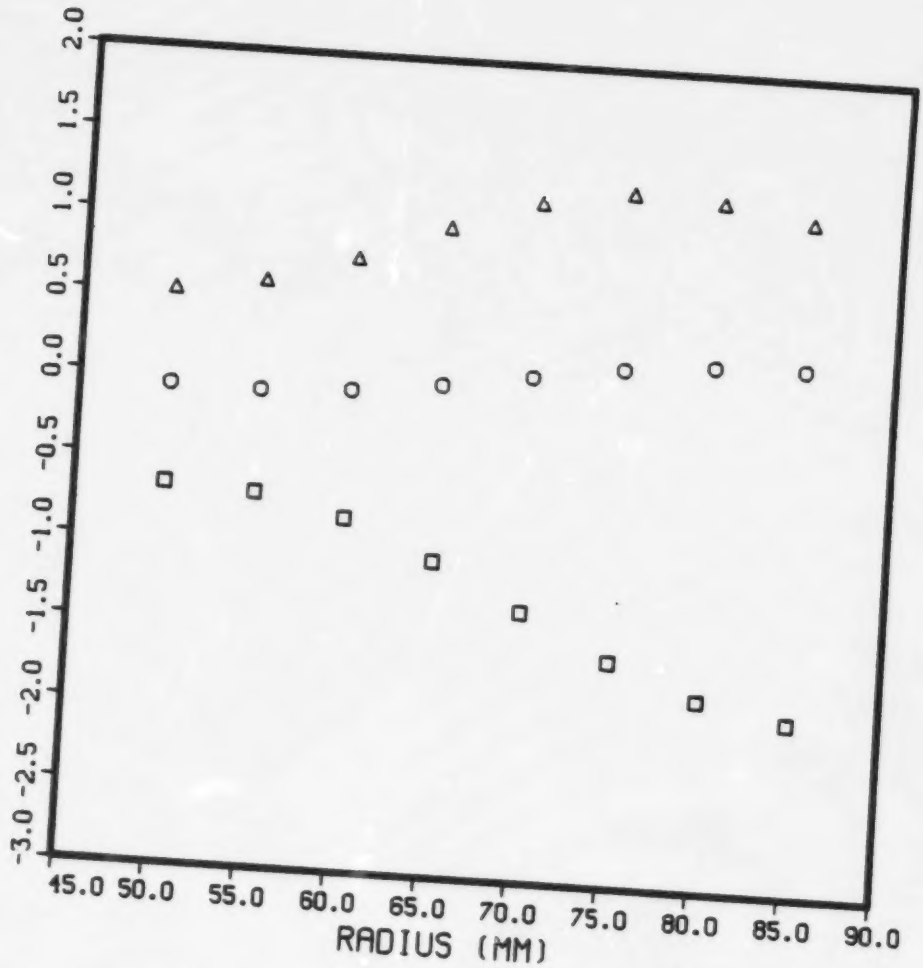

Figure 63: IFRF variable swirl generator secondary flow; S=4.0, $\theta = 90°$, z=2.0 mm; $\square \frac{U_\theta}{U_z}$, $\circ \frac{U_r}{U_z}$, $\triangle \frac{U_t}{U_z}$; $\hat{U}_z$ =19.6 m/s.

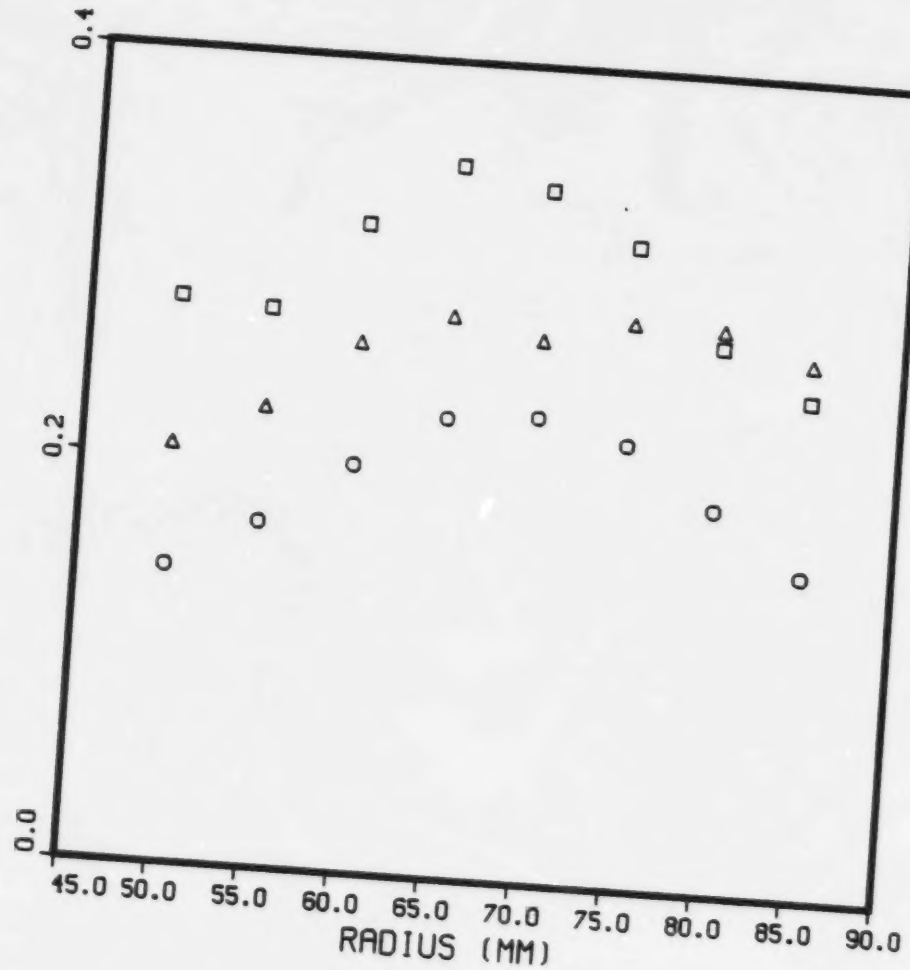

Figure 64: IFRF variable swirl generator secondary flow; S=4.0, $\theta = 90°$, z=2.0 mm; $\square \frac{u'_R}{\hat{U}_z}$, $\circ \frac{u'_\theta}{\hat{U}_z}$, $\triangle \frac{u'_z}{\hat{U}_z}$; $\hat{U}_z$ =19.6 m/s.

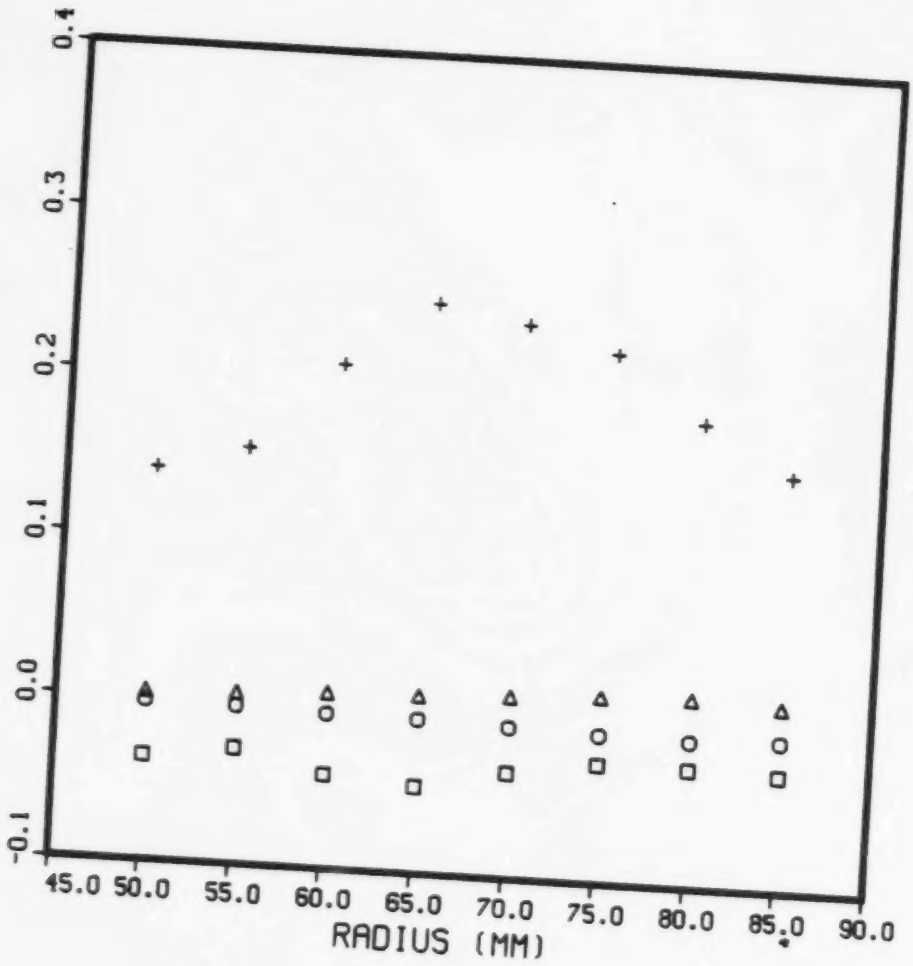

Figure 65: IFRF variable swirl generator secondary flow; S=4.0, $\theta = 90°$, z=2.0 mm; $\square \frac{\overline{u_\theta u_z}}{U_z^2}$, $\circ \frac{\overline{u_r u_z}}{U_z^2}$, $\triangle \frac{\overline{u_r u_\theta}}{U_z^2}$, $+ \frac{\sigma^2}{U_z^2}$; $\hat{U}_z$ =19.6 m/s.

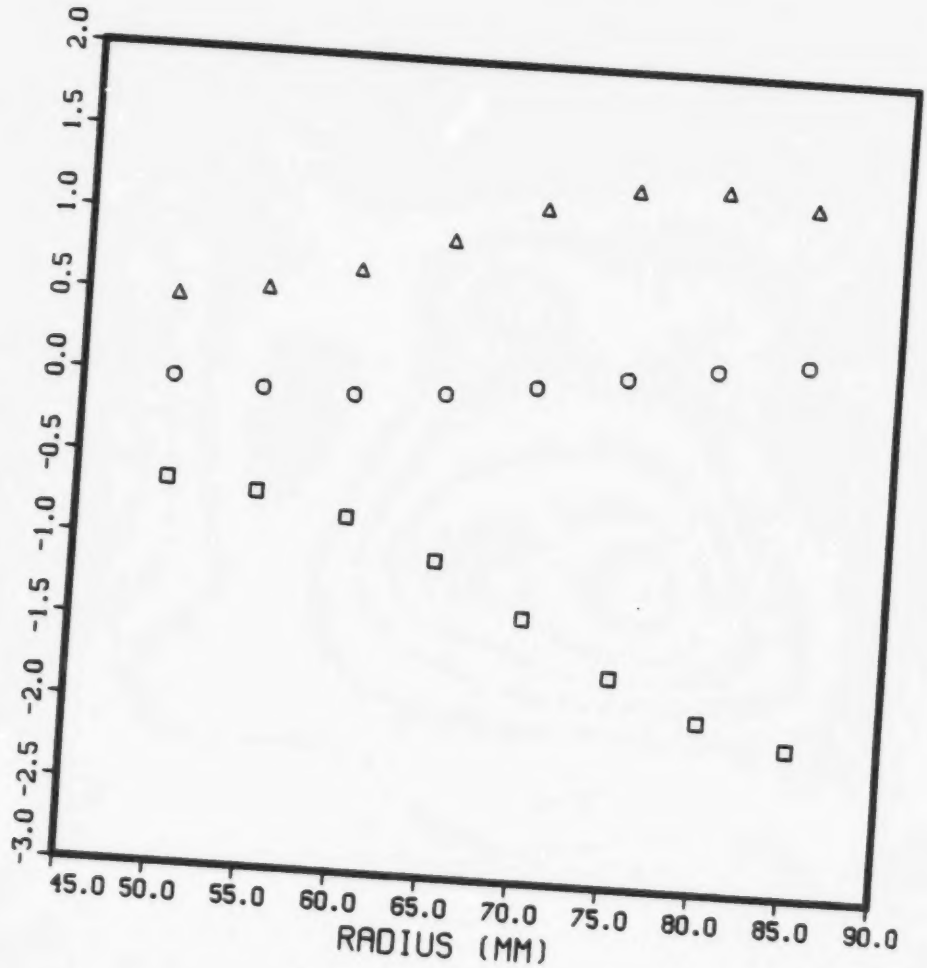

Figure 66: IFRF variable swirl generator secondary flow; S=4.0, $\theta = 90°$, z=2.0 mm; $\square \frac{U_\theta}{\hat{U}_z}$, $\circ \frac{U_r}{\hat{U}_z}$, $\Delta \frac{U_z}{\hat{U}_z}$; $\hat{U}_z$ =7.5 m/s.

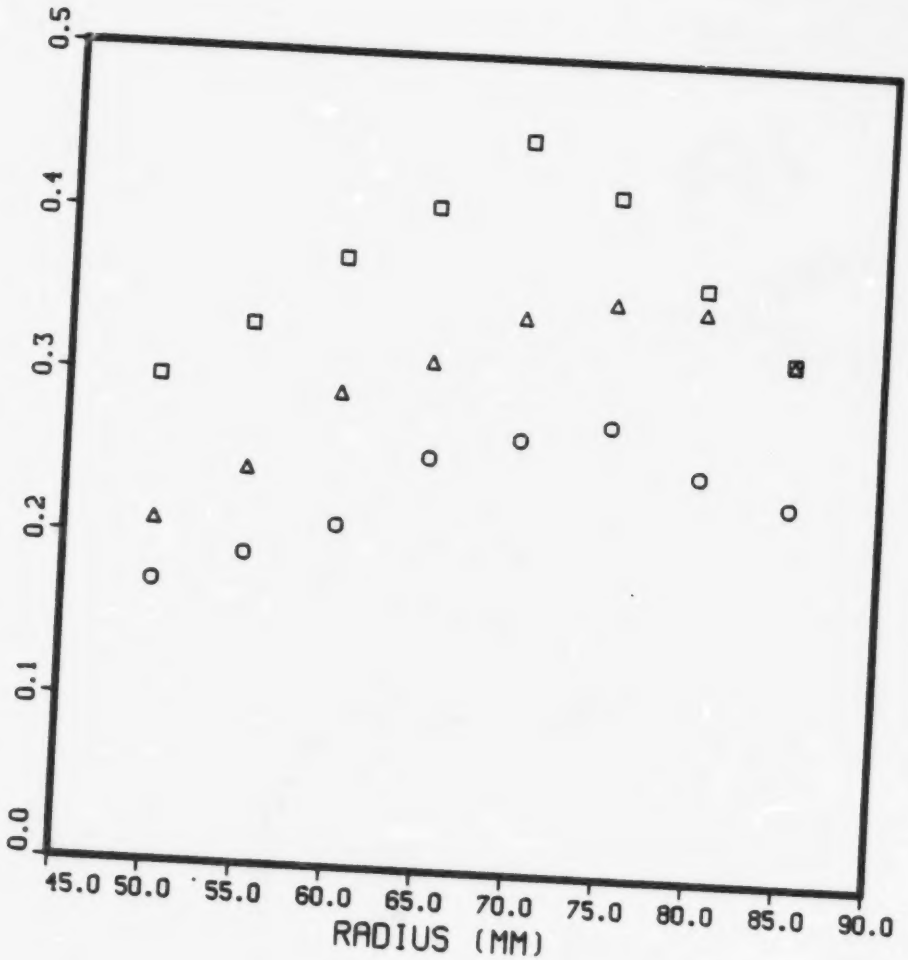

Figure 67: IFRF variable swirl generator secondary flow; S=4.0, $\theta = 90°$, z=2.0 mm; $\Box \frac{u'}{\hat{U}_z}$, $\circ \frac{w'}{\hat{U}_z}$, $\Delta \frac{u'_\theta}{\hat{U}_z}$; $\hat{U}_z = 7.5$ m/s.

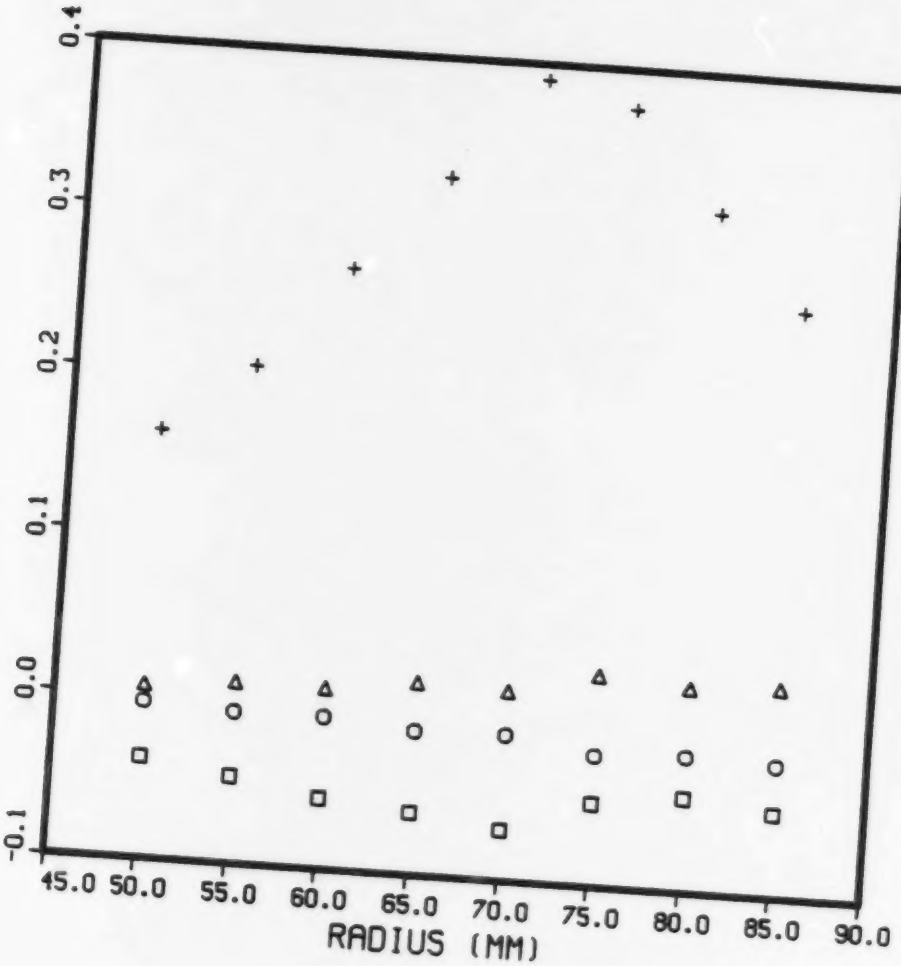

Figure 68: IFRF variable swirl generator secondary flow; S=4.0, $\theta = 90°$, z=2.0 mm; $\square \frac{\overline{u_\theta u_z}}{U_z^2}$, $\circ \frac{\overline{u_r u_z}}{U_z^2}$, $\triangle \frac{\overline{u_r u_\theta}}{U_z^2}$, $+ \frac{q^2}{U_z^2}$; $\hat{U}_z = 7.5$ m/s.

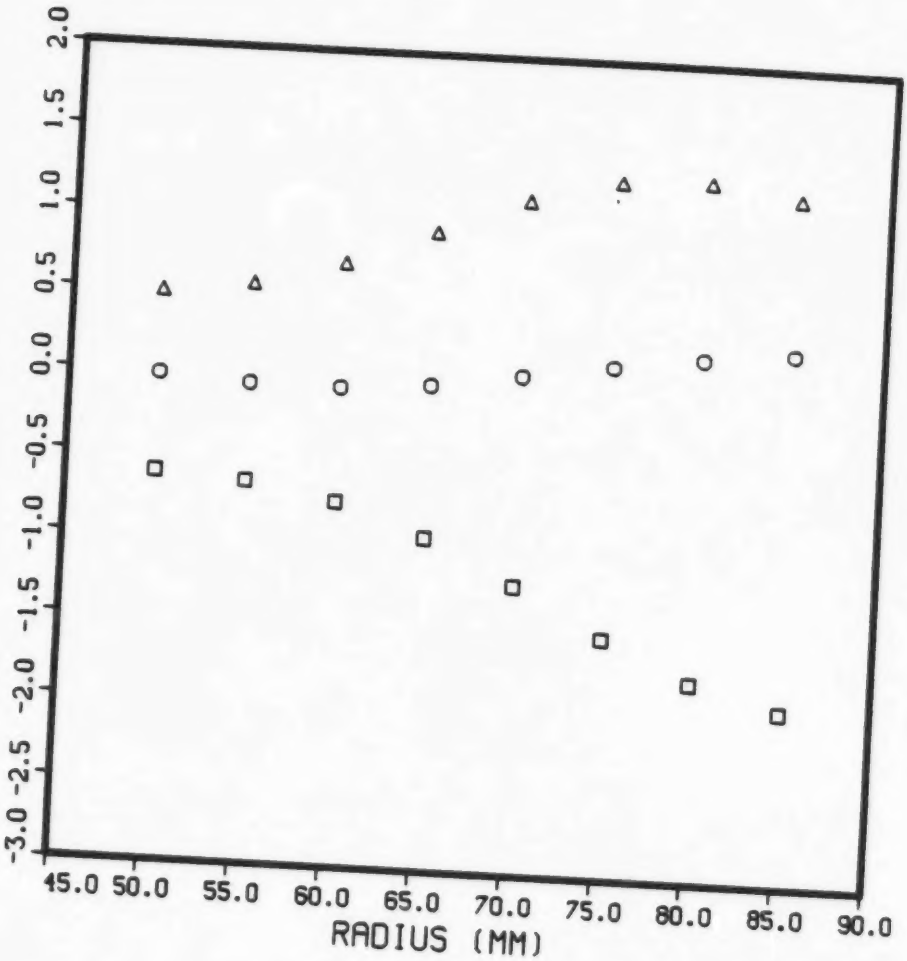

Figure 69: IFRF variable swirl generator secondary flow; S=4.5, $\theta = 90°$, z=4.0 mm; $\square \frac{U_\theta}{U_z}$, $\circ \frac{U_r}{U_z}$, $\triangle \frac{U_z}{U_z}$; $\hat{U}_z$ =17.4 m/s.

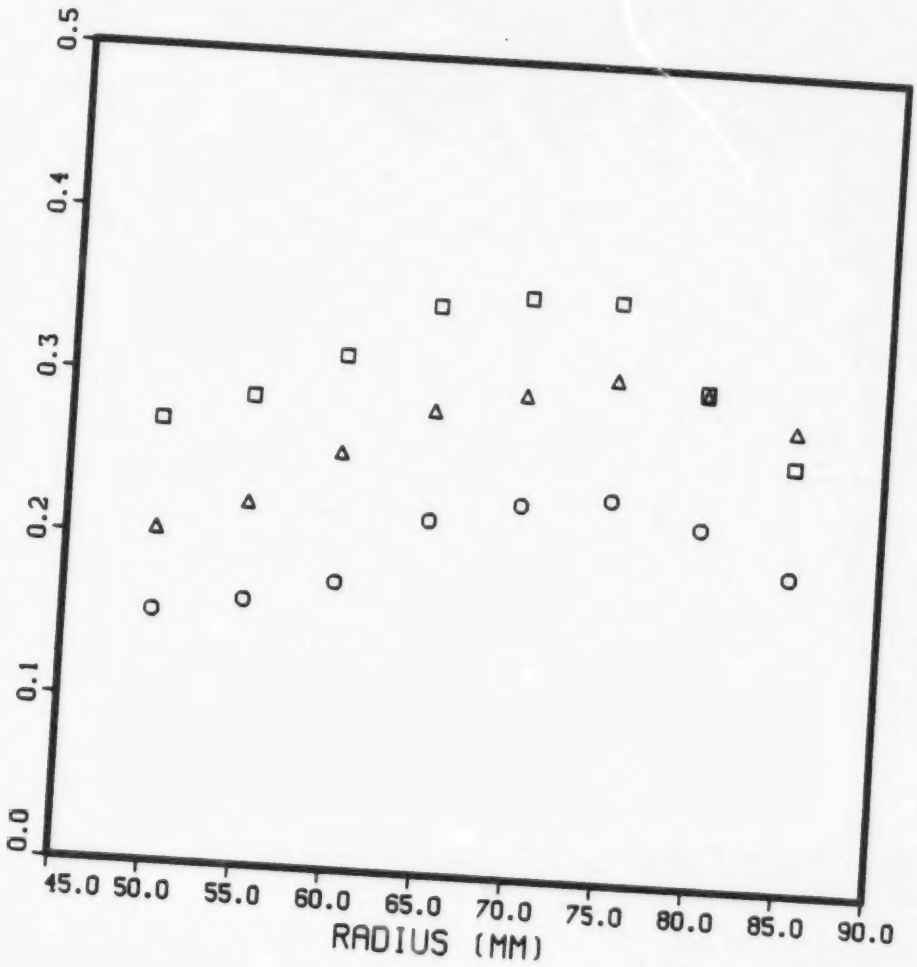

Figure 70: IFRF variable swirl generator secondary flow; S=4.5, $\theta = 90°$, z=4.0 mm; $\Box \frac{u'_z}{\hat{U}_z}$, $\circ \frac{u'_r}{\hat{U}_z}$, $\Delta \frac{u'_\theta}{\hat{U}_z}$; $\hat{U}_z = 17.4$ m/s.

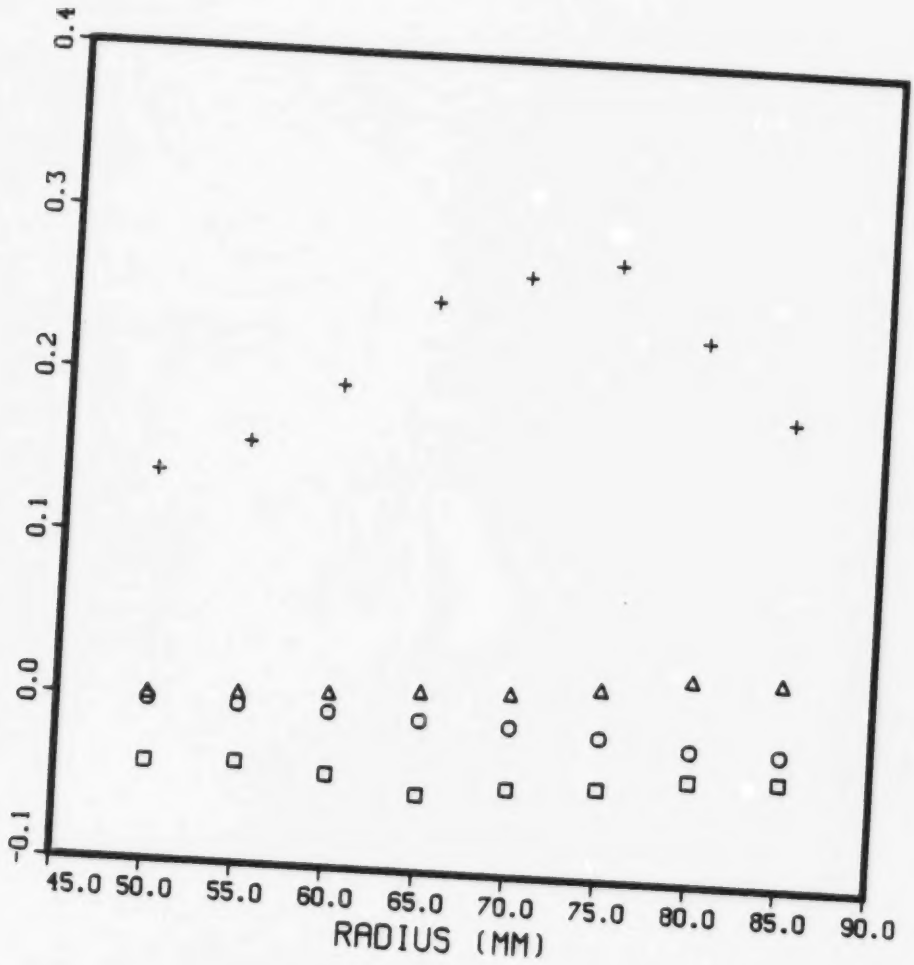

Figure 71: IFRF variable swirl generator secondary flow; S=4.5, $\theta = 90°$, z=4.0 mm; $\square \frac{\overline{u_\theta u_x}}{U_i^2}$, $\circ \frac{\overline{u_r u_x}}{U_i^2}$, $\triangle \frac{\overline{u_r u_\theta}}{U_i^2}$, $+ \frac{q^2}{U_i^2}$; $\hat{U}_z$ =17.4 m/s.

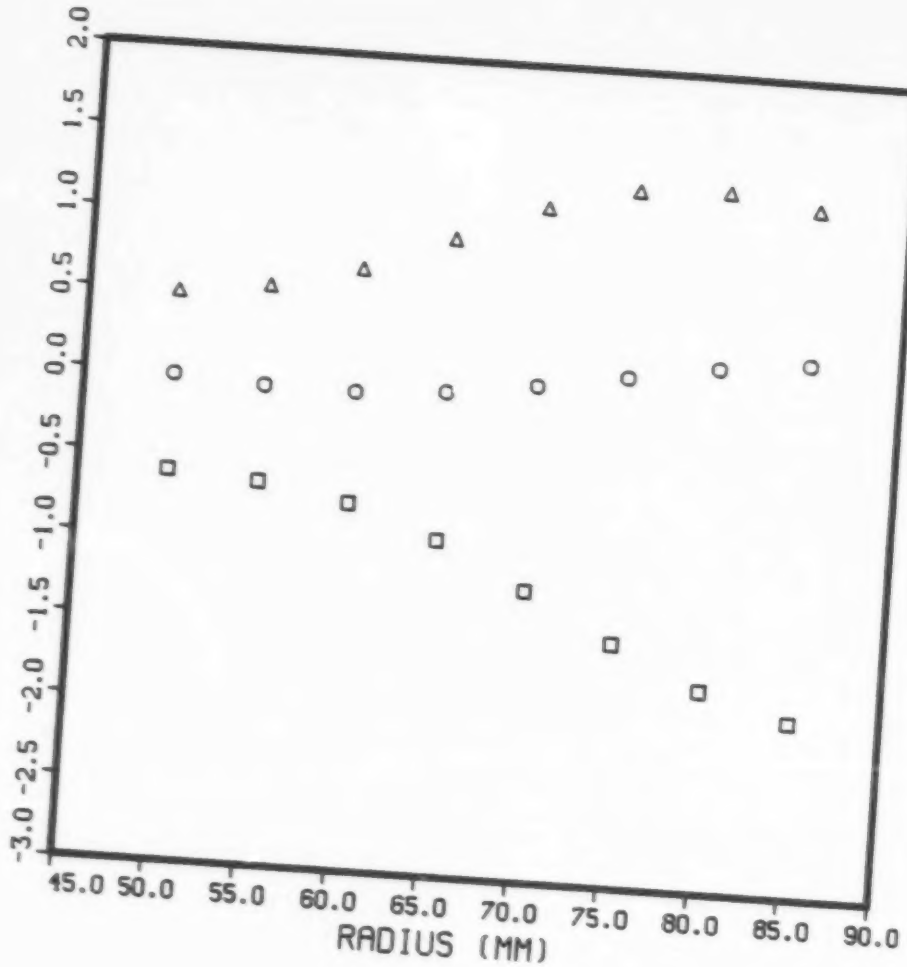

Figure 72: IFRF variable swirl generator secondary flow; S=4 5, $\theta = 90°$, z=4.0 mm; $\square \frac{U_\theta}{U_z}$, $\circ \frac{U_r}{U_z}$, $\triangle \frac{U_r}{U_z}$; $\hat{U}_z = 8.3$ m/s.

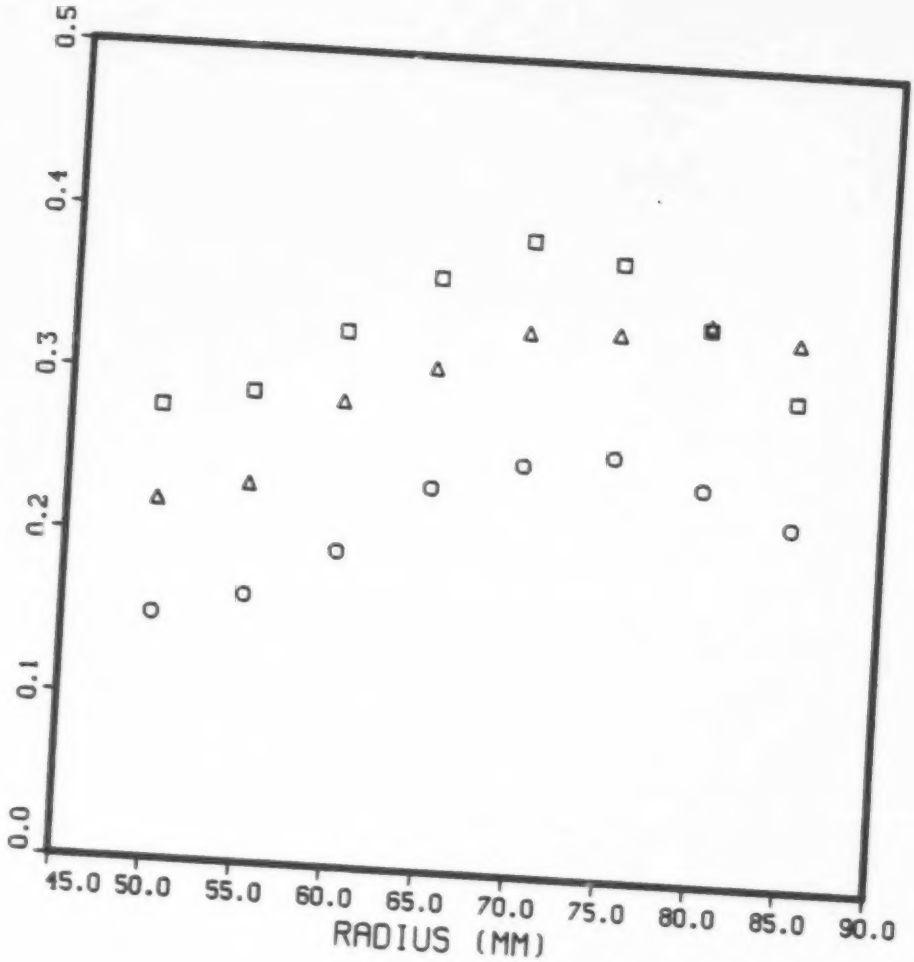

Figure 73: IFRF variable swirl generator secondary flow; S=4.5, $\theta = 90°$, z=4.0 mm; $\Box \frac{u'_z}{\hat{U}_z}$, $\circ \frac{u'_r}{\hat{U}_z}$, $\Delta \frac{u'_\theta}{\hat{U}_z}$; $\hat{U}_z = 8.3$ m/s.

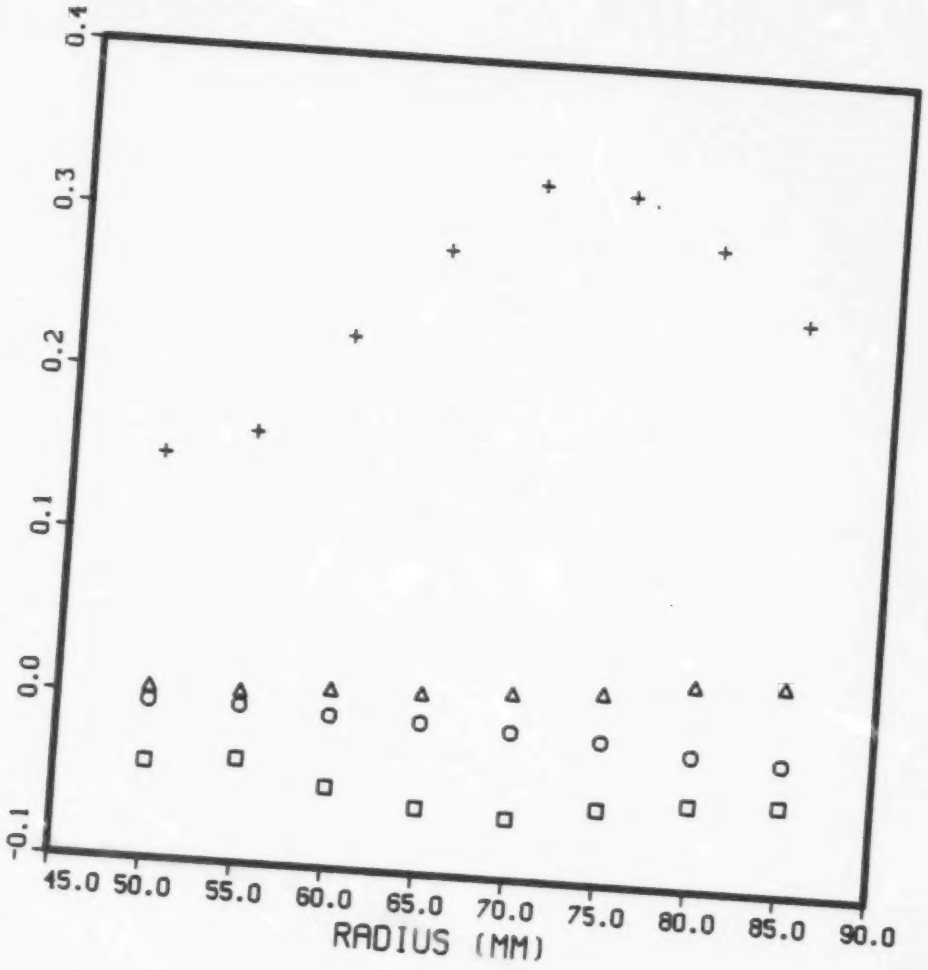

Figure 74: IFRF variable swirl generator secondary flow; S=4.5, $\theta = 90°$, z=4.0 mm; $\square \frac{\overline{u_\theta u_z}}{U_z^2}$, $\circ \frac{\overline{u_r u_z}}{U_z^2}$, $\triangle \frac{\overline{u_r u_\theta}}{U_z^2}$, $+ \frac{q^2}{U_z^2}$; $\hat{U}_z = 8.3$ m/s.